

Punalu‘u Beach Restoration Feasibility Study

Punalu‘u Beach Park, O‘ahu

April 2024



Prepared for:

Hawai‘i Department of Land and Natural Resources
Office of Conservation and Coastal Lands
1151 Punchbowl Street, Suite 131
Honolulu, Hawai‘i 96813

Prepared by:

Sea Engineering, Inc.
Makai Research Pier
41-305 Kalaniana‘ole Hwy
Waimānalo, Hawai‘i 96795

Job No. 25913



This page intentionally left blank

TABLE OF CONTENTS

1. INTRODUCTION	1
2. COASTAL GREEN INFRASTRUCTURE	4
2.1 BEACH NOURISHMENT	5
2.2 DUNES, VEGETATION, AND SHORELINE BERMS	6
2.3 BEACH NOURISHMENT WITH BURIED REVETMENT	7
2.4 BEACH NOURISHMENT WITH STABILIZATION	7
2.4.1 <i>Marine Habitat Enhancement</i>	9
2.5 NATURAL AND ARTIFICIAL REEFS.....	12
2.6 AQUATIC VEGETATION	13
3. PROJECT SITE DESCRIPTION.....	14
3.1 REGIONAL SETTING.....	14
3.2 BEACH CONDITION AND TOPOGRAPHIC SURVEY.....	15
3.2.1 <i>South of Punalu'u Beach Park</i>	16
3.2.2 <i>Southern Portion of Park</i>	19
3.2.3 <i>Central Portion of Park</i>	21
3.2.4 <i>Northern Portion of the Park</i>	22
3.2.5 <i>North of the beach park</i>	25
4. HISTORICAL SHORELINE ANALYSIS.....	28
4.1 HISTORY OF EROSION FRONTING THE COMFORT STATION	31
5. OCEANOGRAPHIC SETTING	39
5.1 BATHYMETRY AND NEARSHORE BOTTOM CONDITIONS	39
5.2 WINDS.....	40
5.3 WATER LEVELS.....	42
5.3.1 <i>Astronomical Tides</i>	42
5.3.2 <i>Sea Level Rise Projections</i>	42
5.3.3 <i>Sea Level Anomalies</i>	45
5.4 WAVES.....	47
5.4.1 <i>General Wave Climate</i>	47
5.4.2 <i>Windward O'ahu Wave Climate</i>	49
5.4.3 <i>Extreme Deepwater Waves</i>	53
6. DESIGN PARAMETERS AND NUMERICAL WAVE MODELING	57
6.1 DESIGN STILL WATER LEVEL.....	58
6.2 OFFSHORE WAVE TRANSFORMATION	58
6.2.1 <i>Prevailing Waves</i>	59
6.2.2 <i>Annual Waves</i>	62
6.2.3 <i>Extreme Waves</i>	64
6.3 NEARSHORE WAVE TRANSFORMATION AND PROCESSES	66
6.3.1 <i>Prevailing Waves</i>	66
6.3.2 <i>Annual Waves</i>	72
6.3.3 <i>50-yr Waves</i>	74

6.4	WAVE RUNUP	76
6.5	ARMOR STONE SIZING.....	78
6.6	UNDERLAYER STONE SIZING.....	78
7.	OFFSHORE SAND SOURCE INVESTIGATIONS.....	79
7.1	INTRODUCTION.....	79
7.2	SAND CHARACTERISTICS AND QUALITY	79
7.3	EXISTING BEACH SAND CHARACTERISTICS.....	80
7.4	OFFSHORE SAND SOURCE INVESTIGATIONS	81
7.5	OVERFILL FACTOR	86
7.6	SEDIMENT TURBIDITY ANALYSIS	88
7.6.1	<i>Methods for Turbidity Testing</i>	88
7.6.2	<i>Turbidity Testing Results</i>	90
8.	OFFSHORE SAND RECOVERY METHODS.....	92
8.1	SMALL-SCALE DREDGING SYSTEMS	92
8.1.1	<i>Subdredge ROV by EDDY Pump</i>	92
8.1.2	<i>Diver-operated Dredge by EDDY Pump</i>	93
8.1.3	<i>Dredge Sled submersible pump and platform by EDDY Pump</i>	94
8.2	TRADITIONAL DREDGING SYSTEMS	95
8.2.1	<i>Clamshell Dredging</i>	96
8.2.2	<i>Submersible Slurry Pump</i>	99
9.	MARINE RESOURCES	102
9.1	OFFSHORE SAND RECOVERY AREA.....	102
9.1.1	<i>Physical Structure</i>	102
9.1.2	<i>Biotic Community Structure</i>	103
9.2	PUNALU‘U BEACH PARK	104
9.2.1	<i>Physical Structure</i>	104
9.2.2	<i>Biotic Community Structure</i>	105
10.	BEACH RESTORATION CONCEPT ALTERNATIVES.....	111
10.1	INTRODUCTION	111
10.2	ALTERNATIVE 1 – BEACH NOURISHMENT.....	111
10.2.1	<i>Alternative 1 – ROM Cost Estimate</i>	114
10.3	ALTERNATIVE 2 – BEACH NOURISHMENT WITH BURIED REVETMENT.....	114
10.3.1	<i>Alternative 2 – ROM Cost Estimate</i>	117
10.4	ALTERNATIVE 3 – STABILIZED POCKET BEACHES	118
10.4.1	<i>Alternative 3 – ROM Cost Estimate</i>	121
10.5	ALTERNATIVE 4 – PARTIALLY STABILIZED POCKET BEACHES	121
10.5.1	<i>Alternative 4 – ROM Cost Estimate</i>	124
10.6	ALTERNATIVE 5 – HYBRID STABILIZED POCKET BEACHES.....	124
10.6.1	<i>Alternative 5 – ROM Cost Estimate</i>	127
11.	WAVE AND SEA LEVEL RISE INUNDATION MODELING.....	128
11.1	PREVAILING WAVES FOR EXISTING SEA LEVEL	128
11.2	ANNUAL WAVES UNDER EXISTING SEA LEVEL.....	134

11.3	PREVAILING WAVES WITH 1.6 FT OF SLR.....	140
11.4	ANNUAL WAVES WITH 1.6 FT OF SLR.....	146
11.5	PREVAILING WAVES WITH 3.2 FT OF SLR.....	152
11.6	ANNUAL WAVES WITH 3.2 FT OF SLR.....	158
12.	SUMMARY, DISCUSSION, AND REGULATORY REQUIREMENTS	164
12.1	SUMMARY	164
12.2	DISCUSSION.....	165
12.3	REGULATORY REQUIREMENTS	166
13.	REFERENCES.....	167
14.	APPENDIX A: PUNALUU BEACH NOURISHMENT MARINE ASSESSMENTS	169

LIST OF FIGURES

FIGURE 1-1.	PUNALU‘U BEACH PARK LOCATION MAP	3
FIGURE 2-1.	VARYING DEGREES OF NATURE-BASED SOLUTIONS (WEBB, ET. AL., 2019).....	4
FIGURE 2-2.	WAIKIKI BEACH NOURISHMENT (24 HOURS POST-CONSTRUCTION)	5
FIGURE 2-3.	BERM STABILIZATION WITH NATIVE VEGETATION.....	6
FIGURE 2-4.	SAMPLE CROSS-SECTION OF BURIED REVETMENT AND DUNE RESTORATION (BOUDREAU ET. AL., 2018).	7
FIGURE 2-5.	NINE ROCK HEADLAND STRUCTURES STABILIZE 4,000 FT OF SAND BEACH AT IROQUOIS POINT	8
FIGURE 2-6.	POCKET BEACH CELLS AT IROQUOIS POINT	9
FIGURE 2-7.	OBSERVED MARINE LIFE WITHIN THE IROQUOIS POINT PROJECT AREA.....	11
FIGURE 2-8.	VARIOUS METHODS OF NATURAL AND ARTIFICIAL REEFS TO REDUCE WAVE ENERGY AT THE SHORELINE (BRIDGES ET. AL., 2021).....	12
FIGURE 2-9.	EXAMPLES OF TYPES OF AQUATIC VEGETATION ALONG A TYPICAL SHORELINE PROFILE (BRIDGES ET. AL., 2021).....	13
FIGURE 3-1.	PUNALU‘U BEACH PARK SITE MAP (REGIONAL VIEW)	15
FIGURE 3-2.	SEI TOPOGRAPHIC SURVEY POINTS AND CONTOURS OVERLAID ON DRONE AERIAL MOSAIC (SURVEY AND DRONE IMAGE DATE: NOVEMBER 22, 2022)	16
FIGURE 3-3.	COMPARISON OF SHORELINE SOUTH OF PUNALU‘U BEACH PARK IN APRIL 2018 (TOP PHOTO) AND NOVEMBER 2022 (BOTTOM PHOTO).....	17
FIGURE 3-4.	FENCE AT SOUTHERN LIMIT OF PUNALU‘U BEACH PARK (NOVEMBER 2022 PHOTO)..	18
FIGURE 3-5.	VIEW OF PROPERTY TO THE SOUTH OF PUNALU‘U BEACH PARK (APRIL 2024 PHOTO) 18	
FIGURE 3-6.	DRONE MOSAIC OVERVIEW OF SOUTHERN AREA OF BEACH PARK (NOVEMBER 22, 2022).....	19
FIGURE 3-7.	SOUTHERN LIMIT OF PUNALU‘U BEACH PARK LOOKING NORTHWEST (NOVEMBER 2022 PHOTO)	20
FIGURE 3-8.	IRONWOOD STUMP, AND ROOTS INDICATING BEACH EROSION (NOVEMBER 2022 PHOTO)	20
FIGURE 3-9.	EPIHEMERAL STREAM FLOW THROUGH BEACH SOUTH OF COMFORT STATION (NOVEMBER 2022 PHOTO)	21

FIGURE 3-10. DRONE MOSAIC OVERVIEW OF CENTRAL AREA OF BEACH PARK (NOVEMBER 22, 2022)	22
FIGURE 3-11. DRONE MOSAIC OVERVIEW OF NORTHERN AREA OF BEACH PARK (NOVEMBER 22, 2022)	23
FIGURE 3-12 . COMPARISON OF NORTHERN AREA SHORELINE IN MARCH 2019 (TOP PHOTO) AND NOVEMBER 2022 (BOTTOM PHOTO)	24
FIGURE 3-13. DRONE MOSAIC OVERVIEW NORTH OF BEACH PARK (NOVEMBER 22, 2022)	25
FIGURE 3-14. COMPARISON OF NORTH PORTION OF PARK IN MARCH 2019 (TOP PHOTO) AND APRIL 2024 (BOTTOM PHOTO)	26
FIGURE 3-15. SAND BEACH ON SOUTH SIDE OF WAI‘ONO STREAM (NOVEMBER 2022)	27
FIGURE 4-1. HISTORICAL SHORELINE CHANGE RATE TRANSECTS FOR PUNALU‘U BEACH PARK (UH CRC)	29
FIGURE 4-2. CRC TRANSECT #166 SHORELINE CHANGE TREND FOR PUNALU‘U BEACH PARK (UH CRC)	30
FIGURE 4-3. HISTORICAL SHORELINE CHANGE FROM 1988-2022, 2006-2022, AND 2015-2022 RELATIVE TO THE UH CRC TRANSECTS (SHOWN IN WHITE)	31
FIGURE 4-4. COMFORT STATION VEGETATION LINE (AUGUST 2008)	33
FIGURE 4-5. COMFORT STATION VEGETATION LINE (JUNE 2012)	33
FIGURE 4-6. COMFORT STATION VEGETATION LINE (AUGUST 2013)	34
FIGURE 4-7. COMFORT STATION VEGETATION LINE (WINTER 2015-2016)	34
FIGURE 4-8. EROSION SCARP AT COMFORT STATION (WINTER 2015-2016)	35
FIGURE 4-9. EROSION PROTECTION FRONTING COMFORT STATION (MAY 2016)	35
FIGURE 4-10. EROSION PROTECTION FRONTING COMFORT STATION (JANUARY 2018)	36
FIGURE 4-11. EROSION PROTECTION FRONTING COMFORT STATION (MARCH 2019)	36
FIGURE 4-12. EROSION PROTECTION FRONTING COMFORT STATION (APRIL 2024)	37
FIGURE 4-13. COMPARISON OF TEMPORARY EROSION AFTER INSTALLATION IN JUNE 2020 (TOP PHOTO) VERSUS ITS CONDITION IN NOVEMBER 2022 (BOTTOM PHOTO)	38
FIGURE 5-1. REGIONAL VIEW OF BATHYMETRY, PUNALU‘U BEACH PARK (ELEVATIONS IN FT RELATIVE TO MSL)	39
FIGURE 5-2. WIND ROSE FOR HONOLULU AIRPORT (1949 TO 1995)	40
FIGURE 5-3. GLOBAL SATELLITE SEA LEVEL RISE VARIABILITY FROM 1993 TO 2022 (SWEET ET AL. 2022)	43
FIGURE 5-4. MEAN SEA LEVEL TREND, MOKU O LO‘E, STATION 1612480, 1957 TO PRESENT (NOAA, 2023)	43
FIGURE 5-5. NOAA 2022 SEA LEVEL RISE PROJECTIONS FOR MOKU O LO‘E ISLAND WITH THRESHOLDS OF +1.6 AND +3.2 FT.	44
FIGURE 5-6. DAILY MAXIMUM MEASURED TIDES AT HONOLULU HARBOR AND CORRESPONDING PREDICTED TIDES AND SEA LEVEL ANOMALY (FEB 1 - OCT 1, 2017)	46
FIGURE 5-7. PREDICTED AND MEASURED TIDES AT HONOLULU HARBOR (DEC 24-26, 2019)	47
FIGURE 5-8. HAWAI‘I DOMINANT SWELL REGIMES	49
FIGURE 5-9. LOCATION OF CDIP BUOYS USED FOR THIS STUDY IN RELATION TO PUNALU‘U BEACH PARK	50
FIGURE 5-10. CDIP BUOY 106 (WAIMEA BAY) WAVE HEIGHT ROSE FROM DECEMBER 2001 TO JUNE 2023	51
FIGURE 5-11. CDIP BUOY 106 (WAIMEA BAY) WAVE PERIOD ROSE FROM DECEMBER 2001 TO JUNE 2023	51

FIGURE 5-12. CDIP BUOY 098 (MOKAPU POINT) WAVE HEIGHT ROSE FROM AUGUST 2000 TO OCTOBER 2023	52
FIGURE 5-13. CDIP BUOY 098 (MOKAPU POINT) WAVE PERIOD ROSE FROM AUGUST 2000 TO OCTOBER 2023	52
FIGURE 5-14. NORTHERLY SWELL SIGNIFICANT WAVE HEIGHT VS. RETURN PERIOD, CDIP 106 (WAIMEA BAY BUOY), DECEMBER 2001 TO JUNE 2023.....	54
FIGURE 5-15. TRADEWIND WAVES SIGNIFICANT WAVE HEIGHT VS. RETURN PERIOD, CDIP 098 (MOKAPU POINT BUOY), AUGUST 2000 TO OCTOBER 2023.....	55
FIGURE 6-1. SWAN UNSTRUCTURED MESH	59
FIGURE 6-2. SWAN MODELED SIGNIFICANT WAVE HEIGHT FOR PREVAILING NORTH SWELL (TOP) AND TRADEWIND WAVES (BOTTOM)	61
FIGURE 6-3. SWAN MODELED SIGNIFICANT WAVE HEIGHT FOR AN ANNUAL NORTH SWELL (TOP) AND TRADEWIND WAVES (BOTTOM)	63
FIGURE 6-4. SWAN MODELED SIGNIFICANT WAVE HEIGHT FOR A 50-YR NORTH SWELL (TOP) AND TRADEWIND WAVES (BOTTOM)	65
FIGURE 6-5. XBEACH-NH MODEL DOMAIN EXTENT	66
FIGURE 6-6. WATER SURFACE SNAPSHOT FROM XBEACH-NH MODEL FOR A PREVAILING NORTH SWELL.....	68
FIGURE 6-7. SIGNIFICANT WAVE HEIGHT FROM XBEACH-NH MODEL FOR A PREVAILING NORTH SWELL.....	68
FIGURE 6-8. DEPTH-AVERAGED FLOW VELOCITY FROM XBEACH-NH FOR A PREVAILING NORTH SWELL.....	69
FIGURE 6-9. WATER SURFACE SNAPSHOT FROM XBEACH-NH MODEL FOR A PREVAILING TRADEWIND WAVES	70
FIGURE 6-10. SIGNIFICANT WAVE HEIGHT FROM XBEACH-NH MODEL FOR A PREVAILING TRADEWIND WAVES	71
FIGURE 6-11. DEPTH-AVERAGED FLOW VELOCITY FROM XBEACH-NH FOR A PREVAILING TRADEWIND WAVES	71
FIGURE 6-12. SIGNIFICANT WAVE HEIGHT FROM XBEACH-NH MODEL FOR ANNUAL TRADEWIND WAVES UNDER EXISTING SEA LEVEL	72
FIGURE 6-13. SIGNIFICANT WAVE HEIGHT FROM XBEACH-NH MODEL FOR ANNUAL TRADEWIND WAVES WITH +1.6FT OF SLR	73
FIGURE 6-14. SIGNIFICANT WAVE HEIGHT FROM XBEACH-NH MODEL FOR ANNUAL TRADEWIND WAVES WITH +3.2FT OF SLR	73
FIGURE 6-15. SIGNIFICANT WAVE HEIGHT FROM XBEACH-NH MODEL FOR 50-YR TRADEWIND WAVES UNDER EXISTING SEA LEVEL	74
FIGURE 6-16. SIGNIFICANT WAVE HEIGHT FROM XBEACH-NH MODEL FOR 50-YR TRADEWIND WAVES WITH +1.6FT OF SLR	75
FIGURE 6-17. SIGNIFICANT WAVE HEIGHT FROM XBEACH-NH MODEL FOR 50-YR TRADEWIND WAVES WITH +3.2FT OF SLR	75
FIGURE 7-1. BEACH SAND SAMPLE LOCATIONS	81
FIGURE 7-2. GRAIN SIZE DISTRIBUTIONS, BEACH SAND SAMPLES.....	81
FIGURE 7-3. JET PROBE AND PUSH CORE LOCATIONS AT OFFSHORE SAND DEPOSIT.....	83
FIGURE 7-4. TYPICAL VIEW OF INTERIOR OF SAND DEPOSIT	84
FIGURE 7-5. INSHORE BOUNDARY OF SEAGRASS AND SAND DEPOSIT	84
FIGURE 7-6. GRAIN SIZE DISTRIBUTIONS OF OFFSHORE SAND SAMPLES.....	85

FIGURE 7-7. COMPARISON OF GRAIN SIZE DISTRIBUTIONS FOR PUNALU‘U BEACH COMPOSITE AND OFFSHORE COMPOSITE SAMPLES	86
FIGURE 7-8. DEAN’S OVERFILL RATIO EXPRESSED AS A SINGLE CURVE (BODGE, 2004).....	87
FIGURE 7-9. 2100Q PORTABLE TURBIDIMETER	89
FIGURE 7-10. LASER NEPHELOMETER OPTICAL CONFIGURATION (SADAR, CASON AND ENGELHARDT 2009)	89
FIGURE 7-11. SEDIMENT TURBIDITY RESULTS FOR SAND SAMPLES TAKEN ON THE SHORELINE OF PUNALU‘U BEACH PARK	90
FIGURE 7-12. SEDIMENT TURBIDITY RESULTS FOR SAND SAMPLES TAKEN AT THE OFFSHORE SAND SITE AT PUNALU‘U.....	91
FIGURE 7-13. COMPARATIVE SEDIMENT TURBIDITY RESULTS FOR THE OFFSHORE AND BEACH COMPOSITE SAMPLES	91
FIGURE 8-1. EDDY PUMP 6” SUBDREDGE ROV (SOURCE: EDDY PUMP).....	93
FIGURE 8-2. SURFACE SUPPLIED AIR DIVER USING A DIVER-OPERATED DREDGE	94
FIGURE 8-3. DREDGE SLED IN USE (SOURCE: EDDY PUMP)	95
FIGURE 8-4. EXAMPLE: ANCHOR AND ANCHOR FLOAT USED IN THE 2012 WAIKIKI BEACH MAINTENANCE PROJECT.....	96
FIGURE 8-5. CLAMSHELL DREDGE WITH ENVIRONMENTAL BUCKET	97
FIGURE 8-6. ENVIRONMENTAL CLAMSHELL BUCKET.....	97
FIGURE 8-7. HOPPER BARGE	98
FIGURE 8-8. SCHEMATIC OF SAND PUMPING ARRANGEMENT (AMERICAN MARINE, 2007).....	100
FIGURE 8-9. HEALY TIBBITTS CRANE BARGE USED IN THE 2012 WAIKIKI BEACH MAINTENANCE PROJECT	100
FIGURE 8-10. PROPOSED SAND RECOVERY PLAN USING HYDRAULIC SUCTION DREDGE.....	101
FIGURE 9-1. VICINITY MAP SHOWING LOCATIONS OF WATER SAMPLING STATIONS, SAND DONOR AREA, SAND REPLENISHMENT AREA, AND DIVER SWIM TRACKS	102
FIGURE 9-2. REPRESENTATIVE IMAGES OF THE CENTER AND PERIMETER OF THE OFFSHORE SAND DEPOSIT	106
FIGURE 9-3. REPRESENTATIVE IMAGES OF SEAGRASS AT THE PERIMETER OF THE OFFSHORE SAND DEPOSIT	107
FIGURE 9-4. REPRESENTATIVE IMAGES OF THE SEAFLOOR AT PUNALU‘U BEACH PARK.	108
FIGURE 9-5. REPRESENTATIVE IMAGES OF MACROALGAE AT PUNALU‘U BEACH PARK.	109
FIGURE 9-6. REPRESENTATIVE IMAGES OF CORALS AT PUNALU‘U BEACH PARK.	110
FIGURE 10-1. BEACH NOURISHMENT CONCEPT PLAN VIEW	113
FIGURE 10-2. TYPICAL SECTION VIEW OF BEACH NOURISHMENT CONCEPT	113
FIGURE 10-3. BEACH NOURISHMENT WITH BURIED REVETMENT CONCEPT PLAN VIEW.....	116
FIGURE 10-4. TYPICAL SECTION VIEW OF BEACH NOURISHMENT WITH BURIED REVETMENT CONCEPT	116
FIGURE 10-5. SECTION VIEW OF BURIED REVETMENT	117
FIGURE 10-6. STABILIZED POCKET BEACHES CONCEPT PLAN VIEW	120
FIGURE 10-7. STABILIZED POCKET BEACHES - STRUCTURE TYPICAL SECTION VIEWS (STEM AND HEAD SECTIONS)	120
FIGURE 10-8. PARTIALLY STABILIZED POCKET BEACHES CONCEPT PLAN VIEW	123
FIGURE 10-9. PARTIALLY STABILIZED POCKET BEACHES - STRUCTURE TYPICAL SECTION VIEWS (STEM AND HEAD SECTIONS).....	123
FIGURE 10-10. HYBRID STABILIZED POCKET BEACHES CONCEPT PLAN VIEW	126

FIGURE 10-11. HYBRID STABILIZED POCKET BEACHES - STRUCTURE TYPICAL SECTION VIEWS (STEM AND HEAD SECTIONS) 126

FIGURE 11-1. MAXIMUM MODELED FLOOD DEPTH FOR EXISTING CONDITIONS FOR EXISTING SEA LEVEL DURING A PREVAILING WAVE EVENT 129

FIGURE 11-2. MAXIMUM MODELED FLOOD DEPTH FOR THE BEACH NOURISHMENT CONCEPT FOR EXISTING SEA LEVEL DURING A PREVAILING WAVE EVENT 130

FIGURE 11-3. MAXIMUM MODELED FLOOD DEPTH FOR STABILIZED POCKET BEACHES CONCEPT FOR EXISTING SEA LEVEL DURING A PREVAILING WAVE EVENT 131

FIGURE 11-4. MAXIMUM MODELED FLOOD DEPTH FOR THE PARTIALLY STABILIZED POCKET BEACHES CONCEPT FOR EXISTING SEA LEVEL DURING A PREVAILING WAVE EVENT 132

FIGURE 11-5. MAXIMUM MODELED FLOOD DEPTH FOR THE HYBRID STABILIZED POCKET BEACHES CONCEPT FOR EXISTING SEA LEVEL DURING A PREVAILING WAVE EVENT 133

FIGURE 11-6. MAXIMUM MODELED FLOOD DEPTH FOR EXISTING CONDITIONS FOR EXISTING SEA LEVEL DURING AN ANNUAL WAVE EVENT 135

FIGURE 11-7. MAXIMUM MODELED FLOOD DEPTH FOR THE BEACH NOURISHMENT CONCEPT FOR EXISTING SEA LEVEL DURING AN ANNUAL WAVE EVENT 136

FIGURE 11-8. MAXIMUM MODELED FLOOD DEPTH FOR STABILIZED POCKET BEACHES CONCEPT FOR EXISTING SEA LEVEL DURING AN ANNUAL WAVE EVENT 137

FIGURE 11-9. MAXIMUM MODELED FLOOD DEPTH FOR THE PARTIALLY STABILIZED POCKET BEACHES CONCEPT FOR EXISTING SEA LEVEL DURING AN ANNUAL WAVE EVENT 138

FIGURE 11-10. MAXIMUM MODELED FLOOD DEPTH FOR THE HYBRID STABILIZED POCKET BEACHES CONCEPT FOR EXISTING SEA LEVEL DURING AN ANNUAL WAVE EVENT 139

FIGURE 11-11. MAXIMUM MODELED FLOOD DEPTH FOR EXISTING CONDITIONS WITH +1.6 FT OF SLR DURING A PREVAILING WAVE EVENT 141

FIGURE 11-12. MAXIMUM MODELED FLOOD DEPTH FOR THE REVETEMENT CONCEPT WITH +1.6 FT OF SLR DURING A PREVAILING WAVE EVENT 142

FIGURE 11-13. MAXIMUM MODELED FLOOD DEPTH FOR STABILIZED POCKET BEACHES CONCEPT WITH +1.6 FT OF SLR DURING A PREVAILING WAVE EVENT 143

FIGURE 11-14. MAXIMUM MODELED FLOOD DEPTH FOR THE PARTIALLY STABILIZED POCKET BEACHES CONCEPT WITH +1.6 FT OF SLR DURING A PREVAILING WAVE EVENT 144

FIGURE 11-15. MAXIMUM MODELED FLOOD DEPTH FOR THE HYBRID STABILIZED POCKET BEACHES CONCEPT WITH +1.6 FT OF SLR DURING A PREVAILING WAVE EVENT 145

FIGURE 11-16. MAXIMUM MODELED FLOOD DEPTH FOR EXISTING CONDITIONS WITH +1.6 FT OF SLR DURING AN ANNUAL WAVE EVENT 147

FIGURE 11-17. MAXIMUM MODELED FLOOD DEPTH FOR THE REVETMENT CONCEPT WITH +1.6 FT OF SLR DURING AN ANNUAL WAVE EVENT 148

FIGURE 11-18. MAXIMUM MODELED FLOOD DEPTH FOR STABILIZED POCKET BEACHES CONCEPT WITH +1.6 FT OF SLR DURING AN ANNUAL WAVE EVENT 149

FIGURE 11-19. MAXIMUM MODELED FLOOD DEPTH FOR THE PARTIALLY STABILIZED POCKET BEACHES CONCEPT WITH +1.6 FT OF SLR DURING AN ANNUAL WAVE EVENT 150

FIGURE 11-20. MAXIMUM MODELED FLOOD DEPTH FOR THE HYBRID STABILIZED POCKET BEACHES CONCEPT WITH +1.6 FT OF SLR DURING AN ANNUAL WAVE EVENT 151

FIGURE 11-21. MAXIMUM MODELED FLOOD DEPTH FOR EXISTING CONDITIONS WITH +3.2 FT OF SLR DURING A PREVAILING WAVE EVENT 153

FIGURE 11-22. MAXIMUM MODELED FLOOD DEPTH FOR THE REVETMENT CONCEPT WITH +3.2 FT OF SLR DURING A PREVAILING WAVE EVENT 154

FIGURE 11-23. MAXIMUM MODELED FLOOD DEPTH FOR THE STABILIZED POCKET BEACHES
CONCEPT WITH +3.2 FT OF SLR DURING A PREVAILING WAVE EVENT 155

FIGURE 11-24. MAXIMUM MODELED FLOOD DEPTH FOR THE PARTIALLY STABILIZED POCKET
BEACHES CONCEPT WITH +3.2 FT OF SLR DURING A PREVAILING WAVE EVENT 156

FIGURE 11-25. MAXIMUM MODELED FLOOD DEPTH FOR THE HYBRID STABILIZED POCKET BEACHES
CONCEPT WITH +3.2 FT OF SLR DURING A PREVAILING WAVE EVENT 157

FIGURE 11-26. MAXIMUM MODELED FLOOD DEPTH FOR EXISTING CONDITIONS WITH +3.2 FT OF
SLR DURING AN ANNUAL WAVE EVENT 159

FIGURE 11-27. MAXIMUM MODELED FLOOD DEPTH FOR THE REVETMENT CONCEPT WITH +3.2 FT OF
SLR DURING AN ANNUAL WAVE EVENT 160

FIGURE 11-28. MAXIMUM MODELED FLOOD DEPTH FOR THE STABILIZED POCKET BEACHES
CONCEPT WITH +3.2 FT OF SLR DURING AN ANNUAL WAVE EVENT 161

FIGURE 11-29. MAXIMUM MODELED FLOOD DEPTH FOR THE PARTIALLY STABILIZED POCKET
BEACHES CONCEPT WITH +3.2 FT OF SLR DURING AN ANNUAL WAVE EVENT 162

FIGURE 11-30. MAXIMUM MODELED FLOOD DEPTH FOR THE HYBRID STABILIZED POCKET BEACHES
CONCEPT WITH +3.2 FT OF SLR DURING AN ANNUAL WAVE EVENT 163

LIST OF TABLES

TABLE 5-1. TIDAL DATUMS AT MOKU O LO‘E, STATION 1612480 (1983-2001 EPOCH)..... 42

TABLE 5-2. NOAA 2022 SEA LEVEL PROJECTION TIMING WITH +1.6 AND +3.2 FT OF SLR..... 45

TABLE 5-3. PEAK RECORDED TIDE LEVELS AT HONOLULU HARBOR (2017 TO PRESENT) 46

TABLE 5-4. NORTHERLY SWELL SIGNIFICANT WAVE HEIGHT VS. RETURN PERIOD, CDIP 106
(WAIMEA BAY BUOY), DECEMBER 2001 TO JUNE 2023..... 54

TABLE 5-5. TOP 10 NORTHERLY SWELL EVENTS RECORDED AT CDIP 106 (WAIMEA BAY BUOY),
DECEMBER 2001 TO JUNE 2023 54

TABLE 5-6. TRADEWIND WAVES SIGNIFICANT WAVE HEIGHT VS. RETURN PERIOD, CDIP 098
(MOKAPU POINT BUOY), AUGUST 2000 TO OCTOBER 2023..... 55

TABLE 5-7. TOP 10 TRADEWIND WAVE EVENTS RECORDED AT CDIP 098 (MOKAPU POINT BUOY),
AUGUST 2000 TO OCTOBER 2023 56

TABLE 6-1. DESIGN WATER LEVEL COMPONENTS RELATIVE TO MSL FOR NUMERICAL MODELING 58

TABLE 6-2. MODELED PREVAILING WAVE CASES (INPUTS TO SWAN MODEL)..... 60

TABLE 6-3. MODELED ANNUAL WAVE CASES (INPUTS TO SWAN MODEL) 62

TABLE 6-4. MODELED 50-YR WAVE CASES (INPUTS TO SWAN MODEL) 64

TABLE 6-5. PREVAILING WAVE RUNUP RESULTS ON BEACH FACE WITH 1:8 SLOPE..... 76

TABLE 6-6. ANNUAL WAVE RUNUP RESULTS ON BEACH FACE WITH 1:8 SLOPE 77

TABLE 6-7. PREVAILING WAVE RUNUP RESULTS ON RUBBLEMOUND STRUCTURE WITH 1:1.5 SLOPE
..... 77

TABLE 6-8. ANNUAL WAVE RUNUP RESULTS ON RUBBLEMOUND STRUCTURE WITH 1:1.5 SLOPE ... 77

TABLE 7-1. DLNR SAND COMPOSITION AND QUALITY REQUIREMENTS FOR BEACH NOURISHMENT 79

TABLE 7-2. SORTING VALUE DESCRIPTIONS 80

TABLE 7-3. PUNALU‘U OFFSHORE SAND SAMPLE SUMMARY 85

TABLE 10-1. BEACH NOURISHMENT DRY BEACH AND BACKSHORE PARAMETERS 112

TABLE 10-2. ALTERNATIVE 1 ROM COST BREAKDOWN 114

TABLE 10-3. BEACH NOURISHMENT WITH BURIED REVETMENT DRY BEACH AND BACKSHORE
PARAMETERS 115



TABLE 10-4. ALTERNATIVE 2 ROM COST BREAKDOWN	117
TABLE 10-5. STABILIZING POCKET BEACHES DRY BEACH AND BACKSHORE PARAMETERS	119
TABLE 10-6. ALTERNATIVE 3 ROM COST BREAKDOWN	121
TABLE 10-7. PARTIALLY STABILIZING POCKET BEACHES DRY BEACH AND BACKSHORE PARAMETERS	122
TABLE 10-8. ALTERNATIVE 4 ROM COST BREAKDOWN	124
TABLE 10-9. HYBRID STABILIZING POCKET BEACHES DRY BEACH AND BACKSHORE PARAMETERS	125
TABLE 10-10. ALTERNATIVE 5 ROM COST BREAKDOWN	127
TABLE 11-1. SUMMARY OF MODELED FLOODING RESULTS FOR ANNUAL WAVES FOR EXISTING SEA LEVEL	128
TABLE 11-2. SUMMARY OF MODELED FLOODING RESULTS FOR ANNUAL WAVES FOR EXISTING SEA LEVEL	134
TABLE 11-3. SUMMARY OF MODELED FLOODING RESULTS FOR PREVAILING WAVES WITH 1.6 FT OF SLR	140
TABLE 11-4. SUMMARY OF MODELED FLOODING RESULTS FOR ANNUAL WAVES WITH 1.6 FT OF SLR	146
TABLE 11-5. SUMMARY OF MODELED FLOODING RESULTS FOR PREVAILING WAVES WITH 3.2 FT OF SLR	152
TABLE 11-6. SUMMARY OF MODELED FLOODING RESULTS FOR PREVAILING WAVES WITH 3.2 FT OF SLR	158

1. INTRODUCTION

Punalu‘u Beach Park, located on the windward coast of O‘ahu (shown in Figure 1-1), suffers from chronic erosion which is being exacerbated by sea level rise due to climate change. The park grounds, park infrastructure, and Kamehameha Highway are low-lying and occasionally inundated by large storm waves. The park is narrow, with the distance between the edge of highway and shoreline being, on average, between about 25 and 80 ft fronting the beach park. In some areas there is no vegetated buffer between the highway and the beach.

Kamehameha Highway is considered vital infrastructure as it is the only road to communities along northeast O‘ahu. Erosion and wave inundation of the highway and backshore are expected to increase in the future as sea level rises. To help protect Kamehameha Highway from flooding and erosion, improve community resiliency to sea level rise and coastal storms, and provide recreational resources and native habitat, the State of Hawai‘i Department of Land and Natural Resources (DLNR), in cooperation with the State of Hawai‘i Department of Transportation (DOT), O‘ahu Metropolitan Planning Organization (OMPO), and City and County of Honolulu Department of Parks and Recreation (DPR), is conducting this green infrastructure feasibility project to identify potential methods to restore the beach at Punalu‘u, O‘ahu. The project is titled "Planning for Improved Resilience to Coastal Hazards through Green Infrastructure at Punalu‘u, O‘ahu".

Sea Engineering, Inc. (SEI) has been contracted by DLNR to conduct in-depth analyses at Punalu‘u Beach Park and develop conceptual design alternatives to address the problems at the beach park and achieve the project objectives. This report documents the results of the feasibility study and includes sections on existing conditions, historical shoreline trends, oceanographic design criteria, offshore sand source investigations, offshore sand recovery methods, marine resources, and concept design alternatives along with detailed numerical modeling of flooding for each concept alternative. It should be noted that this study does not include the costs and assessment of a do-nothing option at the beach park.

Key findings from this study include the following:

- The shoreline at Punalu‘u Beach Park is chronically eroding with historical erosion rates between -2.0 and -3.0 ft/yr (1988-2022). These erosion rates are expected to increase with rising sea levels as more wave energy reaches the shoreline.
- A broad shallow fringing reef protects the shoreline from the highly energetic offshore waves typical for this coastline. As sea level rises, the effectiveness of the reef at reducing waves decreases and backshore inundation increases drastically with both higher water levels and waves at the shoreline. This is shown through numerical modeling discussed in Section 11.
- A suitable offshore sand source exists about 2,000 ft offshore of Punalu‘u Beach Park with sand characteristics that match well with the existing beach sand.
- The most viable method to recover the sand and transport it to shore is to use a hydraulic suction pump deployed off a barge and pump the sand to shore through a temporary

pipeline. Current regulation requires that the sand be dewatered prior to placement on the beach.

- While the source is reasonably close to shore, the windward coast of O‘ahu is one of the most energetic wave environments in Hawai‘i which makes the sand recovery challenging. Because of the challenges and high cost to recover sand it is recommended that stabilizing structures (particularly headland type structures) be used in conjunction with beach nourishment to prevent the need for re-nourishment to maintain the beach.
- Five (5) concept beach alternatives are proposed for Punalu‘u Beach Park along with ROM cost estimates. These concepts are considered nature-based or hybrid nature-based solution and include:
 - Alternative 1 – Beach Nourishment
 - **ROM Cost: \$14,835,000**
 - Alternative 2 – Beach Nourishment with Buried Revetment
 - **ROM Cost: \$22,396,00**
 - Alternative 3 – Stabilized Pocket Beaches
 - **ROM Cost: \$32,910,000**
 - Alternative 4 – Partially Stabilized Pocket Beaches
 - **ROM Cost: \$28,539,000**
 - Alternative 5 – Hybrid Stabilized Pocket Beaches
 - **ROM Cost: \$31,210,000**
- All concepts were modeled under a combination of existing/future sea level and wave conditions. The modeling results show that the alternatives reduce the expected wave inundation at the beach park compared to existing conditions. For the +3.2 ft SLR case, all alternative simulations show no inundation of the backshore park area and highway during prevailing waves compared to extensive induction for existing topography. With annual waves under the same SLR case, flooding of the backshore and highway is reduced from total inundation for existing topography to moderate/extensive inundation of the southern portion of the park and highway for all alternatives.

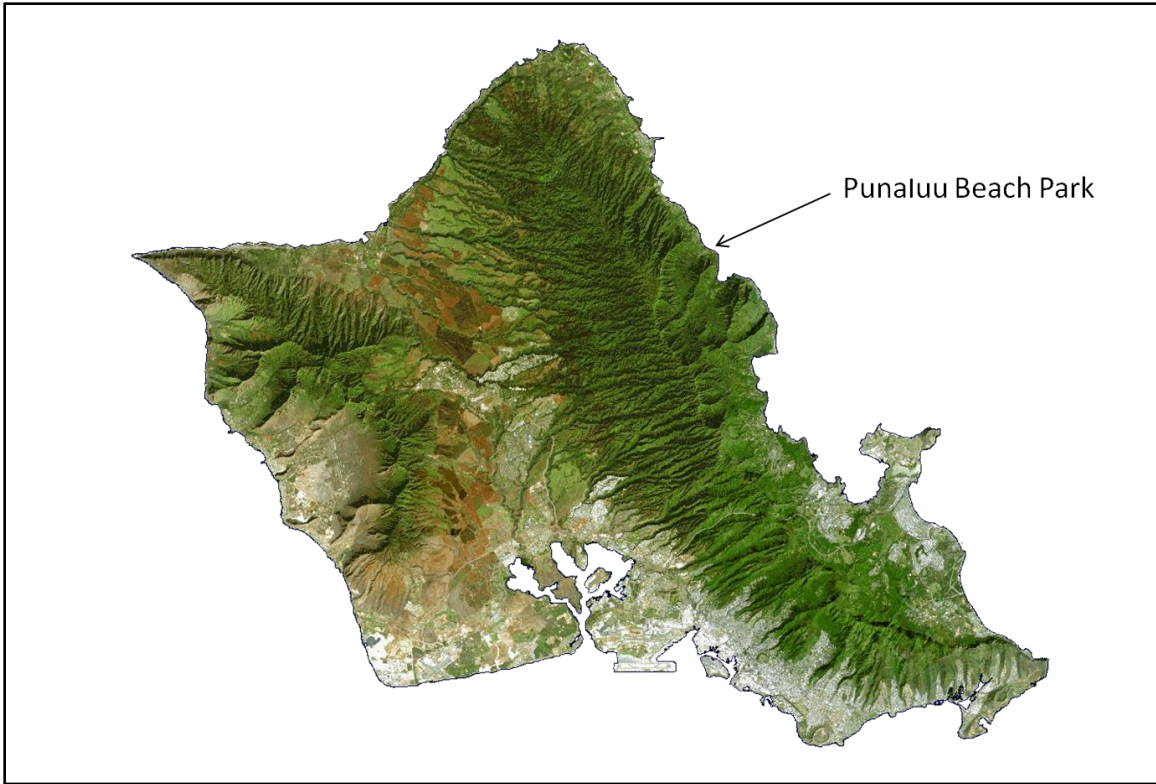


Figure 1-1. Punalu'u Beach Park location map

2. COASTAL GREEN INFRASTRUCTURE

In general terms, coastal green infrastructure uses natural features and/or engineering solutions that mimic natural processes to minimize coastal flooding and erosion. Similar terminology may include, but is not limited to, nature-based solutions, natural infrastructure, living shorelines, and natural and nature-based features (NNBF). The U.S. Department of Transportation Federal Highway Administration (FHWA) report titled “*Nature-Based Solutions for Coastal Highway Resilience*” by Webb, et. al. 2019 provides background information and guidelines for various nature-based solutions and is a useful reference for preliminary selection of possible nature-based solutions for project purpose and site/environmental conditions. The FHWA report states that “A nature-based solution may consist entirely of natural elements (e.g., vegetation, beach, dune) or some combination of natural elements, constructed natural elements, and traditional coastal structures (e.g., sill, breakwater, revetment, seawall).” The latter is termed a *hybrid approach* and is typically implemented in environments with more exposure to waves and/or where a higher order of resilience is desired. Figure 2-1 illustrates the application of varying degrees of nature-based solutions for the environmental setting, exposure, and resilience needs of the project. With respect to coastal highway resilience, the lower right bottom panel in Figure 2-1 would be considered to the Punalu‘u project site due to the open coast wave exposure, low-lying backshore, and critical highway infrastructure.

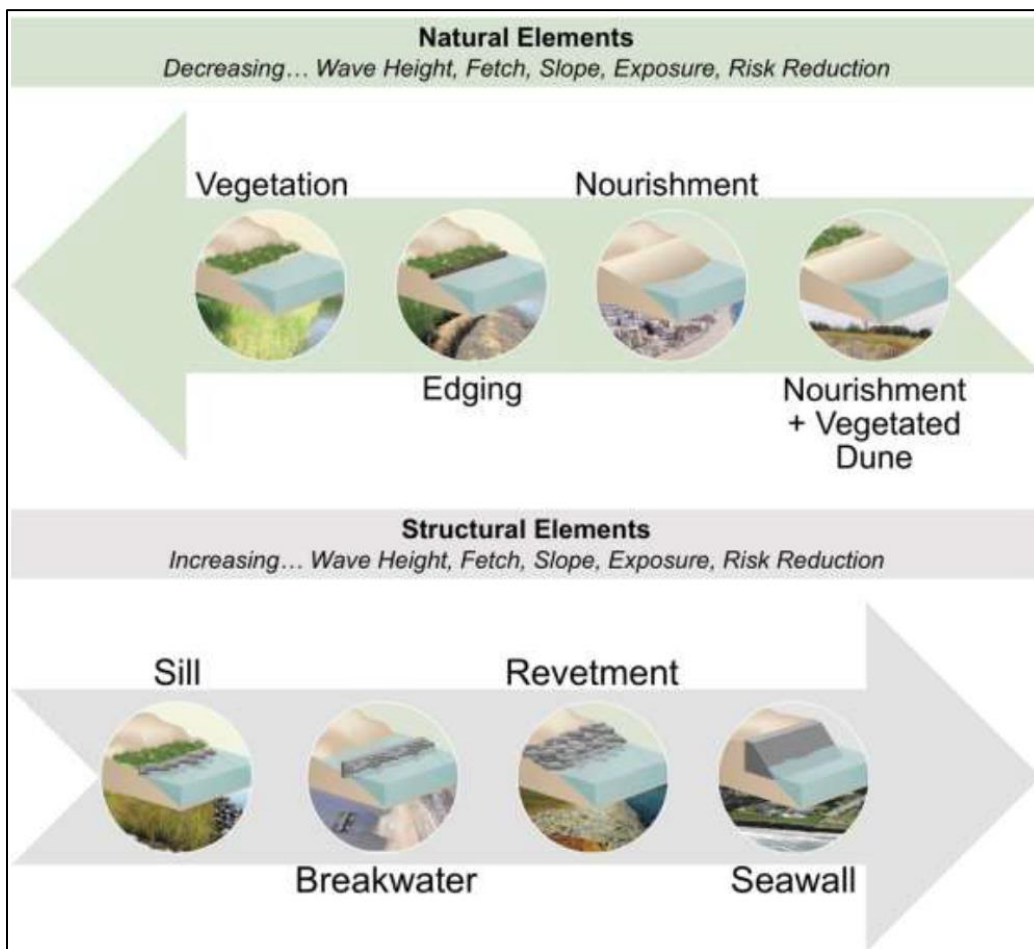


Figure 2-1. Varying degrees of nature-based solutions (Webb, et. al., 2019)

The following sections describe various nature-based solutions which are evaluated to achieve the goals and objectives at Punalu'u Beach Park by restoring the beach to protect Kamehameha Highway from flooding and erosion, improve community resiliency to sea level rise and coastal storms, and provide recreational resources and native habitat.

2.1 Beach Nourishment

Constructing or nourishing a protective beach by placing suitable sand in an appropriately designed manner along a shoreline can be an effective and attractive means of mitigating beach loss, protecting against shoreline recession, protecting the backshore area, and providing for recreational and aesthetic enjoyment. Beaches dissipate incoming wave energy, reducing wave runup, overtopping, and backshore flooding. However, beaches are dynamic coastal landforms, and it is necessary to control the beach shape and size in order to maintain the necessary backshore protection. An example of a recent Hawai'i beach nourishment project is the Waikiki Beach Maintenance project completed by DLNR in 2012 and again in 2021 (Figure 2-2). Approximately 25,000 cy of sand was recovered from nearshore sand deposits off Waikiki Beach and used to nourish 1,700 linear ft of beach. This project widened the beach by about 40 ft. However, Waikiki Beach is chronically eroding and receding, so this is only a temporary improvement, and would have to be repeated every 10 years or so in order to maintain the beach.

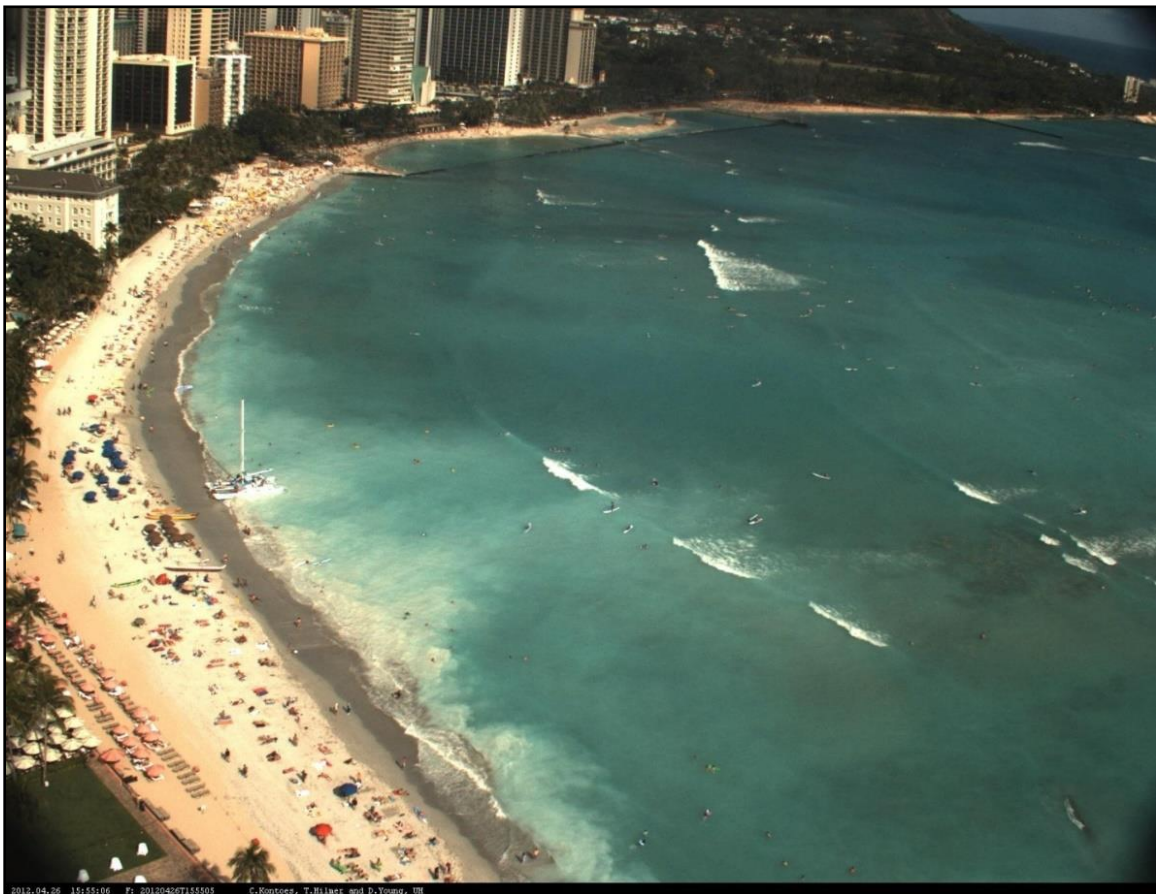


Figure 2-2. Waikiki Beach nourishment (24 hours post-construction)

2.2 Dunes, Vegetation, and Shoreline Berms

On exposed ocean coasts subject to significant wave energy, vegetation alone is typically not sufficient to resist high energy wave-induced erosion. While a strong vegetation root system can slow down the erosion rate and the vegetation itself can help dissipate overtopping waves, in most cases, vegetation is quickly overcome by the erosional forces. However, when used in conjunction with dune systems and beach nourishment combined with erosion control/shore protection methods, vegetation can function to help stabilize low-lying ground behind the primary shore protection structure.

Restoration and maintenance of backshore dunes, and the creation of sand or earthen berms, to function as a levee to block water level rise and wave runup from inundating the backshore can function as a viable solution for flood protection. Beach backshore and upland areas, including storm berms and dunes, are often naturally colonized by specialized vegetation that can help to stabilize the sand. Low-growing native vegetation such as grass (Akiaki), Beach Morning glory (Pohuehue), and Akulikuli can both attract sand and act as a protective mat (Hawai‘i Dune Restoration Manual, 2022). Higher covers such as Naupaka and Pohinahina can offer substantial sand stabilization and help control foot traffic. Although thick Naupaka can offer some resistance to wave action, the primary value for shoreline vegetation is in attracting and protecting sand behind the active beach face as a reserve for times of erosion. Trees such as Naio, Milo, or Beach Heliotrope can provide shade, and their roots can help hold sand in place. Figure 2-3 illustrates active dune stabilization with native vegetation at Kaanapali Beach on Maui.



Figure 2-3. Berm stabilization with native vegetation

2.3 Beach Nourishment with Buried Revetment

One hybrid nature-based solution for beach restoration is to combine beach nourishment and backshore dune, or vegetated berm, enhancement with a buried revetment structure in the backshore. This hybrid approach would provide a risk-reduction benefit for critical backshore infrastructure by protecting the backshore from shoreline retreat while the beach and dune system can function to provide a natural buffer from sea level rise and storms. This approach has been used previously in Hawai'i for the Wailuku-Kahului Wastewater Reclamation Facility on the island of Maui. This facility is considered critical infrastructure, and the county opted for a nature-based approach to protect the backshore (Webb et. al., 2019). Recent aerial imagery from this project shows that the beach and vegetated dune are still in place today and the buried revetment has not yet become exposed. Figure 2-4 shows a sample cross-section of a buried revetment with dune restoration.

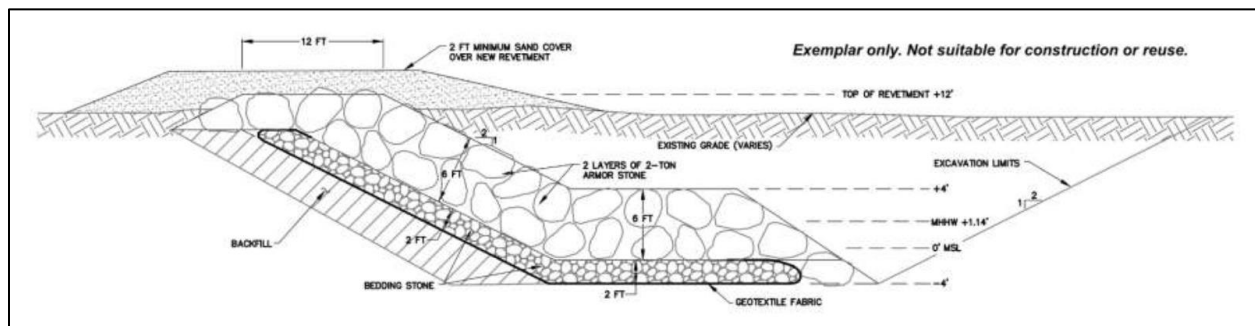


Figure 2-4. Sample cross-section of buried revetment and dune restoration (Boudreau et. al., 2018).

2.4 Beach Nourishment with Stabilization

On chronically eroding shorelines which would necessitate extensive regular nourishment in order to maintain the beach, and for which periodic sand nourishment alone is not cost effective, or a sustainable source of suitable sand is not available, structures can be used to stabilize the beach fill and reduce significantly the need for re-nourishment activities.

Stabilizing structures can be designed to prevent longshore and offshore transport of sand and limit erosion of an existing beach. Where there is significant sand volume available, and adverse impacts to downdrift shorelines are not a problem, these structures can be used to trap sand and build a protective beach. However, modern coastal engineering practice typically includes a regional perspective that considers the stability of adjacent beaches and shorelines, and thus structure emplacement may also involve beach fill so as to not remove sand from the overall beach system. For a long shoreline reach a groin "field" is typically utilized, with the distance between groins a function of the design wave conditions, the length of the individual groins, and the extent of shoreline re-adjustment desired. A sandy shoreline would also adjust its position between groins so as to align itself parallel to the incident wave crests, possibly resulting in landward recession of the shoreline on the updrift side and accretion on the downdrift side. The use of headland type stabilizing structures, in lieu of traditional straight structures, can create individual beach cells with a predictable stable beach configuration. Headland type structures mimic the effect of natural rock headlands on sandy shorelines and can provide stabilized pocket beach cells.

For the recently constructed Iroquois Point beach nourishment project, the improvement plan was beach nourishment with stabilization, consisting of the construction of nine rock rubblemound T-head (headland type) groin structures, recovery of 95,000 cubic yards of sand from the side of the Pearl Harbor channel, and placement of the sand in the pocket beach cells created by the groins (see Figure 2-5 and Figure 2-6). This is the largest single beach nourishment project ever accomplished in Hawai'i. The design consisted of engineered pocket beach/headland structures ("tuned" T-head groins). Based on numerical modeling of wave approach, the headland structure locations, head lengths, and orientations are designed so that they are tuned to the prevailing incident wave approach. The gap between structure heads produces an arc-shaped shoreline, the location of which is a function of the gap width and orientation. This design methodology, which was based on replicating natural headland pocket beaches, has been shown to result in predictable stable beach configurations.

Porous rock groins can provide marine habitat if installed on disturbed or sandy bottoms. A beach and stabilizing structures do, however, occupy a large marine area and have a large footprint. They are also typically significantly more costly than standalone shoreline armoring.



Figure 2-5. Nine rock headland structures stabilize 4,000 ft of sand beach at Iroquois Point



Figure 2-6. Pocket beach cells at Iroquois Point

2.4.1 Marine Habitat Enhancement

The nearby Iroquois Point beach nourishment and stabilization project illustrates the marine habitat enhancement potential of rock rubblemound structures. The nearshore area fronting the project is marginal marine habitat, due primarily to little bottom relief and complexity and sand scour. The stabilizing structures and sand fill were placed primarily on new sea bottom created by the erosion and recession of the shore, and which did not have established benthic flora and fauna. It was also an area of active sand movement, which resulted in scouring and stress on benthic organisms.

The shoreline stabilization project created new reef fish habitat in the form of boulder groins and sand fill. Approximately 0.4 acres of intertidal boulder habitat and 0.7 acres of shallow subtidal boulder habitat was created. The rock groins provide bare, stable surfaces for recruitment of corals, algae, and invertebrates. In addition, the void space between rocks provides habitat and shelter for cryptic benthic (crabs, shrimps, worms etc.) and sessile organisms (sponges and tunicates) which provide foraging resources for fishes, as well as shelter for juvenile fish. Reef fishes prefer topographically complex reefs, with various size holes and crevices to accommodate different size fish, and the groins provide habitat for many different fish. The sand fill created approximately 1.7 acres of intertidal and 2.9 acres of subtidal stable sand habitat, providing habitat for small worms, crustaceans, and echinoderms, which in turn are foraged by bottom feeding fishes.

The post-construction marine ecosystem monitoring shows that the project has resulted in a significant change in marine species diversity and density. In the general project area (groins and beach cells combined), there has been a 25-fold increase in fish abundance, not counting small baitfish, and a doubling of species richness (number of species). Fish biomass is more than six times greater than prior to construction. The greatest change occurred in the vicinity of the new

habitat created by the rock groin structures. Other changes in the vicinity of the groins includes an increase in crustose coralline algae cover from 1% to 60%, coral cover increase from 0% to 0.6% and macroinvertebrate cover from 1.4% to 6.3%. Coral abundance in the groin vicinity increased from 0 to 16 colonies per 10m², with the most common coral species being *Pocillopora damicornis*. These changes are attributable to the creation of hard, stable habitat for colonization. The wide sand beach also provides sunbathing opportunity for endangered Hawaiian monk seals, who regularly haul out and rest on the beach.

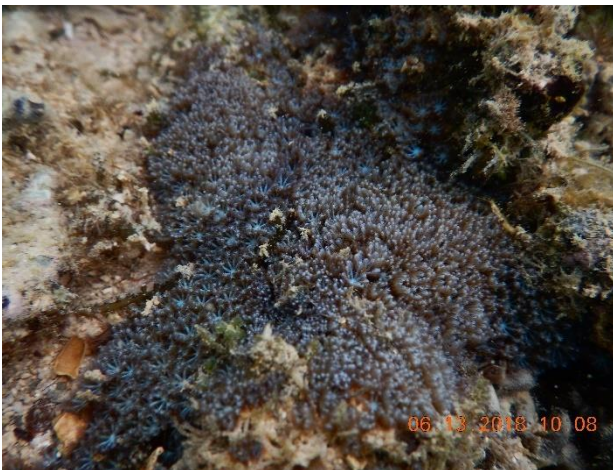
Figure 2-7 illustrates post project increase in marine life, and the photo collage is representative of marine life in the new project habitat. As a Department of the Army permit condition the entire project area has been declared a “No Fishing Zone” so that the fish are protected.



Coral and Sea Cucumber



Convex Crab



Soft Coral



Hard Coral



Hawaiian Sargent Fish



Hawaiian Monk Seal

Figure 2-7. Observed marine life within the Iroquois Point project area

2.5 Natural and Artificial Reefs

Natural reefs in Hawai'i provide protection from wave energy reaching the shoreline through the process of depth-induced wave breaking and friction. As sea levels rise, the effectiveness of the reef at reducing wave energy is expected to diminish if reef growth cannot keep up with sea level rise. Artificial reefs are submerged engineered structures to mimic a natural reef system by providing a platform for a variety of marine habitat. Figure 2-8 illustrates various methods ranging from natural reefs to artificial reef systems to attenuate wave energy. While artificial reefs have the potential to reduce waves, flooding, and coastal erosion in certain regions, their use is still in the research and development phase and further work is still needed for full scale implementation (Bridges et. al., 2021). To-date, offshore reef structures have not been implemented in Hawai'i, and their application is not yet considered practical. Pilot projects have been proposed on Oahu and, in the future, may provide additional insight into these nature-based solutions and how they may perform in regard to shoreline response and flood mitigation in Hawai'i.

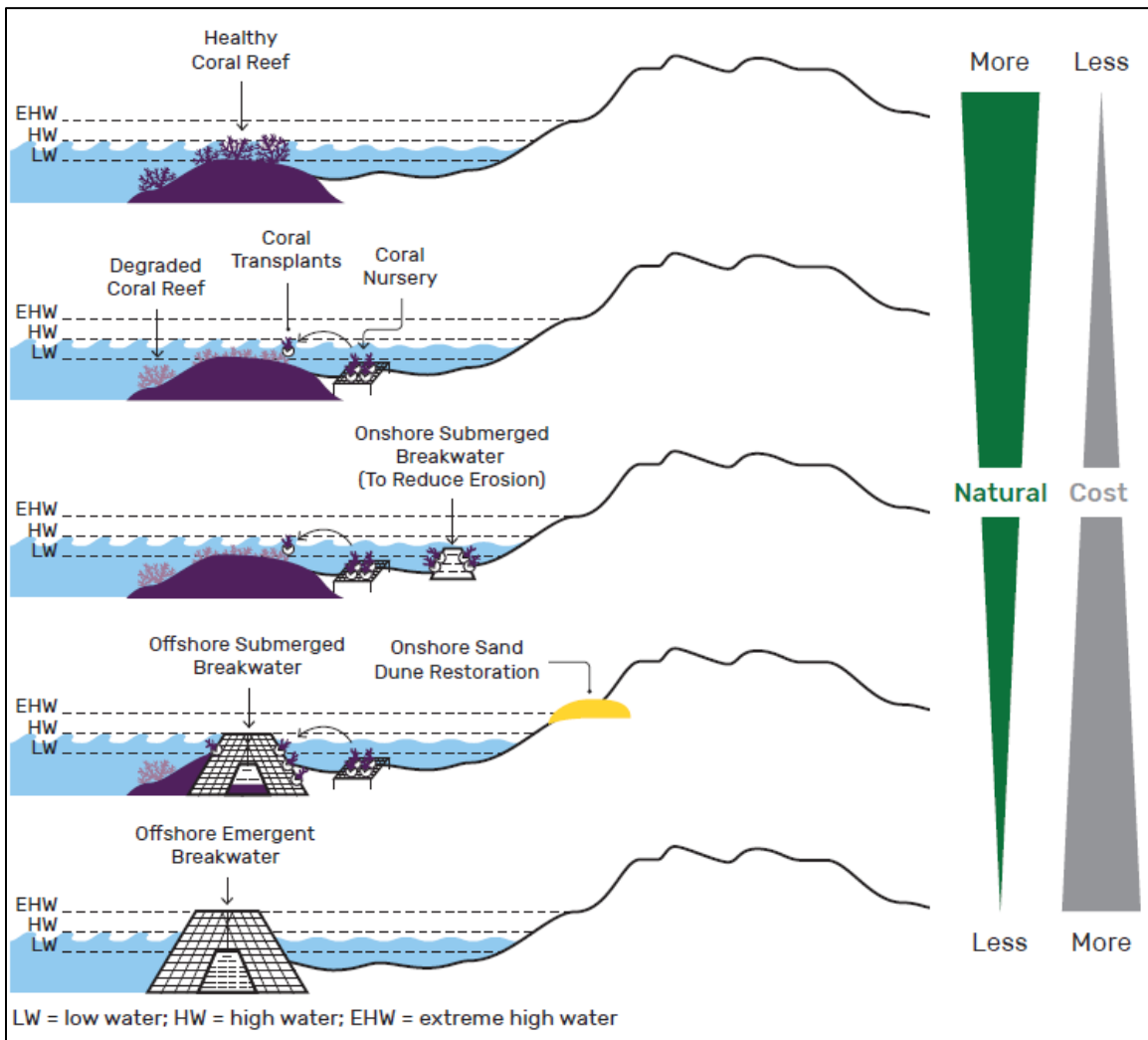


Figure 2-8. Various methods of natural and artificial reefs to reduce wave energy at the shoreline (Bridges et. al., 2021)

2.6 Aquatic Vegetation

Aquatic vegetation may include saltwater marshes, mangroves, and Kelp within nearshore waters to dissipate wave energy, minimize sediment loss, and reduce flooding along a shoreline (see Figure 2-9). Saltwater marshes or wetlands typically consist of a native plant species over a broad flat area such as a mudflat within the intertidal zone. Mangroves have the potential to dissipate wave energy through their dense canopy and provide some shoreline stabilization through their complex root system, however they are an invasive species in Hawai‘i. In general, these approaches generally require large broad areas to be effective at reducing wave energy at the shoreline and are considered feasible only in very sheltered, low-lying embayments and estuaries. Additionally, due to the broad shallow reef flat fronting the Punalu‘u shoreline, the use of aquatic vegetation further offshore such as Kelp, which is not native to Hawai‘i, or seagrass beds is likely not an effective solution due to the hard seafloor substrate. Seagrass beds were observed within the nearshore sand channel at Punalu‘u which provides more suitable substrate for these types of aquatic species.

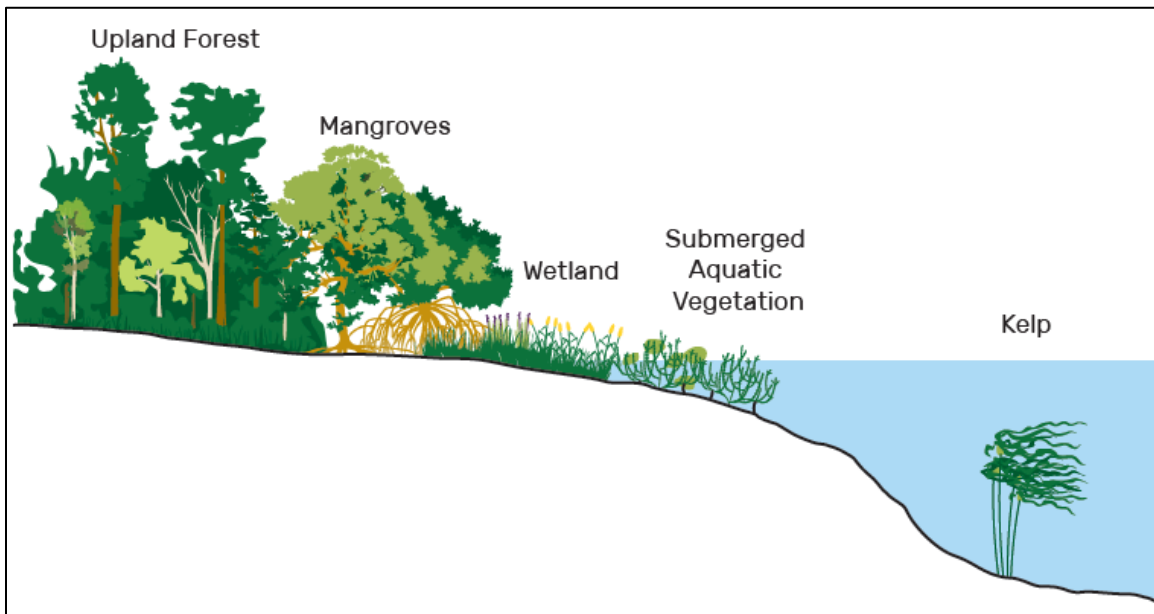


Figure 2-9. Examples of types of aquatic vegetation along a typical shoreline profile (Bridges et. al., 2021)

3. PROJECT SITE DESCRIPTION

3.1 Regional Setting

Punalu‘u Beach Park is approximately 1,500 ft in length, running southeast-northwest along O‘ahu’s windward coastline. The beach park is located within the Ko‘olauloa Moku and Punalu‘u Ahupua‘a. The park is a narrow, 2.8-acre strip of coastal plain located between Kamehameha Highway and the shoreline. A regional view of the park and park features is shown on Figure 3-1. Park width from the edge of the road to the shoreline varies between about 25 and 80 ft with some areas where the edge of highway is immediately adjacent to the sand beach. The northern half of the park is generally wider than the southern half. A comfort station is located in the central region of the park with shower facilities located on the north side of the comfort station and picnic tables are found throughout the park. Two ephemeral streams pass through the park approximately 150 ft south and 300 ft north of the comfort station. The makai edge of highway is immediately adjacent to the sand beach at the stream mouth locations. The park ends about 380 ft south of Wai‘ono Stream.

The Punalu‘u Beach Park shoreline is fronted by a shallow reef that extends nearly 2,000 ft offshore along most of the park. LiDAR and topographic survey data shows that depths measured over the reef are typically 3 to 5 ft below mean sea level (MSL), occasionally reaching 6 ft. Offshore of this reef is the open ocean. The dominant wave energy is produced by the northeast tradewinds and north swell. The shallow reef dissipates a high percentage of the offshore wave energy through broken waves. The waves over the reef are depth limited, meaning that the maximum wave height is a function of water depth. More wave energy can impact the shoreline at higher water levels. At low tide, very little wave energy was observed reaching the shoreline.

North of the park, a deep paleo channel, referred to as the Punalu‘u Sand Channel, extends from the mouth of Wai‘ono Stream and divides the fringing reef. The offshore substrate in this region includes alluvial basalt cobbles and boulders that are likely derived from the nearby streams.



Figure 3-1. Punalu‘u Beach Park site map (regional view)

3.2 Beach Condition and Topographic Survey

SEI completed an aerial drone and topographic survey of the Punalu‘u shoreline on November 22, 2022. Beach profile data was collected at approximately 50 ft spacing along the shoreline using a Real-Time Kinematic (RTK) Global Positioning System (GPS). A drone aerial photographic survey was conducted concurrently with the topographic survey and the photographs collected by the drone were compiled together to produce a detailed aerial mosaic of the Punalu‘u study area. Figure 3-2 shows the beach survey points and contours overlaid on the collected drone mosaic. Beach sand samples were also collected at six (6) locations along the shoreline. These sand samples were analyzed for grain size and turbidity which is discussed in Sections 7.3 and 7.6 of this report.

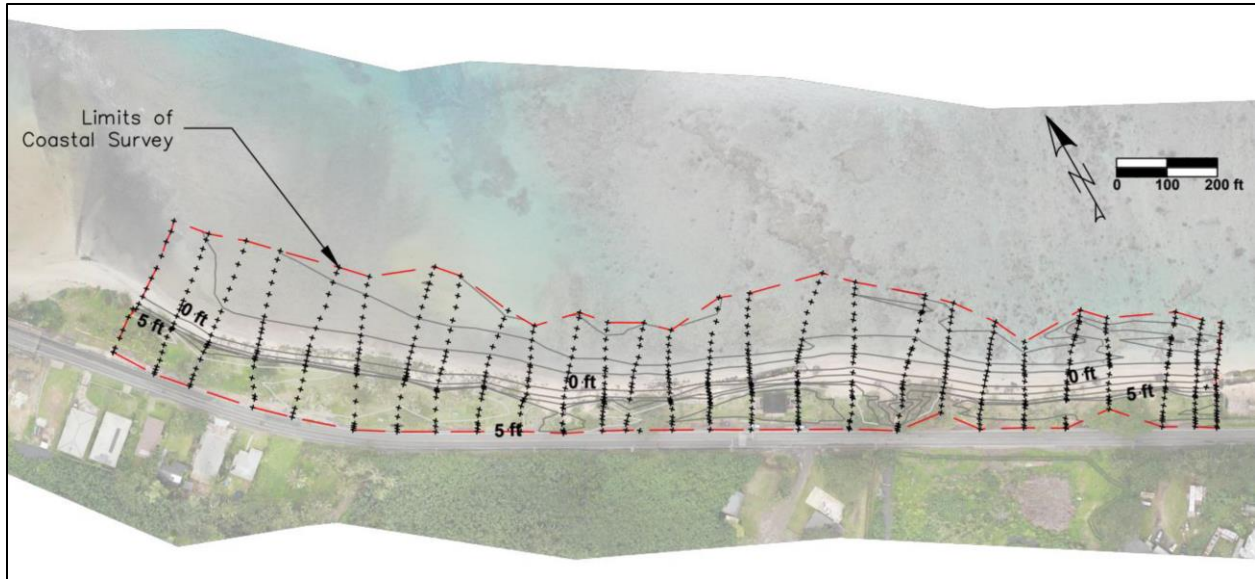


Figure 3-2. SEI topographic survey points and contours overlaid on drone aerial mosaic (survey and drone image date: November 22, 2022)

The following sections describe the shoreline conditions based on the SEI November 22, 2022, survey. The Punalu‘u shoreline can be subdivided into five (5) general segments, including the private properties south of the beach park, southern portion of park, central portion of park, northern portion of park, and north of the beach park to Wai‘ono Stream.

3.2.1 South of Punalu‘u Beach Park

South of Punalu‘u Beach Park, the shoreline fronts eight private parcels which have employed various erosion control measures to protect against chronic beach erosion in this area. Figure 3-3 shows a comparison between April 2018 and November 2022 of some of the erosion control attempts fronting the private homes and the evident beach loss since 2018. These measures may have slowed the land loss due to erosion; however, most are showing signs of failure and the beach is narrow or completely eroded fronting the structures. A wooden fence, shown in Figure 3-4, separates the beach park from these private parcels. A more recent photo from April 2024, shows part of the fence, erosion control measures, and house have been removed from the property to the south (Figure 3-5) since the initial site visit in 2022.



Figure 3-3. Comparison of shoreline south of Punalu'u Beach Park in April 2018 (top photo) and November 2022 (bottom photo)



Figure 3-4. Fence at southern limit of Punalu'u Beach Park (November 2022 photo)



Figure 3-5. View of property to the south of Punalu'u Beach Park (April 2024 photo)

3.2.2 Southern Portion of Park

Figure 3-6 shows an overview of the southern portion of the park. This area generally consists of a low-lying, sandy coastal plain with low-relief historic dune features inland of the erosion scarp. The backshore is grassy and generally level, with typical elevations varying between about +5 and +7 ft MSL. No modern, frontal dune was evident along this portion of the park, indicating that historical dunes were graded flat with or prior to the construction of the park and the seaward edge of any shorefront dune has eroded away. The shoreline has receded past a line of ironwood trees, and now only stumps and roots remain on the beach face (Figure 3-7 and Figure 3-8). One- to two-foot-high erosion scarps are typical along the southern portion of the park, becoming less pronounced, though persistent, toward the comfort station. The coastal substrate in this portion of the park is primarily carbonate sediment with lobes of clay-rich outwash deposits interbedded amongst the sand. The sandy substrate is preferentially eroded, leaving clay layers exposed and overhanging erosion scarps in several areas. This section is particularly susceptible to both erosion and overwash of the waves.

The backshore transitions into hard-packed unvegetated coastal plain amongst the ironwood trees. An ephemeral stream about 150 ft south of the comfort station has a broad mouth with a sandy beach spit formed across much of its width (Figure 3-9). The stream flow has cut a narrow channel through the beach face. The coastal plain is somewhat lower on the south side of the channel. The typical beach width in the southern half of the park was about 40 ft as measured from the scarp to the beach toe, and the beach had a typical slope of about 1V:8H. Beyond the beach toe, the profile quickly changed to a mixture of fossil reef, coral rubble, and sand with typical depths of 2 to 3 ft below MSL.

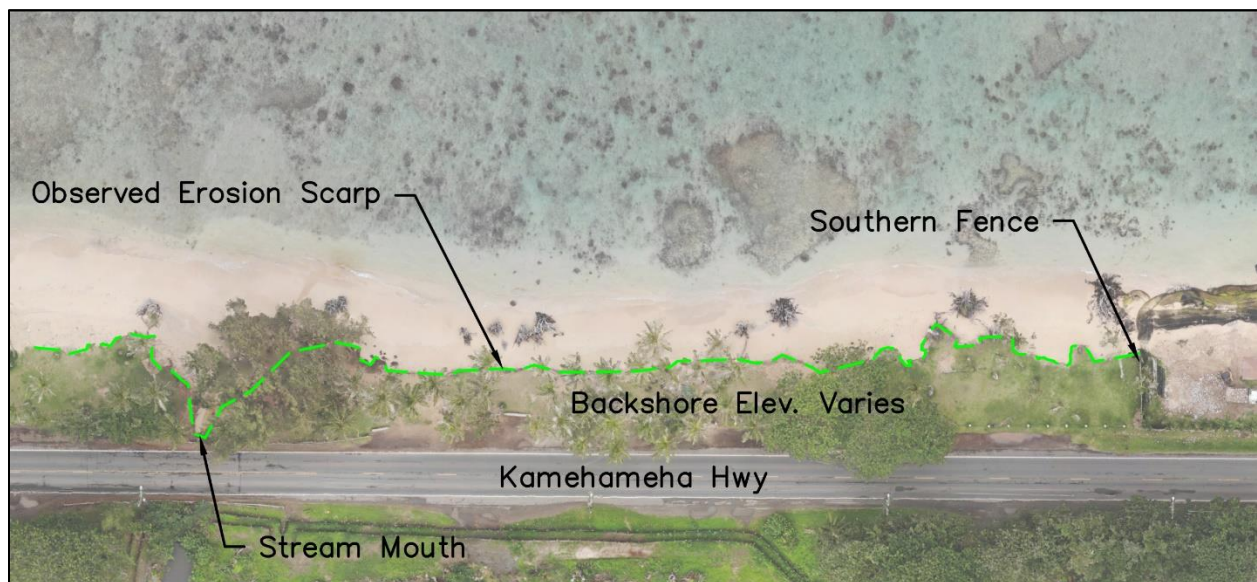


Figure 3-6. Drone mosaic overview of southern area of beach park (November 22, 2022)



Figure 3-7. Southern limit of Punalu'u Beach Park looking northwest (November 2022 photo)



Figure 3-8. Ironwood stump, and roots indicating beach erosion (November 2022 photo)



Figure 3-9. Ephemeral stream flow through beach south of comfort station (November 2022 photo)

3.2.3 Central Portion of Park

The central portion of Punalu‘u Beach Park consists of the area around the comfort station between the streams to the south and north as shown in Figure 3-10. The backshore area around the comfort station has elevations between about +6 and +7 ft MSL. The backshore area around the comfort station has elevations between about +6 and +7 ft MSL, gradually decreasing to +4 to +5 ft msl near the streams. An erosion scarp is evident along a majority of the shoreline in this region except for portions of the temporary erosion protection fronting the comfort station. A minor salient, or seaward protrusion in the shoreline, is noted between the comfort station and the intermittent stream mouth to the south. This salient gradually diminishes just south of the comfort station where the shoreline transitions to being fronted by a line of partially-buried basalt boulders and several concrete pile butts.

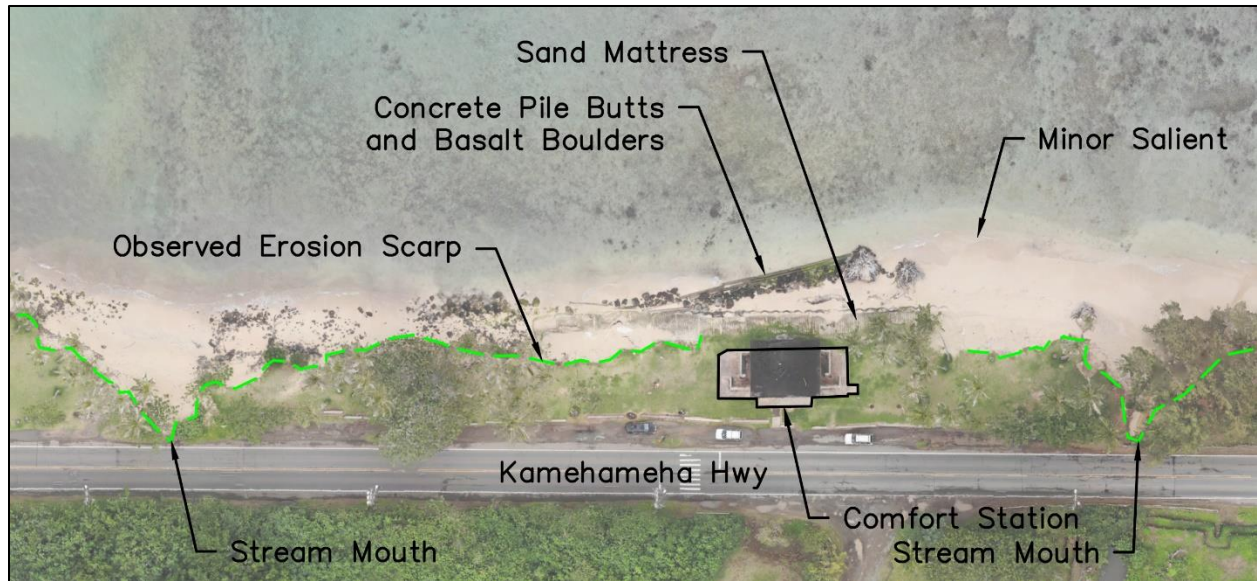


Figure 3-10. Drone mosaic overview of central area of beach park (November 22, 2022)

3.2.4 Northern Portion of the Park

The northern portion of Punalu‘u Beach Park consists of the area between the ephemeral stream (or may be better described as a drainage ditch or outfall) north of the comfort station and the northern limit of the beach park as shown in Figure 3-11. An erosion scarp is evident along this entire region. Backshore elevations in this area are generally lower than the central and southern area of the park with elevations between about +4.5 and +5.5 ft MSL. However, the width of the backshore between the edge of road and observed erosion scarp is greater in this area compared to the central and southern areas with widths between about 30 and 90 ft. The shoreline in this area had little to no beach sand during the time of the survey and was dominated by basalt boulders between the erosion scarp and the water line. Figure 3-12 shows a comparison of the shoreline between March 2019 and November 2022. The offshore is composed of basalt gravel and cobbles as opposed to limestone reef fronting most of the beach park. This condition begins at the ephemeral stream and continues northward beyond Wai‘ono Stream. The Punalu‘u sand channel comes close to the shoreline near the ephemeral stream where nearshore water depths are slightly deeper due to the presence of this channel. The sand channel is likely a paleochannel historically when sea level was lower.

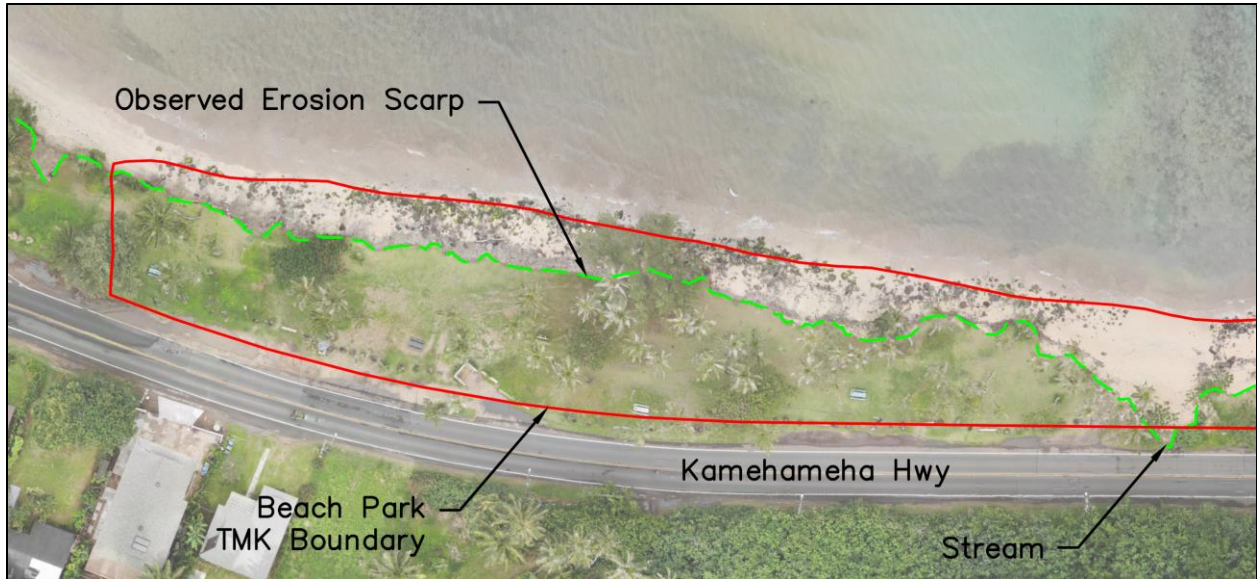


Figure 3-11. Drone mosaic overview of northern area of beach park (November 22, 2022)

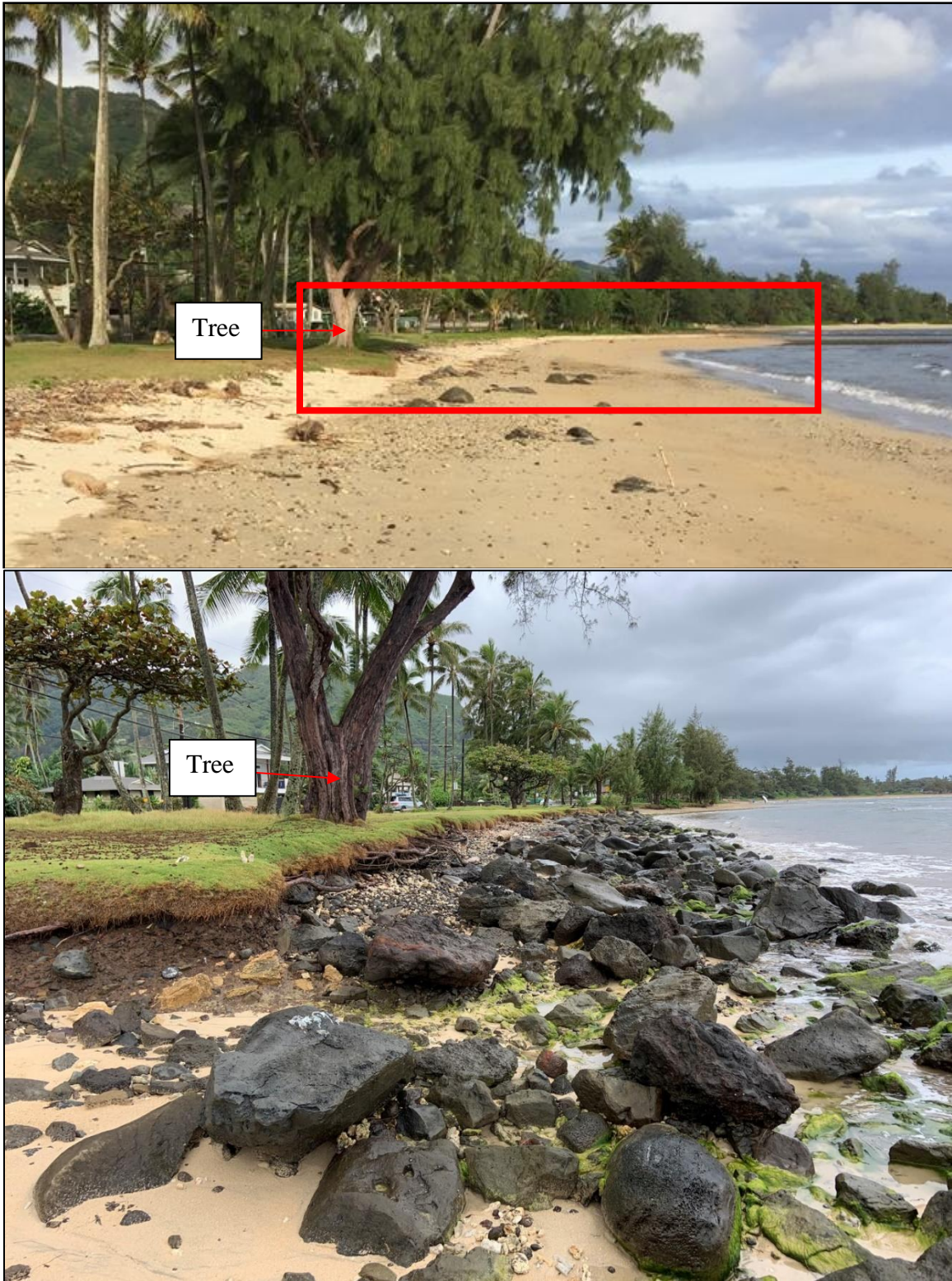


Figure 3-12 . Comparison of northern area shoreline in March 2019 (top photo) and November 2022 (bottom photo)

3.2.5 North of the beach park

The area north of the beach park is shown in Figure 3-13. The backshore in this area served as a construction staging area and temporary road realignment for the South Punalu'u Bridge replacement project completed in 2012. The project utilized a temporary steel bridge makai of the bridge replacement which required removal of much of the backshore vegetation in the area. The area was re-vegetated at the end of the project and heavily irrigated. Figure 3-14 shows a comparison of the vegetated shoreline in March 2019 and April 2024. It is evident from the comparison that the vegetated berm has receded, and the thick plant beds no longer exist between the sand beach and backshore area. An erosion scarp now exists between the beach and the backshore in this area. Figure 3-15 shows the beach further north on the south side of Wai'ono Stream. This area showed no signs of an erosion scarp but frequent overwash in this area has deposited fresh sand and limited vegetative growth. Signs of sand accumulation coupled with offshore sand transport from stream discharge was evident fronting the Wai'ono Stream mouth.

The offshore substrate north of the beach park is composed of basalt gravel and cobbles as opposed to limestone reef fronting most of the beach park. This condition begins at the ephemeral stream and continues northward beyond Wai'ono Stream.



Figure 3-13. Drone mosaic overview north of beach park (November 22, 2022)



Figure 3-14. Comparison of north portion of park in March 2019 (top photo) and April 2024 (bottom photo)



Figure 3-15. Sand beach on south side of Wai'ono Stream (November 2022)

4. HISTORICAL SHORELINE ANALYSIS

Generally, sandy shorelines in Hawai‘i are dynamic and change in response to incident wave conditions, such as high surf, which can quickly alter beach width. Punalu‘u’s shoreline is on the windward side of O‘ahu, where it is subject to nearly constant tradewinds and subsequent waves year-round. Additionally, in the winter months, swell events originating from the northern Pacific Ocean impact the shorelines on the northern and eastern sides of O‘ahu.

A series of historical aerial photographs can be used to show shoreline trends. The University of Hawai‘i (UH) Climate Resilience Collaborative (CRC) has undertaken historical analysis of O‘ahu’s shoreline and has produced a shoreline change map for the Punalu‘u region based on survey data and aerial imagery from 1928 to 2015. The CRC analysis involves measuring the migrating location of the beach toe, which serves as the shoreline change reference feature, along a transect. The CRC analysis employed a weighted linear regression (WLR) methodology to provide a best fit for a long-term shoreline change trend. The transects along the project shoreline are numbered 152 through 174 and are shown in Figure 4-1.

The UH CRC analysis at Punalu‘u Beach Park finds a slight overall accretion trend with rates of between about 0.2 ft/yr and 0.6 ft/yr over the full data set going back to 1928. However, the WLR method employed by CRC is standardized for island-wide analysis and does not capture the site-specific historical shoreline change trend at the beach park. Figure 4-2 below shows transect #166 from the UH CRC analysis and how the calculated shoreline change rate fits to the data points. The individual data points representing the shoreline position indicate that the beach accreted up to the early 1970s followed by beach recession up to 2015. Since the historical change trend using the WPR is applied to the entire data set, the accretional trend between 1928 and the early 1970s following by erosional trends is not captured in the published rates.

To better capture more recent shoreline change trends at the beach park, SEI analyzed the historical shoreline positions since 1988 using the End Point Rate (EPR) method by first establishing the beach toe in each aerial image, to remain consistent with CRC methods. The EPR method calculates the distance of shoreline movement by the time elapsed between two aerial images. The EPR method is useful for calculating overall change and greater sub trends of shoreline migration by breaking up shoreline changes into smaller time periods. Figure 4-3 shows the average annual erosion hazard determined using the EPR method for the project shoreline from 1988-2022, 2006-2022, and 2015-2022. Aerial images from the UH CRC Historical Mosaic archives were used to compare the past shoreline location to the November 2022 shoreline derived from the high-resolution drone aerial imagery. Red bars represent erosion while green bars represent accretion. The shoreline trend has been erosion, between -0.1 ft/year at northern transects to almost -6.0 ft/year at the southern end of the beach.

Coastal erosion is expected to worsen with increasing sea level rise. A 2015 study found that, due to increasing sea level rise, average shoreline recession (erosion) in Hawai‘i is expected to be nearly twice the historical extrapolation by 2050, and nearly 2.5 times the historical extrapolation by 2100 (Anderson et al., 2015).

This analysis indicates that the last four to five decades have been dominated by erosion with evidence of accelerating erosion in the last decade or two in the southern section of the park. This

trend of chronic erosion is evidenced by erosion scarps along the entire length of the coastline. Overwash deposits along much of the park indicate that the sandy beach face is still routinely overtopped by waves. The entire length of the park is susceptible to erosion with erosion rates between -2.0 and -3.0 ft/yr based on the historical rate since 1988 using the EPR.



Figure 4-1. Historical shoreline change rate transects for Punalu'u Beach Park (UH CRC)

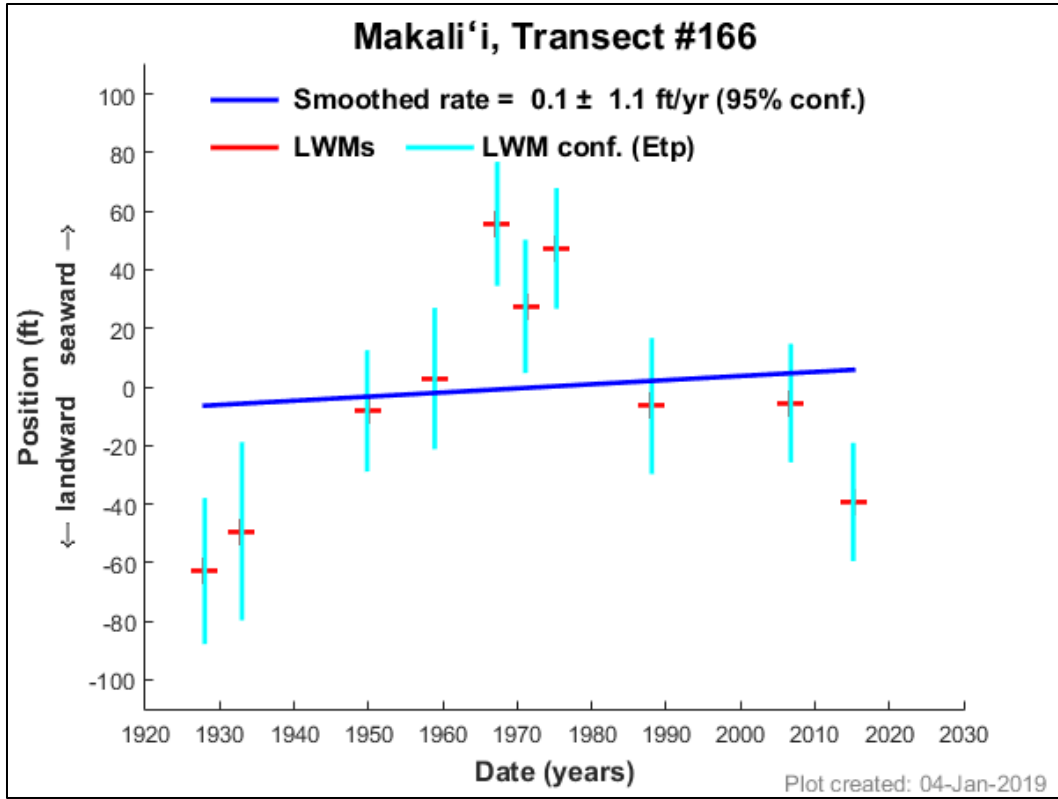


Figure 4-2. CRC transect #166 shoreline change trend for Punalu'u Beach Park (UH CRC)

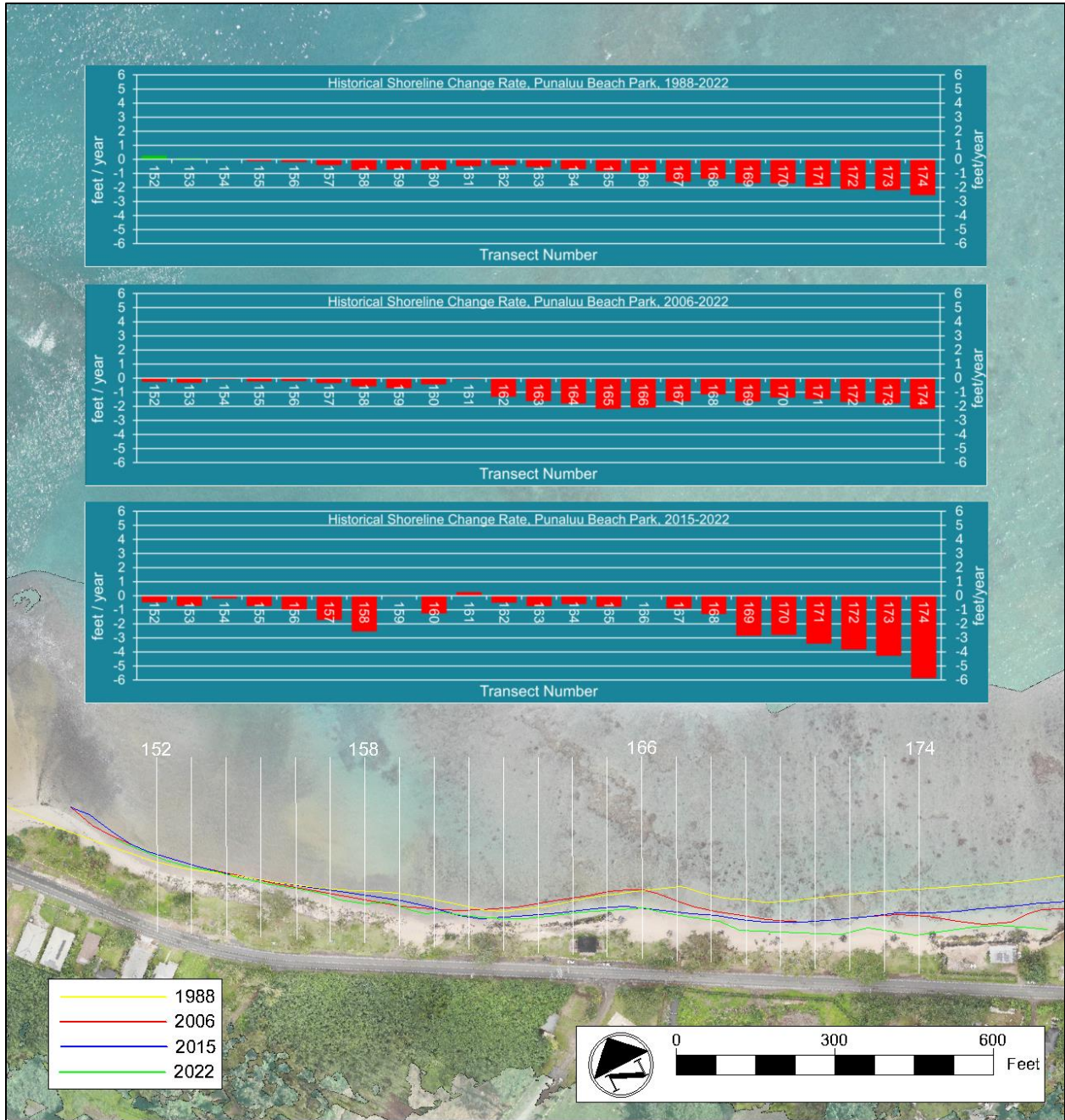


Figure 4-3. Historical shoreline change from 1988-2022, 2006-2022, and 2015-2022 relative to the UH CRC transects (shown in white)

4.1 History of Erosion Fronting the Comfort Station

There have been significant episodic chronic problems in the area fronting the comfort station, as evidenced by both the elevation of the erosion scarp and the presence of the temporary armoring along the face. A series of photographs are presented that show the dynamic nature of the shoreline fronting the comfort station. Figure 4-4 **Error! Reference source not found.** was taken in August of 2008 and shows the gradual transition from backshore to the beach. There was no scarp apparent

at that time; however, the bank appeared slightly steeper than the beach face. A June 2012 site visit followed a period of erosion that produced distinct scarping at the vegetation line and exposure of boulders (Figure 4-5). The face and base of the scarp were becoming covered with grass, and by August 2013, the scarp had turned into a vegetated bank with a lesser amount of scarping (Figure 4-6).

The shoreline fronting the comfort station experienced further erosion during the winter of 2015-2016, resulting in an erosion scarp approaching the foundation of the comfort station (Figure 4-7 and Figure 4-8). The erosion fully exposed a row of large basalt boulders (Figure 4-9) that were previously buried and only partially visible (Figure 4-5). These boulders may be evidence of past attempts to protect the shoreline. Emergency protection in the form of sandbags and geotextile aprons were installed in April-May 2016 (Figure 4-9). That protection slowly failed as the beach continued to erode (Figure 4-10). In February 2019 a large North Pacific low-pressure system generated a large north swell lasting several days, causing significant erosion at Punalu‘u Beach Park. Figure 4-11 shows the condition of the comfort station in March 2019 after the large north swell event. Additional emergency protection in the form of sandbags wrapped in a geotextile blanket and a sand filled mattress were installed in June 2020. The total length of the mattress was approximately 220 ft fronting the comfort station. Figure 4-12 shows a recent photo of the temporary shore protection fronting the comfort station. Figure 4-13 shows an aerial view comparison of the installed temporary protection between its installation in 2020 to 2022. From this comparison it is evident that the erosion control measures have deteriorated north of the comfort station and the backshore area is continuing to erode with the presence of the erosion scarp landward of the installed protection. Fronting and south of the comfort station the erosion control system is still in place, however, the toe is becoming exposed, and the remaining section of the apron is expected to deteriorate.

It is clear from the photographs and historical shoreline positions that this shoreline is susceptible to chronic erosion that can affect the comfort station.



Figure 4-4. Comfort station vegetation line (August 2008)



Figure 4-5. Comfort station vegetation line (June 2012)



Figure 4-6. Comfort station vegetation line (August 2013)



Figure 4-7. Comfort station vegetation line (winter 2015-2016)



Figure 4-8. Erosion scarp at comfort station (winter 2015-2016)



Figure 4-9. Erosion protection fronting comfort station (May 2016)



Figure 4-10. Erosion protection fronting comfort station (January 2018)



Figure 4-11. Erosion protection fronting comfort station (March 2019)



Figure 4-12. Erosion protection fronting comfort station (April 2024)



Figure 4-13. Comparison of temporary erosion after installation in June 2020 (top photo) versus its condition in November 2022 (bottom photo)

5. OCEANOGRAPHIC SETTING

5.1 Bathymetry and Nearshore Bottom Conditions

Figure 5-1 presents a regional view of the offshore depths fronting Punalu'u Beach Park. The offshore bottom is composed of distinct areas of reef and sand. A shallow reef flat extends approximately 2,000 ft offshore. The reef flat is composed of fossil or living reef, which dissipates nearshore wave energy. Depths over the reef flat are typically 4 to 5 ft MSL, occasionally reaching 6 ft deep. The shallow reef is bounded on the north and offshore by deep relict stream channel referred to as the Punalu'u Sand Channel. An additional smaller channel through the reef can be seen in the bathymetry offshore of Punalu'u Point to the south. This channel cuts through the reef, and although it diminishes near shore, it does provide a pathway for circulation over the reef to exit offshore. The channel joins the Punalu'u Sand Channel on the offshore side of the reef.

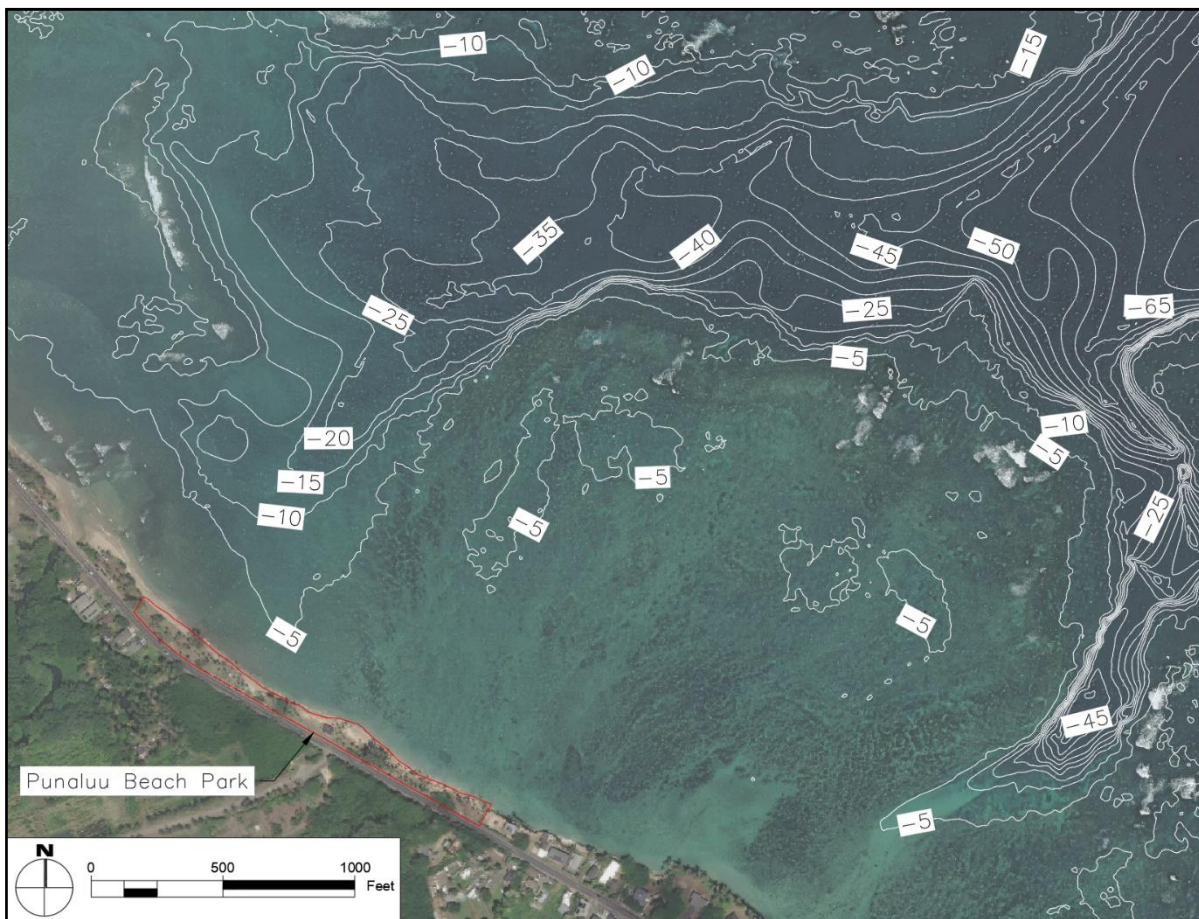


Figure 5-1. Regional view of bathymetry, Punalu'u Beach Park (elevations in ft relative to MSL)

5.2 Winds

The prevailing wind throughout the year is the northeasterly trade wind. Its average frequency varies from more than 90% during the summer season to only 50% in January, with an overall annual frequency of 70%. Westerly, or Kona, winds occur primarily during the winter months, generated by low pressure or cold fronts that typically move from west to east past the islands. Figure 5-2 shows a wind rose diagram applicable to the site based on wind data recorded at Honolulu International Airport between 1949 and 1995.

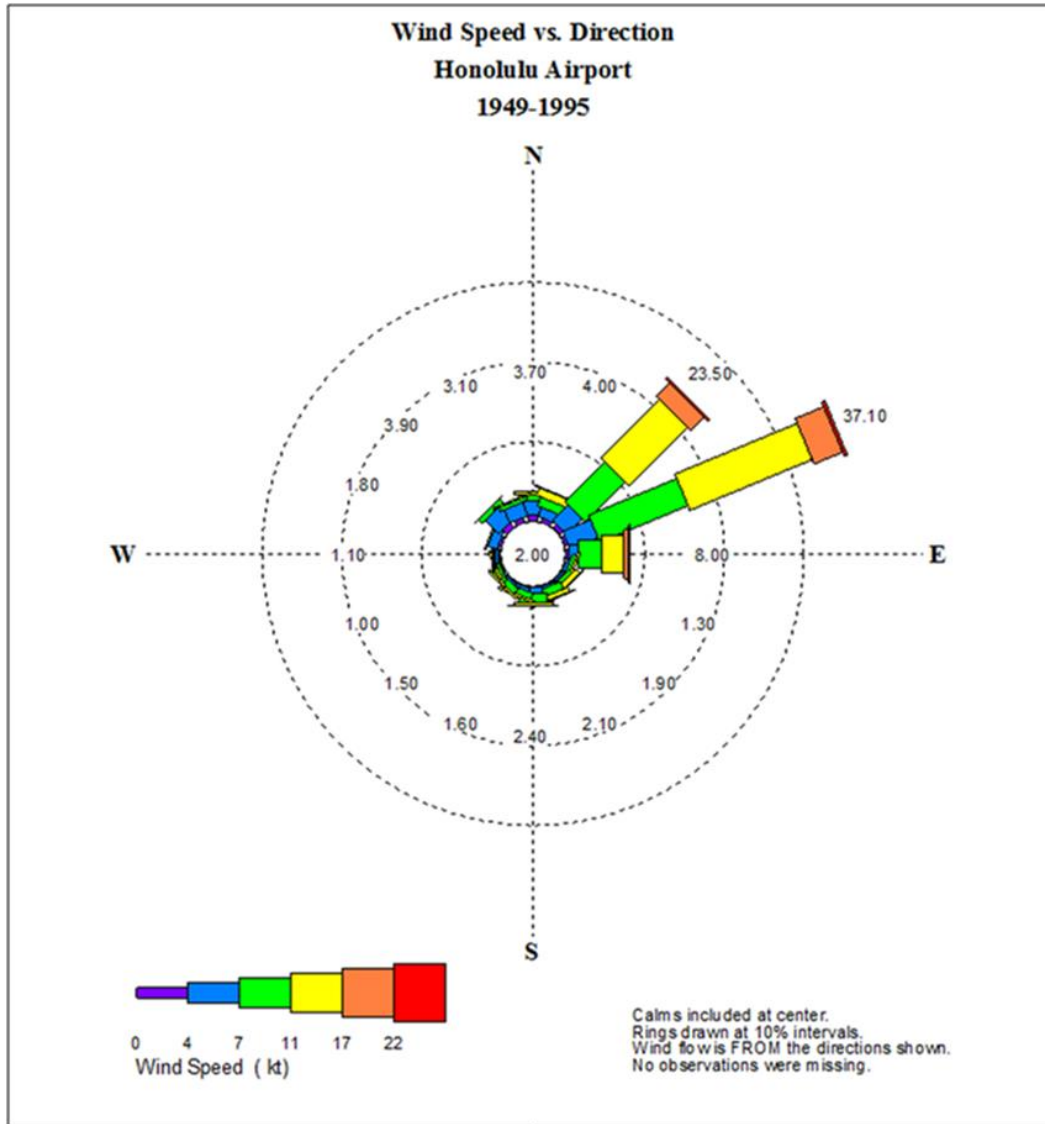


Figure 5-2. Wind rose for Honolulu Airport (1949 to 1995)

Tradewinds are produced by the outflow of air from the Pacific Anticyclone high pressure system, also known as the Pacific High. The center of this system is typically located well north and east of the Hawaiian chain and moves to the north and south seasonally. In the summer months, the center moves to the north, causing the tradewinds to be at their strongest from May through

September. In the winter, the center moves to the south and often displaced by low pressure systems, resulting in decreasing tradewind frequency from October through April. During these months, the tradewinds continue to blow; however, their average monthly frequency decreases to 50%.

During the winter months, wind patterns of a more transient nature increase in prevalence. Winds from extra-tropical storms can be very strong from almost any direction, depending on the strength and position of the storm. The low-pressure systems associated with these storms typically track west to east across the North Pacific north of the Hawaiian Islands. At Honolulu Airport, wind speeds resulting from these storms have on several occasions exceeded 60 mph. Kona winds are generally from a southerly to southwesterly direction, usually associated with slow-moving low-pressure systems known as Kona lows which typically transit from west to east through the vicinity of the island chain. These storms are often accompanied by heavy rains.

Punalu‘u Beach Park is directly exposed to tradewind waves and associated waves developed by these wind patterns. The exposure to tradewinds at Punalu‘u makes offshore sand recovery work challenging which requires the use of moored floating platforms.

The shoreline at Punalu‘u Beach Park is oriented towards the northwest direction while the mean wind direction is primarily from the east-northeast to northeast directions. Locally generated waves over the reef flat from these wind patterns may cause sediment transport and morphological changes along the shoreline in addition to offshore swell. Beaches typically orient themselves towards the nearshore wave crest and any difference in wave angle to shoreline angle will likely cause longshore sediment transport and shoreline change in the direction of the wave orientation. Because of this, sand would likely be transported to the northwest along the shoreline when the winds are coming from the east-northeast and alternatively sand may move to the southeast along the shoreline when winds approach from the north-northeast direction. Since most of the wind comes from the east-northeast direction, the mean movement of sand from local wind waves is expected to move from southeast to northwest along the shoreline.

Climate change effects on the future wind climate is still not well understood and an active area of research currently. A United States Geological Survey (USGS) paper by Storlazzi et. al. in 2015 titled “Future Wave and Wind Projections for United States and United States-Affiliated Pacific Islands” looked at the future wind and wave climate based on Representative Concentration Pathways (RCP) scenarios 4.5 and 8.5, which correspond to moderately mitigated and unmitigated greenhouse gas emissions, respectively, for four atmosphere-ocean global climate models (Storlazzi et. al., 2015). They generally found in the Hawai‘i region that mean and extreme wind speeds during all seasons slightly decreased or did not change between present day and mid-century for both RCP4.5 and RCP 8.5 and direction of the wind typically shifted clockwise to a more easterly approach. For end of century, they found a similar trend for RCP4.5 and RCP8.5 and further clockwise directional shift of the wind directions. Another study by Garza, et. al., 2012, investigated the change in wind patterns on Oahu at local wind stations since 1973 and found that the tradewinds have been typically weakening and shifting from a northeast to more easterly direction. This clockwise shifting of the tradewind direction may have implications for Punalu‘u Beach Park which may experience southeast to northwest sand transport during more easterly

tradewinds as discussed previously. This trend may also continue into the future with climate change.

5.3 Water Levels

5.3.1 Astronomical Tides

Tides in the Hawaiian Islands are semi-diurnal with pronounced diurnal inequalities (i.e., two high and low tides each 24-hour period with different elevations). Variation of the tidal range results from the relative position of the moon and the sun. During full moon and new moon phases, the moon and sun act together to produce larger "spring" tides; when the moon is in its first or last quarter, smaller "neap" tides occur. The cycle of spring to neap tides and back is half the 27-day period of the moon's revolution around the earth and is known as the fortnightly cycle. The combination of diurnal, semi-diurnal and fortnightly cycles dominate variations in sea level throughout the Hawaiian Islands.

The offshore diurnal tide reaches Hawai'i Island first, then sweeps across Maui, O'ahu, and finally Kaua'i. Tidal predictions and historical extreme water levels are provided by the National Oceanic and Atmospheric Administration (NOAA), National Ocean Service (NOS), Center for Operational Oceanographic Products and Services (COOPS). The nearest tide station to the project site is located in Kaneohe Bay on Moku o Lo'e (Coconut) Island on the windward side of O'ahu. The water level tidal datum data from this station is shown in Table 5-1. The mean sea level (MSL) datum is used as the design elevation reference datum in this study.

Table 5-1. Tidal datums at Moku o Lo'e, Station 1612480 (1983-2001 Epoch)

Datum	Elevation (ft, MLLW)	Elevation (ft, MSL)
Highest Astronomical Tide (HAT)	+2.91	+1.86
Mean Higher High Water (MHHW)	+2.12	+1.07
Mean High Water (MHW)	+1.80	+0.75
Mean Sea Level (MSL)	+1.05	0.00
Mean Low Water (MLW)	+0.31	-0.74
Mean Lower Low Water (MLLW)	0.00	-1.05
Lowest Astronomical Tide (LAT)	-0.82	-1.87

5.3.2 Sea Level Rise Projections

Global mean sea level is the average height of the entire ocean surface. The present rate of global mean sea level change is +3.1 mm/yr (Sweet et al., 2022, Figure 5-3), where a positive number represents a rising sea level. Global mean sea level rise has accelerated over preceding decades compared to the mean of the 20th century (Sweet et al., 2017). Regional effects cause sea levels to increase in some parts of the planet while decreasing or remaining relatively stable in other areas. In the contiguous United States (U.S.), sea level has risen on average by 6.5 inches (in) since 1950 (Sweet et al., 2018). Based on the Honolulu tide station, sea level has risen by about 4.5 inches (in) since 1950. Factors contributing to the observed rise in sea level include melting of land-based glaciers and ice sheets and thermal expansion of the ocean water column.

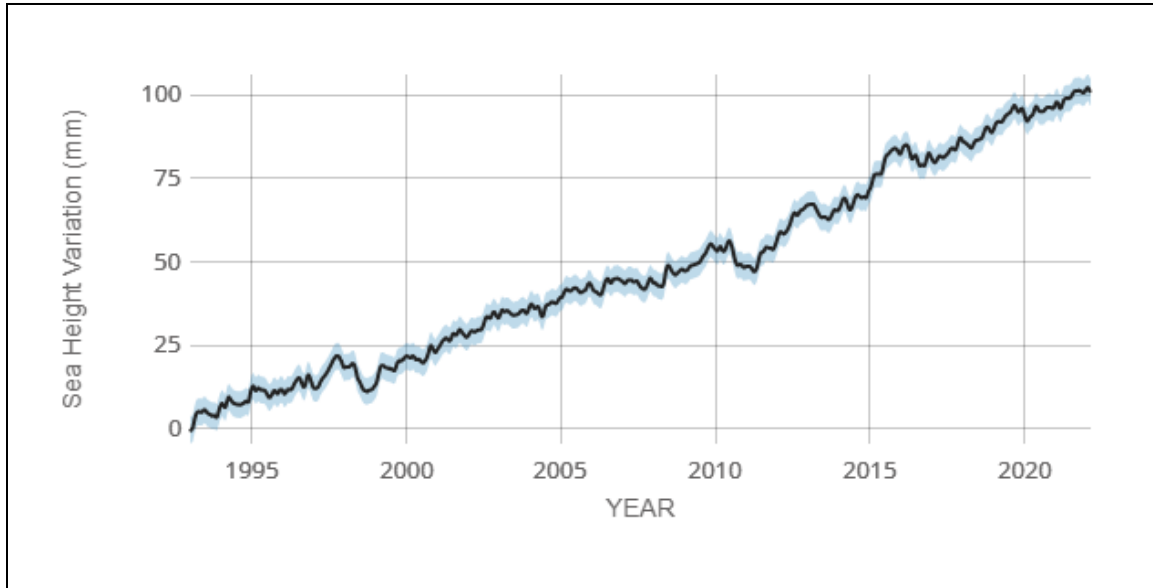


Figure 5-3. Global satellite sea level rise variability from 1993 to 2022 (Sweet et al. 2022)
 (Black line shows the average sea level rise during the time period.)

Sweet et. al. (2017 and 2022) identifies specific regions that are susceptible to a greater-than-average rise in sea level. Hawai‘i thus far has seen a rate of sea level rise less than the global average, however, this is expected to change in the future. Hawai‘i is in the “far-field” regarding the effects of melting land ice. This means that the effects of melting land ice have been significantly less in Hawai‘i compared to areas nearer to the ice melt. Over the next few decades, these effects are expected to spread to Hawai‘i, which is then projected to experience a sea level rise greater than the global average.

The relative sea level trend for Moku o Lo‘e Island for the period of 1957 to present is shown in Figure 5-4 (NOAA, 2023) with a value of $+1.65 \pm 0.50$ mm/yr. Figure 5-4 also shows interannual anomalies exceeding 0.5 ft (15 cm) in magnitude due to natural oceanic variability from processes such as the El Niño-Southern Oscillation (ENSO) and the Pacific Decadal Oscillation (PDO).

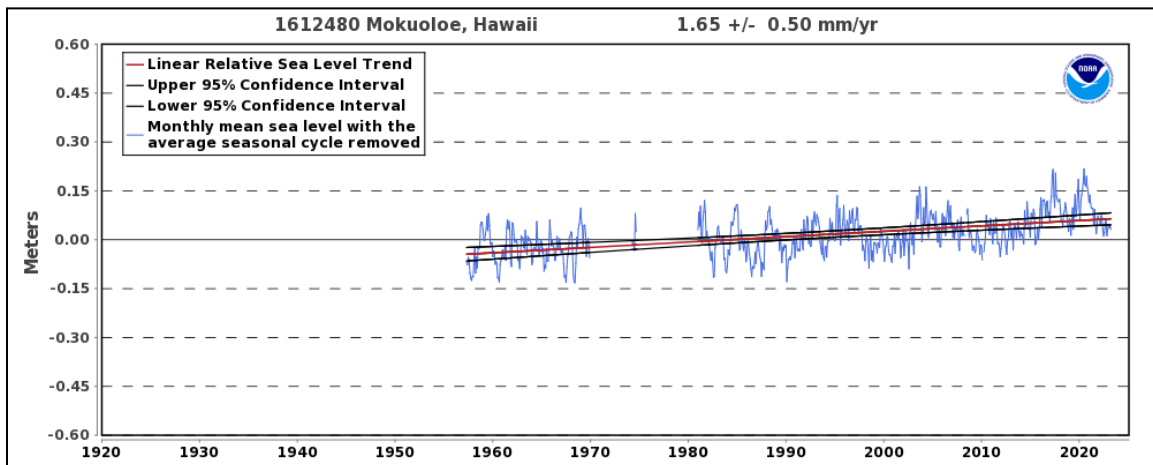


Figure 5-4. Mean sea level trend, Moku o Lo‘e, Station 1612480, 1957 to present (NOAA, 2023)



The Sea Level Rise and Coastal Flood Hazard Scenarios and Tools Interagency Task Force (NOAA 2022) recently revised their sea level change projections through 2150, considering up-to-date scientific research and measurements. The Task Force consists of representatives from the National Aeronautics and Space Administration (NASA), National Oceanic and Atmospheric Administration (NOAA), U.S. Environmental Protection Agency (EPA), U.S. Geological Survey (USGS), U.S. Army Corps of Engineer (USACE), and additional partners within academia. The most recent report entitled *Global and Regional Sea Level Rise Scenarios for the United States: Updated Mean Projections and Extreme Water Level Probabilities Along U.S. Coastlines* (Sweet, et al., 2022), provides the most up to date sea level rise projections for all the U.S. states and territories. Five (5) scenarios are also included in the NOAA 2022 report including *Low*, *Intermediate-Low*, *Intermediate*, *Intermediate-High*, and *High* and correspond to mean sea level values of 1.2, 2.0, 3.8, 5.8, and 7.9 ft, respectively, for Honolulu by the year 2100. These values are referenced to a baseline 0 in 2000 and are adjusted accordingly to the current tidal epoch defining MSL.

For this study, SLR values of +1.6 and +3.2 ft were chosen for assessment and development of conceptual shoreline restoration alternatives. The upper bound of +3.2 ft is currently adopted by the State of Hawai‘i for planning and design purposes and was derived from the 2013 IPCC Fifth Assessment Report as the global mean sea level rise by 2100. SLR of +1.6 ft was chosen as half of +3.2 ft as a mid-level value to represent potential sea level mid-century. The USACE Sea Level Rise Analysis Tool¹ (SLAT) was utilized in this study to look at the projected timings of when +1.6 and +3.2 ft of SLR may occur. The tool allows visualization of various sea level change projections at a specific tide station and accounts for local effects including vertical land motion and historical sea level trends. Figure 5-5 shows the SLAT output for Moku o Lo‘e Island tide station for the NOAA 2022 projections. Table 5-2 lists the timings of when +1.6 and +3.2 ft may occur based on the NOAA 2022 projections.

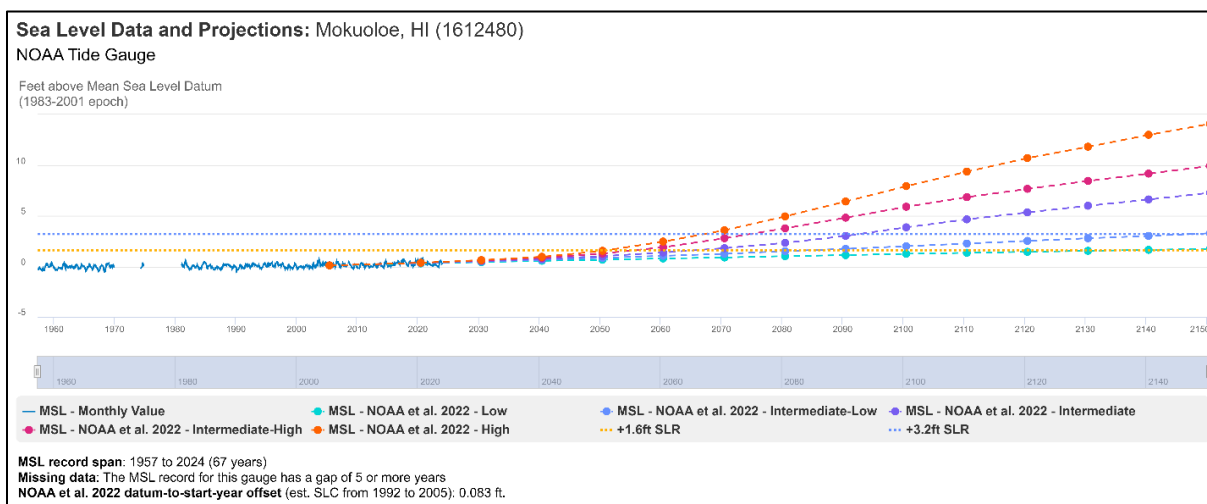


Figure 5-5. NOAA 2022 sea level rise projections for Moku o Lo‘e Island with thresholds of +1.6 and +3.2 ft

¹ <https://www.usace.army.mil/corpsclimate/Public-Tools-Developed-by-USACE/Sea-Level-Change/>

Table 5-2. NOAA 2022 sea level projection timing with +1.6 and +3.2 ft of SLR

Curve	Timing (year)
Intersections with +1.6 ft SLR	
NOAA et al. 2022 – Low	2138
NOAA et al. 2022 – Intermediate-Low	2085
NOAA et al. 2022 – Intermediate	2066
NOAA et al. 2022 – Intermediate-High	2056
NOAA et al. 2022 – High	2051
Intersections with +3.2 ft SLR	
NOAA et al. 2022 – Low	None
NOAA et al. 2022 – Intermediate-Low	2148
NOAA et al. 2022 – Intermediate	2093
NOAA et al. 2022 – Intermediate-High	2075
NOAA et al. 2022 – High	2067

5.3.3 Sea Level Anomalies

The ocean surface does not have a consistent elevation. In this study, sea level anomalies are defined as the difference between the measured and predicted tides recorded at the Moku o Lo‘e NOAA tide station. Sea level anomalies occur as a result of processes such as El Niño, global warming, geostrophic currents due to the rotation of the earth, and mesoscale eddies that propagate across the ocean.

Hawai‘i is subject to periodic extreme tide levels due to large oceanic eddies and other oceanographic phenomena that have recently been recognized and that sometimes propagate through the Hawaiian Islands. Mesoscale eddies produce tide levels that can be up to 0.5 ft higher than normal for periods up to several weeks (Firing and Merrifield, 2004). An additional temporary sea level rise on the order of 0.5 ft has also been associated with phenomena related to the El Niño / Southern Oscillation (ENSO).

In 2017, Hawai‘i experienced anomalous sea levels which caused significant inundation of low-lying urban areas such as Waikiki, Ala Wai Boulevard, and Mapunapuna. The daily maximum recorded tides at Honolulu Harbor from February through October 2017 are shown in Figure 5-6. The plot also shows the corresponding predicted tide and sea level anomalies for the daily maximum recorded tide. Table 5-3 extends this data, presenting the recorded and predicted tides at Honolulu Harbor from February 2017 to present.

The media widely reported that the flooding was the result of *King Tides* referring to peak annual astronomic tides; however, sea level anomalies during those high-water events ranged from approximately 0.5 foot to 1 foot above the astronomical tide, contributing significantly to the high water levels. The occurrence of summer swells during this period of elevated water levels added to the inundation. The end of 2019 also marked an extended period of large sea level anomalies. Figure 5-7 shows the extreme water levels from December 24 to 27, 2019. During this time period, sea level anomalies of +0.6 to +1.1 ft MLLW added to the winter *King Tides* resulting in the highest recorded water level at Honolulu Harbor of +3.4 ft MLLW.

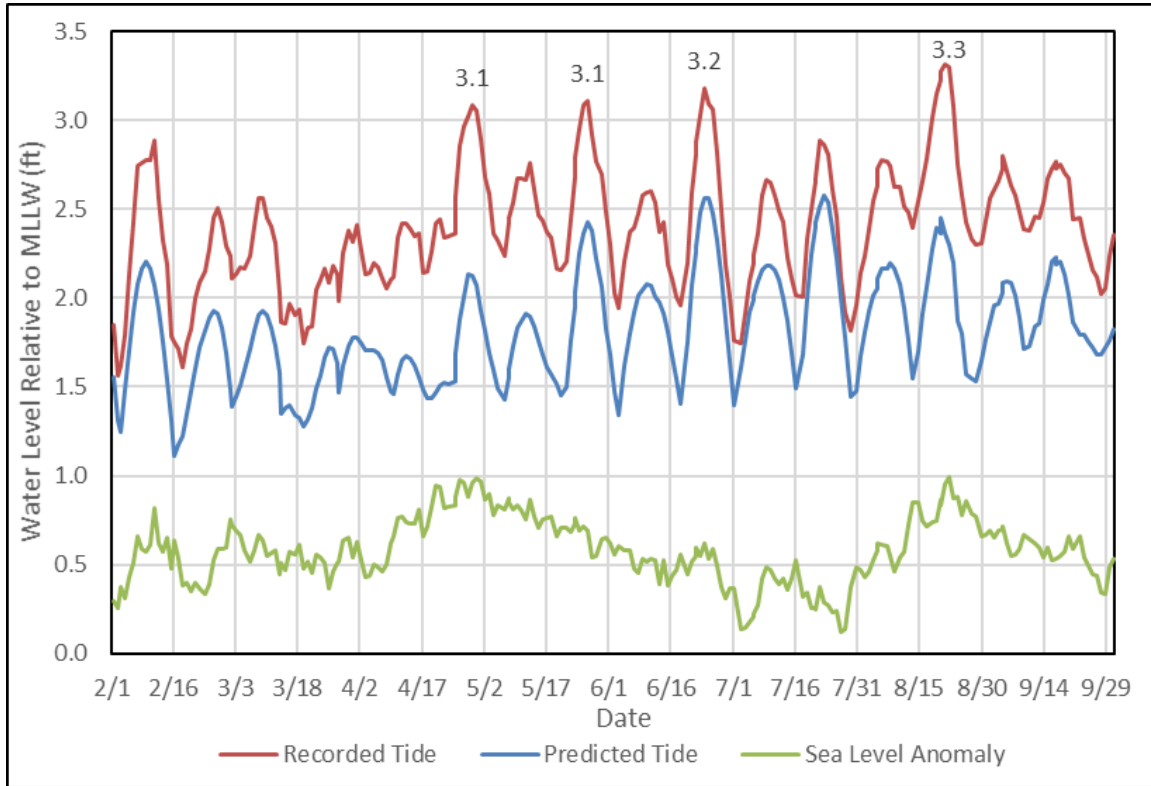


Figure 5-6. Daily maximum measured tides at Honolulu Harbor and corresponding predicted tides and sea level anomaly (Feb 1 - Oct 1, 2017)

Table 5-3. Peak recorded tide levels at Honolulu Harbor (2017 to present)

Date	Recorded Tide (ft, MLLW)	Predicted Tide (ft, MLLW)	SLA (ft)
12/25/2019	3.4	2.4	1.0
08/20/2017	3.3	2.4	0.9
08/21/2017	3.3	2.3	1.0
08/19/2017	3.3	2.4	0.9
07/19/2020	3.3	2.4	0.9
07/20/2020	3.3	2.5	0.8
12/26/2019	3.3	2.4	0.9
07/21/2020	3.2	2.4	0.8
07/04/2020	3.2	2.5	0.7
11/15/2020	3.2	2.5	0.7

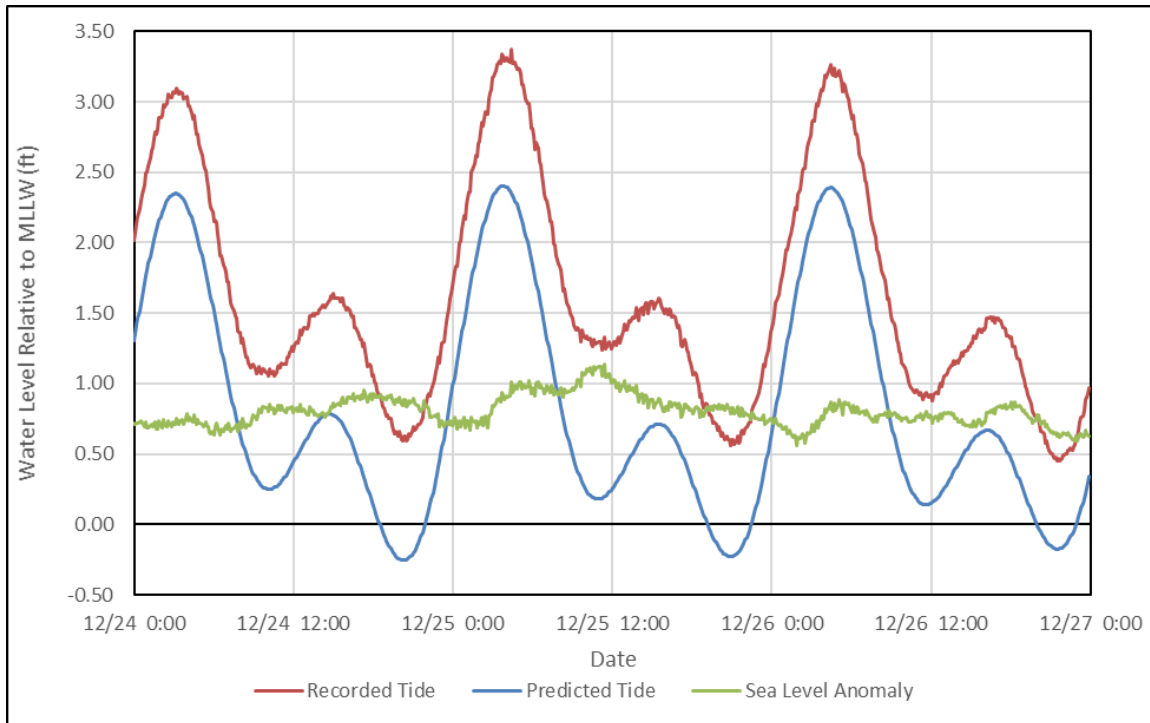


Figure 5-7. Predicted and measured tides at Honolulu Harbor (Dec 24-26, 2019)

5.4 Waves

5.4.1 General Wave Climate

The wave climate in Hawai‘i is typically characterized by four general wave types. These include northeast tradewind waves, southern swell, North Pacific swell, and Kona wind waves. Tropical storms and hurricanes also generate waves that can approach the islands from virtually any direction. Unlike winds, any and all of these wave conditions may occur at the same time. The dominant swell regimes for Hawai‘i are shown in Figure 5-8.

Tradewind waves occur throughout the year and are the most persistent April through September when they usually dominate the local wave climate. They result from the strong and steady tradewinds blowing from the northeast quadrant over long fetches of open ocean. Tradewind deepwater waves are typically between 3 to 8 ft high with periods of 5 to 10 seconds, depending upon the strength of the tradewinds and how far the fetch extends east of the Hawaiian Islands. The direction of approach, like the tradewinds themselves, varies between north-northeast and east-southeast and is centered on the east-northeast direction. The Punalu‘u project site is directly exposed to tradewind waves.

Southern swell is generated by storms in the southern hemisphere and is most prevalent during the summer months of April through September. Traveling distances of up to 5,000 miles, these waves arrive with relatively low deepwater wave heights of 1 to 4 ft and periods of 14 to 20 seconds. Depending on the positions and tracks of the southern hemisphere storms, southern swells approach between the southeasterly and southwesterly directions. The Punalu‘u project site is sheltered from southern swell.

During the winter months in the northern hemisphere, strong storms are frequent in the North Pacific in the mid latitudes and near the Aleutian Islands. These storms generate large North Pacific swells that range in direction from west-northwest to northeast and arrive at the northern Hawaiian shores with little attenuation of wave energy. These are the waves that have made surfing beaches on the north shores of O‘ahu and Maui famous. Deepwater wave heights often reach 15 ft and in extreme cases can reach 30 ft. Periods vary between 12 and 20 seconds, depending on the location of the storm. The Punalu‘u project site is partially exposed to swell approach from the north and northwest; however, swell from east of north can directly approach the site.

Kona storm waves do not directly approach the project site; however, these waves are fairly infrequent, occurring only about 10 percent of the time during a typical year. Kona waves typically range in period from 6 to 10 seconds with heights of 5 to 10 ft, and approach from the southwest. Deepwater wave heights during the severe Kona storm of January 1980 were about 17 ft. These waves had a significant impact on the south and west shores of O‘ahu.

Severe tropical storms and hurricanes obviously have the potential to generate extremely large waves, which in turn could potentially result in large waves at the project site. Recent hurricanes impacting the Hawaiian Islands include Hurricane Iwa in 1982 and Hurricane Iniki in 1992. Iniki directly hit the island of Kauai and resulted in large waves along the southern shores of all the Hawaiian Islands. Damage from these hurricanes was extensive. More recently, Hurricane Douglas in 2020 passed north of Oahu within about 30 mi category 1 storm. Although not a direct landfall, the storm caused wave inundation and overwash along low-lying regions of the Windward Oahu coastline. Hurricane Dora in 2023 passed south of the Hawaiian Islands and did not directly impact the islands but may have caused strong gradient winds to develop over the island chain. These strong gradient winds have the potential for elevated surf and local wind waves along the Windward coastline and at the project shoreline.

Climate change effects on the future wave climate is still not well understood and an active area of research currently. The same USGS paper by Storlazzi et. al. in 2015, discussed in Section 5.2, also looked at the future wave climate based on RCP scenarios 4.5 and 8.5 for four atmosphere-ocean global climate models. They generally found in the Hawai‘i region that mean and extreme waves during all seasons slightly decreased or did not change between present day and mid-century for both RCP4.5 and RCP 8.5 (Storlazzi et. al., 2015). For end of the century, they found a similar reduced or unchanged trend for RCP4.5 but found that extreme waves in the summer months may increase for RCP8.5 (Storlazzi et. al., 2015).

Another study by Knutson et. al. in 2015, studied how future climate change may affect tropical storm and hurricane frequency and intensity within all ocean basins for RCP4.5. Their paper titled “Global Projections of Intense Tropical Cyclone Activity for the Late Twenty-First Century from Dynamical Downscaling of CMIP5/RCP4.5 Scenarios” reports that tropical cyclone intensity and frequency in the Northeast Pacific may increase by 8.2 and 16.3 percent, respectively. Hurricane intensity and frequency in the Northeast Pacific showed a similar trend with an increase of 7.8 and 19.3 percent, respectively (Knutson et. al., 2015). They also noted that stronger category storms may increase in frequency with climate change in the Northeast Pacific basin.

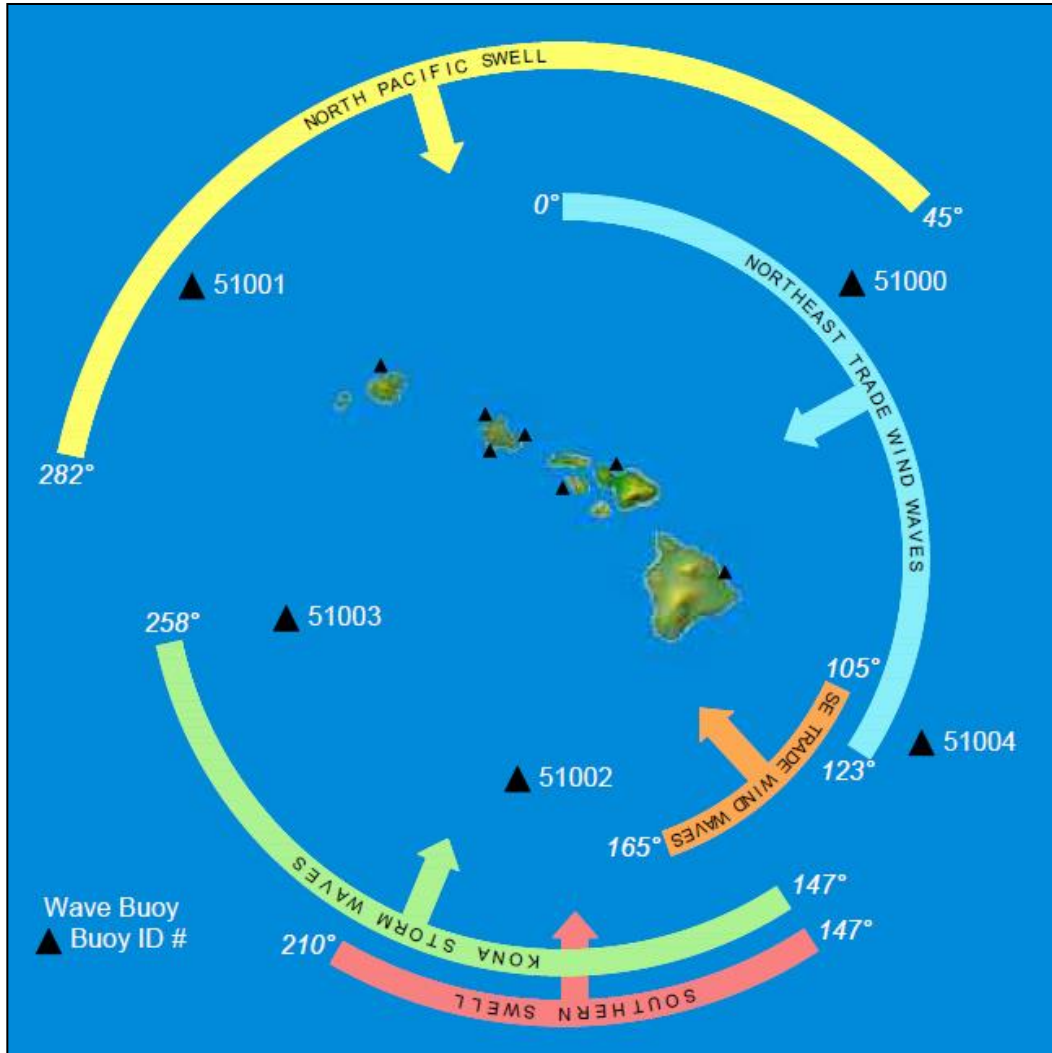


Figure 5-8. Hawai'i dominant swell regimes

5.4.2 Windward O'ahu Wave Climate

Wave conditions for this area have been measured by the Coastal Data Information Program (CDIP), at three nearby locations, designated as Station 106 ("Waimea Bay"), Station 225 ("Kaneohe Bay, WETS"), and Station 098 ("Mokapu Point"). Station 106, which is located approximately 16.5 miles northwest of the project site in a water depth of roughly 656 ft (200 m), recorded data from 2002 to present with full exposure to north pacific swell. Stations 225 and 098 are located approximately 10.6 and 17.0 miles southeast, respectively, of the project site both in water depths of roughly 280 ft (85 m). Stations 225 and 098 recorded data since 2016 and 2000, respectively, and are both exposed to tradewind waves and partially exposed to north pacific swell. These buoy locations relative to the project site are shown in Figure 5-9.

Each buoy measures and records its motion due to passing waves. This data is used to compute spectral wave energy and direction at half-hour increments and derives important wave parameters such as significant wave height, peak direction, and peak period from those measurements. The

entire dataset from Station 106 and Station 098 was utilized to generate wave height and wave period rose plots, which are a form of histogram that conveys a parameter’s directional dependence. Figure 5-10 and Figure 5-11 show the wave height and period rose plots, respectively, for Station 106 (Waimea). Figure 5-12 and Figure 5-13 show the wave height and period rose plots, respectively, for Station 098 (Mokapu). In general, the plots show peak values centered on two primary directions: northwest swell from 315° (seen at Waimea) and tradewind waves from 67.5° (seen at both Waimea and Mokapu). Punalu‘u Beach Park is most susceptible to northerly swell rather than northwest swell due to the northern-most tip of O‘ahu blocking much of the northwest swell energy from reaching the park. The rose plots indicate that the study shoreline is susceptible to elevated surf throughout the year due to its exposure to both northerly (winter) and tradewind waves. The wave period rose plot shows that the north and swell peaks are primarily composed of longer period (>14 seconds) swell while the tradewind waves are composed of shorter period (<10 seconds) waves, as would be expected.

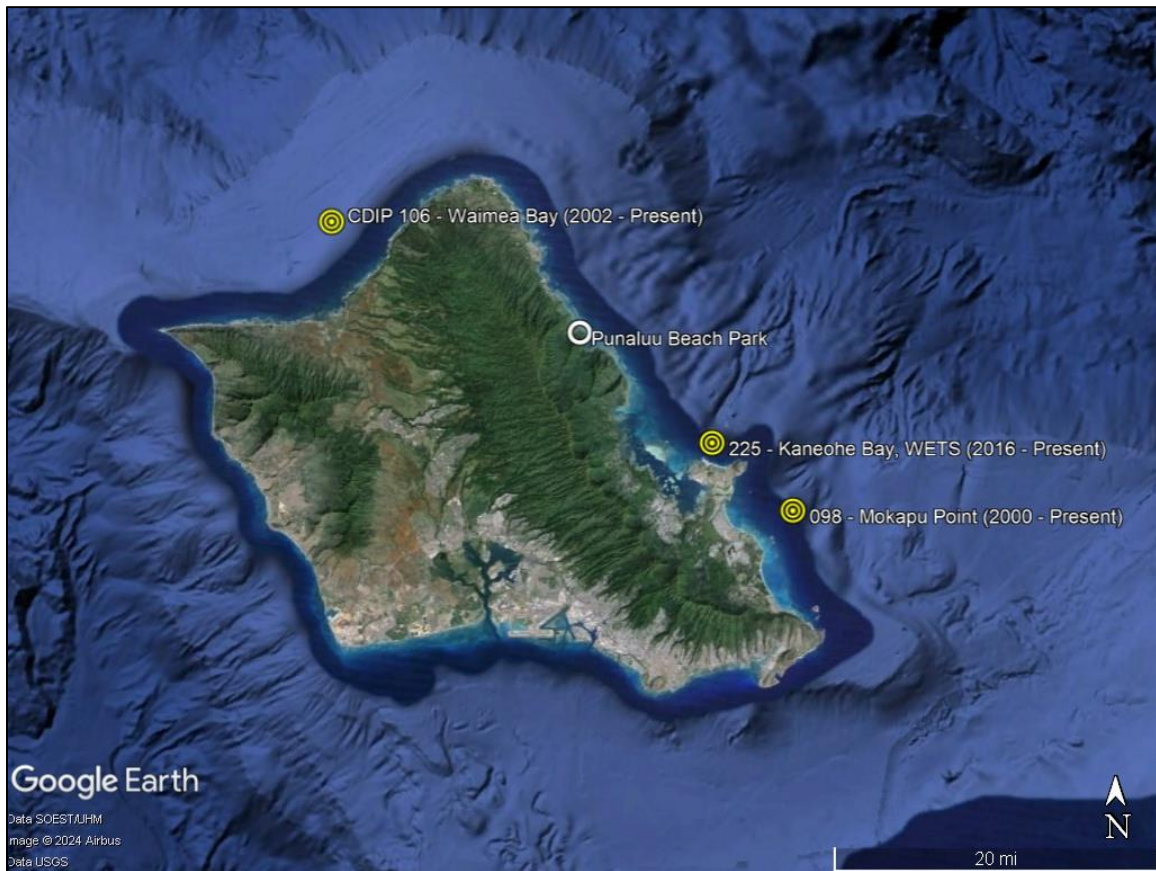


Figure 5-9. Location of CDIP buoys used for this study in relation to Punalu‘u Beach Park

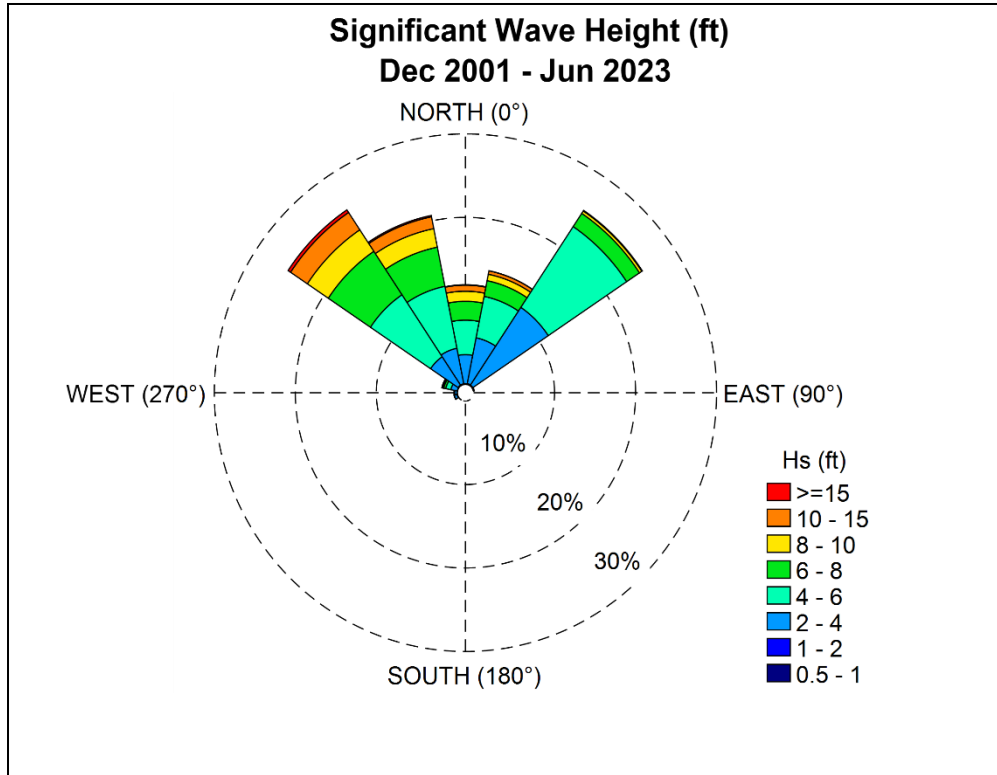


Figure 5-10. CDIP Buoy 106 (Waimea Bay) wave height rose from December 2001 to June 2023

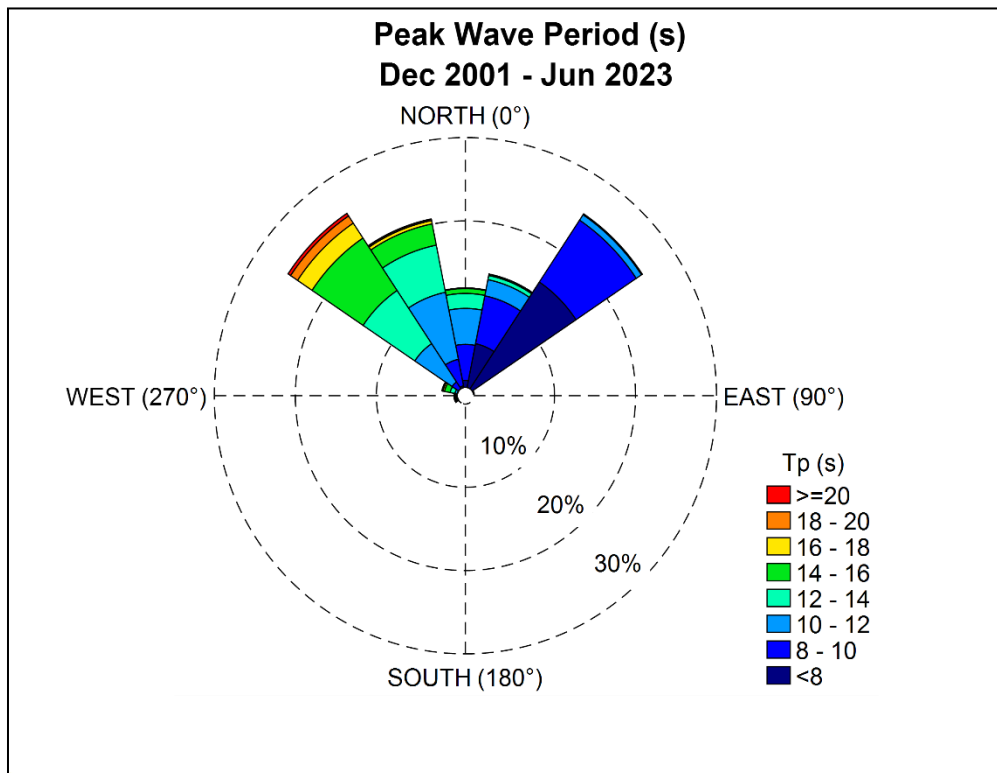


Figure 5-11. CDIP Buoy 106 (Waimea Bay) wave period rose from December 2001 to June 2023

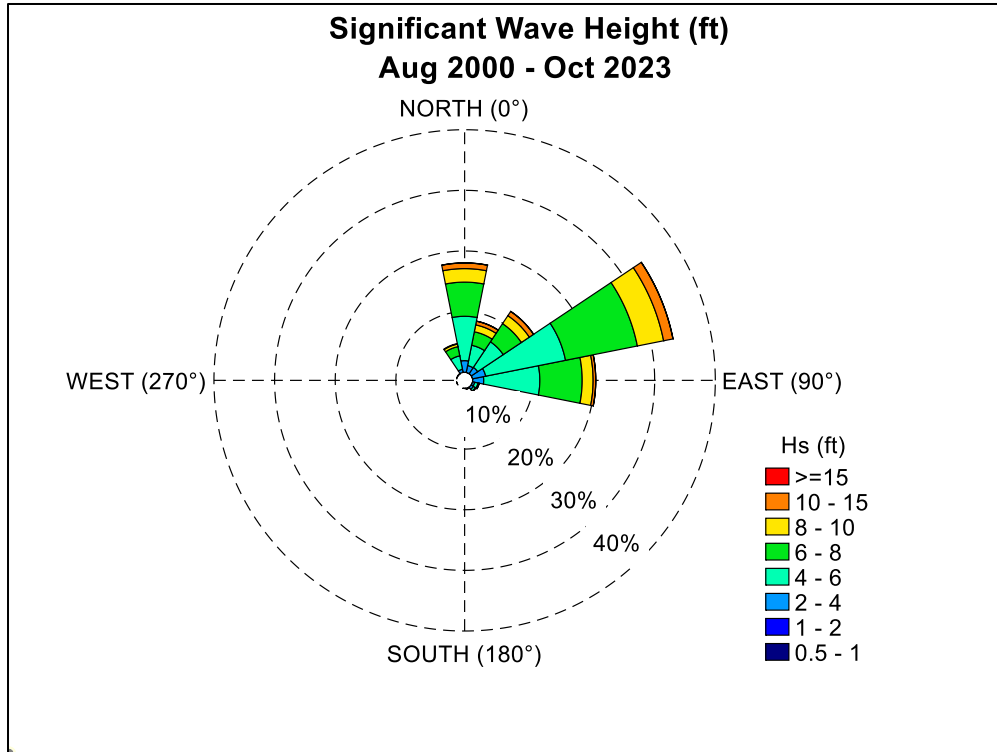


Figure 5-12. CDIP Buoy 098 (Mokapu Point) wave height rose from August 2000 to October 2023

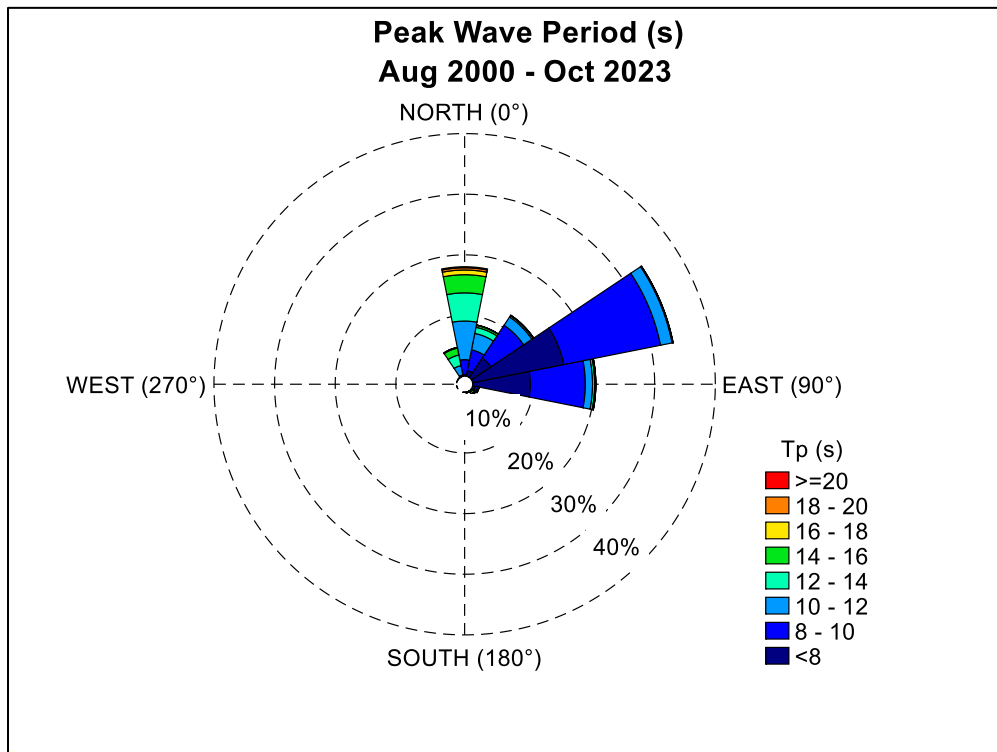


Figure 5-13. CDIP Buoy 098 (Mokapu Point) wave period rose from August 2000 to October 2023

5.4.3 *Extreme Deepwater Waves*

Historical wave buoy and hindcast data allows the prediction of extreme wave events. These are infrequent, large, powerful, low probability wave events that are typically used for design purposes. For example, a 50-year return period wave event is an extreme event with a 1/50 (i.e., 2%) chance of occurring in any given year. Because the project shoreline is vulnerable to multiple wave regimes (north pacific swell and tradewind waves) extreme deep water wave heights for each event were determined based on the available buoy data.

The available buoy wave height data was used to generate a Weibull extreme value distribution for return period wave heights. The Weibull Distribution is a tool for relating the size of wave to the frequency of occurrence at a given location. The analysis requires a long-term data set with well-documented wave events. These events are then sorted by size, and frequency of occurrence can be assessed by how often these events occur in the record. The relationship is logarithmic, and a linear fit can be established with a best fit linear regression of the data. Though not all wave events will be co-located on the line, its general trend represents the nature of the size and frequency relationship of wave events at a specific location. An extreme wave return-period analysis using the Weibull Distribution was performed for waves associated with north pacific swell and tradewind waves.

5.4.3.1 *North Pacific Swell*

For extreme deepwater waves associated with north pacific swell, wave buoy data was compiled from the Coastal Data Information Program (CDIP) buoy station 106 located offshore from Waimea Bay approximately 16.5 miles to the northwest of the project site (Figure 5-9). This buoy was chosen for its full exposure to north pacific swell and its longer timeseries of wave data, which makes it more reliable for return period analysis. Wave data for this buoy spans over a 21-year period from December 2001 to June 2023. Extreme wave heights were investigated by filtering the buoy data by direction and period for waves approaching from the north to north-northeast direction, with periods of 12 seconds or greater. The distribution of wave height versus return period (probability of wave height occurring in any given year) is shown on Figure 5-14 and Table 5-4. The ten largest wave events associated with North Pacific swell during the period of record are shown on Table 5-5.

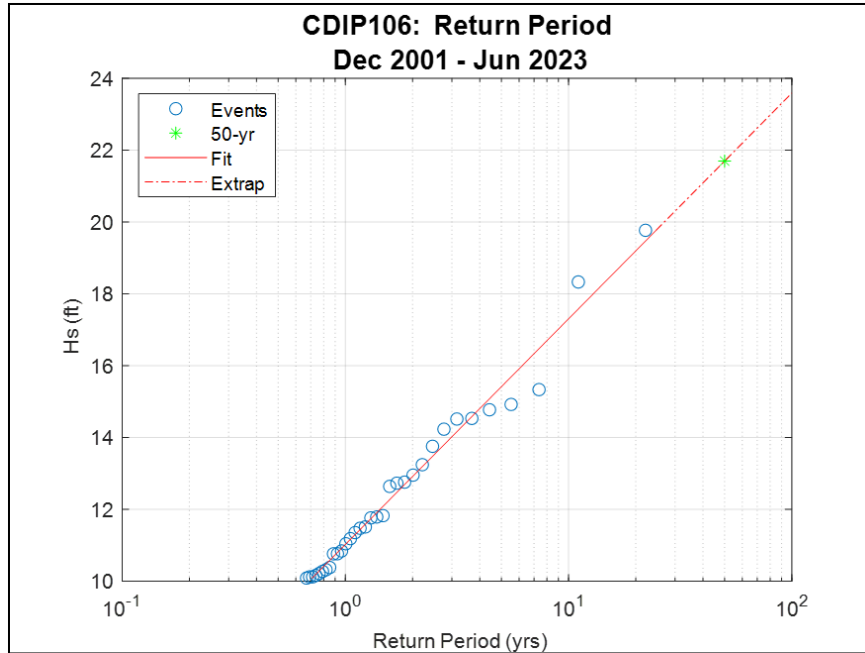


Figure 5-14. Northerly swell significant wave height vs. return period, CDIP 106 (Waimea Bay buoy), December 2001 to June 2023

Table 5-4. Northerly swell significant wave height vs. return period, CDIP 106 (Waimea Bay buoy), December 2001 to June 2023

Return Period	Hs (ft)
1	11.0
5	15.4
10	17.3
25	19.8
50	21.7

Table 5-5. Top 10 northerly swell events recorded at CDIP 106 (Waimea Bay buoy), December 2001 to June 2023

Date	Hs (ft)	Tp (sec)	Dp (deg. TN)
2009-03-14	19.8	15	10
2013-11-13	18.3	17	359
2003-11-29	15.3	13	3
2002-11-30	14.9	17	359
2021-03-14	14.8	12	8
2019-12-02	14.5	14	359
2009-11-12	14.5	13	18
2022-11-25	14.2	17	356
2020-02-08	13.8	13	13
2021-12-05	13.2	15	359

5.4.3.2 Tradewind Waves

For extreme deepwater waves associated with tradewind waves, wave buoy data was compiled from CDIP buoy station 098 located offshore from Mokapu Point approximately 17.0 miles to the southeast of the project site (Figure 5-9). Wave data for this buoy spans a 22-year period between August 2000 and October 2023. Extreme wave heights were investigated by filtering the buoy data by direction and period for waves approaching from the northeast to east-southeast directions, with periods of 12 seconds or less. Wave height versus return period (probability of wave height occurring in any given year) is shown on Figure 5-15 and

Table 5-6. The ten largest wave events associated with tradewind swell during the period of record are shown in Table 5-7.

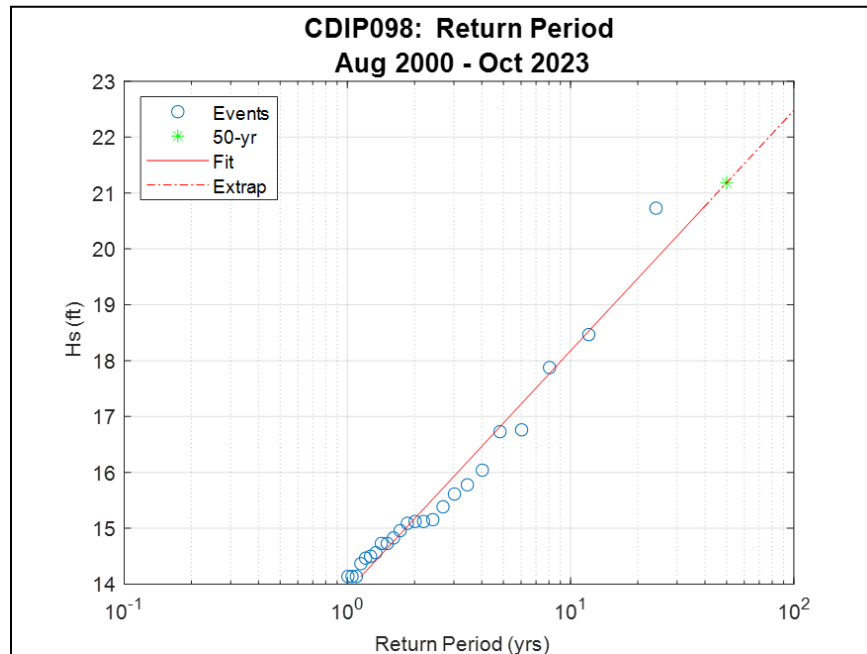


Figure 5-15. Tradewind waves significant wave height vs. return period, CDIP 098 (Mokapu Point buoy), August 2000 to October 2023

Table 5-6. Tradewind waves significant wave height vs. return period, CDIP 098 (Mokapu Point buoy), August 2000 to October 2023

Return Period	Hs (ft)
1	13.9
5	16.9
10	18.2
25	19.9
50	21.2

Table 5-7. Top 10 tradewind wave events recorded at CDIP 098 (Mokapu Point buoy), August 2000 to October 2023

Date	Hs (ft)	Tp (sec)	Dp (deg. TN)
2001-12-14	20.7	11.8	84.5
2002-01-19	18.5	11.8	62.0
2018-09-12	17.9	11.1	84.9
2017-01-22	16.8	9.1	35.7
2013-01-05	16.7	9.9	58.2
2023-02-10	16.0	9.9	73.3
2003-11-22	15.8	11.1	31.1
2015-12-20	15.6	9.9	69.5
2008-01-27	15.4	10.5	50.8
2007-12-29	15.2	11.1	74.7

6. DESIGN PARAMETERS AND NUMERICAL WAVE MODELING

The development of beach restoration concepts requires determination of the design water level and wave conditions along the study shoreline. As deepwater waves propagate toward shore, they begin to encounter and be transformed by the ocean bottom. In shallow water, the wave speed becomes related to the water depth. As waves slow down with decreasing depth, the process of wave shoaling steepens the wave and increases the wave height. Wave breaking occurs when the wave profile shape becomes too steep to be maintained. This typically occurs when the ratio of wave height to water depth is about 0.78 and is a mechanism for dissipating the wave energy. Wave energy is also dissipated due to bottom friction. The phenomenon of wave refraction is caused by differential wave speed along a wave crest as the wave passes over varying bottom contours and can cause wave crests to converge or diverge and may locally increase or decrease wave heights. Not strictly a shallow water phenomenon, wave diffraction is the lateral transmission of wave energy along the wave crest and would cause the spreading of waves in a shadow zone, such as occurs behind a breakwater or other barrier. Two numerical wave models, SWAN and XBeach-NH were utilized for this study to simulate the wave transformation from deep water to the study shoreline.

SWAN

Simulating Waves Nearshore (SWAN) is a third-generation wave model developed by Delft University of Technology that computes random, short-crested wind-generated waves in coastal regions and inland waters (*Booij et al, 1999*). The SWAN model can be applied as a steady state or non-steady state model and is fully spectral (over the total range of wave frequencies). Wave propagation is based on linear wave theory, including the effect of wave generated currents. SWAN provides many output quantities, including two-dimensional spectra, significant wave height and mean wave period, and average wave direction and directional spreading. For this study, the SWAN model was used to transform waves from deep water to intermediate water depths just offshore from the Punalu‘u region. SWAN model results were used to provide wave parameter input for the nearshore numerical wave model, XBeach.

XBeach-NH

As waves move into shallow water, bathymetry has a greater influence on wave behavior. Waves interact with the bottom, dissipating more energy through depth-induced breaking and bottom friction. Results of the SWAN model for the prevailing, annual, and extreme 50-year wave conditions were modeled from just offshore of the study area into the nearshore region using the XBeach non-hydrostatic (XBeach-NH) numerical model. XBeach is an open-source numerical wave model originally developed to simulate hydrodynamic and morphological processes along sandy shorelines. The XBeach-NH module (*Stelling and Zijlema, 2003*) computes the depth-averaged flow due to waves and currents using the non-linear shallow water equations and includes a non-hydrostatic pressure term. The governing equations are valid from intermediate to shallow water and can simulate most of the phenomena of interest in the nearshore zone and in harbor basins, including shoaling and refraction over variable bathymetry, reflection and diffraction near structures, energy dissipation due to wave breaking and bottom friction, breaking-induced longshore/cross-shore (“rip”) currents, and harbor oscillations. XBeach-NH is a phase resolving model, meaning that wave crests and troughs are modeled and propagated in time and space. The result is an accurate representation of wave heights and wave patterns across the domain.

6.1 Design Still Water Level

Wave models require an estimation of the still water level across the model domain for the modeled conditions. In the present analysis, the total still water level rise (see Section 5.3) considered is a linear combination of the following components:

1. Astronomical tide
2. Sea level rise
3. Sea level anomaly
4. Wave setup

An astronomical tide of +1.1 ft MSL is used for models of design wave conditions. This is equivalent to the mean higher high water (MHHW) level, relative to MSL, as measured at the Moku o Lo‘e tidal station and is typical of a high tide condition at the Punalu‘u shoreline.

Two (2) sea level rise values including +1.6 and +3.2 ft are included in the numerical modeling of nearshore waves. Additionally, existing sea level is included in the nearshore wave modeling to assess current conditions along the shoreline and how they may change with rising sea levels.

A local sea level anomaly of +0.25 ft MSL is also included as part of the design water level. This is a typical value commonly used for planning and design purposes and represents typical anomaly levels which may be present during a design event.

Another design water level component is wave setup which is a complex phenomenon and occurs at the shoreline due to breaking waves offshore. Wave setup is most accurately predicted using the XBeach-NH numerical wave model and is calculated as part of the simulated wave transformation by the model.

The total still water levels used for numerical modeling is +1.35, +2.95, and +4.55 ft MSL for each of the SLR cases in this study (Table 6-1).

Table 6-1. Design water level components relative to MSL for numerical modeling

Component	Exist Level (ft)	+1.6 ft Level (ft)	+3.2 ft Level (ft)
Astronomical Tide	+1.10	+1.10	+1.10
Sea Level Rise	0.00	+1.60	+3.20
Sea Level Anomaly	+0.25	+0.25	+0.25
TOTAL:	+1.35	+2.95	+4.55

6.2 Offshore Wave Transformation

For this study, an unstructured mesh grid was developed for the SWAN model that covers the island of O‘ahu specifically surrounding the northwest and eastern facing shorelines (see Figure 6-1). Unstructured mesh grids allow for coarse resolution in offshore regions where waves are not influenced by the seafloor and fine resolution nearshore where wave transformation is more of a function of the water depth. The resolution of the SWAN domain varies from 0.6 mi (1 km)

offshore in deepwater to 656 ft (200 m) in intermediate water depths within the model domain. The grid resolution is further refined around the Punalu'u region to a resolution of 164 ft (50 m).

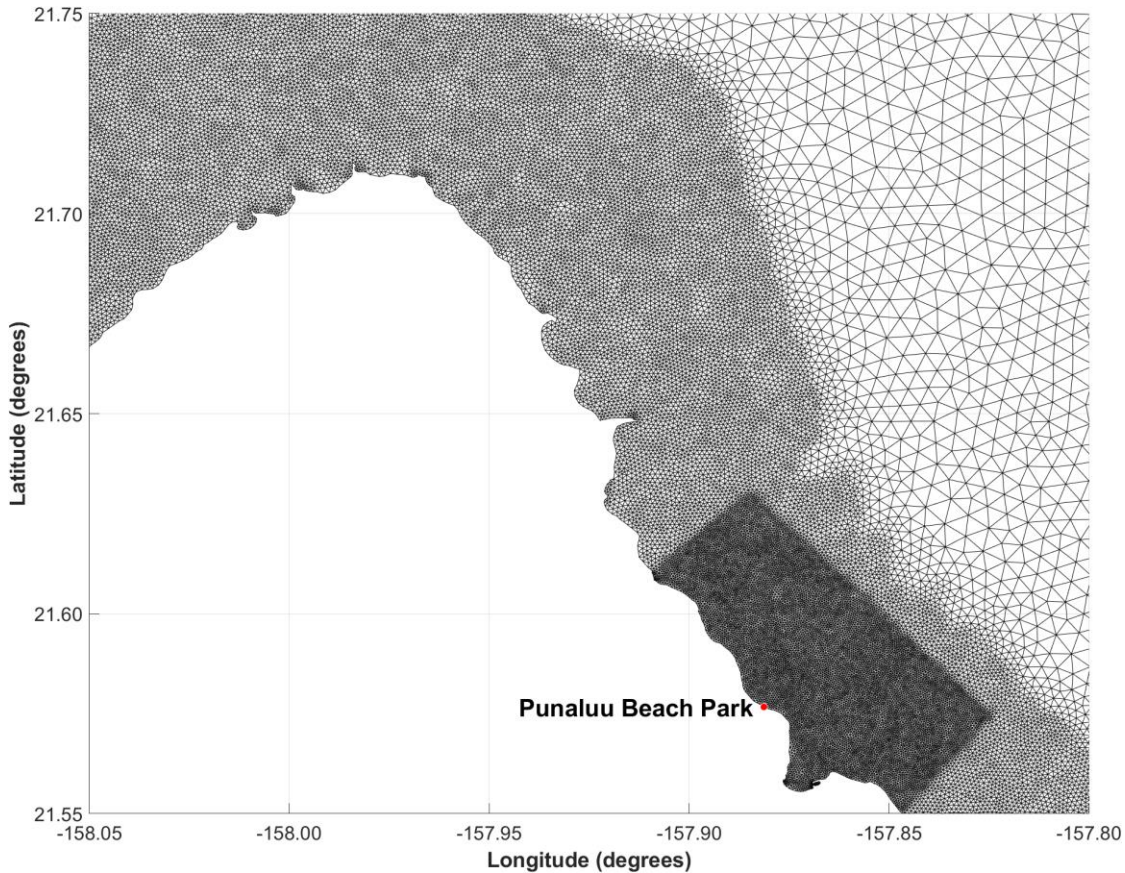


Figure 6-1. SWAN unstructured mesh

6.2.1 Prevailing Waves

The most prevalent waves that reach the Punalu'u shoreline are winter northerly swells and tradewind waves. Table 6-2 lists the prevailing deepwater wave parameters (see Section 5.4) used as input for the SWAN model for each prevailing wave condition. These parameters are applied along all boundaries of the unstructured SWAN grid. Figure 6-2 shows the modeled output for significant wave height near the project site for both prevailing north swell and tradewind waves. The results illustrate the propagation of offshore wave energy associated with typical winter (north swell) and tradewind waves along the windward Oahu coastline and where wave energy may converge or diverge based on the seafloor contours. For both north swell and tradewind waves, wave energy appears to focus to the north and east of Punalu'u and slightly diverge to the northeast. More energy is distributed along the offshore reef edge and closer to shore for tradewind waves than north swell which may influence nearshore wave processes differently in the surrounding region. Nearshore wave processes are modeled using XBeach-NH (see Section 6.3).



Table 6-2. Modeled prevailing wave cases (inputs to SWAN model)

Wave Case	Deepwater Wave Parameters		
	Hs (ft)	Tp (sec)	Dir. (deg. TN)
North Swell	3.1	12.5	360.0
Tradewind Waves	6.0	8.0	67.5

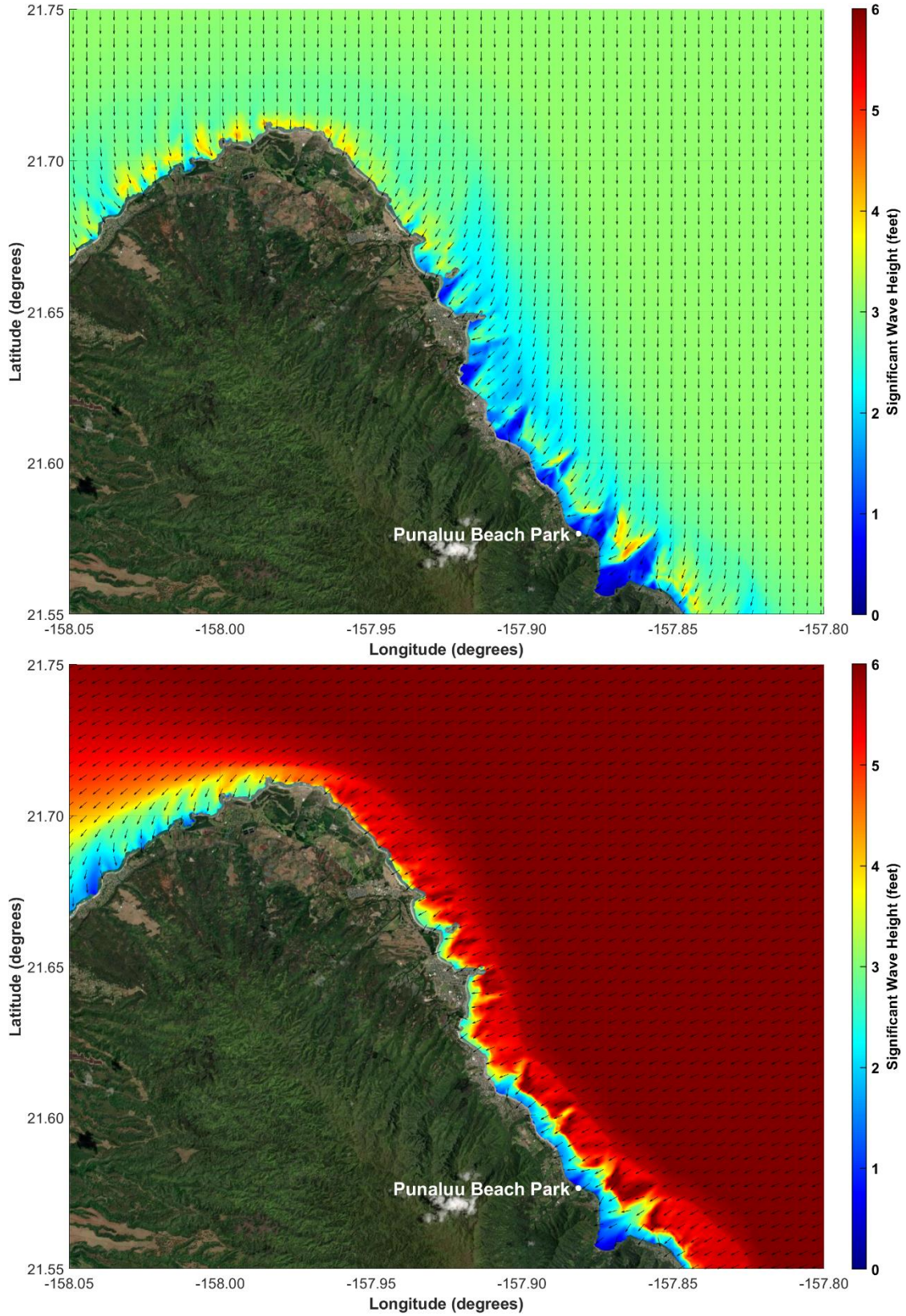


Figure 6-2. SWAN modeled significant wave height for prevailing north swell (top) and tradewind waves (bottom)

6.2.2 Annual Waves

Table 6-3 lists the annual deepwater wave parameters (see Section 5.4) used as input for the SWAN model for each wave condition. These parameters are applied along all boundaries of the unstructured SWAN grid. Figure 6-3 shows the modeled output for significant wave height near the project site for both the annual north swell and tradewind wave events. Similar to prevailing waves, both north swell and tradewind wave energy appears to focus to the north and east of Punalu'u and slightly diverge to the northeast. More energy is distributed along the offshore reef edge and closer to shore for tradewind waves than north swell which may influence nearshore wave processes differently in the surrounding region. Nearshore wave processes are modeled using XBeach-NH (see Section 6.3).

Table 6-3. Modeled annual wave cases (inputs to SWAN model)

Wave Case	Deepwater Wave Parameters		
	Hs (ft)	Tp (sec)	Dir. (deg. TN)
North Swell	11.0	15.0	5.0
Tradewind Waves	13.9	10.0	67.5

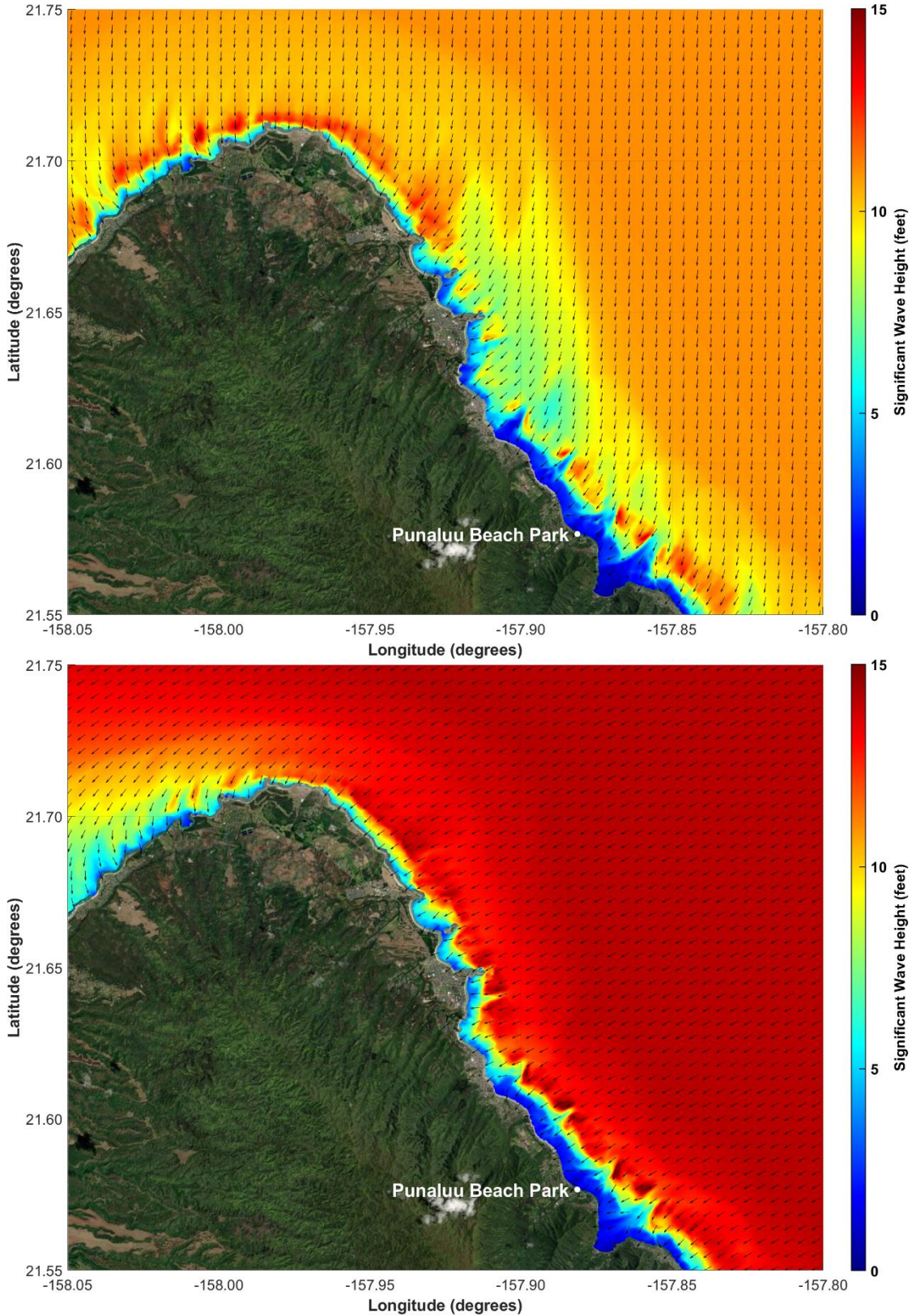


Figure 6-3. SWAN modeled significant wave height for an annual north swell (top) and tradewind waves (bottom)

6.2.3 Extreme Waves

Table 6-4 lists the 50-yr deepwater wave parameters (see Section 5.4) used as input for the SWAN model for each wave condition. These parameters are applied along all boundaries of the unstructured SWAN grid. Figure 6-4 shows the modeled output for significant wave height near the project site for both the 50-yr north swell and tradewind wave events. Both north swell and tradewind wave energy appears to be more evenly distributed along the offshore reef than the prevailing and annual wave cases. This is likely attributed to larger waves which break in deeper water and essentially along most of the offshore edge of the reef flat in the surrounding area. More energetic offshore waves will drive more energetic nearshore processes such as wave setup, currents, and nearshore wave heights. Nearshore wave processes are modeled using XBeach-NH (see Section 6.3).

Table 6-4. Modeled 50-yr wave cases (inputs to SWAN model)

Wave Case	Deepwater Wave Parameters		
	Hs (ft)	Tp (sec)	Dir. (deg. TN)
North Swell	21.7	15.0	5.0
Tradewind Waves	21.2	12.0	67.5

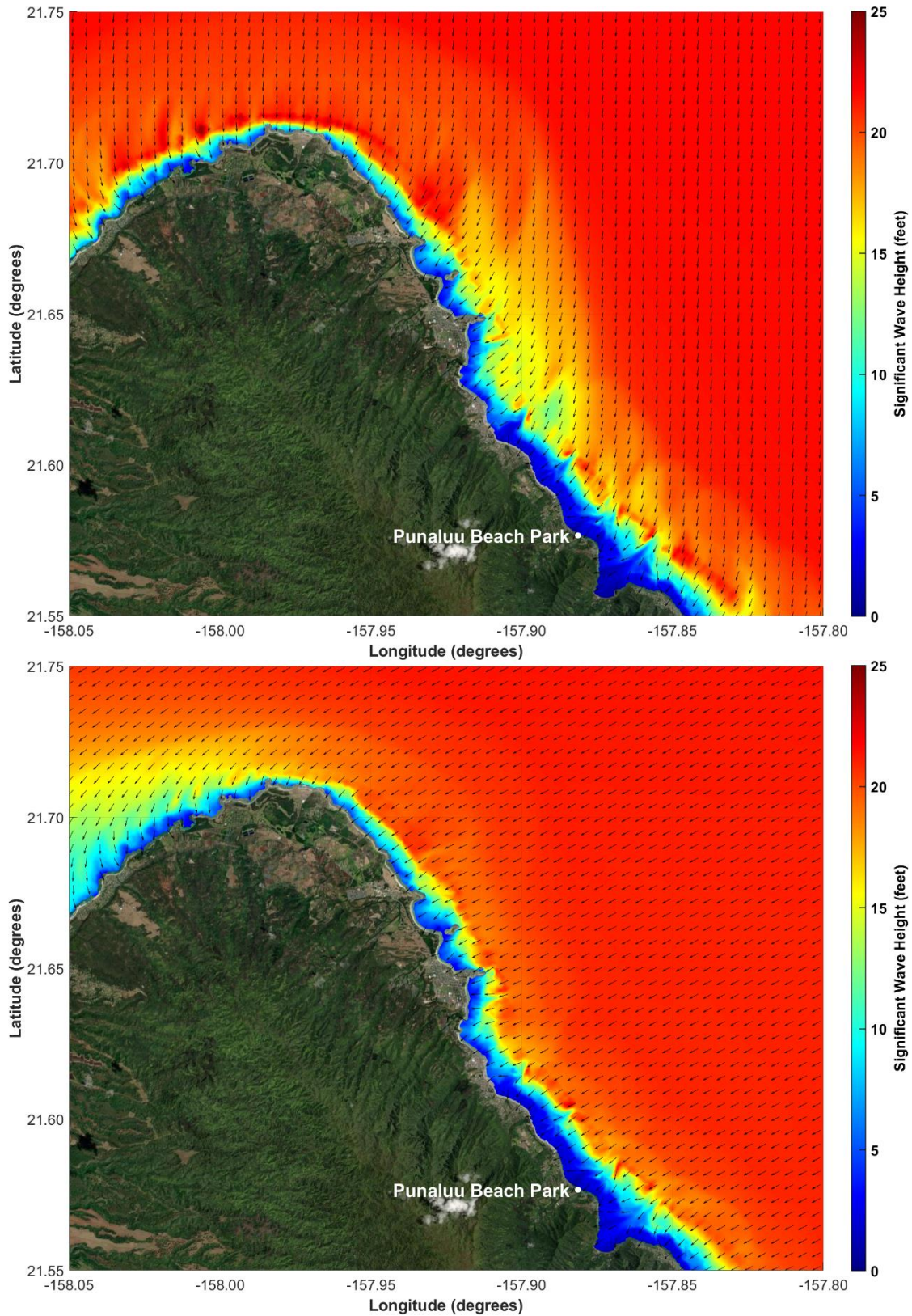


Figure 6-4. SWAN modeled significant wave height for a 50-yr north swell (top) and tradewind waves (bottom)

6.3 Nearshore Wave Transformation and Processes

The XBeach-NH model was used to simulate the wave transformation from intermediate water depths to the project site shoreline and surrounding nearshore waters. Model bathymetry was adapted from a combination of the USACE SHOALS LiDAR dataset, the *Continuously Updated Digital Elevation Model (CUDEM) - Ninth Arc-Second Resolution Bathymetric-Topographic Tiles for the Hawaiian Islands*, and the topographic data collected by SEI of the beach and nearshore waters on November 22, 2022 (see Section 3.2). A model resolution of 6.6 ft (2 m) was chosen. Figure 6-5 shows the XBeach-NH model extent. Results from the SWAN model runs were used as input to the XBeach-NH model runs for prevailing, annual, and extreme 50-yr wave cases associated with tradewind waves. The output parameters from XBeach-NH include water surface elevation, significant wave height, wave setup, and depth-averaged velocity over the model domain.

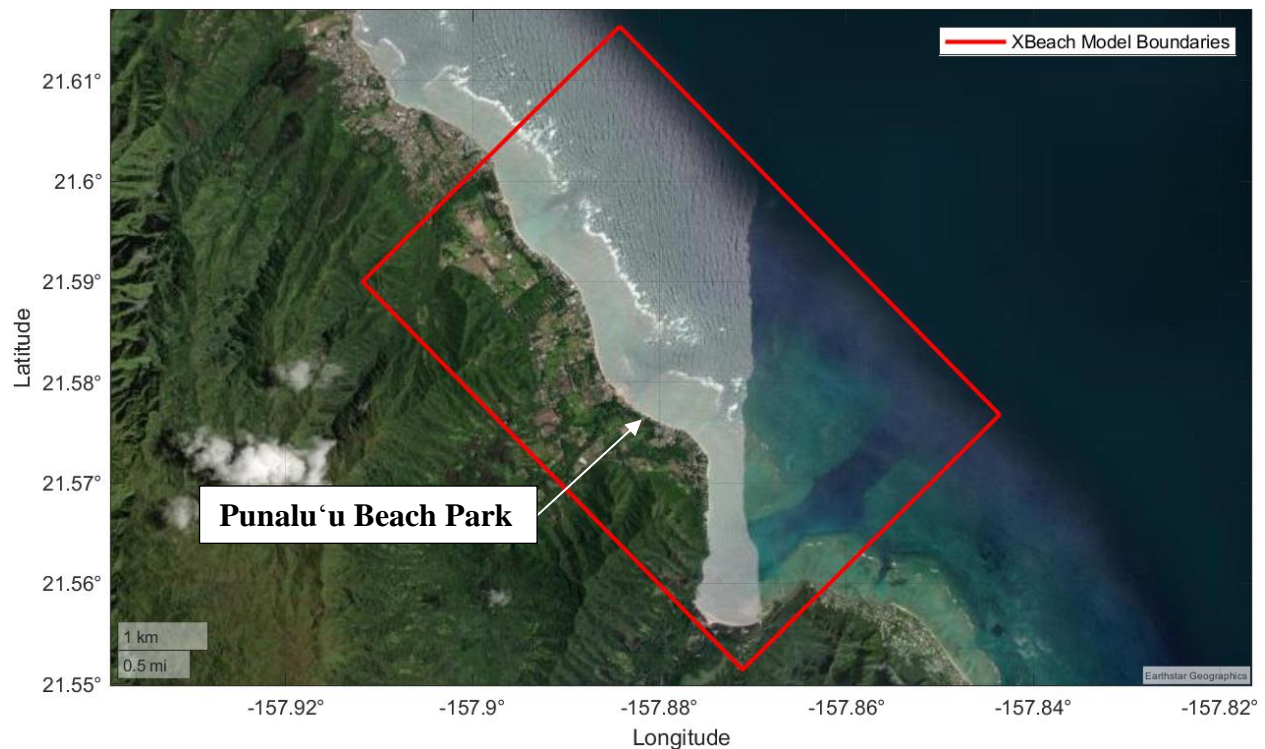


Figure 6-5. XBeach-NH model domain extent

6.3.1 Prevailing Waves

6.3.1.1 North Swell

Figure 6-6, Figure 6-7, and Figure 6-8 show the XBeach-NH model outputs for water surface elevation (single snapshot), significant wave height, and depth-averaged flow velocity for a prevailing north swell.

The modeled nearshore wave patterns show signs of multiple wave fronts incoming over the reef flat. Wave fronts refracted over the deeper Punalu‘u sand channel north of the comfort station approach from a northerly directly once they reach the shoreline while wave fronts refracted by

the deeper channel south of the beach park approach from a more easterly direction near shoreline. Wave fronts coming directly over the reef flat from the northeast appear to approach the nearshore straight on. As these various wave fronts cross over each other, wave heights may increase (constructive wave crests) or decrease (destructive wave crests) causing significant variability in the distribution of wave height and energy along the shoreline and in the nearshore. This difference in wave crest and shoreline orientation may promote longshore sediment transport in the direction of the wave propagation.

The modeled significant wave height along the Punalu‘u shoreline varies with wave heights up to 1.5 ft on the shallow reef flat and wave heights less than 1 ft in the deeper sand channel north of the comfort station. This is expected as the waves in the deeper channel will maintain their speed while the waves over the shallower reef slow down. The shallower areas will generally attract more wave energy than the deep channels as wave refract over the complex bottom. The model results provide a useful tool in identifying areas along the shoreline that attract more wave energy than other areas. The southern portion of the Punalu‘u shoreline shows more wave energy than the northern portion beach park. This may partially explain why historical erosion rates of the shoreline are larger towards the south end of the park.

Depth-averaged flow patterns from the model show a north to south flow of water along the shoreline north of the Punalu‘u sand channel and south to north flow south of the sand channel. Modeled flow paths converge at the sand channel and are redirected offshore from the beach park. This trend in nearshore currents is likely attributed to the oblique wave approach discussed previously and the deep-water channel providing a release conduit for wave-elevated water levels across the reef flat. These flow patterns may promote longshore sediment transport during the winter months with north pacific swell. Any sediment suspended off the beach by the waves and into the nearshore waters may be carried by these nearshore currents until they settle to the seafloor.

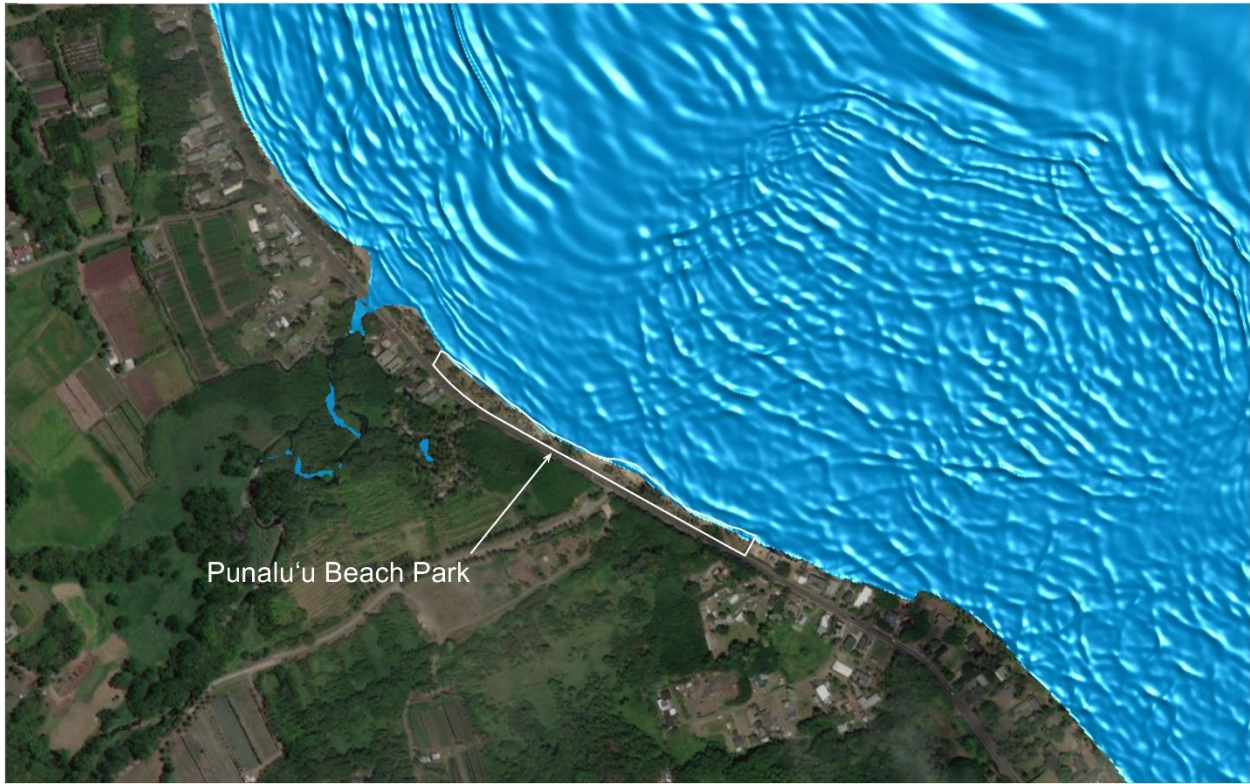


Figure 6-6. Water surface snapshot from XBeach-NH model for a prevailing north swell

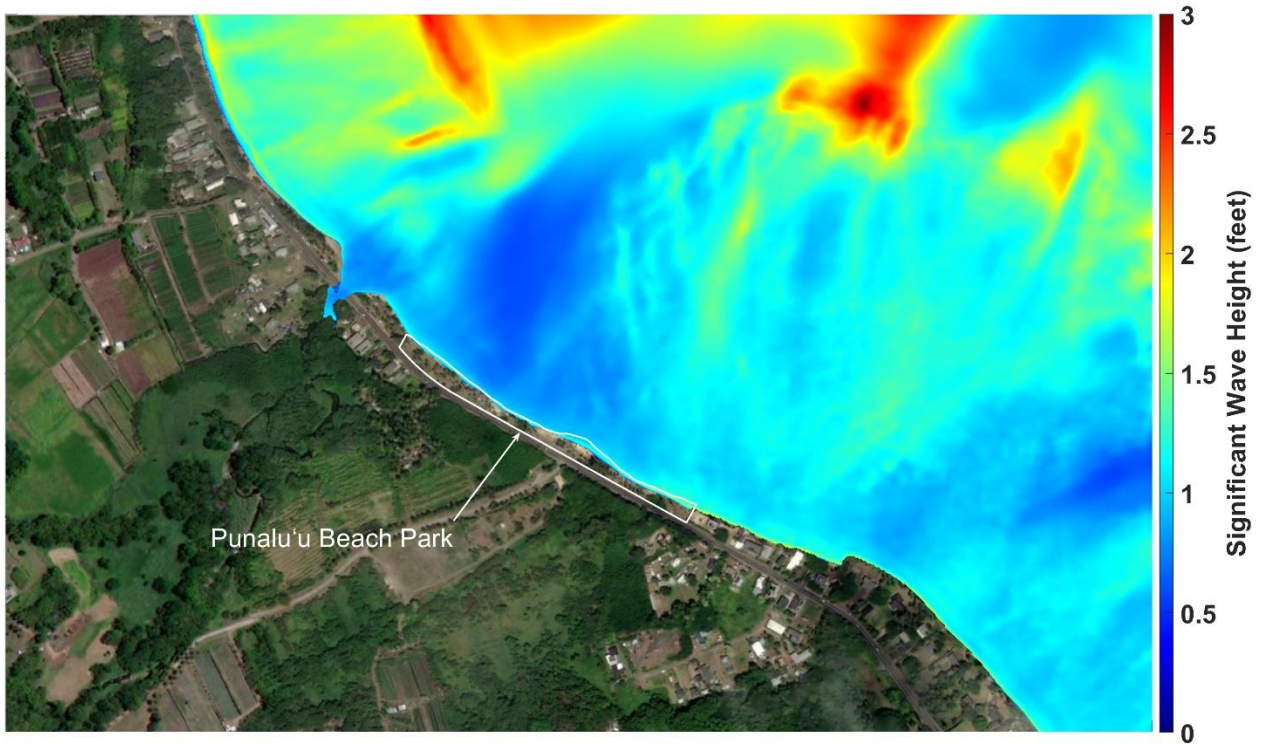


Figure 6-7. Significant wave height from XBeach-NH model for a prevailing north swell

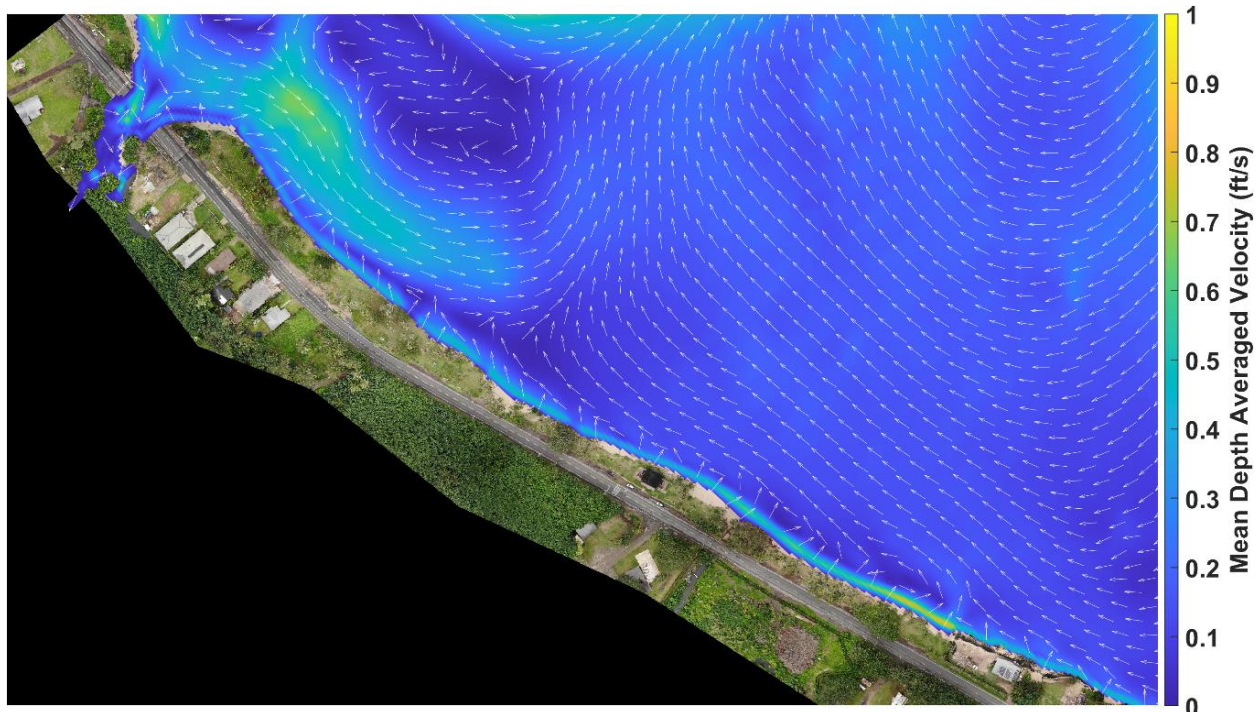


Figure 6-8. Depth-averaged flow velocity from XBeach-NH for a prevailing north swell

6.3.1.2 Tradewind Waves

Figure 6-9, Figure 6-10, and Figure 6-11 show the XBeach-NH model outputs for water surface elevation (single snapshot), significant wave height, and depth-averaged flow velocity for a prevailing tradewind wave.

Similar to north swell, the modeled nearshore wave patterns for tradewind waves show signs of multiple wave fronts incoming over the reef flat. For this case the wave crests are closer together which is likely attributed to the shorter wave period associated with these waves. Wave fronts refracted over the deeper Punalu'u sand channel north of the comfort station approach from a northerly direction once they reach the shoreline while wave fronts refracted by the deeper channel south of the beach park approach from a more easterly direction near shoreline. Wave fronts coming directly over the reef flat from the northeast appear to approach the nearshore straight on. As these various wave fronts cross over each other, wave heights may increase (constructive wave crests) or decrease (destructive wave crests) causing significant variability in the distribution of wave height and energy along the shoreline and in the nearshore. The difference between wave crest and shoreline orientation may promote longshore sediment transport in the direction of the wave propagation.

Similar to prevailing north swell, the modeled significant wave height for tradewind waves along the Punalu'u shoreline varies with wave heights up to 1.5 ft on the shallow reef flat and wave heights less than 1 ft in the deeper sand channel north of the comfort station. This is expected as the waves in the deeper channel will maintain their speed while the waves over the shallower reef slow down. The shallower areas will generally attract more wave energy than the deep channels as wave refract over the complex bottom. The model results provide a useful tool in identifying

areas along the shoreline that attract more energy than other areas. The southern portion of the Punalu'u shoreline experiences more wave energy than the northern portion beach park. This may explain why historical erosion rates of the shoreline are larger towards the south end of the park. Because this pattern is seen for both north swell and tradewind wave conditions, the south end of the shoreline likely experiences these conditions throughout most of the year.

Depth-averaged flow patterns from the model for the tradewind wave case show similar patterns as the north swell wave case. North to south flow of water is observed along the shoreline north of the Punalu'u sand channel and south to north flow south of the sand channel. Modeled flow paths converge at the sand channel and are redirected offshore from the beach park. These flow patterns may promote longshore sediment transport during tradewind wave conditions. Any sediment suspended off of the beach by the waves and into the nearshore waters may be carried by these nearshore currents until they settle to the seafloor. These results suggest that sand eroded from Punalu'u beach may be transported by a combination of nearshore waves and currents away from the shoreline and out of the beach system via the sand channel.

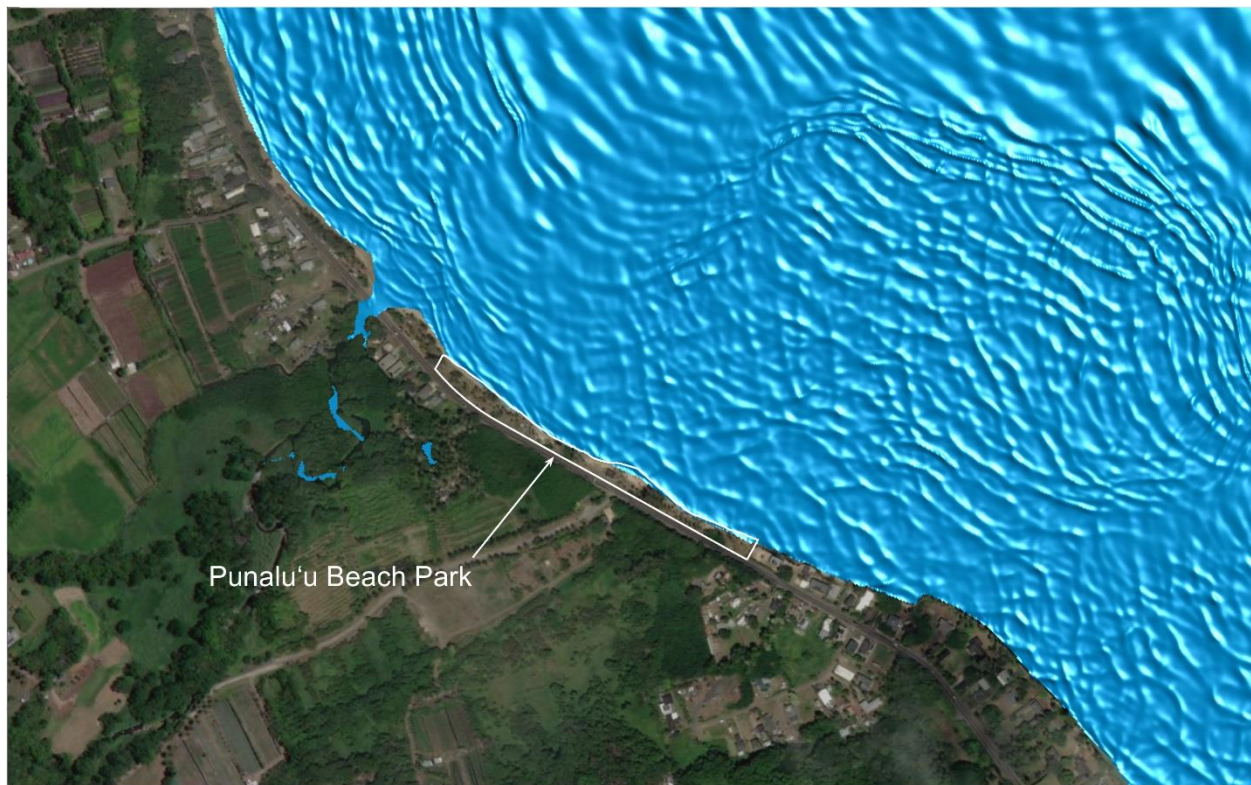


Figure 6-9. Water surface snapshot from XBeach-NH model for a prevailing tradewind waves

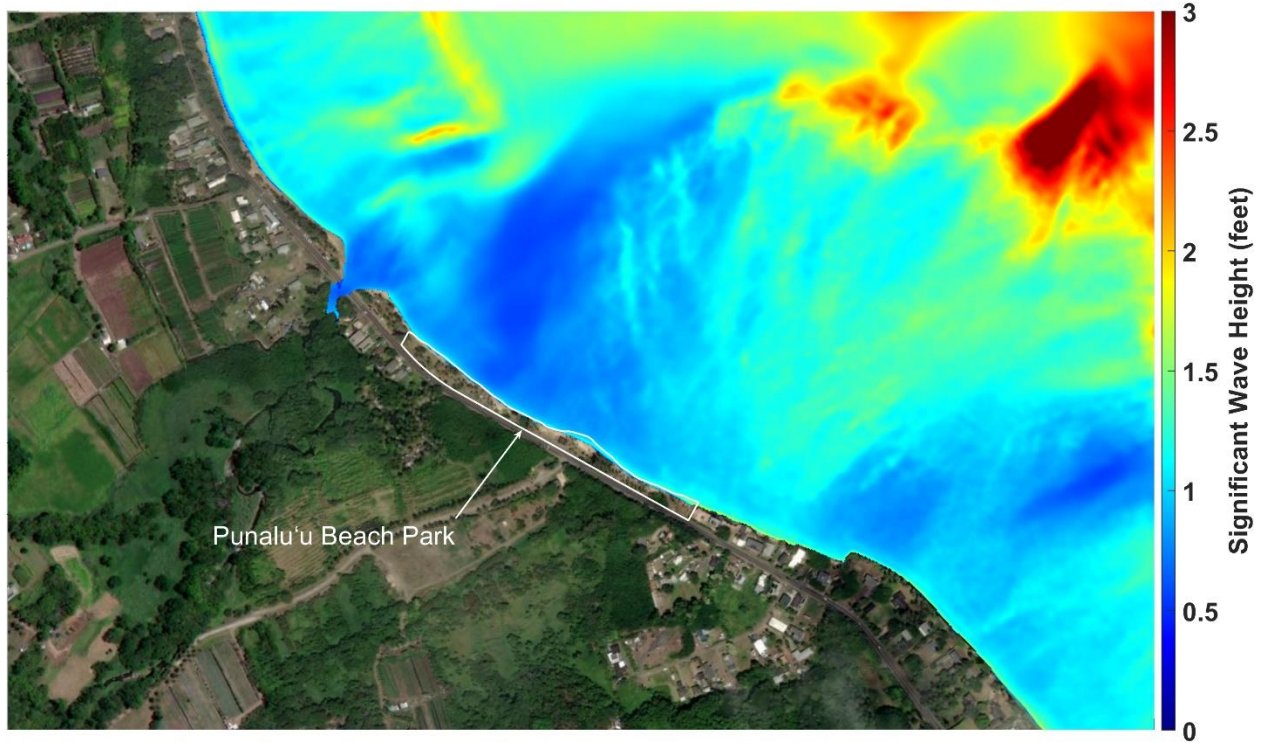


Figure 6-10. Significant wave height from XBeach-NH model for a prevailing tradewind waves

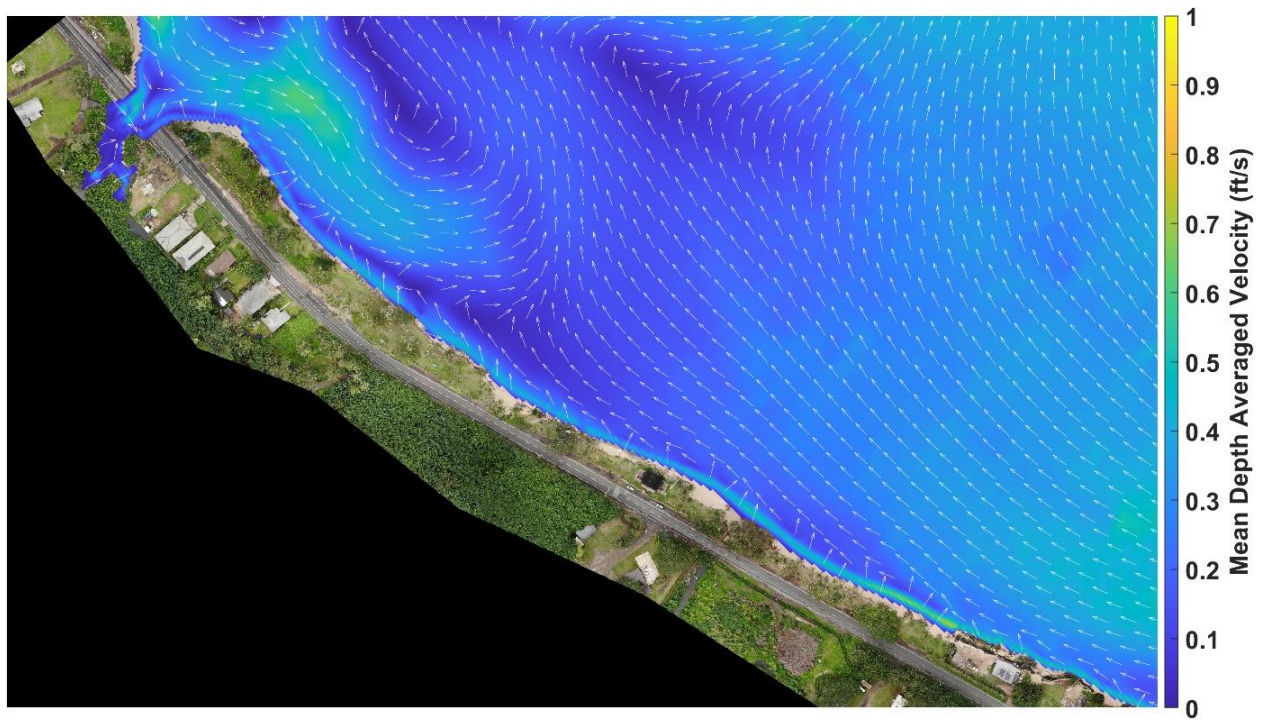


Figure 6-11. Depth-averaged flow velocity from XBeach-NH for a prevailing tradewind waves

6.3.2 Annual Waves

Similar to the prevailing wave case, it was found that tradewind waves produced larger waves near the shoreline than north swell for the annual return period events. Figure 6-12 through Figure 6-14 show the XBeach-NH modeled significant wave height for the annual tradewind wave cases under existing sea level and +1.6 and +3.2 ft of SLR. Higher wave energy is represented in the figures by the color red. The sequence of figures below shows the increase in wave energy as indicated by the red color moving closer to shore. This increase in nearshore wave energy is due to sea level rise, as larger waves are able to cross over the reef and reach the shoreline. It should be noted that the offshore reef is not adjusted to account for reef growth/accretion over time. This is a conservative assumption for modeling purposes and likely reef growth/accretion will not be able to keep up with future SLR.

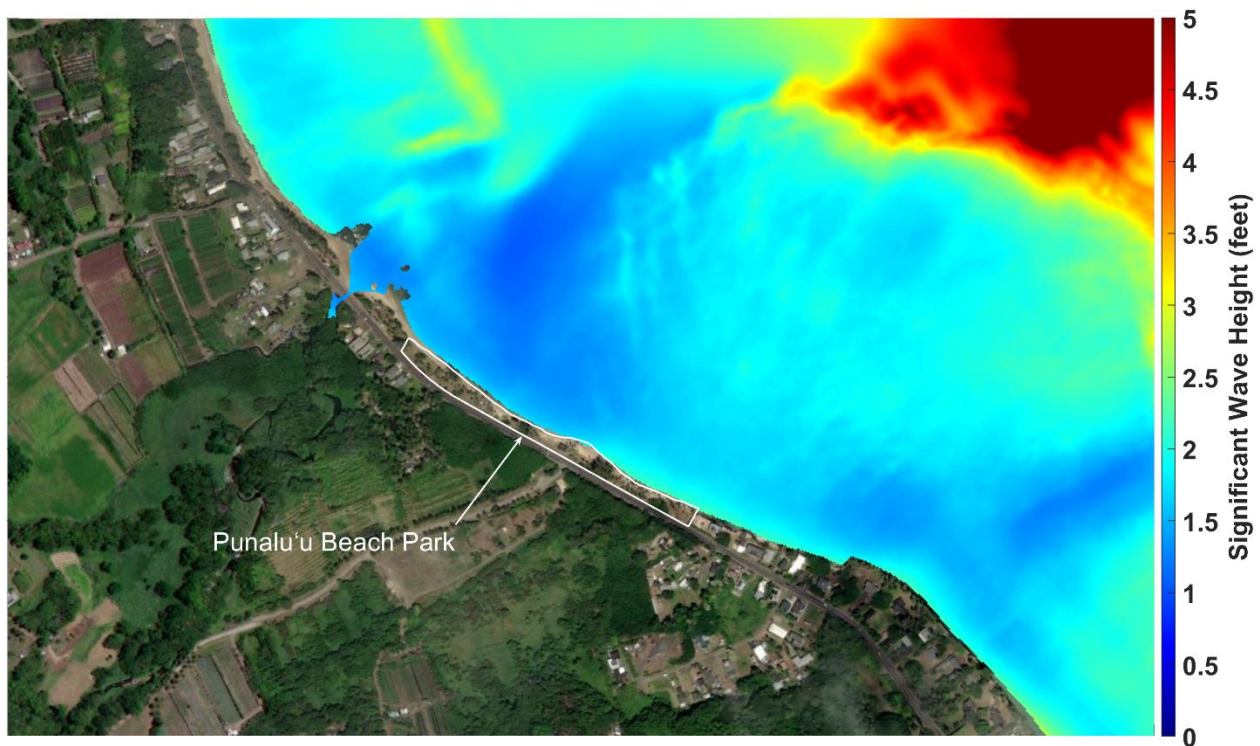


Figure 6-12. Significant wave height from XBeach-NH model for annual tradewind waves under existing sea level

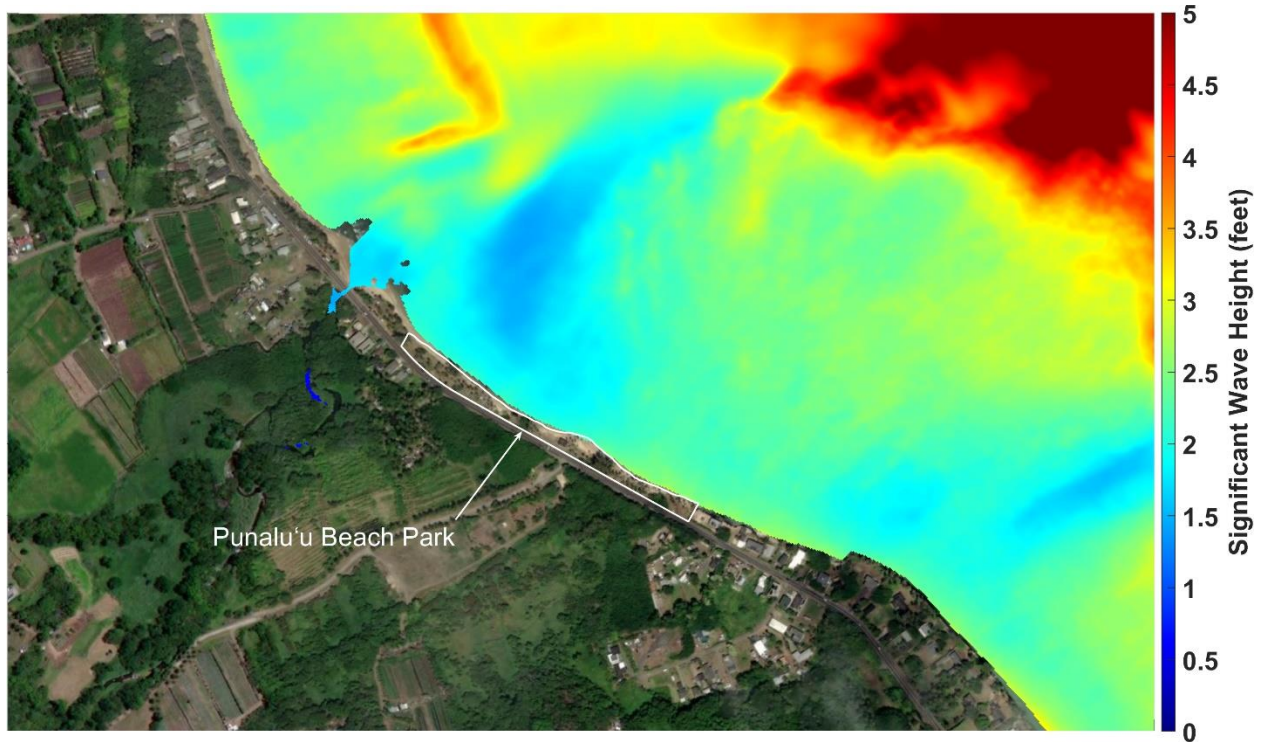


Figure 6-13. Significant wave height from XBeach-NH model for annual tradewind waves with +1.6ft of SLR

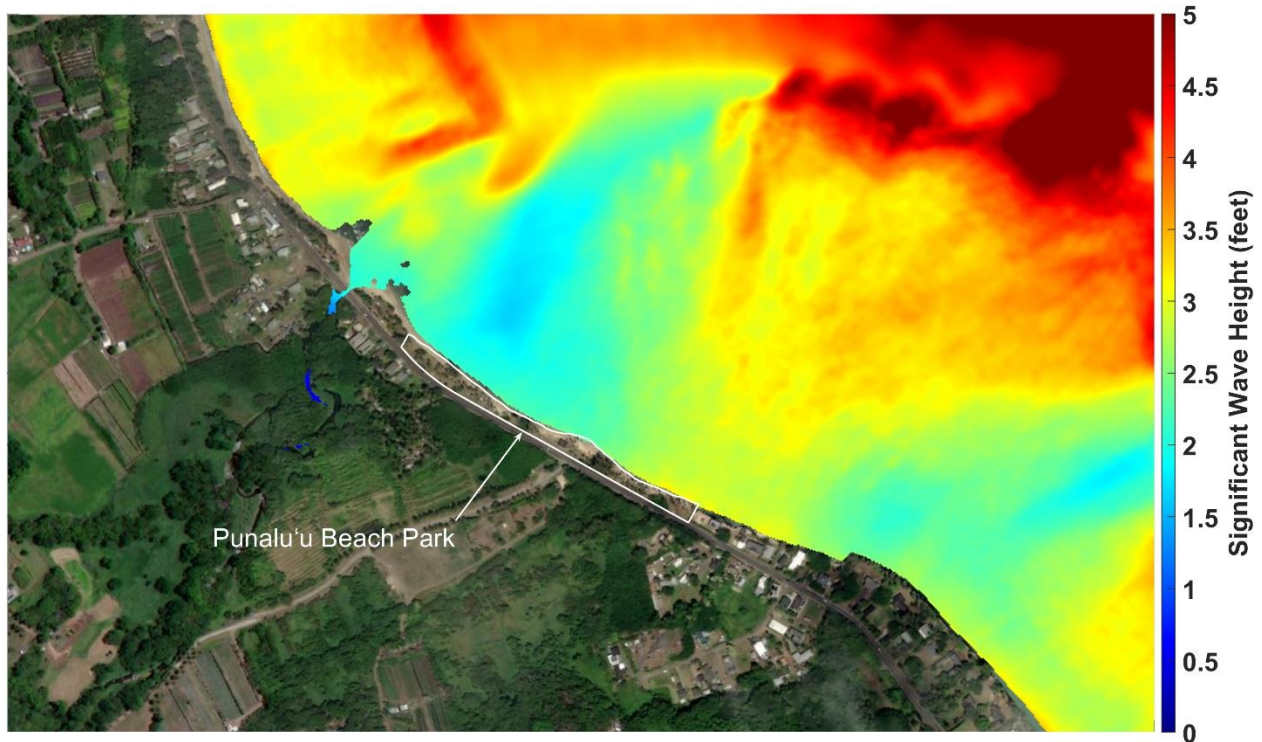


Figure 6-14. Significant wave height from XBeach-NH model for annual tradewind waves with +3.2ft of SLR

6.3.3 50-yr Waves

Similar to the annual wave case, it was found that tradewind waves produced the larger waves near the shoreline than north swell for the 50-yr return period events. Figure 6-15 through Figure 6-17 show the XBeach-NH modeled significant wave height for the annual tradewind wave cases under existing sea level and +1.6 and +3.2 ft of SLR. These model results show the increase in nearshore wave energy due to sea level rise as larger waves are able to cross over the reef and reach the shoreline. The model shows a significant increase in wave energy reaching the shoreline for the 50-yr wave case with up to 4 ft waves fronting the beach park at the southern end.

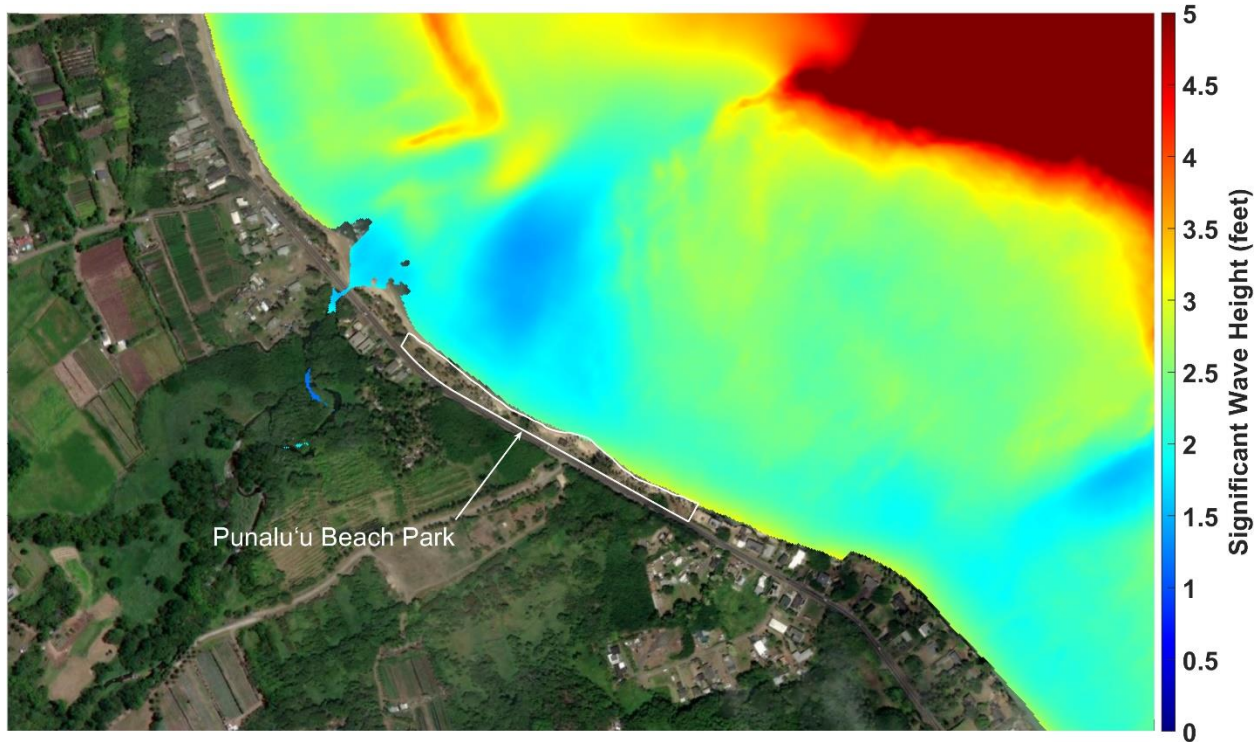


Figure 6-15. Significant wave height from XBeach-NH model for 50-yr tradewind waves under existing sea level

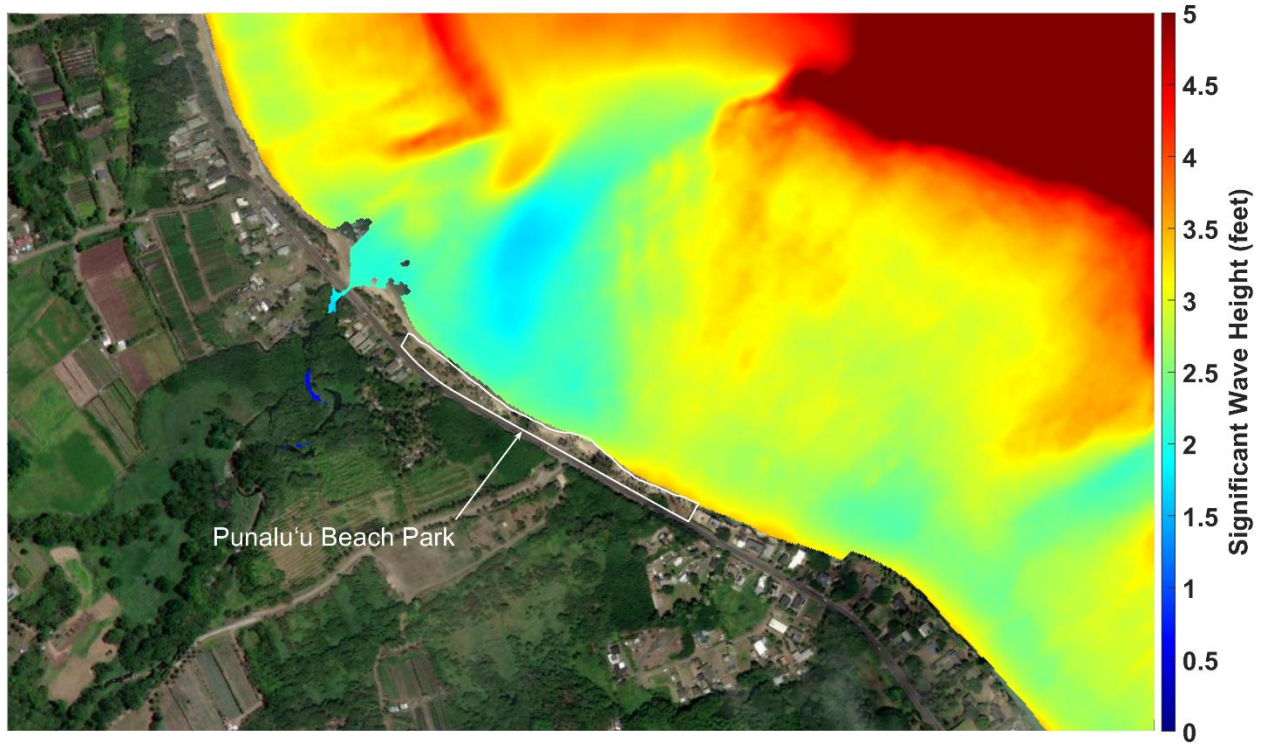


Figure 6-16. Significant wave height from XBeach-NH model for 50-yr tradewind waves with +1.6ft of SLR

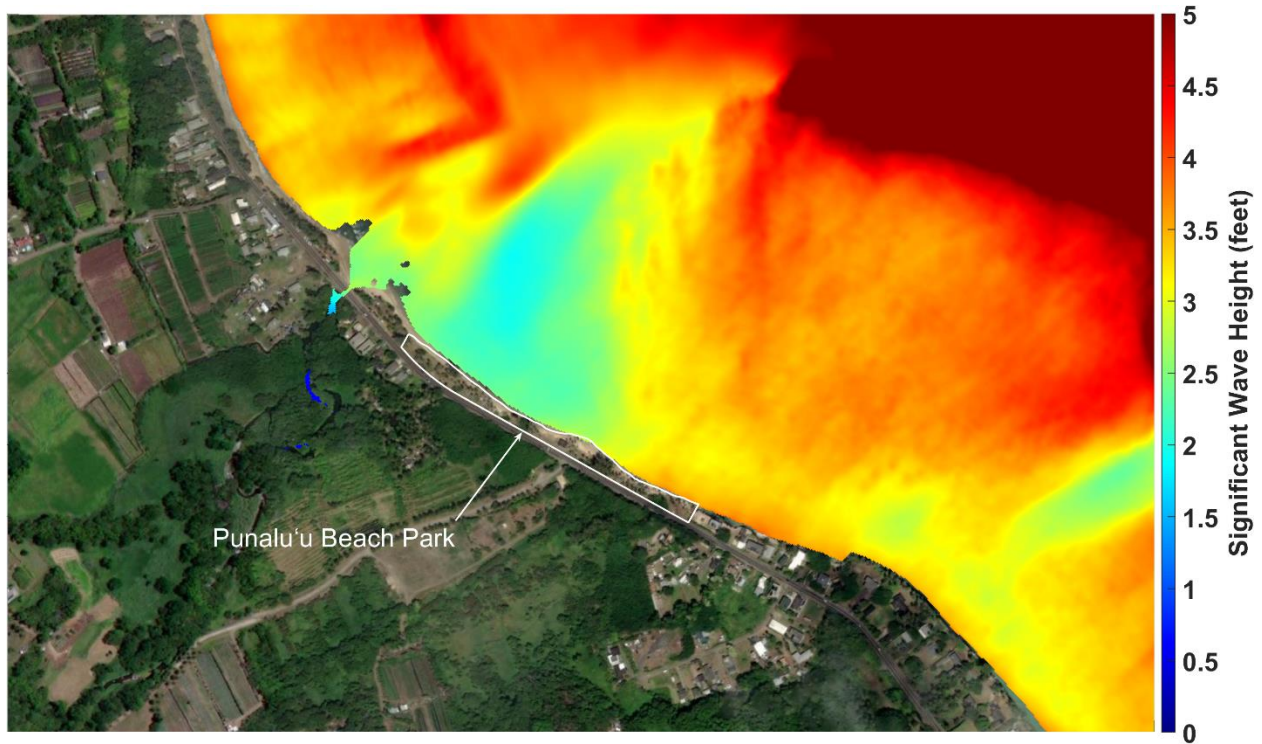


Figure 6-17. Significant wave height from XBeach-NH model for 50-yr tradewind waves with +3.2ft of SLR

6.4 Wave Runup

Development of coastal protection alternatives requires runup elevations at the site to determine the required height of beach fill and shoreline structure features to minimize wave runup and overtopping. For this study, a 2% overtopping threshold ($R_{2\%}$) is assumed and is found using the methodology outlined in the Eurotop Manual on wave overtopping of sea defenses and related structures (Van der Meer et al., 2016). This manual gives general and design guidance on wave runup and overtopping using a semi-probabilistic approach based on a large international dataset of physical model tests. The equation for determining $R_{2\%}$ for a typical beach face is shown in the equation below:

$$\frac{R_{2\%}}{H_{m0}} = 1.07 * \left(4 - \frac{1.5}{\sqrt{\xi_{m-1,0}}} \right)$$

where,

H_{m0} is the significant wave height at the beach toe

$R_{2\%}$ is the runup elevation exceeded by 2% of the incoming waves

$\xi_{m-1,0}$ is the surf similarity parameter (ratio of beach steepness to wave steepness)

For rubblemound structures with a permeable core, the equation for maximum wave runup reduces to:

$$\frac{R_{2\%}}{H_{m0}} = 2.14$$

The significant wave height for the runup analysis from each wave condition was determined from the XBeach-NH model results presented in the previous sections. The model results show both north swell and tradewinds waves produced similar wave heights near the shore with tradewinds slightly larger. Tradewind wave conditions were chosen for design of crest elevation and armor stability for this study.

Wave runup on a beach face was assessed for both the prevailing and annual tradewind wave conditions for existing sea level and for both +1.6 and +3.2 ft of SLR. These results are shown in Table 6-5 and Table 6-6 for prevailing and annual wave conditions, respectively.

Table 6-5. Prevailing wave runup results on beach face with 1:8 slope

SLR Condition	$R_{2\%}$ (ft, MSL)
Existing	4.3
+1.6 ft SLR	7.4
+3.2 ft SLR	10.4

Table 6-6. Annual wave runup results on beach face with 1:8 slope

SLR Condition	$R_{2\%}$ (ft, MSL)
Existing	5.6
+1.6 ft SLR	8.5
+3.2 ft SLR	12.4

The wave runup on rubble mound structures was also assessed for both the prevailing and annual tradewind wave conditions for existing sea level and for both +1.6 and +3.2 ft of SLR. These results are shown in Table 6-7 and Table 6-8 for prevailing and annual wave conditions, respectively.

Table 6-7. Prevailing wave runup results on rubblemound structure with 1:1.5 slope

SLR Condition	$R_{2\%}$ (ft, MSL)
Existing	3.3
+1.6 ft SLR	6.0
+3.2 ft SLR	8.5

Table 6-8. Annual wave runup results on rubblemound structure with 1:1.5 slope

SLR Condition	$R_{2\%}$ (ft, MSL)
Existing	4.0
+1.6 ft SLR	6.8
+3.2 ft SLR	10.1

The largest calculated wave runup is produced by the annual tradewind wave event, reaching an elevation of +12.4 and +10.1 ft (MSL) for the beach face and rubblemound structure, respectively. For prevailing wave conditions, the largest runup values have elevations of +10.4 and +8.8 ft (MSL) for the beach face and rubblemound structure, respectively. These maximum runup elevations are associated with the +3.2 ft SLR scenario.

To design shoreline concepts for +3.2 ft of SLR, beach crest and stabilizing structure elevations would require minimum heights of +10.4 and +8.8 ft (MSL) so that overtopping would not occur during typical wave conditions. Additionally, backshore elevation should be high enough to limit overtopping during stronger annual wave events. This would require the backshore to be elevated to +12.4 ft (MSL). Due to the existing low-lying nature of the beach park, highway, and surrounding areas, designing shoreline concepts for +3.2 ft SLR may be impractical since most of the surrounding regions will likely be inundated. As an alternative, the shoreline concepts developed in this study use a design SLR of +1.6 ft for specifying the beach fill and stabilizing structure elevations. The calculated runup elevations for SLR of +1.6 ft are 6 ft for prevailing waves on a rubblemound structure and 8.5 ft for the annual wave on the beach backshore. However, consideration is given for +3.2 ft of SLR by ensuring the developed concepts plans are adaptable to high sea levels by accommodating the option to raise elevations as necessary.

6.5 Armor Stone Sizing

Structure stone size is based on extreme wave conditions discussed in Section 5.4.3. The analyses presented in Section 5.4.3 included large swell events (50-yr wave) for both north swell and tradewind waves. Tradewind waves were found to produce larger waves at the shoreline and were used for armor sizing. Hurricanes may also produce large waves at the study shoreline, however, due to the infrequency of these events in Hawai'i, the 50-yr tradewind wave case is chosen as the design condition. The scenario of +3.2 ft of SLR is chosen when choosing the design nearshore wave heights from the XBeach-NH model. This ensures that any shoreline stabilizing structures are stable across all SLR scenarios and adaptable to higher sea levels without requiring reconstruction with larger armor stone. The required armor stone weight for stability under this design wave height is given by the Hudson Formula (Coastal Engineering Manual, 2006).

$$W = \frac{w_r H^3}{K_D (S_r - 1)^3 \cot \theta}$$

where,

W = weight in pounds of an individual armor stone

w_r = unit weight of the stone, 160 lb/ft³

H = wave height, 4.8 ft (stabilizing structure) or 4.3 ft (revetment)

K_D = armor stone stability coefficient, 2 for stabilizing structure, 1.4 for revetment

S_r = specific gravity of the stone relative to seawater, use 2.5

$\cot \theta$ = cotangent of the stabilizing beach structure side slope, use 1.5

The resultant armor stone weight for the offshore headland structure would be approximately 1,800 lbs with a corresponding nominal diameter of 2.2 ft. A range of $\pm 25\%$ of the median weight is typically utilized, which yields a stone weight range of 1,300 to 2,300 lbs. It is recommended that the armor stone be keyed-and-fitted for an added level of stability.

For a shoreline revetment, the same formula is used, substituting 4.3 ft for the wave height and 1.4 for the armor stone stability coefficient, resulting in an armor stone weight of 1,800 lbs with a nominal diameter of 2.2 ft. A range of $\pm 25\%$ of the median weight is typically utilized, which yields a stone weight range of 1,300 to 2,300 lbs. It is recommended that armor stone for a revetment also be keyed-and-fitted for an added level of stability.

6.6 Underlayer Stone Sizing

The underlayer stone is sized at approximately 1/10 the armor weight, resulting in underlayer stone size between about 130 to 230 lbs for both the stabilizing beach structure and for the revetment. The sizing is important for providing porosity for energy dissipation rather than reflection, to achieve interlocking between the armor and underlayer, and to ensure that the underlayer material cannot be removed through voids in the armor layer.

Existing basalt boulders along the shoreline described in Sections 3.2.4 and 4.1 may be used for either armor or underlayer stone in either the headland or revetment structures to reduce the amount of stone to be imported to the site.

7. OFFSHORE SAND SOURCE INVESTIGATIONS

7.1 Introduction

A key component to the success of beach maintenance is the availability of suitable sand for beach nourishment. The potential sources of sand must be carefully evaluated in terms of quality, quantity, cost, and general feasibility. The majority of Hawai'i beaches are composed of calcareous (calcium carbonate) sand, made of skeletal fragments of marine organisms such as corals, coralline algae, mollusks, echinoids, and forams. The composition of sand is determined by the relative abundance of each species and therefore varies with location.

In the past, sand for beach nourishment was typically obtained from other beaches on O'ahu or from on-land deposits that were commercially available. However, these sources are no longer available. Offshore deposits present an alternative source of sand. These deposits can be dredged and transported to shore. Offshore sand deposits can be a suitable cost-effective source of sand for beach fill and nourishment, particularly when considering the lack of suitable, natural sand from onshore sources. Offshore sand deposits occurring within the same littoral cell can have grain size characteristics and composition that are very similar to the adjacent beach sand.

7.2 Sand Characteristics and Quality

The State Department of Land and Natural Resources (DLNR) beach nourishment guidelines specify that fill sand used to nourish a beach must meet several specific requirements which are summarized below in Table 7-1.

Table 7-1. DLNR sand composition and quality requirements for beach nourishment

Overall Composition	<p>Similar in composition, grain size distribution, color and texture to existing coastal system at the placement site</p> <ul style="list-style-type: none"> • may require more restrictive standards than the individual parameters listed below • if existing beach sediment is outside the individual parameters below, nourishment sand will be measured in comparison to the existing site-specific sand, rather than the parameters listed below <p>No construction debris, toxic materials or foreign matter</p> <p>No material that results in cementation of the beach</p>
Silt, Clay or Colloids; #230 Sieve	≤2%
Grain diameter <0.125mm; #120 Sieve	≤50%
Coarse Sediments ≥4.76mm; #4 Sieve	≤10%
Coarse gravel, cobbles, material >3/4inch (19.05mm)	≤ % on existing or native beach

The majority of the current fill sand requirements are related to grain size. In order to ascertain the grain size characteristics, a sieve analysis is performed, which is done by mechanically shaking a sand sample through a series of sieves of decreasing screen size. The material captured on each sieve is weighed, and this establishes the grain size distribution curves. The median diameter (grain diameter that is finer than 50% of the sample), or D_{50} , is often used by engineers to quantify the grain size of a sample. Similarly, D_{16} and D_{84} are obtained, and they are used to quantify the range of grain sizes present in a sample known as sorting, σ , defined by:

$$\sigma = \frac{\phi_{84} - \phi_{16}}{4} - \frac{\phi_{95} - \phi_5}{6.6}$$

where $\phi = -\log_2(D)$ where D is given in millimeters. Descriptive sorting values are presented in Table 7-2.

Table 7-2. Sorting value descriptions

Sorting Range (ϕ units)	Description
0.00 – 0.35	very well sorted
0.35 – 0.50	well sorted
0.50 – 0.71	moderately well sorted
0.71 – 1.00	moderately sorted
1.00 – 2.00	poorly sorted
2.00 – 4.00	very poorly sorted
4.00 – ∞	extremely poorly sorted

Color and abrasion resistance are also important characteristics of fill sand. While natural calcareous beaches range in color from light brown to white, sand in offshore deposits usually turns a gray color as a result of anaerobic conditions typically produced by a lack of wave action and associated mixing. Even though an offshore sand source may be suitable in terms of grain size characteristics, a gray color can be undesirable.

7.3 Existing Beach Sand Characteristics

Sand samples were obtained on November 22, 2022, at six locations along the beach as shown on Figure 7-1. At each location, samples were obtained from the upper beach face and the lower beach face, each within the swash zone. Since there was little noticeable difference between the upper and lower samples at each location, the two samples at each location were combined. The grain size distributions are shown in Figure 7-2 and show the median grain size D_{50} to be in the range of 0.24 and 0.57 mm. The composite distribution for the six samples has a D_{50} of 0.32 mm with an average sorting value of 0.9, which according to Table 7-2 categorized the beach sand to be considered moderately sorted.



Figure 7-1. Beach sand sample locations

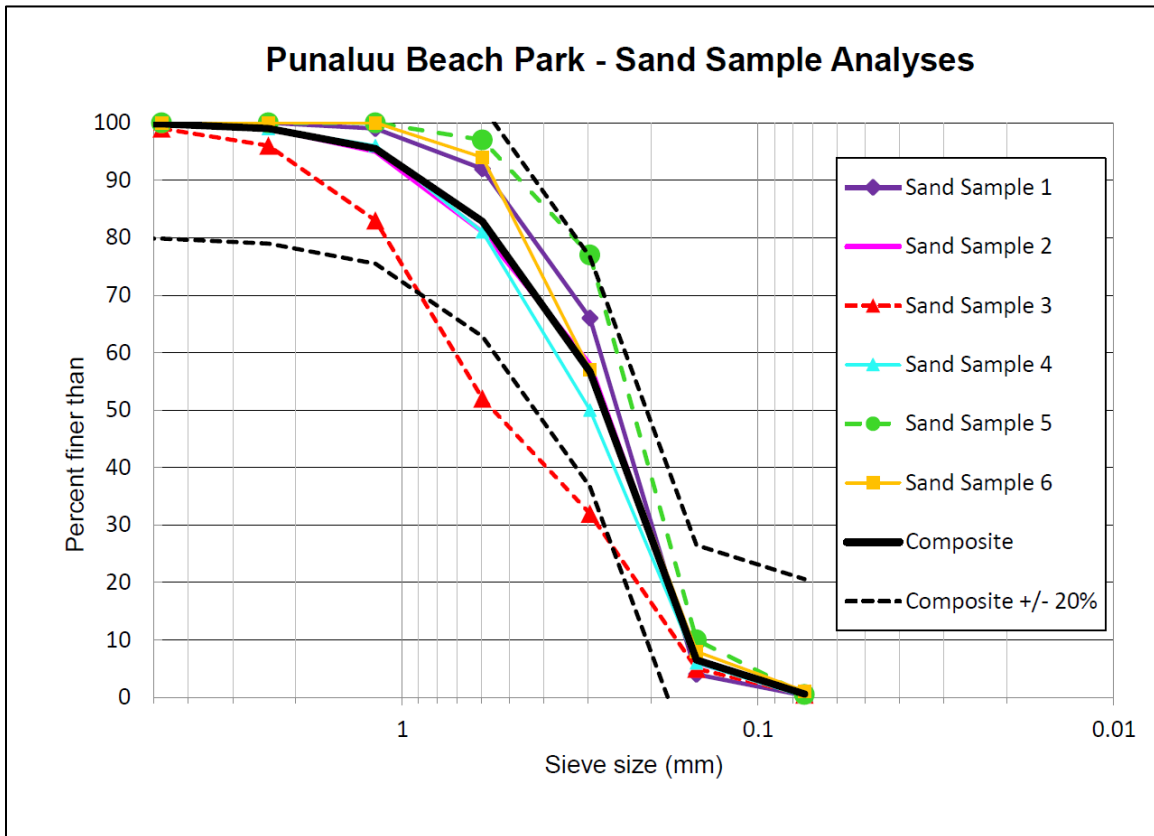


Figure 7-2. Grain size distributions, beach sand samples

7.4 Offshore Sand Source Investigations

Observations of aerial photographs, as well as knowledge of the region, resulted in field investigations of a sand deposit within the relict stream channel offshore of the north part of the Punalu'u Beach Park. The deposit is shown in Figure 7-3. The center of the sand deposit is located approximately 2,000 ft offshore of Punalu'u Beach Park.

Scuba divers performed an investigation of the sand deposit. Jet probing was conducted to determine the thickness of sediments overlying consolidated or hard bottom substrate. The jet probe consists of an eight-foot long pipe connected to a scuba tank by a flexible hose. A diver jets the pipe and hose vertically into the sediment deposit until “refusal” is encountered or the end of the probe is reached. The refusal can be described as hard, crunchy, or soft; hard indicates a solid bottom, crunchy indicates a gravel layer, and soft indicates that the hole is collapsing and seizing the pipe or that there is insufficient hose to penetrate further. The divers also obtained sand samples at certain jet probe locations by using a push-coring device that drives an acrylic tube into the sand. The practical limit of penetration within a sand deposit is about 3 to 4 ft. When the tube is removed, the sand core is extracted. The sand core can then be divided into top, middle, and bottom samples. The divers also took photographs of the sand deposit at each location and logged written observations. The jet probe and push core locations are shown in Figure 7-3.

Jet probe penetration averaged between 5 and 8 ft for all samples, and in some instances, the probe was pushed into the sand beyond its limit without encountering refusal. Cobbles were encountered, primarily in the offshore end of the deposit and along the north and south perimeters of the deposit.

Beach quality sand was located within the outlined area shown in Figure 7-3. Sand ripples on the seafloor of the inshore part of the sand deposit are shown in Figure 7-4. Inshore of this area existing beds of seagrass were observed as shown in Figure 7-5. Offshore from this area consisted of finer grained sand with cobbles, darker gray in color, and algae covered, and thus less suitable for placement on the beach. Jet probe penetration also reduced in the offshore direction which infers the limited sand volume in this region.

The areas with suitable sand were bounded for the purpose of estimating the amount of sand potentially available in the deposit, such that determinations could be made about the adequacy of the deposit for nourishing the beach. The sand deposit area covers approximately 45,000 square yards, or about 9.3 acres. The jet probe data for the area was used to estimate the volume of available sand within the deposit and corresponds to an estimated sand volume of 100,000 cubic yards.

Grain size distributions and sediment characteristics were determined for each core sample obtained and are shown in Figure 7-6 and Table 7-3, respectively. Comparison of composite offshore and beach samples are shown Figure 7-7. Also shown are the $\pm 20\%$ bounds identified in the DLNR guidelines. The grain size analyses show the median diameter, D_{50} , of the beach sand to be in the range of about 0.24 mm to 0.57 mm, and the offshore sand to be in the range of 0.24 mm to 0.47 mm. The composite median diameters are 0.32 mm for the beach sand and 0.31 mm for the offshore sand.

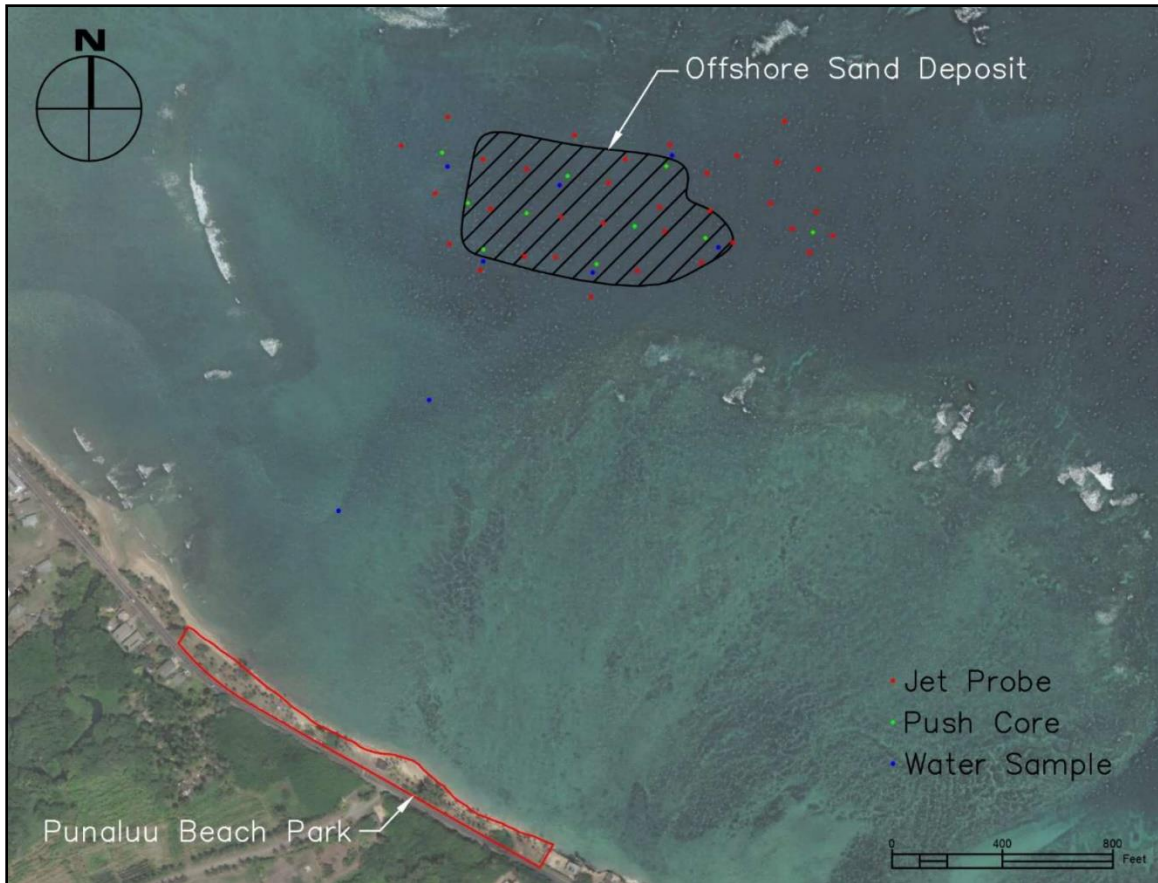


Figure 7-3. Jet probe and push core locations at offshore sand deposit



Figure 7-4. Typical view of interior of sand deposit



Figure 7-5. Inshore boundary of seagrass and sand deposit

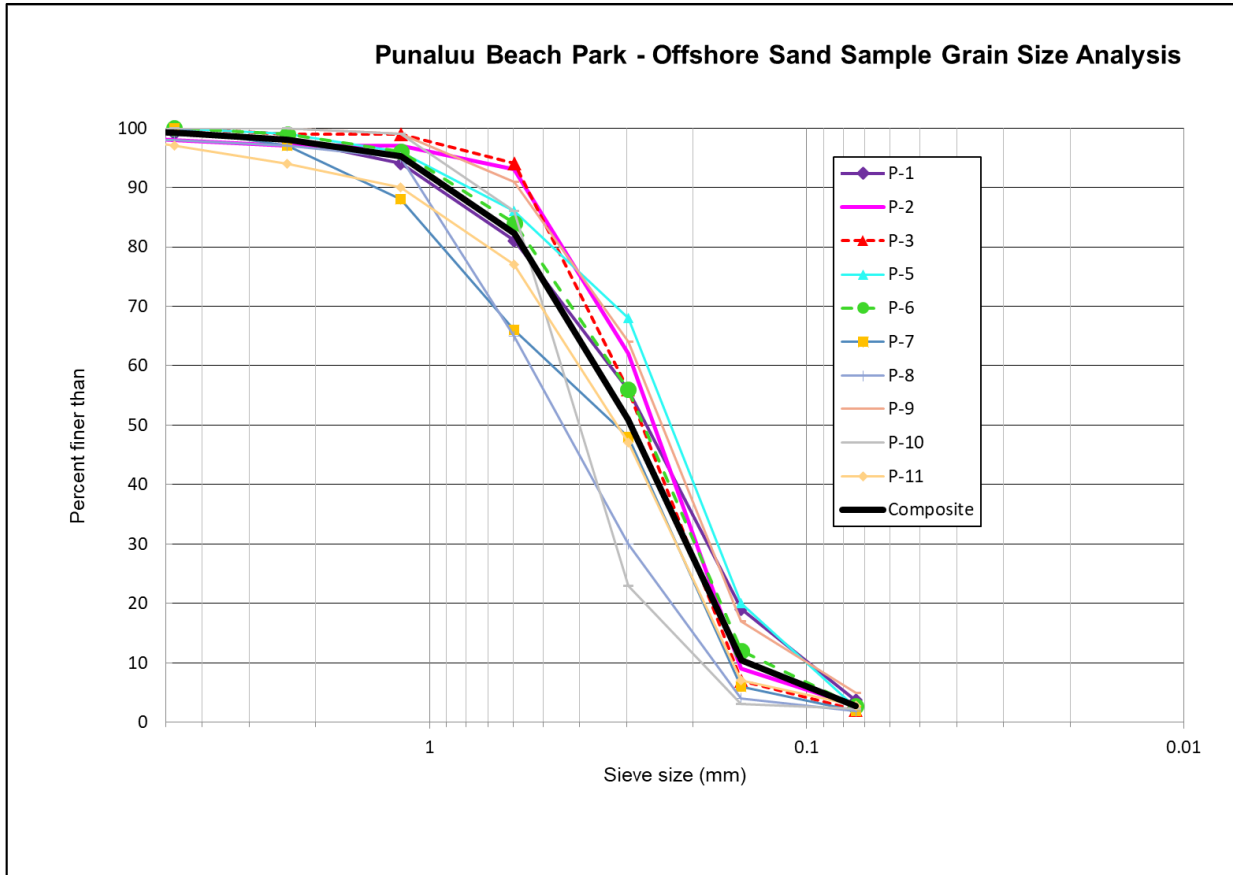


Figure 7-6. Grain size distributions of offshore sand samples

Table 7-3. Punalu'u offshore sand sample summary

Location ID	D_{50} (mm)	Sorting σ	% fines	Source	Year
P-1	0.27	1.2	3.7	SEI	2023
P-2	0.26	0.9	2.8	SEI	2023
P-3	0.28	0.8	2.1	SEI	2023
P-5	0.24	1.1	2.4	SEI	2023
P-6	0.28	1.0	2.7	SEI	2023
P-7	0.33	1.1	1.9	SEI	2023
P-8	0.47	1.0	1.8	SEI	2023
P-9	0.25	1.0	4.9	SEI	2023
P-10	0.42	0.7	2.3	SEI	2023
P-11	0.33	1.1	2.8	SEI	2023

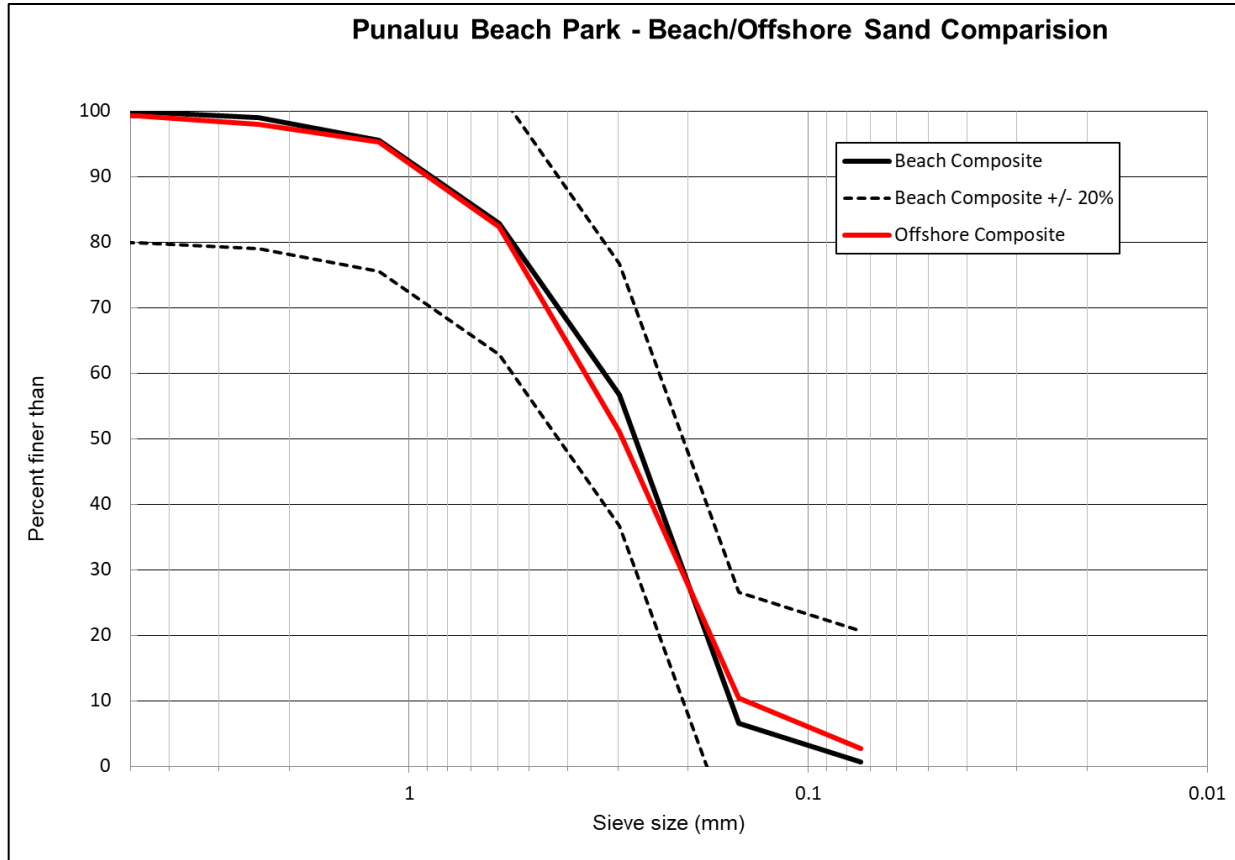


Figure 7-7. Comparison of grain size distributions for Punalu'u Beach composite and offshore composite samples

7.5 Overfill Factor

A beach undergoes an adjustment period following nourishment. The beach equilibrium profile is achieved as sand moves cross shore and alongshore and there may be an accompanying decrease in beach volume. This loss of sand is compensated for through an overfill ratio, which describes the compatibility of the native beach and borrow sands and is dependent on the size distributions of the native and nourishment (borrow) sand.

The overfill ratio is determined based on the sand size characteristics of the two sands and represents the volume of fill necessary to yield the desired beach volumes calculated previously. Bodge (2004) compared overfill ratio methods and developed an expression that is believed to produce more accurate results than the previous methods.

The mean grain size, M , and sorting, σ , for the native and borrow sands are calculated as presented in the Coastal Engineering Manual (2006) as

$$M = \frac{(\phi_{16} + \phi_{50} + \phi_{84})}{3}$$

$$\sigma = \frac{(\phi_{84} - \phi_{16})}{4} + \frac{(\phi_{95} - \phi_5)}{6}$$

The dimensionless grain size difference is calculated as

$$M'_b - M'_n = \frac{M_b - M_n}{\sigma_b}$$

where subscripts n and b refer to the native and borrow sand, and the overfill ratio is read from Figure 7-8.

The composite grain size distributions for the offshore sand (“borrow”) and the beach sand (“native”) were shown previously in Figure 7-7. The mean diameter M_b for the composite Punalu‘u offshore sand is 1.6ϕ with a sorting σ_b of 0.9ϕ , while the mean diameter of the native beach sand M_n is found to be 1.6ϕ . These values produce a dimensionless grain size difference of 0.0, which is used along with Figure 7-8 to yield an overfill ratio of $K = 1.0$. Thus, no additional sand would be necessary to achieve the final desired volume of beach. This also indicates that the offshore sand had good compatibility with the beach sand.

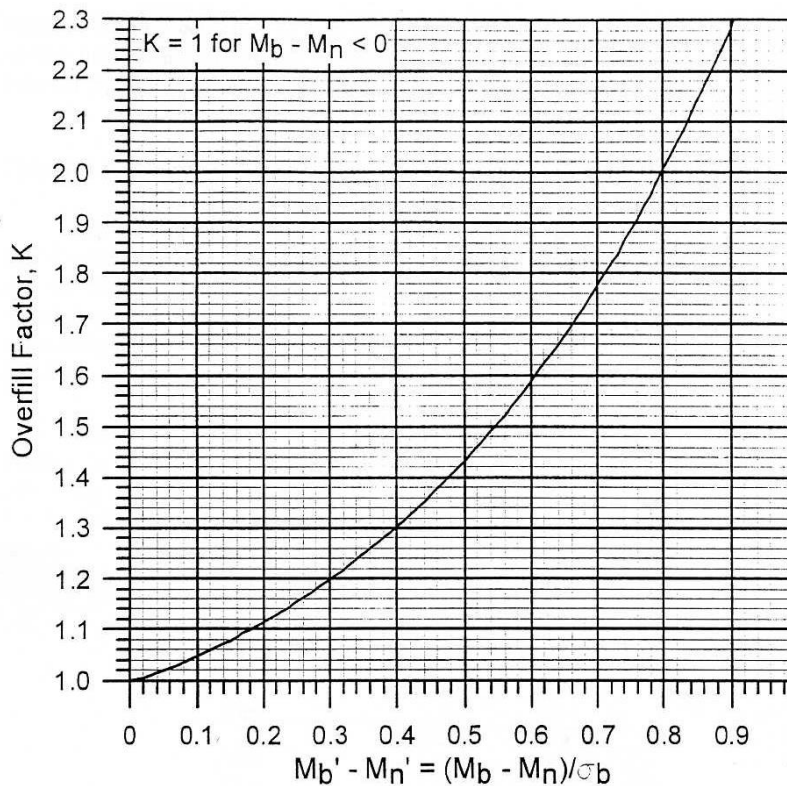


Figure 7-8. Dean’s overfill ratio expressed as a single curve (Bodge, 2004).

7.6 Sediment Turbidity Analysis

Turbidity occurs when fine sediment particles are suspended in the water column, reducing water transparency. Turbidity can occur at the offshore sand dredging site or along the beach where sand is placed. Beach restoration projects can generate turbidity plumes that can be unsightly and affect water visibility for days. Although sand fill placed on a beach must closely match the existing beach sand with respect to grain size, offshore sand will typically have a higher percentage of fine particles than native beach sand. Additionally, fines may be generated during dredging and placement of offshore sand onto the beach. After placement, wave action can suspend the fines creating turbidity plumes offshore of the nourished area.

Laboratory turbidity tests were performed on numerous sand samples from the potential borrow site offshore of Punalu‘u Beach Park, along with samples from transects measured during the beach survey of the shoreline. Turbidity was determined by measuring the scattering of the light through sample cells that contained distilled water and sand in suspension.

Ten (10) sand samples from the potential sand borrow site offshore of Punalu‘u Beach Park, shown in Figure 7-3, were tested and compared with six (6) samples taken at Punalu‘u Beach (locations shown in Figure 7-1). The potential borrow area offshore of the beach park was sampled using a diver-operated push core mechanism to extract sediment cores. The layers of substrate were then divided into sections and tested for sand characteristics. Samples from this area are labeled P#. Punalu‘u Beach was sampled in six (6) locations all along the beach park and are labeled B# and also were tested for sediment characteristics.

7.6.1 Methods for Turbidity Testing

Turbidity was measured using a Hach 2100Q Portable Turbidimeter (Figure 7-9). The instrument has an optical laser configuration that measures the scattering of the light passing through the sample cell (Figure 7-10). Turbidity is measured in Nephelometric Turbidity Units (NTUs), a standard turbidity unit for United States environmental monitoring. The instrument was calibrated once before the first experiment using the manufacturer’s 20, 100, 800 NTU StablCal primary calibration standards and the 10 NTU primary verification standard. The cells used for the turbidity readings were glass Hach Lab Turbidimeter Sample Cells.

All sample bottles and sample cells were meticulously cleaned. The sample bottles were cleaned with tap water, while the sample cells were cleaned with tap water and filled with distilled water, then left filled for a minimum of 24 hours. The sample cells remained filled with distilled water until use to avoid contamination from air. Before each turbidity test, the cells were emptied, cleaned with tap water, and filled once more with distilled water until overflowing. The outside walls were treated with a thin coating of Hach silicone oil to cover imperfections and scratches and to minimize stray light.

Test samples were prepared with one tablespoon of dry sand placed in a 120 mL Polystyrene sample bottle. The bottle was then filled with 100 mL of distilled water. Preceding each turbidity test run, the sample bottle was shaken vigorously to emulate turbulence. The suspension was immediately poured into a cleaned Hach cell, which was then inverted three times following the manufacturer’s guidelines and placed in the machine. The turbidity runs began immediately upon cell insertion within the analyzer.

A reading was taken for each sample at the following time intervals: 30 seconds, 1 minute, 2 minutes, 5 minutes, 10 minutes, 20 minutes, 1 hour, 2 hours, 4 hours, 6 hours and 24 hours.



Figure 7-9. 2100Q Portable Turbidimeter

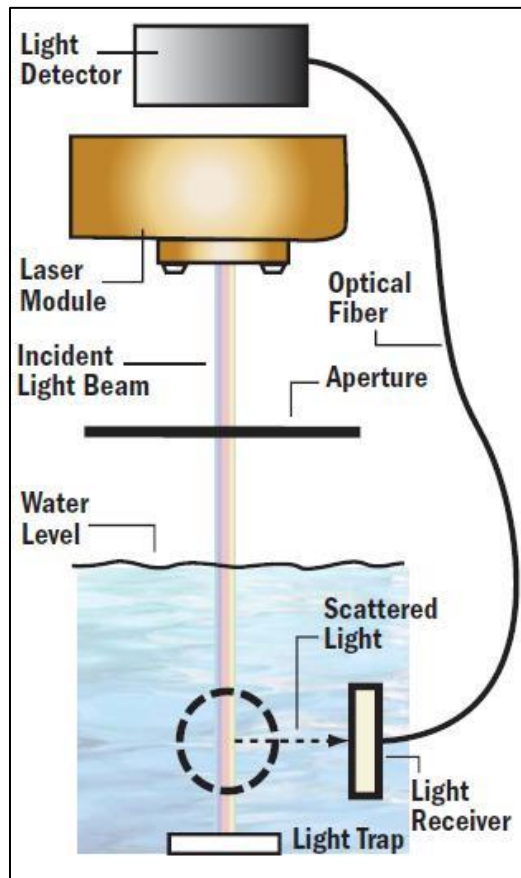


Figure 7-10. Laser Nephelometer Optical Configuration (Sadar, Cason and Engelhardt 2009)

7.6.2 Turbidity Testing Results

Data are plotted as turbidity versus time. Sample results from the Punalu‘u Beach Park are shown in Figure 7-11. Sample results from the offshore sand deposit area are plotted in Figure 7-12. Punalu‘u Beach Park samples had initial turbidity values ranging from 37 to 153 NTUs, with an average value of 48 NTUs. All offshore samples tested showed initial turbidity that decreased exponentially with time. Offshore samples had initial turbidity values ranging from 307 to over 1000 NTUs, with an average value of 293 NTUs.

Sand from within the offshore sand deposits will be mixed during excavation, transport, and placement on the beach. Average values for the usable area in the deposit are important, as they are representative of the material that will eventually be placed on the beach. The composite samples from the offshore deposit area had higher average initial turbidity readings than the samples from Punalu‘u Beach Park, with average values of 293 and 48 NTUs respectively.

After 6 hours, the average Punalu‘u Beach Park turbidity fell to 13 NTUs and the average offshore deposit turbidity fell to 10 NTUs. After 24 hours, the averages for both the Punalu‘u Beach Park and offshore deposit samples had turbidity values between 5 and 6 NTUs. This shows that, while after initial placement of offshore deposit sediment on the beach may lead to temporary nearshore turbidity, over time, the sediment will settle and integrate well into the Punalu‘u Beach Park environment.

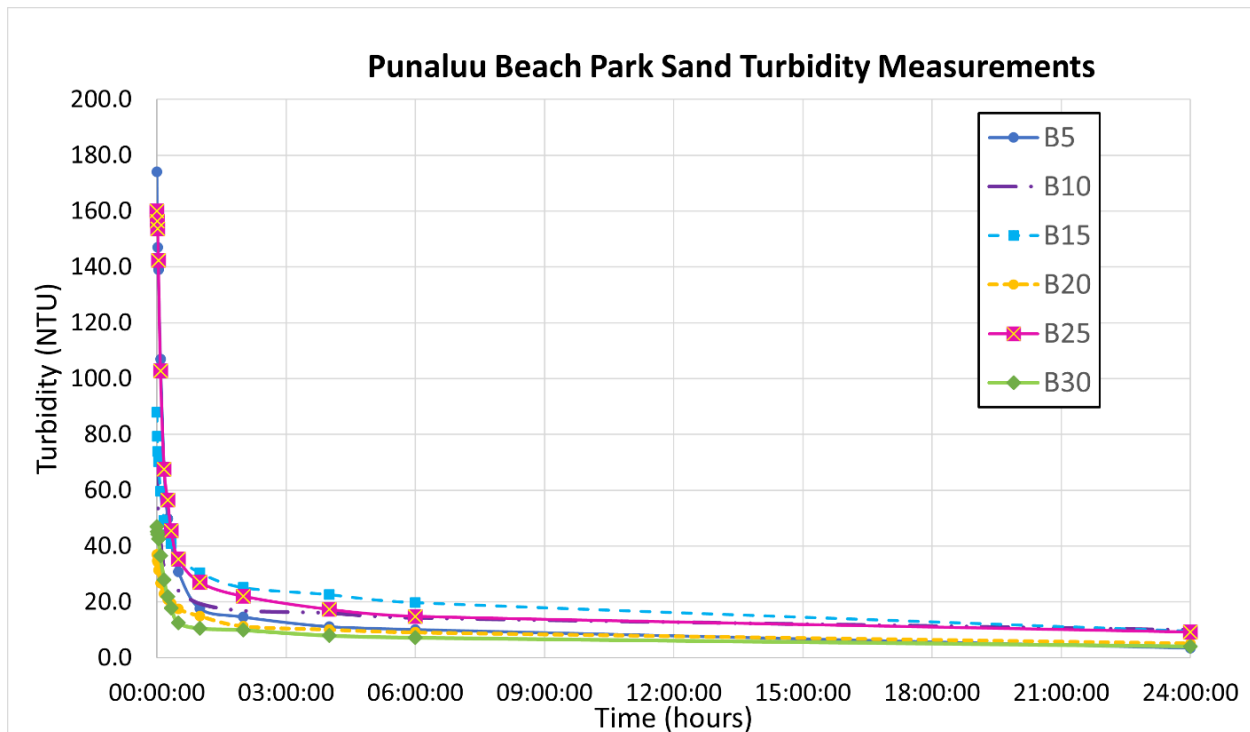


Figure 7-11. Sediment turbidity results for sand samples taken on the shoreline of Punalu‘u Beach Park

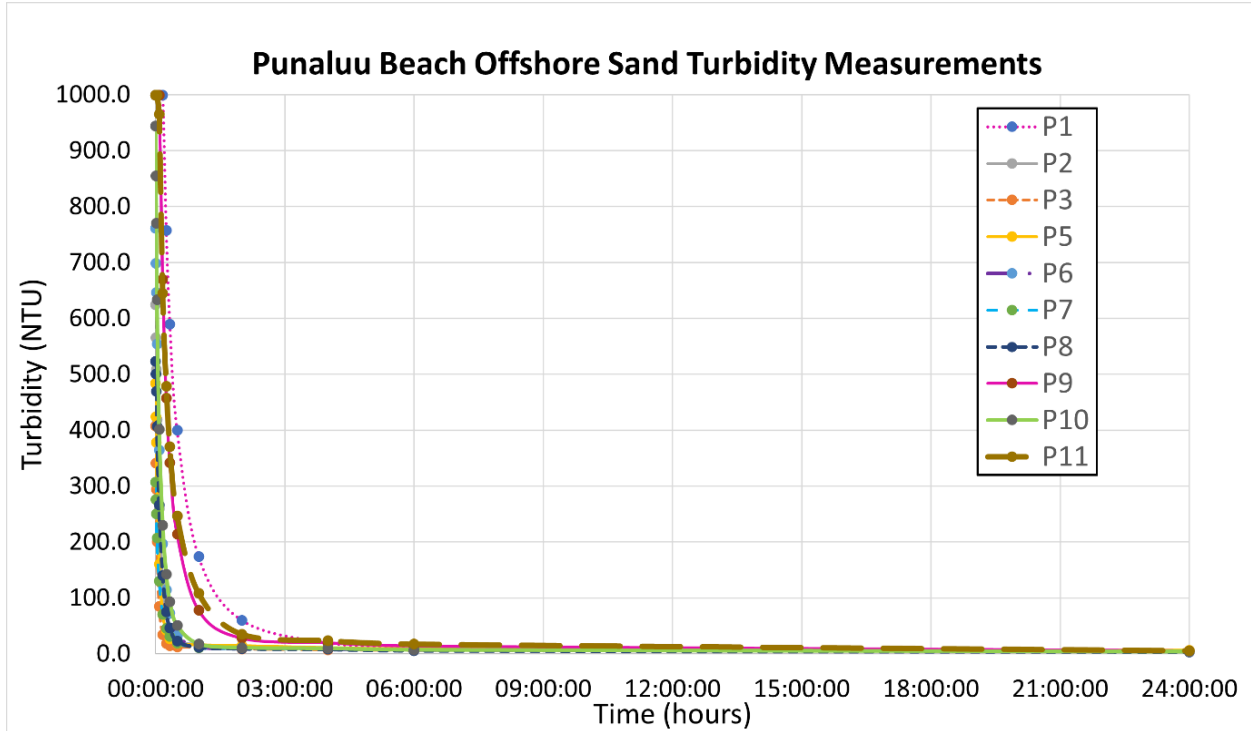


Figure 7-12. Sediment turbidity results for sand samples taken at the offshore sand site at Punalu'u

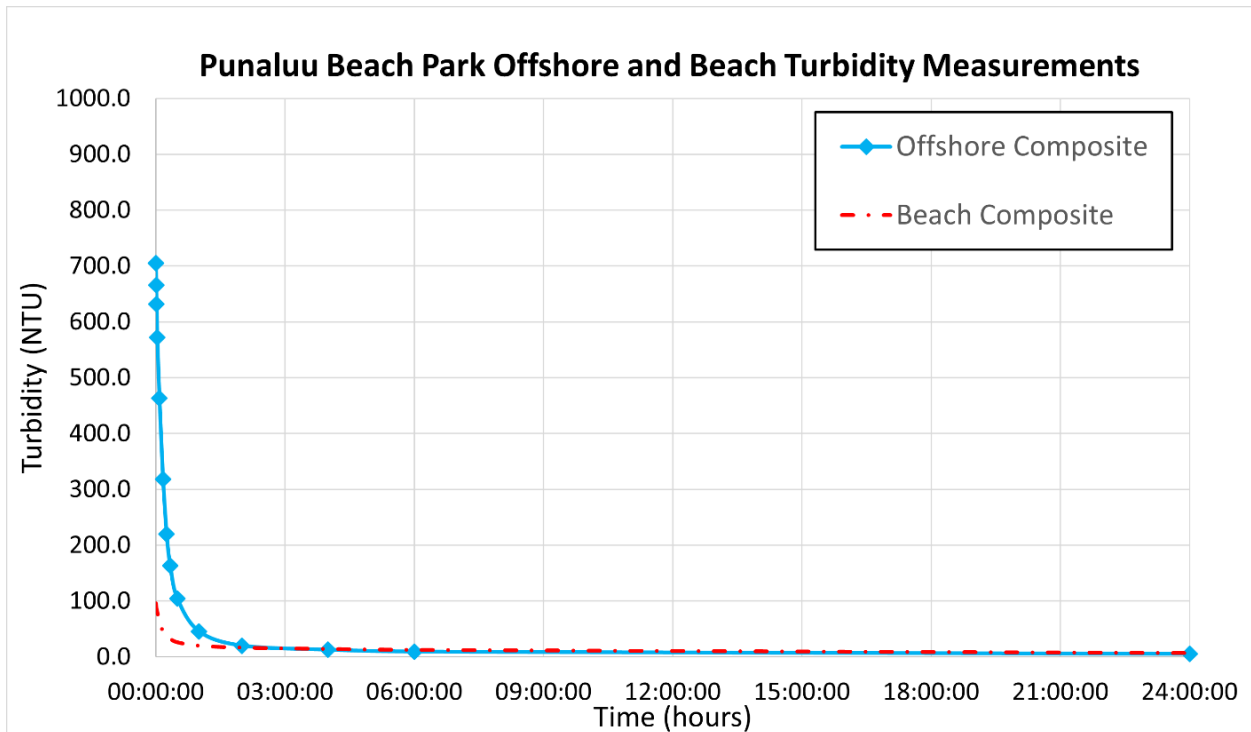


Figure 7-13. Comparative sediment turbidity results for the offshore and beach composite samples

8. OFFSHORE SAND RECOVERY METHODS

The offshore sand source is shown in Section 7 to be a satisfactory sand source option for beach nourishment along Punalu‘u Beach Park. The following subsections describe both small-scale and traditional dredging techniques and their suitability for sand recovery and transport at Punalu‘u. A range of techniques is presented herein.

8.1 Small-Scale Dredging Systems

8.1.1 *Subdredge ROV by EDDY Pump*

The Subdredge ROV is an electric-powered tracked hydraulic pump manufactured by EDDY Pump Corporation (Figure 8-1). The pump was developed for the U.S. Army and U.S. Navy for Logistics-Over-the-Shore (LOTS) operations for early entry forces and areas that are too dangerous for human operators. It is fully submersible and capable of being operated remotely from shore. The ROV is equipped with a hydraulic pump with a discharge pipe diameter of 6 inches that is reportedly capable of pumping an estimated 60 cubic yards of sand per hour on average via a pipeline to shore. An umbilical would run along the pipeline providing power and control to the ROV. An electric power unit located on shore would power the pump and a small submersible hydraulic power unit mounted on the ROV. The hydraulic power unit would drive all auxiliary functions (i.e., ROV movement). RTK GPS provides location data to the landside operator.

If deployed/operated from shore, the Subdredge ROV system could only operate up to 1,000 ft away from the shoreline and would not be able to reach the Punalu‘u sand deposit which is located about 2,000 ft offshore. The ROV would also have to transit through the sand channel to reach the offshore deposit and may impact seagrass beds which were identified within the sand channel area. Alternatively, the ROV system may be deployed/operated from an offshore vessel or barge moored over the sand deposit, however, this setup would not offer any advantages over a traditional submersible slurry pump system (described in Section 8.2.2). Based on these considerations, the Subdredge ROV is not recommended for sand recovery at Punalu‘u Beach Park.



Figure 8-1. Eddy Pump 6” Subdredge ROV (source: EDDY Pump)

8.1.2 Diver-operated Dredge by EDDY Pump

An alternative small-scale dredging method would be a diver-operated dredge system. A diver-operated dredge has a suction head that can be manipulated and operated by a diver without assistance from a support vessel or construction equipment. Diver-operated dredges are used in the mining/fracking industry and shipyard operations. Using a diver to manipulate the suction hose offers a level of precision that cannot be achieved by simply lowering a pump over the side of a vessel (i.e., a Toyo pump). Figure 8-2 shows a diver on surface supplied air manipulating a diver-operated dredge nozzle.

Sand recovery using a diver-operated dredge would require a full commercial diving team to be OSHA compliant. Due to the distance from the shoreline to the offshore deposit at Punalu‘u, the dive team would likely have to work from an offshore vessel moored over the sand deposit versus directly from the shoreline. The diver-operated dredge system uses smaller diameter pumps than available traditional submersible slurry pumps resulting in a fraction of the production rates. Dredging duration could extend 1 to 2 years with costs becoming prohibitive. Due to increased costs associated with utilizing a commercial dive team and lower production rates, the diver-operated dredge system is not recommended for sand recovery at Punalu‘u Beach Park.



Figure 8-2. Surface supplied air diver using a diver-operated dredge

8.1.3 *Dredge Sled submersible pump and platform by EDDY Pump*

The Dredge Sled by EDDY Pump is a remote-controlled floating dredge system best suited for calm environments such as lagoons, ponds, and settling basins (Figure 8-3). The system consists of a floating platform referred to as a sled. The sled is cabled through winches to anchor points on shore. The winches control the position of the sled, which is the platform for a submersible EDDY Pump. A battery-operated winch on the sled raises and lowers the pump from the seafloor.

The Dredge Sled is best used in very calm conditions such as ponds and settling basins and is not recommended for use in wave environments. Therefore, Dredge Sled or other similar technologies is not recommended for sand recovery at Punalu‘u Beach Park.



Figure 8-3. Dredge Sled in use (source: Eddy Pump)

8.2 Traditional Dredging Systems

Traditional dredging systems consist of utilizing clamshell buckets or submersible slurry pumps to recover sand from an offshore deposit for beach nourishment purposes. As discussed in the previous section, typical small-scale dredging systems are better suited for nearshore sand recovery working from shore and not suitable at Punalu'u Beach Park. Due to the distance of the deposit from the shoreline and the volume of sand needed for nourishment, industrial scale dredging methods are more practical and most feasible at Punalu'u Beach Park compared to small-scale dredging methods. There are various ways to accomplish these operations, some of which store the sand onboard the dredging vessel or deliver it to nearby barges or ships, while others transport the sand directly through a pipeline to the shore. Storing the sand on the dredging vessel requires that the vessel return to a commercial harbor on a regular basis to discharge recovered materials, requiring considerable time, energy, and harbor space. If the sand is pumped to shore, booster pumps and additional barges may be necessary if the distance to the project beach is excessive. The third strategy would be placement of the dredged sand in ships or barges that could be cycled through the recovery and delivery process close to the project site to increase dredging efficiency. This would allow for simultaneous loading and offloading of pairs of these barges and would allow the dredge barge to remain in place for the duration of the recovery effort.

All of these techniques require that the dredge barge be anchored with a stable, minimum four-point mooring in the recovery area. Anchors would be placed within the sand field and marked with floats or buoys, as depicted in Figure 8-4. A four-point mooring would allow the barge to change locations within the recovery area and remain securely anchored without having to adjust

anchor placement. The sand recovery site is located along the energetic windward coast, fully exposed to prevailing tradewind seas and partially exposed to north Pacific swell. Dredging at this location will therefore be challenging, requiring specialized equipment and mooring systems, careful planning to maximize more favorable sea conditions, and allowance for significant standby and down time due to rough seas.

There are several potential dredging techniques that might be employed for the study area, all of which are discussed in the following sections.



Figure 8-4. Example: anchor and anchor float used in the 2012 Waikiki Beach Maintenance Project

8.2.1 *Clamshell Dredging*

Clamshell dredging, shown in Figure 8-5, describes the process of mechanically scooping and lifting the sediment, in this case sand, from the seafloor. An environmental clamshell bucket, such as the one shown in Figure 8-6, is lowered from a crane in the open position, and upon the clamshell reaching the bottom, the crane operator closes the clamshell jaws and lifts the material out of the water. The operator then rotates the crane and opens the bucket to dispense the material into a waiting barge, such as a hopper barge (Figure 8-7).



Figure 8-5. Clamshell dredge with environmental bucket
(http://www.conedison.com/ehs/2009annualreport/environmental_stewardship)



Figure 8-6. Environmental clamshell bucket
(http://www.alibaba.com/product-free/107658423/Environmental_clamshell_grab.html)



Figure 8-7. Hopper barge
(<http://www.thecargogroup.net/>)

Clamshell dredging is often used in association with a large barge, such as the hopper barge shown in Figure 8-7, on which the sediment is deposited. Once the sediment is onboard the barge, transport is accomplished by either moving the barge to a dock and offloading or using a waterborne sand delivery system to deliver the sand to the shoreline.

The benefits of using clamshell dredging are that it is very mobile, it can operate at any depth that the crane cable can reach, it can be used in moderate swell conditions, and it can recover a wide variety of material types. Additionally, little specialized equipment beyond the clamshell is needed for dredging operations. The technology of the environmental buckets helps to reduce environmental impacts due to turbidity and increase efficiency in recovering sand, reducing time and cost of the operation. Additionally, the amount of water that is accumulated from the clamshell dredging process is much less than with hydraulic dredging presented in the next section, and the small amount of water can be discharged at an approved location.

The drawbacks are that it is less efficient than other dredging systems, such as those utilizing hydraulic or slurry pumps, and it requires the sand deposits to be thick enough that the clamshell does not reach hard substrate. This method also requires a suitable location to offload the sand. The closest potential offload location is the Heeia Small Boat Harbor. This harbor is over 12 miles

away from the dredging site, resulting in long, costly transits through typically rough tradewind seas.

8.2.2 *Submersible Slurry Pump*

Submersible slurry pumps, referred to as “Toyo Pumps” after the largest supplier of such, are distinguishable by the way that they are lowered from overhead and suspended above the sediment they are pumping. The pumps can be hydraulically or electrically driven and are available in a range of sizes. Models are available with up to 400 hp. Toyo DP75B (75hp) hydraulic pumps were used successfully for dredging both the 2007 Kuhio Beach restoration project and 2012 Waikiki Beach Maintenance Project. Respectively, the projects pumped approximately 10,000 and 24,000 cu. yd. of sand from offshore onto the beach within the Kuhio Beach crib walls.

Several equipment elements are required to successfully recover sand utilizing a submersible pump. A barge and crane are necessary to position a hydraulic or electric powered pump over the sand bottom. The crane can move the pump across a small area, dependent on the crane size and length of its boom. Accessing different portions within the recovery area is achieved by repositioning of the pump barge using a minimum four-point mooring system. Additionally, depending on the size of the slurry pump, a booster pump may be required if the distance to the shoreline is excessive. An additional piece of equipment called a “jet ring” can be mounted on the pump to aid in entraining sand to increase the percent of sand in the slurry. This jet ring requires a water pump on deck and an additional 4-inch water hose connected to the submersible pump. An illustration of this dredge system is shown on Figure 8-8, taken from the Kuhio Beach project after-action report (American Marine, 2007). Figure 8-9 shows the Healy Tibbitts dredge barge used in the 2012 Waikiki Beach Maintenance Project.

The benefit of the submersible pump is its precise positioning and ability to reach into tight spaces. Using a crane-tip GPS unit to locate the pump, the operator can accurately position the pump to within a few feet of any location to effectively remove the sand from near the edges and corners of the recovery area. In addition, sand recovery with a slurry pump can be more efficient than mechanical recovery when a high sand to water ratio can be achieved.

The primary drawbacks to the submersible pump are that the operation is labor intensive, and it requires dewatering. Operation requires a crane operator, a rigger, and several people to handle the pumps, generators, and pipelines on deck. Additionally, the pump must be held at a relatively constant height above the sand. If the pump is lifted too high it will not entrain the sand, and if it is too low the slurry will become too concentrated, and the pipeline may clog. Maintaining this balance is especially difficult for the crane operator in the presence of swells greater than one to two feet; however, the dredge equipment can be operated from an ocean-going barge, which provides reasonable seaworthiness. Submersible pumping requires that the slurry be properly dewatered, which increases on-land space requirements. For example, the 2012 Waikiki Maintenance project utilized a one-acre dewatering basin within Kuhio Beach Park, requiring the Diamond Head basin to be completely closed to the public. Given the location of the offshore deposit identified in Section 7, hydraulically pumping sand to shore is the most viable option compared to clamshell dredging. Figure 8-10 shows a potential sand recovery layout for Punalu‘u. While the source is reasonably close to shore, the windward coast of O‘ahu is one of the most energetic wave environments in Hawai‘i which makes the sand recovery challenging in this region.

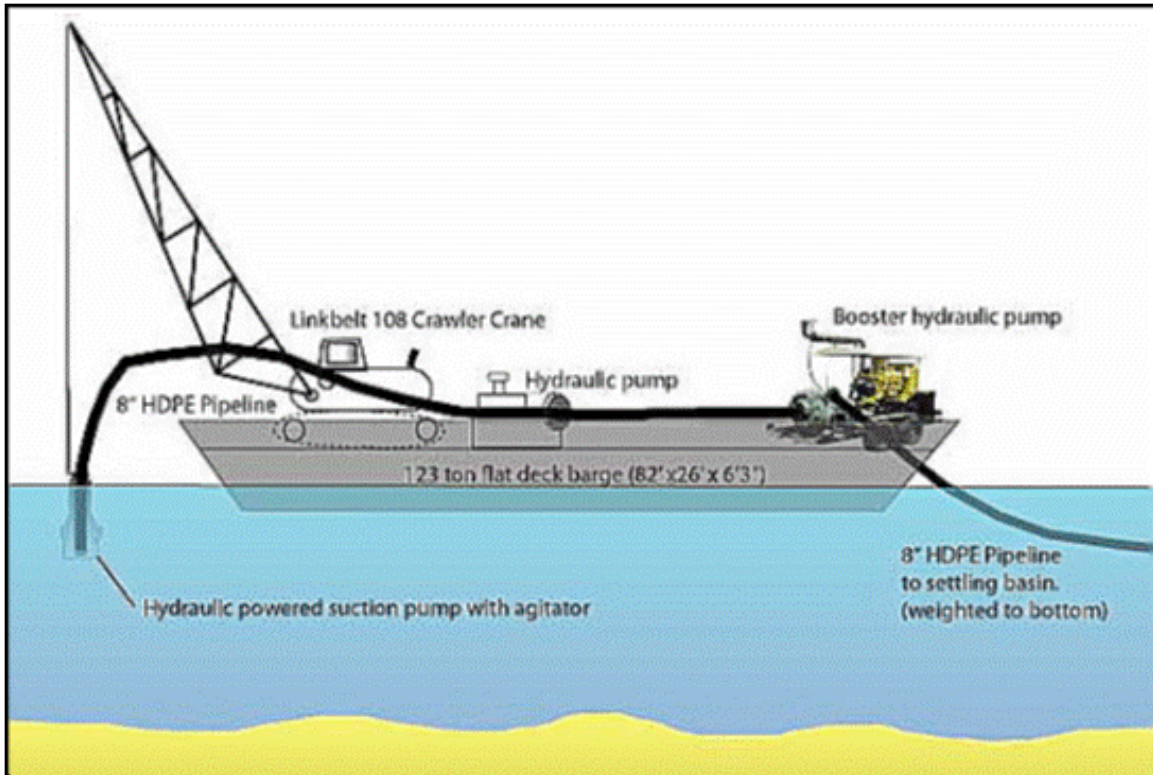


Figure 8-8. Schematic of sand pumping arrangement (American Marine, 2007)



Figure 8-9. Healy Tibbitts Crane Barge used in the 2012 Waikiki Beach Maintenance Project

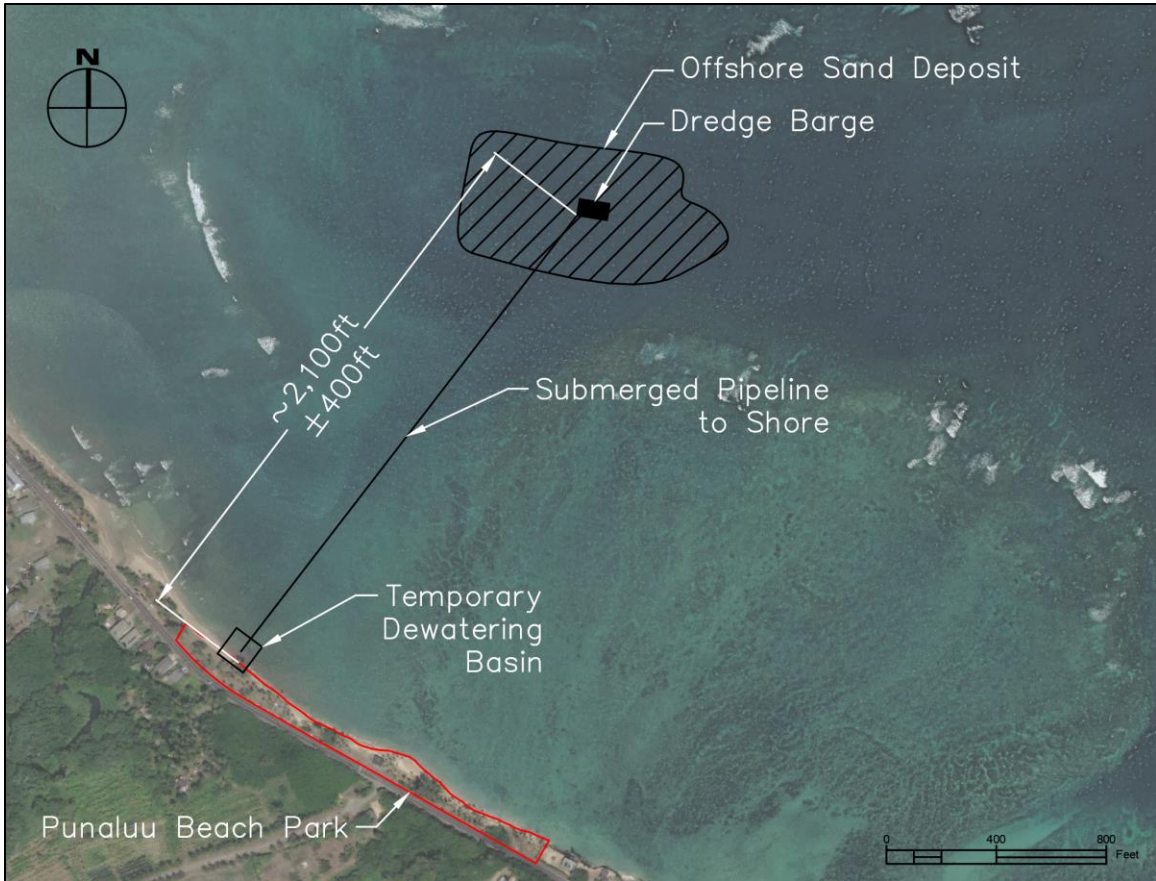


Figure 8-10. Proposed sand recovery plan using hydraulic suction dredge

9. MARINE RESOURCES

Water quality and marine biology of both the park's nearshore waters and offshore sand recovery site were assessed by Marine Research Consultants Inc. (MRCI) for this study. Fieldwork for the water chemistry and marine biology assessment at the sand recovery area was conducted on September 6, 2023, and water chemistry samples were collected at six stations at the sand recovery area and at two stations in the channel leading to Punalu'u Beach Park. Fieldwork for the water chemistry and marine biology assessment at the beach park was conducted on January 4, 2024, and water chemistry was investigated along two transects extending from the shoreline to points offshore deemed to be at or beyond the limit of influence from material emission at the shoreline. Figure 9-1 shows the water sampling and marine biology assessment locations. Results from the marine resources assessment are presented in Appendix A and summarized below.

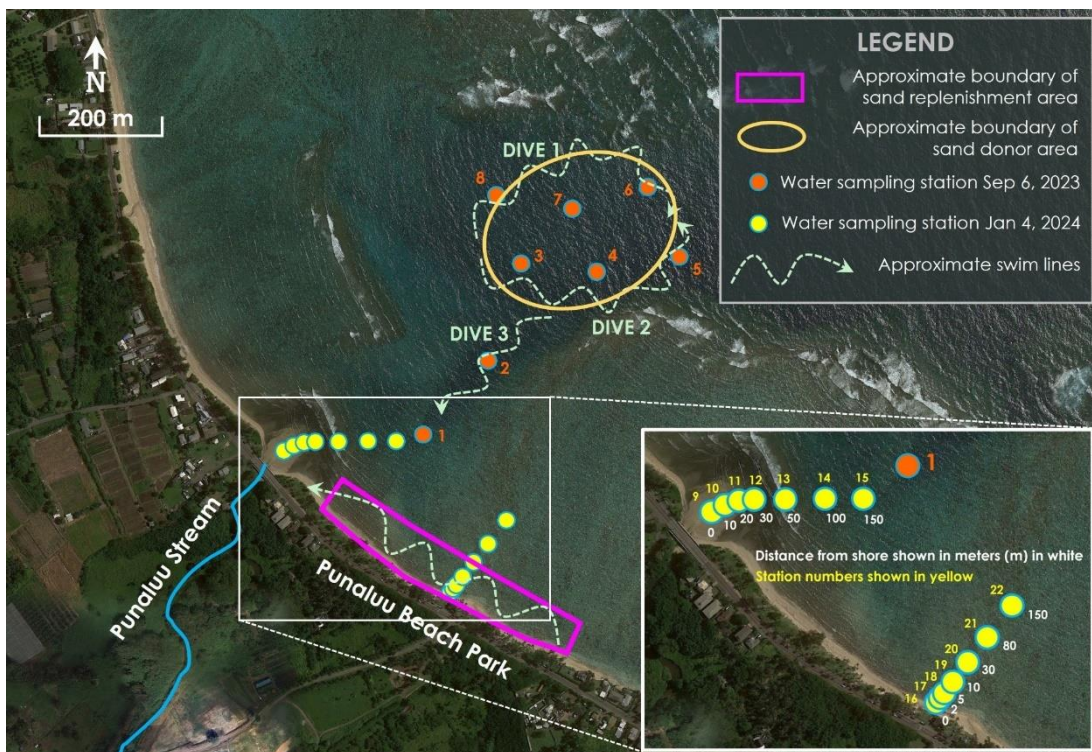


Figure 9-1. Vicinity map showing locations of water sampling stations, sand donor area, sand replenishment area, and diver swim tracks

9.1 Offshore Sand Recovery Area

9.1.1 Physical Structure

The sand recovery area consists of a bed of uniform sand with no macrobiotic components. The sand surface is structured into waves that cover the entirety of the area. The seafloor outside of the perimeter of the bed of sand transitions to hard substrate consisting of coral rock rubble and limestone fossil reef. The presence of living coral tissue buried in sand waves indicates that the sand likely moves into, out of, and around the sand bed along the perimeter. The south edge of the patch is adjacent to a vertical wall that reaches to within several feet of the surface of the water.

The wall provides a solid surface for the attachment of stony corals. Figure 9-2 presents photographs of the seafloor in the vicinity of the sand recovery area.

9.1.2 *Biotic Community Structure*

As macrobiota were not present within the sand bed, biotic community structure analysis will focus on the community immediately surrounding the sand bed. Best management practices should be mandated to protect these nearby resources during all in-water operations.

9.1.2.1 *Seagrass*

One primary resource in the vicinity of the sand donor bed is seagrass. Dense meadows of seagrass rim the perimeter of the west edge of the sand deposit as well as throughout the channel between the donor area and the shore (Figure 9-3). Note, seagrass was not observed within the bounds of the sand recovery area. It is likely that the shifting nature of the sand bed prevents colonization by seagrass as this species requires substrate with some stability. Seagrass is present in areas of hard substrate covered with sand and sand pockets between areas of hard substrate.

9.1.2.2 *Coral*

Corals were common on the hard substrate outside the perimeter of the sand deposit. When considering the entire survey area around the outside of the sand donor site, eight species of stony corals were documented. *Montipora capitata*, *M. patula*, *Pocillopora meandrina*, and *Porites evermanni* can be considered common; while *Montipora flabellata*, *Pavona varians*, *Pocillopora damicornis*, and *Porites lobata* can be considered rare within the survey area. At the time of the survey, the water column above the sand donor area was highly turbid owing to resuspended fine-grained sediment and sand. As a result of persistent wave energy, it is likely that these conditions are common and corals in this zone have adapted to the high turbidity and low light conditions present in the coastal area of the northeast shore of O'ahu.

The nearly vertical wall on the south side of the sand donor bed provided adequate hard substrate above the scour of sand for coral colonization. This wall was estimated to have coral cover of approximately 40% (Figure 9-2). The most common species of coral on the wall were encrusting and plating colonies of *Montipora capitata* and *M. patula* followed by mounding and encrusting colonies of *P. lobata* and branching colonies of *Pocillopora meandrina*. Crustose coralline algae and turf algae were also common on the vertical wall.

9.1.2.3 *Algae*

The most common algal group at the sand donor area was turf algae, which colonized nearly all available abiotic hard substrate. The turf algae collected sand and fine-grained sediment and often created a carpet of sediment-bound turf.

With respect to macroalgae, 18 species/species groups were identified in the sand survey area. However, none of the observed macroalgal species groups were classified as abundant. Species/species groups classified as common were cyanobacteria, *Acanthophora spicifera*, and crustose coralline algae. Tufts of cyanobacteria were found on the seafloor attached to small stones in the sand as well as to larger expanses of hard substrate. *Acanthophora spicifera* was common

on the west side of the sand bed and was often found growing in conjunction with other macroalgae. *Acanthophora spicifera* is a red alga that is classified as invasive alien species by the Hawai‘i Department of Land and Natural Resources, Division of Aquatic Resources (DAR). In the 50 years since its unintended introduction from Guam, *A. spicifera* has become one of the most successful and abundant algae on Hawaiian reef flats. Crustose coralline algae were ubiquitous throughout the survey area and was commonly found on the wall off the south end of the donor bed as well as on rubble and boulders.

9.1.2.4 *Fish*

Fish were relatively uncommon within the sand survey area. Fish paucity is likely partially a result of low detectability owing to poor visibility at the time of the survey. In total, 26 species of fish were detected. The most common and conspicuous groups were the surgeonfish and damselfish, which were comprised of 3 species and 5 species, respectively. The wrasses were also well-represented with 4 species, however, 3 of these 4 species were considered rare within the survey area.

The saddle wrasse (*Thalassoma duperrey*) and the blackfin chromis (*Chromis vanderbiltili*) were the only species classified as abundant around the perimeter of the sand donor bed. The saddle wrasse was ubiquitous throughout the survey area and both juveniles and adults were observed. The blackfin chromis was commonly observed schooling over large coral heads in groups of up to 50 individuals. A group of Hawaiian Dascyllus (*Dascyllus albisella*) was schooling over a rock with mixed encrusting corals.

9.1.2.5 *Non-Coral Invertebrates*

In general, non-coral macro-invertebrates were conspicuously sparse around the perimeter of the sand bed with only five species/species groups detected. All of the species observed around the perimeter of the sand bed were classified as rare (low abundance at the site) except for the collector urchin (*Tripneustes gratilla*), which can be considered common within the survey area.

9.2 Punalu‘u Beach Park

9.2.1 *Physical Structure*

The seafloor offshore of the beach park consists primarily sand beach in the inter-tidal zone transitioning to mixed sand and rubble immediately offshore (Figure 9-4). The sand and rubble zone extends seaward for the entire offshore range of the study area and beyond. In general, the amount of sand decreases while the amount of solid rock bottom increases with distance from shore. Sand beds are also more common and persist further from shore at the northwest end of the survey area near the mouth of the Punalu‘u Stream. Occasional boulders and cracks forming small ledges add some rugosity to an otherwise flat, sloping seafloor in the nearshore zone. The entire sand/rubble/rock zone within the study area is shallow in depth, never deeper than approximately 2 m. The offshore area beyond the sandy intertidal zone consists of a relatively homogeneous environment with little distinct zonation in physical structure.

9.2.2 Biotic Community Structure

9.2.2.1 Algae

The biotic composition of the reef community fronting Punalu‘u Beach Park can generally be considered an algal dominated system. Most of the sand and rubble/rock surfaces were covered with a variety of turf and macroalgae (Figure 9-4). In total, 30 macroalgae species/species groups were identified in the Punalu‘u Beach Park survey area. The most common species/species groups were *Acanthophora spicifera*, crustose coralline algae, and cyanobacteria (Figure 9-5). These three macroalgae were categorized as abundant. *Acanthophora spicifera* is a red alga that is classified as an invasive alien species by the Hawai‘i Department of Land and Natural Resources, Division of Aquatic Resources (DAR). In the 50 years since its unintended introduction from Guam, *A. spicifera* has become one of the most successful and abundant algae on Hawaiian reef flats. *Halophila* spp. was not observed within the Punalu‘u beach Park survey area.

9.2.2.2 Coral

Reef building corals were present throughout the rubble and rock zones. However, colonies were generally isolated with no true accreting reef structure. Over the entire survey area along Punalu‘u Beach Park, six species of stony corals were documented, and only *Porites lobata* was considered common (Figure 9-6). It was estimated that corals accounted for less than 1% of bottom cover.

9.2.2.3 Non-Coral Macroinvertebrates

In general, non-coral macro-invertebrates were conspicuously sparse on the reef flat with only five species/species groups detected. All of the species observed at Punalu‘u Beach Park were classified as rare (low abundance at the site) with three sightings or fewer. Two species of sea cucumbers were detected (*Actinopyga varians* and *Holothuria atra*), one sea star (*Ophiocoma erinaceus*), one sea urchin (*Echinometra mathaei*), and several sponges. All five of these species/groups are common nearshore Hawai‘i organisms.

9.2.2.4 Fish

Fish were relatively uncommon on the reef flat, and the fish that were observed were generally small (less than 20 cm). In total, 11 species of fish were detected. The most common and conspicuous groups were the surgeonfish and wrasses, which were each comprised of 3 species. The ringtail surgeonfish (*Acanthurus blochii*) the Hawaiian whitespotted pufferfish (*Canthigaster jactator*), and the saddle wrasse (*Thalassoma duperrey*) were the only fish observed to be common within the survey area. No species of fish were observed to be abundant. The majority of fish were observed under small ledges and sheltering in boulders. The relative paucity of fish is likely a result of the lack of shelter for fish on the flat bottom structure of the nearshore area at Punalu‘u Beach Park.

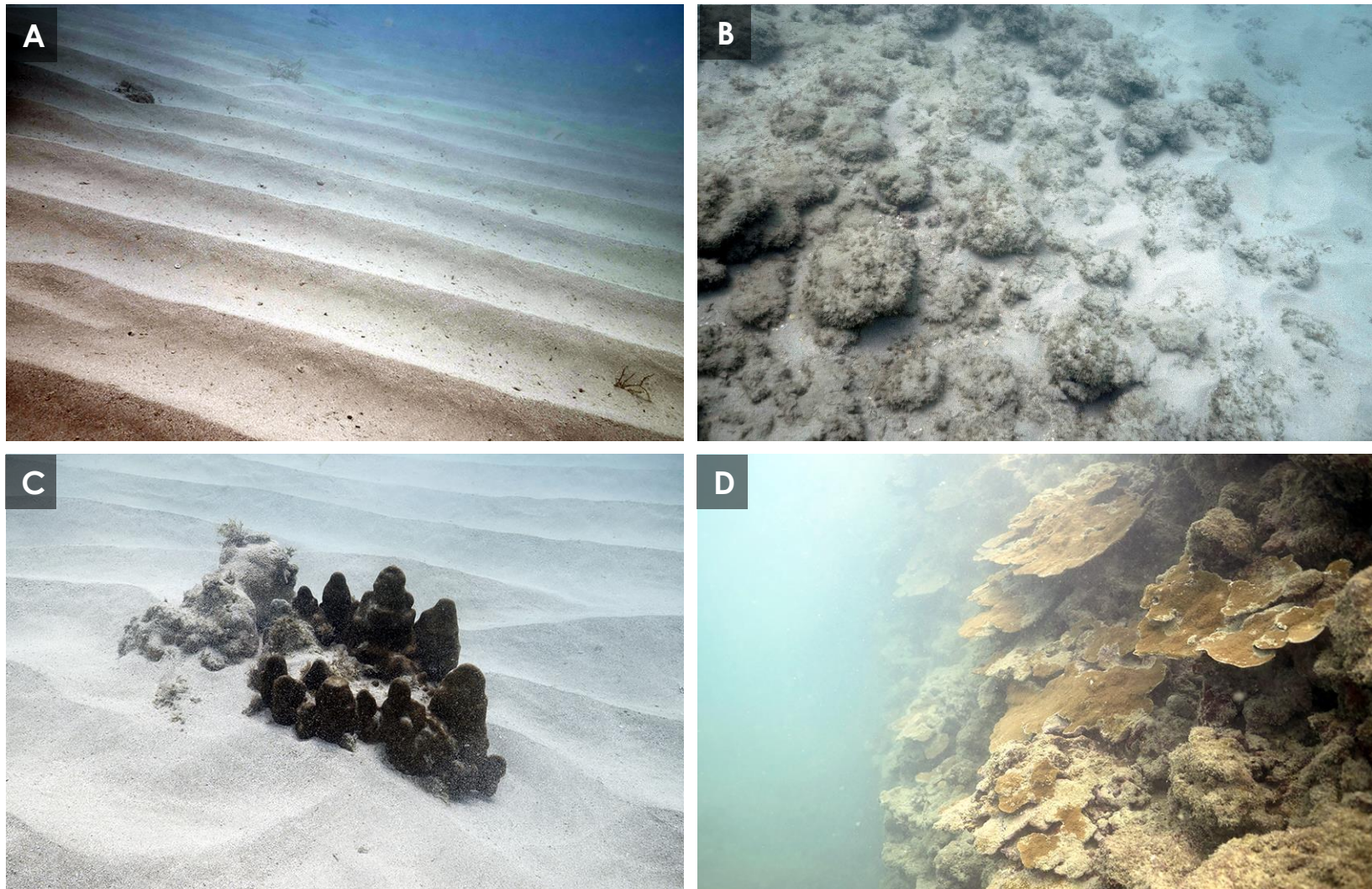


Figure 9-2. Representative images of the center and perimeter of the offshore sand deposit

Notes: A – Uniform bed of sand with sand waves in center of donor area; B – Rubble at edge of sand bed; C – Vertical wall at south side of sand bed; and D – partially buried coral at edge of sand bed

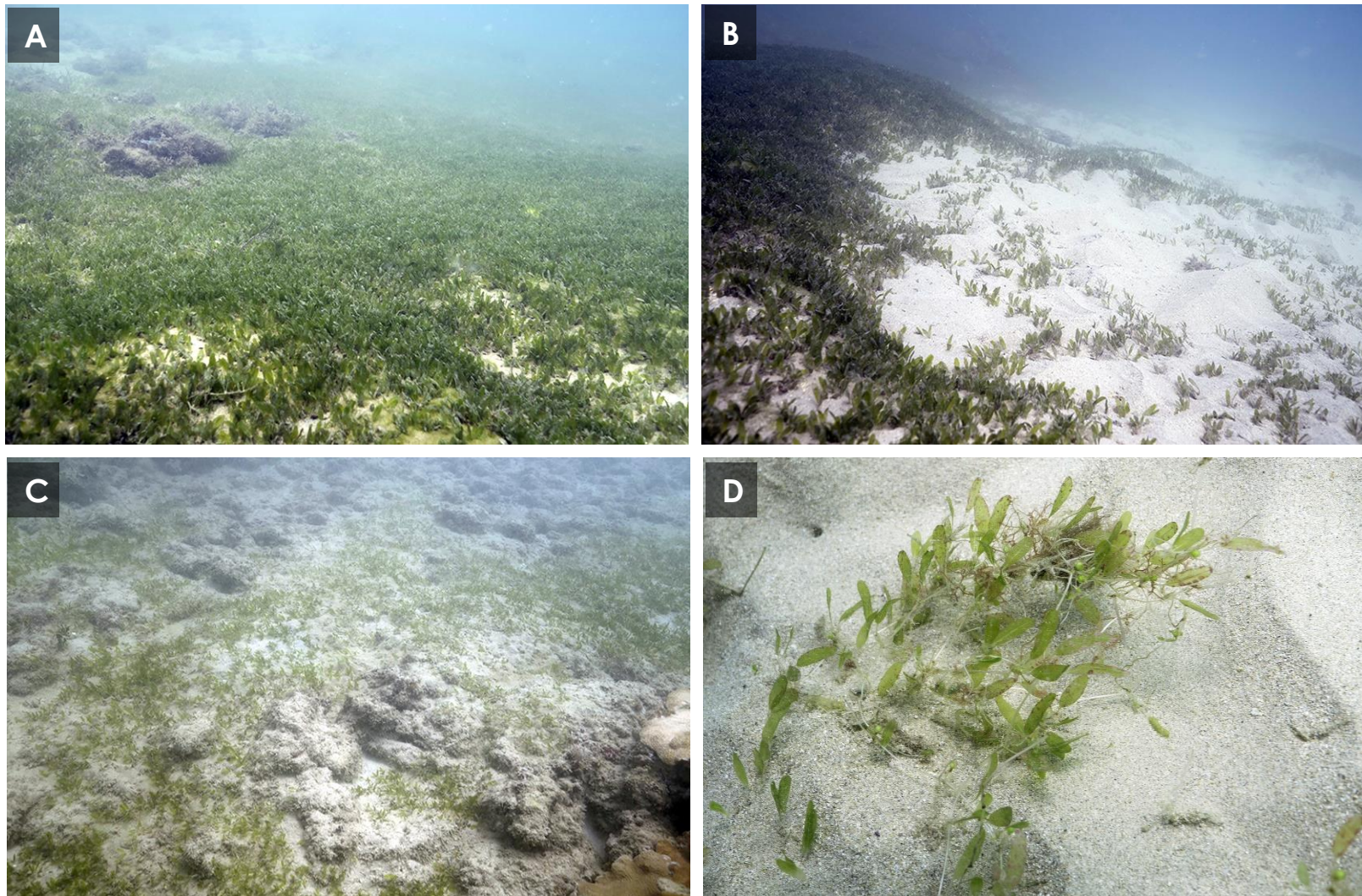


Figure 9-3. Representative images of seagrass at the perimeter of the offshore sand deposit

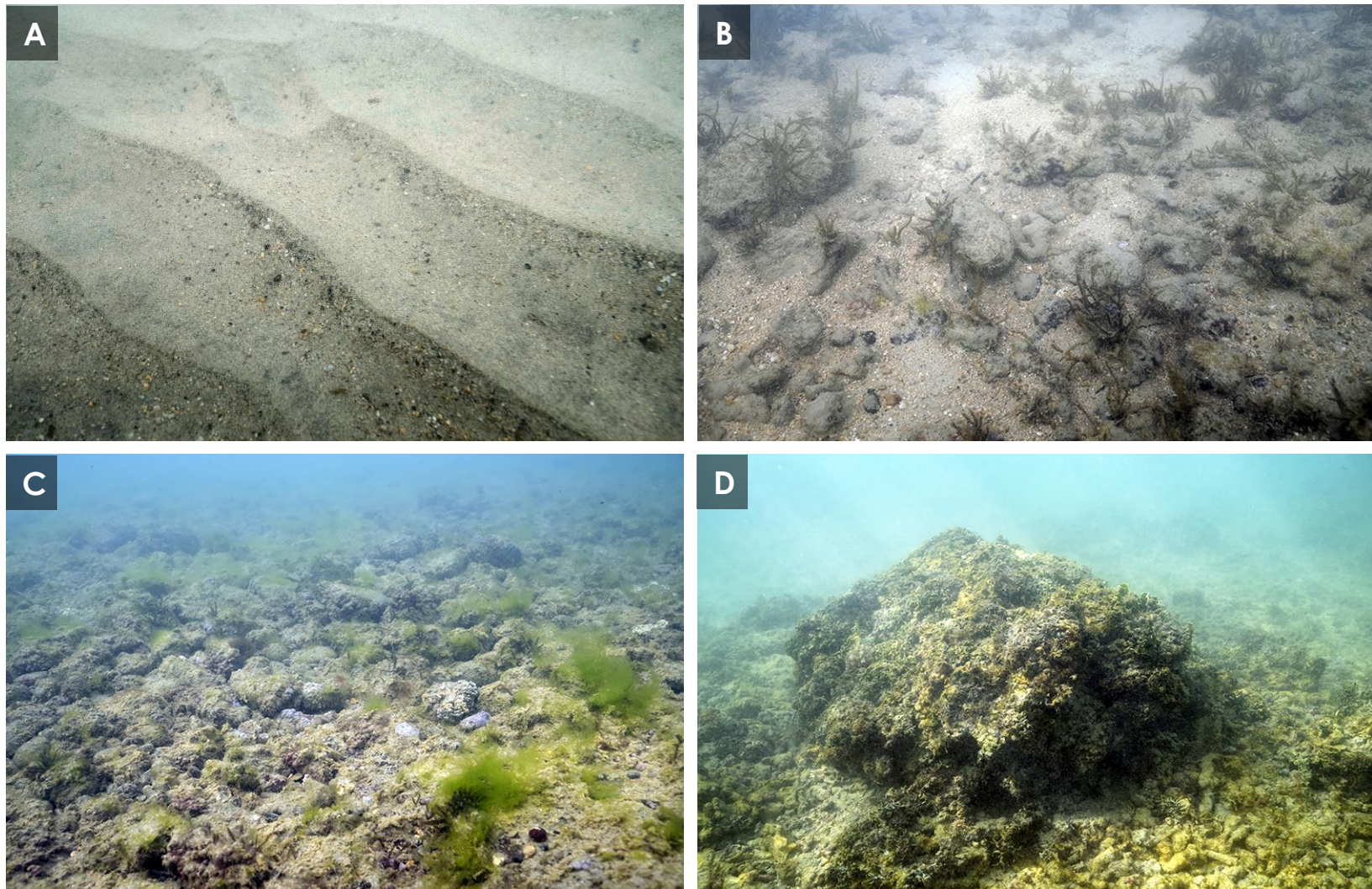


Figure 9-4. Representative images of the seafloor at Punalu'u Beach Park.

Notes: A – Sand waves; B and C – Mix of sand and rock rubble with turf and macroalgae ; and D – Boulder covered with turf and macroalgae

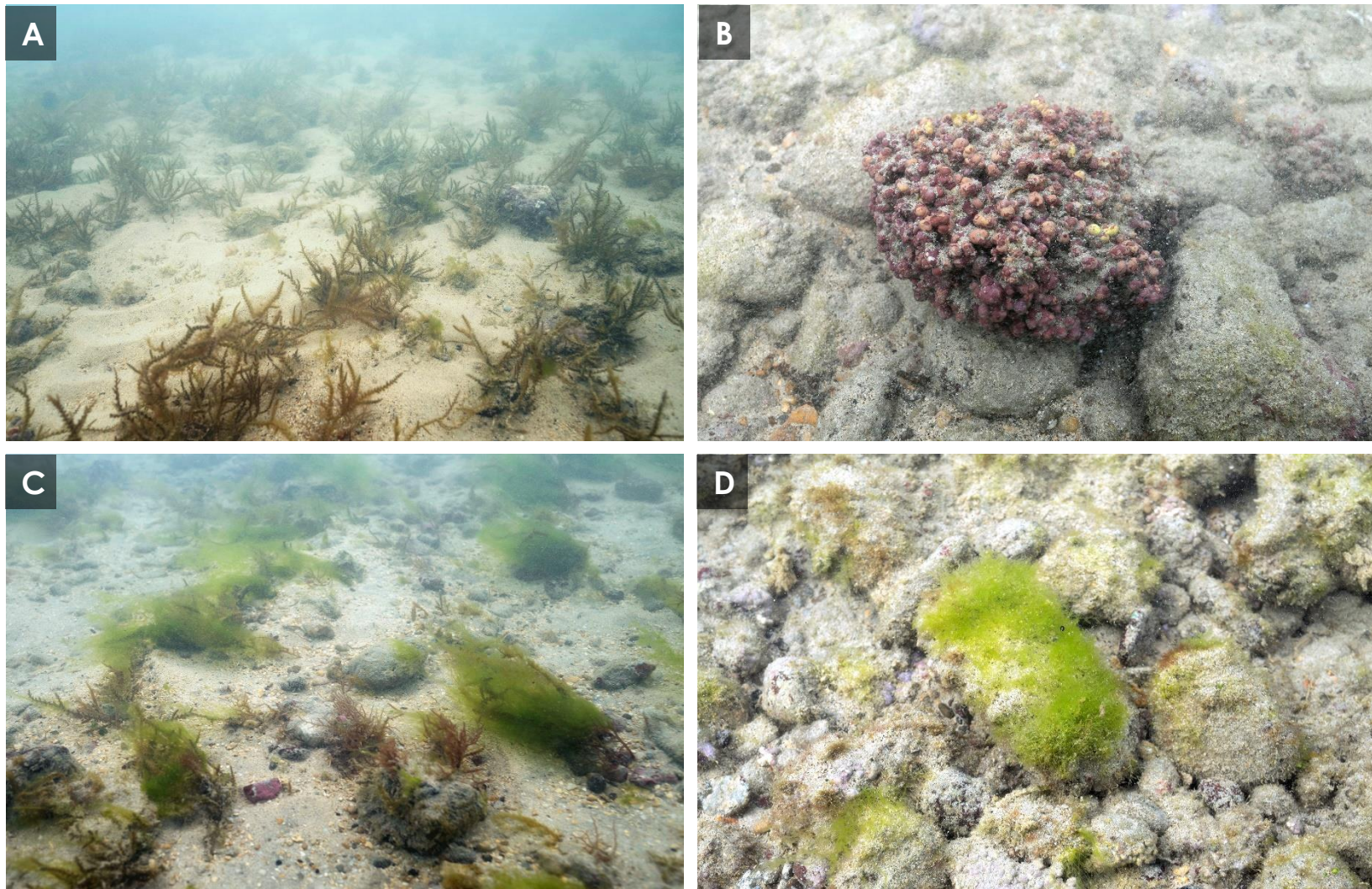


Figure 9-5. Representative images of macroalgae at Punalu'u Beach Park.

Notes: A – *Acanthophora spicifera*; B – Crustose Coralline Algae; C – Cyanobacteria (green) ; and D – *Boodlea composita*.

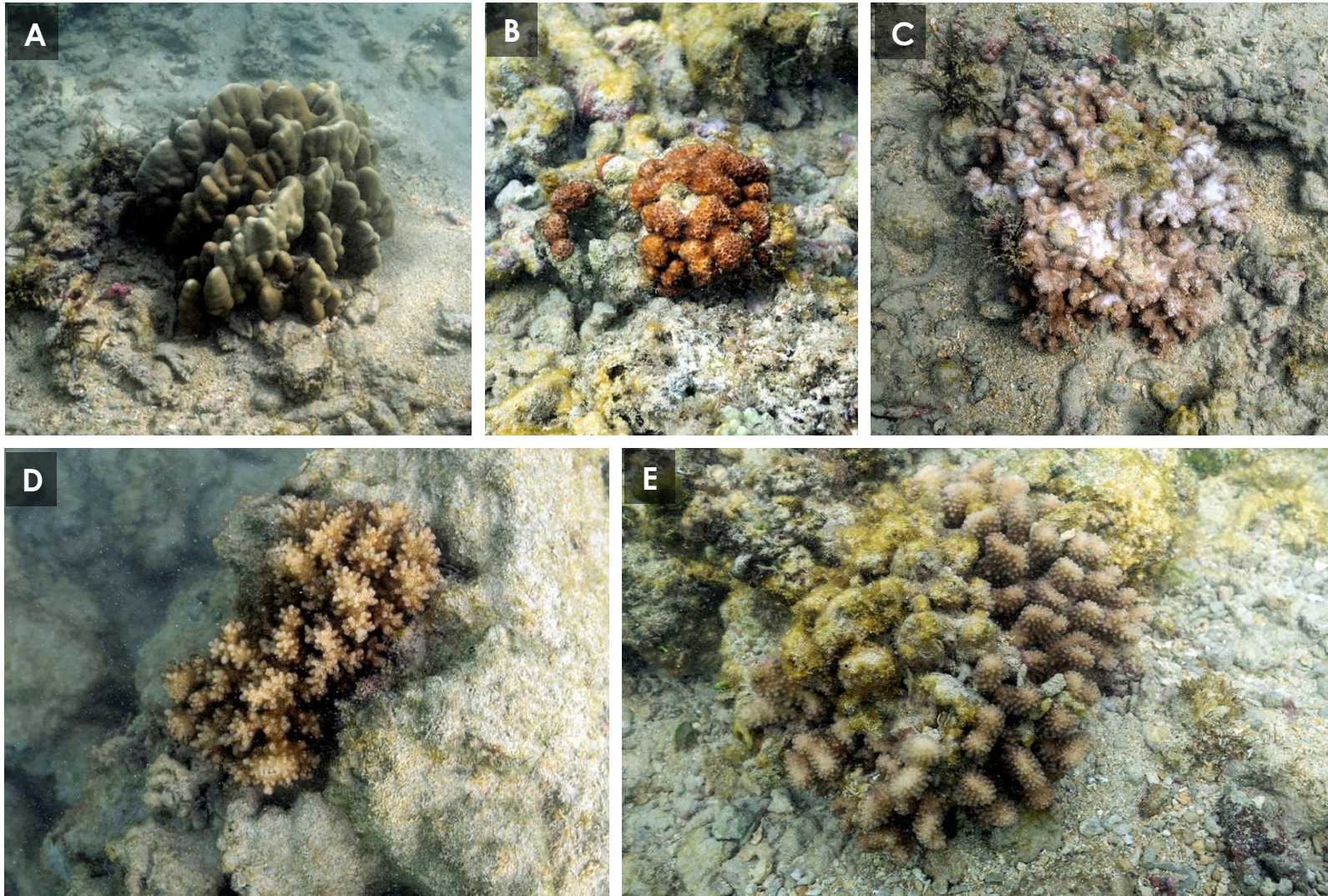


Figure 9-6. Representative images of corals at Punalu'u Beach Park.

Notes: A – *Porites lobata*; B – *Cyphastrea ocellina*; C – *Montipora capitata*; D – *Pocillopora damicornis*; and *Pocillopora meandrina*

10. BEACH RESTORATION CONCEPT ALTERNATIVES

10.1 Introduction

The primary objectives for this project are the following:

- protect Kamehameha Highway from flooding and erosion,
- improve community resiliency to sea level rise and coastal storms,
- provide recreational resources and native habitat, and
- restore the beach at Punalu‘u Beach Park.

Existing conditions at the project site limit shoreline improvement options to some extent. The backshore area, in its current form, between the existing erosion scarp and highway is narrow and low-lying which limits the creation of a natural dune system by adding sand to the backshore area as a standalone option for long-term restoration of the beach. To meet the project objectives listed above, the general strategy involves advancement seaward of the current shoreline position to restore the beach resource. Due to the low-lying backshore, the general strategy would also involve raising the backshore elevation to protect against future sea level rise and wave flooding.

The following section summarizes five (5) concept alternatives selected from the range of alternatives discussed in Section 2 which each meet the project objectives to varying degrees. Rough Order of Magnitude (ROM) cost estimates are also provided along with each alternative. Each alternative follows a nature-based or hybrid nature-based approach and the associated advantages and disadvantages of each are discussed.

10.2 Alternative 1 – Beach Nourishment

Alternative 1 consists of beach nourishment coupled with dune restoration or a vegetated berm enhancement and would involve placing sand along the Punalu‘u Beach Park shoreline. The sand would be placed along approximately 1,800 ft of shoreline between Wai‘ono Stream and the fence separating the beach park from the private properties to the southeast. The beach would have a crest elevation of +8.0 ft MSL and a beach slope of 1V:8H. For comparison, the existing beach slope is also 1V:8H but only has a crest elevation of between +4.5 and +6.5 MSL. This concept would require 46,000 cy of sand and would advance the beach toe about 50 ft seaward from its current position. The backshore area would be enhanced by the addition of a vegetated berm or dune up to an elevation of +8.5 ft MSL. Based on historical erosion rates, the beach may only last between 15 and 25 years before it recedes to its pre-project position. Follow-up beach re-nourishment would likely be required every 10 years to maintain the beach width. Erosion rates may accelerate due to increasing sea level rise. Table 10-1 summarizes the change in dry beach width/area (measured from the backshore vegetated berm or dune to MHHW) and the backshore vegetated berm or dune width/area (measured from edge of highway road shoulder). The concept plan for this alternative is shown in Figure 10-1 and typical section shown in Figure 10-2.

The advantages and disadvantages of Alternative 1 – Beach Nourishment are as follows:

Advantages

- Sand fill would provide a natural buffer from storm waves and high-water levels.
- Improves lateral shoreline access.
- Improves access to and from the water.
- Provides wide sand beach for recreation.

Disadvantages

- Sand fill for beach nourishment would be subject to chronic and likely accelerating erosion occurring in the project area, and thus is not expected to remain in the medium to long term (15 to 25 years).
- Periodic beach re-nourishment may be required to maintain the beach.
- Because there are no stabilizing structures, rapid, catastrophic sand loss is possible due to severe wave events.
- Additional offshore sand surveys would be required to determine availability of offshore sand for follow-up re-nourishment activities.

Table 10-1. Beach nourishment dry beach and backshore parameters

	Existing	Proposed
Avg. Dry Beach Width (ft)	0 to 20	70
Dry Beach Area (sq.ft.)	43,830	135,800
Avg. Backshore Width (ft)	45	65
Backshore Area (sq.ft.)	86,555	122,850

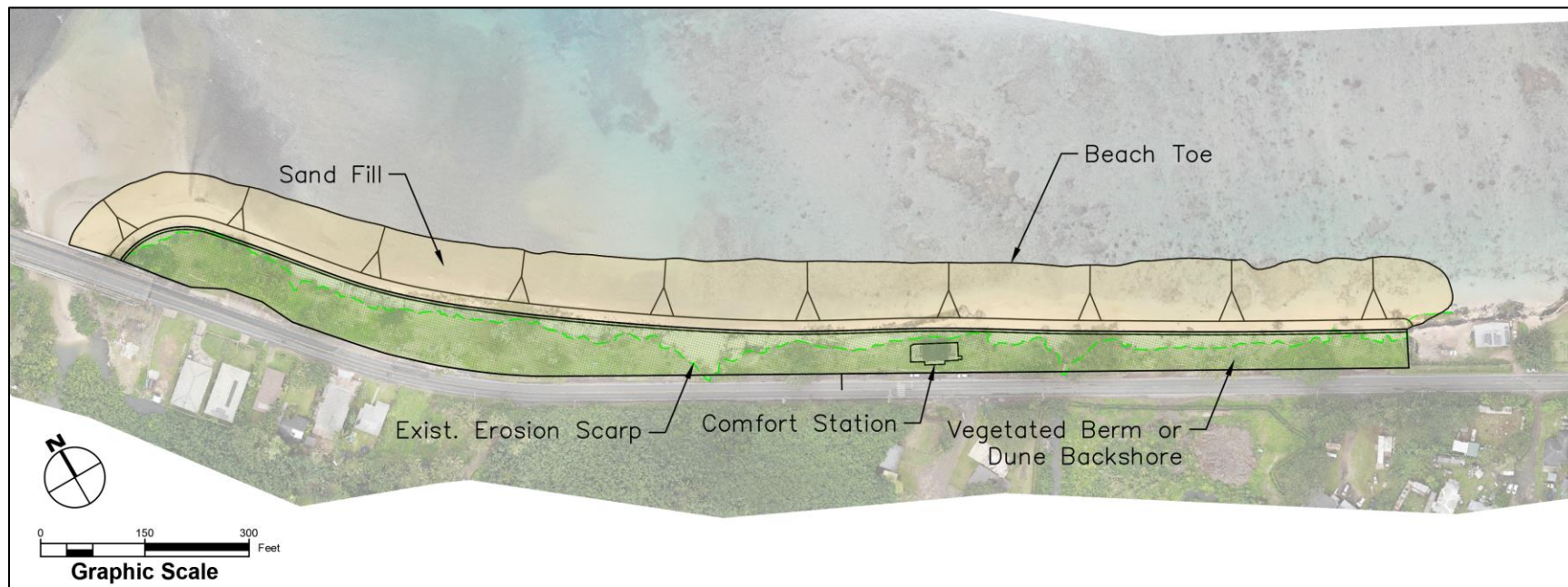


Figure 10-1. Beach nourishment concept plan view

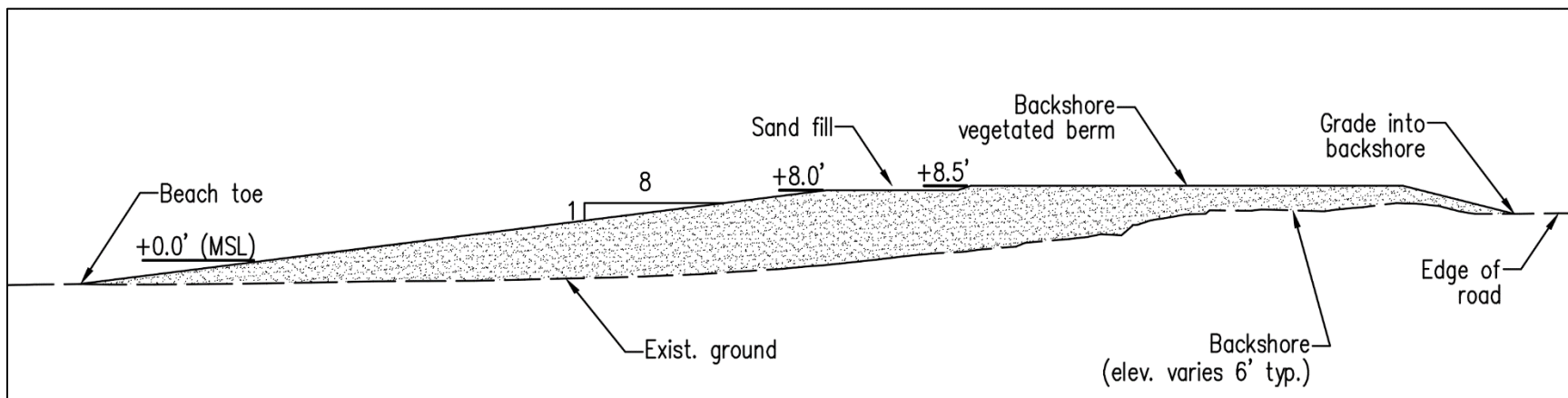


Figure 10-2. Typical section view of beach nourishment concept



10.2.1 Alternative 1 – ROM Cost Estimate

Table 10-2 below summarizes the ROM cost estimate breakdown for Alternative 1 – Beach Nourishment. The cost for sand recovery and placement are separated from the backshore work costs. The unit rate to recover and place 46,000 cy of sand is \$280/cy. This unit rate is expected to increase with decreasing volumes of sand due to the fixed costs associated with construction activities. The total ROM cost for this alternative is \$14,835,000. The ROM cost does not include the recurring nourishment efforts that would be needed to maintain the beach width.

Table 10-2. Alternative 1 ROM cost breakdown

Sand Recovery and Placement Task Descriptions:	ROM Cost Breakdown
Construction Mobilization and Demobilization	\$295,000
Environmental Controls and Safety Measures	\$450,000
Water Quality Monitoring and Surveying Services	\$180,000
Installation of HDPE Pipeline from Sand Recovery Area to the Shoreline	\$1,575,000
Dewatering Basin Construction	\$650,000
Hydraulic Suction Dredging of Offshore Sand and Transport to Dewatering Basin	\$8,740,000
Spread Dredged Sand Along Beach	\$920,000
Weather Contingency	\$75,000
Subtotal:	\$12,885,000
Backshore Vegetated Berm or Dune Construction Task Descriptions:	
Construction Mobilization and Demobilization	\$50,000
Environmental Controls and Safety Measures	\$100,000
Backshore Dune Construction	\$1,800,000
Subtotal:	\$1,950,000
Total:	\$14,835,000

10.3 Alternative 2 – Beach Nourishment with Buried Revetment

Beach nourishment at Punalu‘u is anticipated to only last between 15 and 25 years based on the historical erosion rates (see Section 4). At a minimum, the beach would likely migrate landward at the historic erosion rate, however, with future sea level rise, this erosion rate is expected to increase, and the beach may last less than 15 years. To improve the resiliency of the beach park to sea level rise, a buried revetment structure installed within the backshore of the beach nourishment would act as a backstop and serve to protect the backshore area when the beach erodes back to its pre-project position. The buried revetment would tie into the existing bridge abutment to the north of the park and extend south to the existing fence separating the private homes and the beach park. The location of the buried revetment seaward of the existing erosion scarp would preserve the backshore area to be used by park users even after the beach has eroded. Alternatively, the buried revetment could be installed adjacent to the highway behind the existing park backshore area to allow additional time before the backstop is exposed by shoreline erosion. However, this option would require the removal of the comfort station and any other infrastructure within the beach park since it would not be protected from erosion. The backshore area would be enhanced by the addition of a vegetated berm or dune up to an elevation of +8.5 ft MSL. Table 10-3 summarizes the change in dry beach width/area (measured from the backshore vegetated berm or dune to

MHHW) and the backshore vegetated berm or dune width/area (measured from edge of highway road shoulder). The concept plan for this alternative is shown in Figure 10-3 and typical sections shown in Figure 10-4 and Figure 10-5.

The advantages and disadvantages of Alternative 2 – Beach Nourishment with Buried Revetment are as follows:

Advantages

- Improves lateral shoreline access.
- Improves access to and from the water.
- Provides wide beach for recreation.
- Buried revetment would protect the backshore and highway from shoreline erosion.

Disadvantages

- Sand fill for beach nourishment would be subject to chronic and likely accelerating erosion occurring in the project area, and thus is not expected to remain in the medium to long term (15 to 25 years).
- Because there are no stabilizing structures, rapid, catastrophic sand loss is possible due to severe wave events.
- Periodic beach re-nourishment may be required to maintain the beach.
- Continued erosion of the sand beach could eventually lead to exposure of the revetment, leaving the shoreline armored and without a restored sand beach.
- An exposed revetment would likely interrupt any natural beach processes.
- Additional offshore sand surveys would be required to determine availability of offshore sand for follow-up re-nourishment activities.
- Higher cost than standalone beach nourishment.
- Sourcing suitable stone size and quality may be challenging.

Table 10-3. Beach nourishment with buried revetment dry beach and backshore parameters

	Existing	Proposed
Avg. Dry Beach Width (ft)	0 to 20	70
Dry Beach Area (sq.ft.)	43,830	135,800
Avg. Backshore Width (ft)	45	65
Backshore Area (sq.ft.)	86,555	122,850

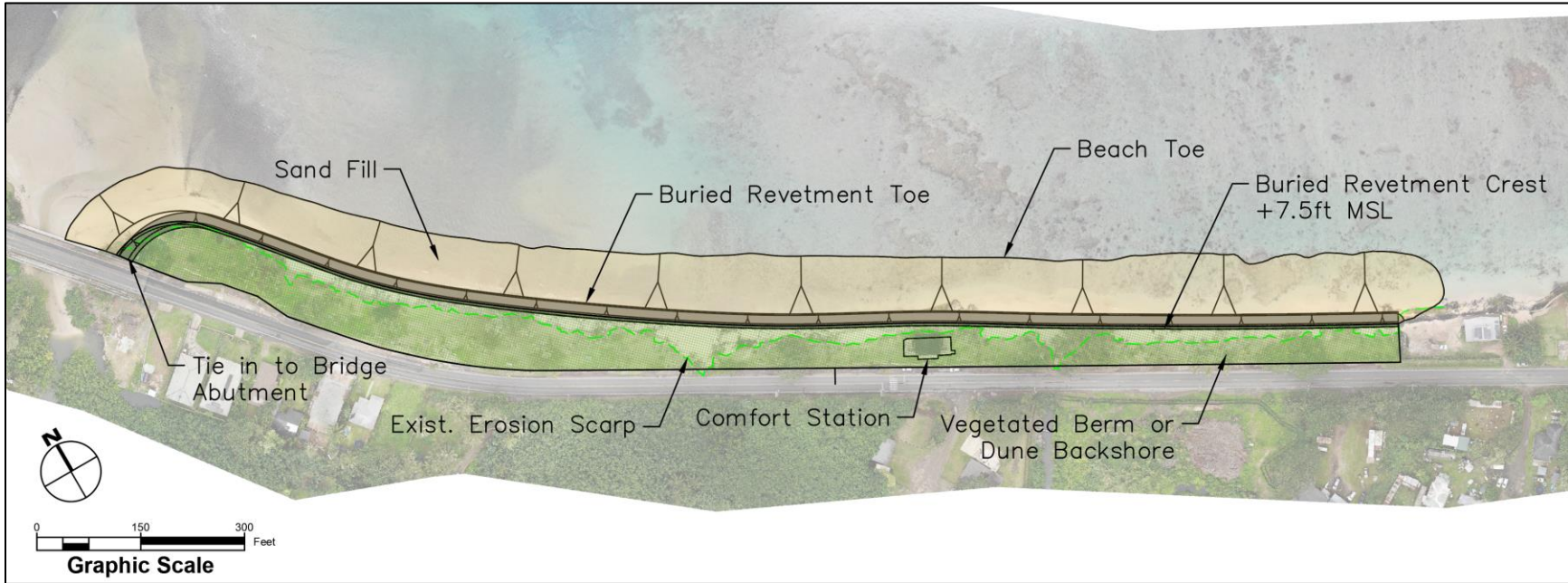


Figure 10-3. Beach nourishment with buried revetment concept plan view

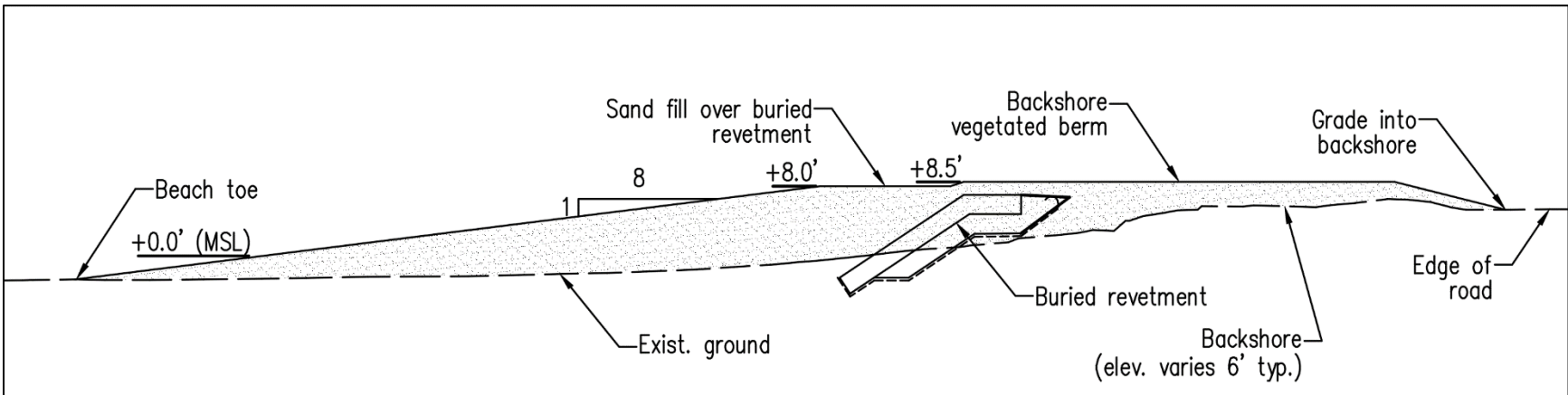


Figure 10-4. Typical section view of beach nourishment with buried revetment concept

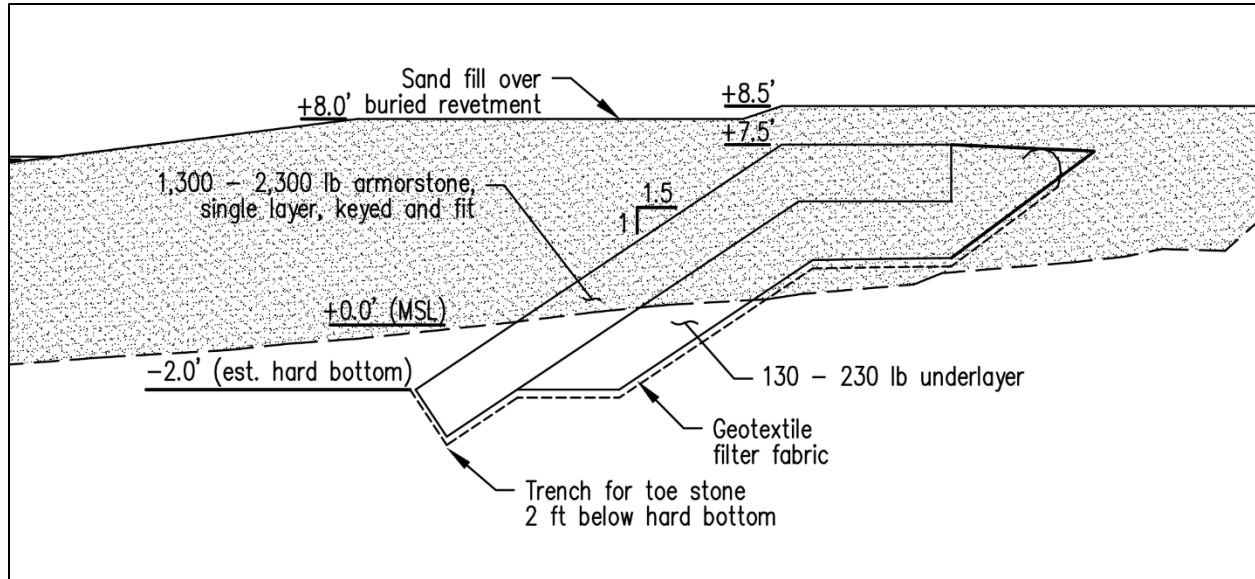


Figure 10-5. Section view of buried revetment

10.3.1 Alternative 2 – ROM Cost Estimate

Table 10-4 below summarizes the ROM cost estimate breakdown for Alternative 2 – Beach Nourishment with Buried Revetment. The total ROM cost for this alternative is \$22,396,000.

Table 10-4. Alternative 2 ROM cost breakdown

Sand Recovery and Placement Task Descriptions:	ROM Cost Breakdown
Construction Mobilization and Demobilization	\$295,000
Environmental Controls and Safety Measures	\$450,000
Water Quality Monitoring and Surveying Services	\$180,000
Installation of HDPE Pipeline from Sand Recovery Area to the Shoreline	\$1,575,000
Dewatering Basin Construction	\$650,000
Hydraulic Suction Dredging of Offshore Sand and Transport to Dewatering Basin	\$8,740,000
Spread Dredged Sand Along Beach	\$920,000
Weather Contingency	\$75,000
Subtotal:	\$12,885,000
Revetment Construction Task Descriptions:	
Construction Mobilization and Demobilization	\$250,000
Environmental Controls and Safety Measures	\$525,000
Water Quality Monitoring and Surveying Services	\$256,000
Construct Buried Revetment	\$6,330,000i
Weather Contingency	\$200,000
Subtotal:	\$7,561,000
Backshore Dune Construction Task Descriptions:	
Construction Mobilization and Demobilization	\$50,000
Environmental Controls and Safety Measures	\$100,000

Backshore Dune Construction	\$1,800,000
Subtotal:	\$1,950,000
Total:	\$22,396,000

10.4 Alternative 3 – Stabilized Pocket Beaches

This alternative includes beach nourishment and construction of five (5) pocket beach headland structures and one stabilizing structure at the north end of the shoreline. The stabilizing structures would be spaced between 325 and 350 ft apart and would extend between 205 and 230 ft from the existing erosion scarp. The heads would extend between 72 and 84 ft to either side of the stem, at angles ranging from 90° to 120° in order to best orient the gaps between heads parallel to the typical wave approach. The straight stabilizing structure at the north end of the shoreline would tie into the existing bridge abutment and extend about 170 ft offshore. This structure would serve to stabilize and protect the shoreline north of the beach park from any potential downdrift effects caused by northern most headland structure. To minimize the structure footprints, the headland sections (seaward ends) would have crest elevations of +6.5 ft MSL while the stems (landward ends) would have elevations of +8.5 ft MSL to limit sand exchange between adjacent pocket beach cells. The beach would have a crest elevation of +8.0 ft MSL and a beach slope of 1V:10H. The backshore area would be enhanced by the addition of a vegetated berm or dune up to an elevation of +8.5 ft MSL. Table 10-5 summarizes the change in dry beach width/area (measured from the backshore vegetated berm or dune to MHHW) and the backshore vegetated berm or dune width/area (measured from edge of highway road shoulder). The plan view for this alternative is shown in Figure 10-6 and typical section views of the structure heads and stems are shown in Figure 10-7.

The advantages and disadvantages of Alternative 3 – Stabilized Pocket Beaches are as follows:

Advantages

- Improves lateral shoreline access.
- Improves access to and from the water.
- Provides a wide beach for recreation.
- Sand fill is protected from erosion, minimizing or possibly eliminating need for renourishment maintenance.
- Structures may provide improved marine habitat and biomass/biodiversity.

Disadvantages

- Larger footprint than standalone beach nourishment.
- Higher cost than standalone beach nourishment.
- Sourcing suitable stone size and quality may be challenging.
- Alters view plane and character of beach.

Table 10-5. Stabilizing pocket beaches dry beach and backshore parameters

	Existing	Proposed
Avg. Dry Beach Width (ft)	0 to 20	90
Dry Beach Area (sq.ft.)	43,830	156,730
Avg. Backshore Width (ft)	45	50
Backshore Area (sq.ft.)	86,555	91,290

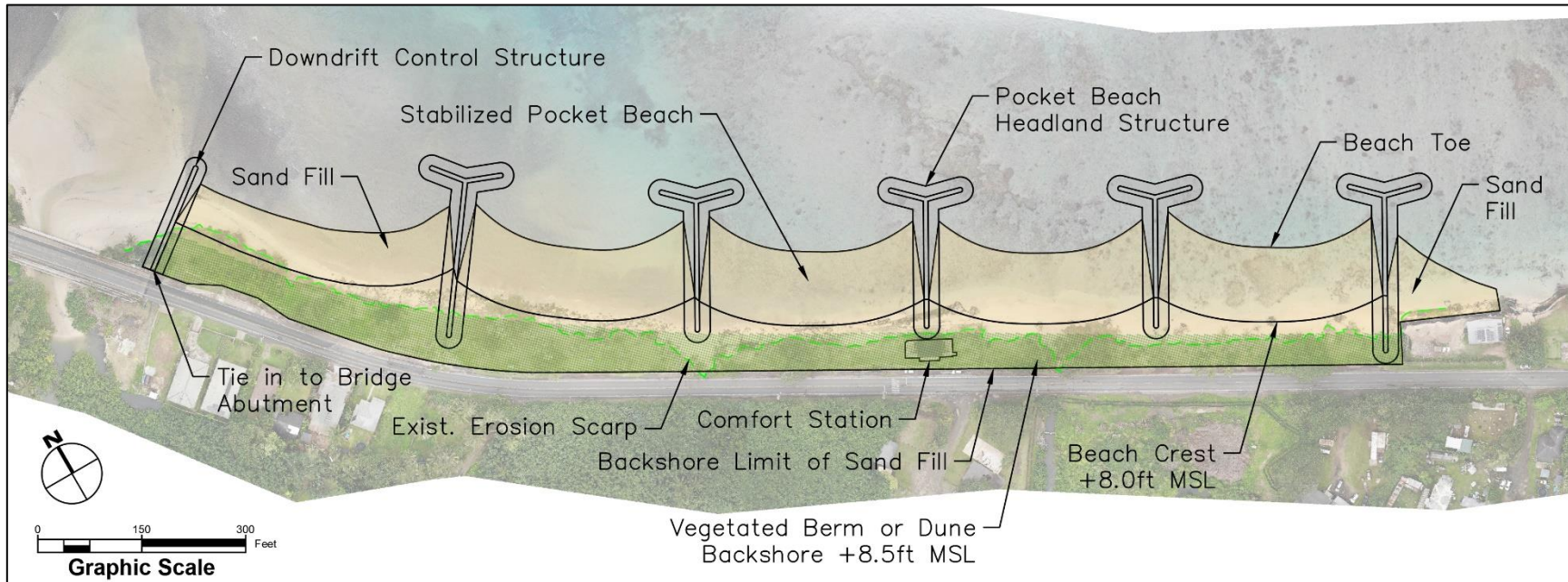


Figure 10-6. Stabilized pocket beaches concept plan view

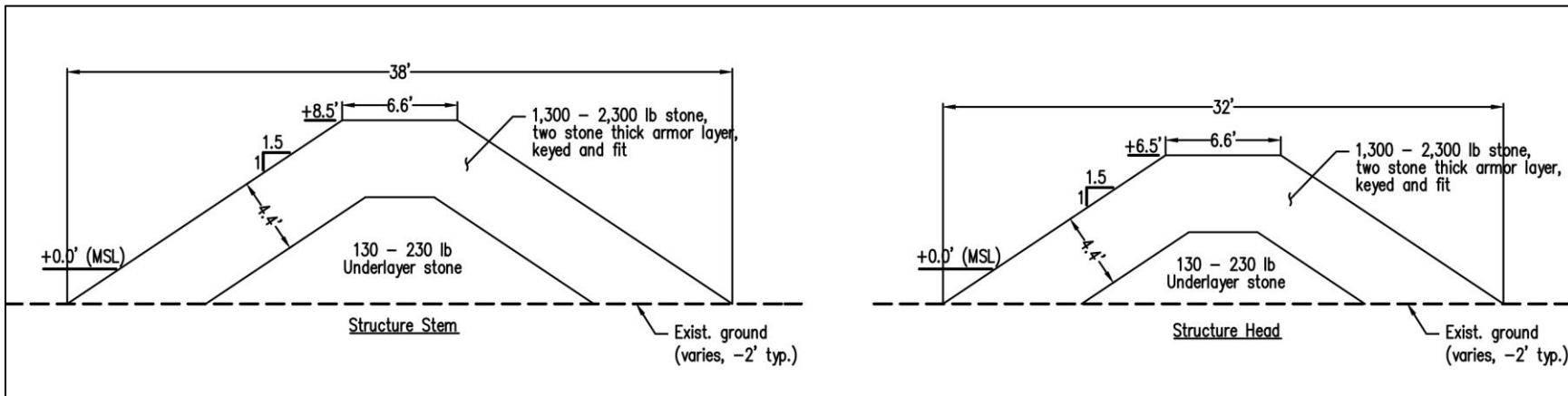


Figure 10-7. Stabilized pocket beaches - structure typical section views (stem and head sections)



10.4.1 Alternative 3 – ROM Cost Estimate

Table 10-6 below summarizes the ROM cost estimate breakdown for Alternative 3 – Stabilized Pocket Beaches. The total ROM cost for this alternative is \$32,910,000. The ROM cost does not include the recurring nourishment efforts that would be needed to maintain the beach width.

Table 10-6. Alternative 3 ROM cost breakdown

Sand Recovery and Placement Task Descriptions:	ROM Cost Breakdown
Construction Mobilization and Demobilization	\$295,000
Environmental Controls and Safety Measures	\$450,000
Water Quality Monitoring and Surveying Services	\$180,000
Installation of HDPE Pipeline from Sand Recovery Area to the Shoreline	\$1,575,000
Dewatering Basin Construction	\$650,000
Hydraulic Suction Dredging of Offshore Sand and Transport to Dewatering Basin	\$8,740,000
Spread Dredged Sand Along Beach	\$920,000
Weather Contingency	\$75,000
Subtotal:	\$12,885,000
Stabilizing Structure Construction Task Descriptions:	
Construction Mobilization and Demobilization	\$250,000
Environmental Controls and Safety Measures	\$647,000
Water Quality Monitoring and Surveying Services	\$128,000
Furnish and Install Five (5) Headland Structures	\$14,750,000
Furnish and Install Downdrift Control Structure	\$2,100,000
Weather Contingency	\$200,000
Subtotal:	\$18,075,000
Backshore Dune Construction Task Descriptions:	
Construction Mobilization and Demobilization	\$50,000
Environmental Controls and Safety Measures	\$100,000
Backshore Dune Construction	\$1,800,000
Subtotal:	\$1,950,000
Total:	\$32,910,000

10.5 Alternative 4 – Partially Stabilized Pocket Beaches

Alternative 4 includes beach nourishment and construction of six (6) straight stabilizing structures to partially stabilize the beach. These stabilizing structures have a smaller footprint than the headland structures and would reduce the potential longshore sediment transport along the shoreline. However, without the headland feature on these structures, sand may still be transported offshore and away from the beach system. Sand may also pass around the seaward ends of the structures. The backshore area would be enhanced by the addition of a vegetated berm or dune up to an elevation of +8.5 ft MSL. Table 10-7 summarizes the change in dry beach width/area (measured from the backshore vegetated berm or dune to MHHW) and the backshore vegetated berm or dune width/area (measured from edge of highway road shoulder). The plan view for this

alternative is shown in Figure 10-8 and typical section views of the structure heads and stems are shown in Figure 10-9.

The advantages and disadvantages of Alternative 4 – Partially Stabilized Pocket Beaches are as follows:

Advantages

- Improves lateral shoreline access.
- Improves access to and from the water.
- Provides wide beach for recreation.
- Sand fill is partially protected from erosion, reducing the frequency of renourishment maintenance.
- Structures may provide improved marine habitat and biomass/biodiversity.

Disadvantages

- Larger footprint than standalone beach nourishment.
- Rip currents may develop along structure stems posing a risk to swimmers.
- Sand may still be lost from the system.
- Higher cost than standalone beach nourishment.
- Sourcing suitable stone size and quality may be challenging.
- Alters view plane and character of beach.

Table 10-7. Partially stabilizing pocket beaches dry beach and backshore parameters

	Existing	Proposed
Avg. Dry Beach Width (ft)	0 to 20	75
Dry Beach Area (sq.ft.)	43,830	131,770
Avg. Backshore Width (ft)	45	50
Backshore Area (sq.ft.)	86,555	91,290

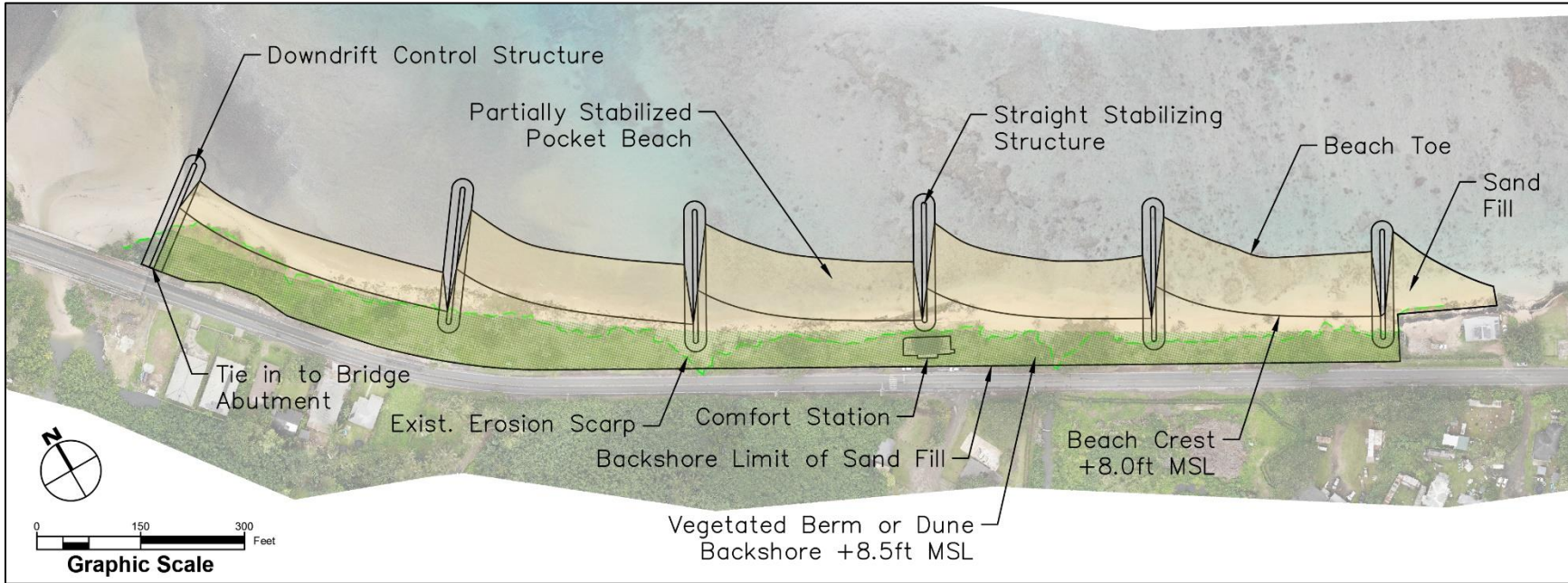


Figure 10-8. Partially stabilized pocket beaches concept plan view

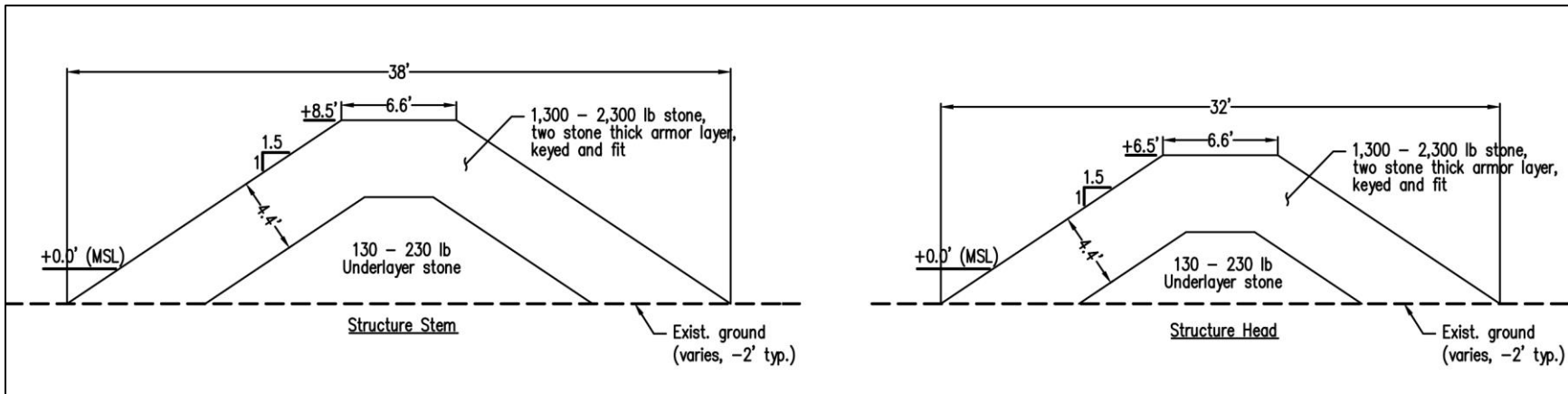


Figure 10-9. Partially stabilized pocket beaches - structure typical section views (stem and head sections)



10.5.1 Alternative 4 – ROM Cost Estimate

Table 10-8 below summarizes the ROM cost estimate breakdown for Alternative 4 – Partially Stabilized Pocket Beaches. The total ROM cost for this alternative is \$28,539,000.

Table 10-8. Alternative 4 ROM cost breakdown

Sand Recovery and Placement Task Descriptions:	ROM Cost Breakdown
Construction Mobilization and Demobilization	\$295,000
Environmental Controls and Safety Measures	\$450,000
Water Quality Monitoring and Surveying Services	\$180,000
Installation of HDPE Pipeline from Sand Recovery Area to the Shoreline	\$1,575,000
Dewatering Basin Construction	\$650,000
Hydraulic Suction Dredging of Offshore Sand and Transport to Dewatering Basin	\$8,740,000
Spread Dredged Sand Along Beach	\$920,000
Weather Contingency	\$75,000
Subtotal:	\$12,885,000
Stabilizing Structure Construction Task Descriptions:	
Construction Mobilization and Demobilization	\$250,000
Environmental Controls and Safety Measures	\$550,000
Water Quality Monitoring and Surveying Services	\$104,000
Furnish and Install Six (6) Straight Stabilizing Structures	\$12,600,000
Weather Contingency	\$200,000
Subtotal:	\$13,704,000
Backshore Dune Construction Task Descriptions:	
Construction Mobilization and Demobilization	\$50,000
Environmental Controls and Safety Measures	\$100,000
Backshore Dune Construction	\$1,800,000
Subtotal:	\$1,950,000
Total:	\$28,539,000

10.6 Alternative 5 – Hybrid Stabilized Pocket Beaches

Alternative 5 consists of a combination of Alternatives 3 and 4 by utilizing headland type stabilizing structures in the critical area of the park surrounding the comfort station and straight stabilizing structures towards the north and south portions of the park. The backshore area would be enhanced by the addition of a vegetated berm or dune up to an elevation of +8.5 ft MSL. Table 10-9 summarizes the change in dry beach width/area (measured from the backshore vegetated berm or dune to MHHW) and the backshore vegetated berm or dune width/area (measured from edge of highway road shoulder). The plan view for this alternative is shown in Figure 10-10 and typical section views of the structure heads and stems are shown in Figure 10-11.

The advantages and disadvantages of Alternative 4 – Partially Stabilized Pocket Beaches are as follows:

Advantages

- Improves lateral shoreline access.
- Improves access to and from the water.
- Provides wide beach for recreation.
- Sand fill is well protected from erosion, minimizing the need for renourishment maintenance.
- Structures may provide improved marine habitat and biomass/biodiversity.

Disadvantages

- Larger footprint than standalone beach nourishment.
- Rip currents may develop along structure stems posing a risk to swimmers.
- Sand may still be lost from the system.
- Higher cost than standalone beach nourishment.
- Sourcing suitable stone size and quality may be challenging.
- Alters view plane and character of the beach.

Table 10-9. Hybrid stabilizing pocket beaches dry beach and backshore parameters

	Existing	Proposed
Avg. Dry Beach Width (ft)	0 to 20	75
Dry Beach Area (sq.ft.)	43,830	132,355
Avg. Backshore Width (ft)	45	50
Backshore Area (sq.ft.)	86,555	91,290

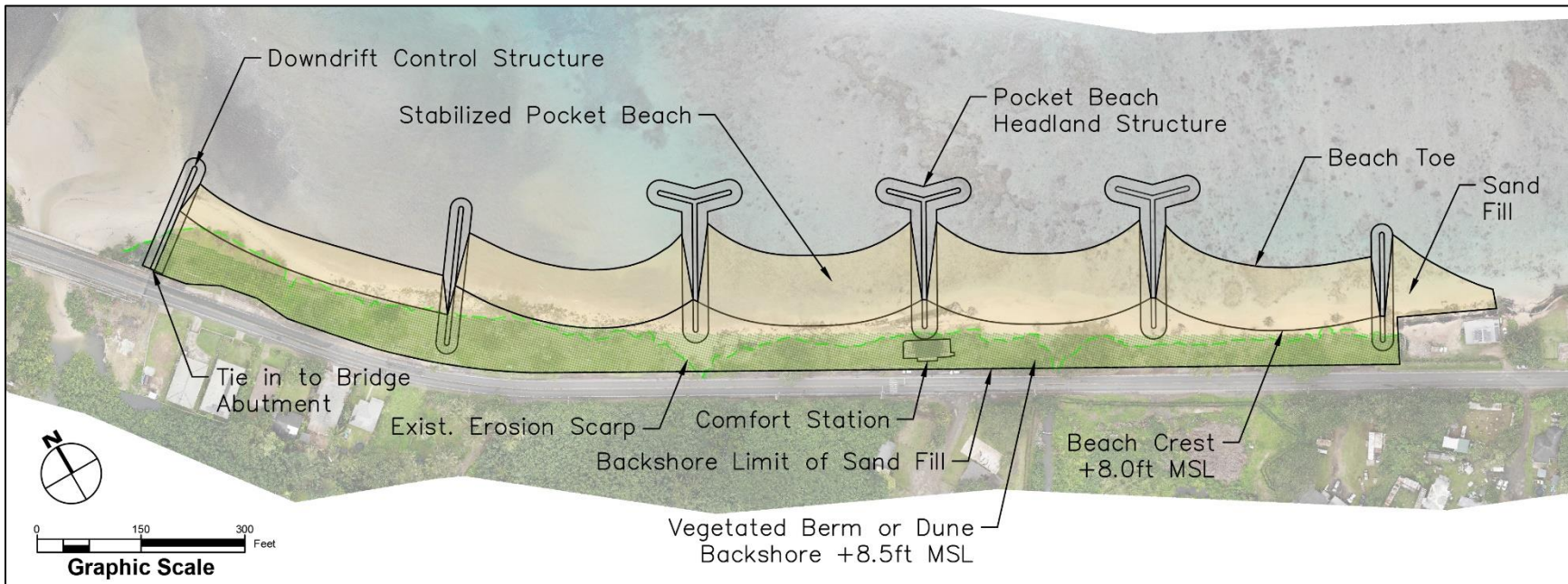


Figure 10-10. Hybrid stabilized pocket beaches concept plan view

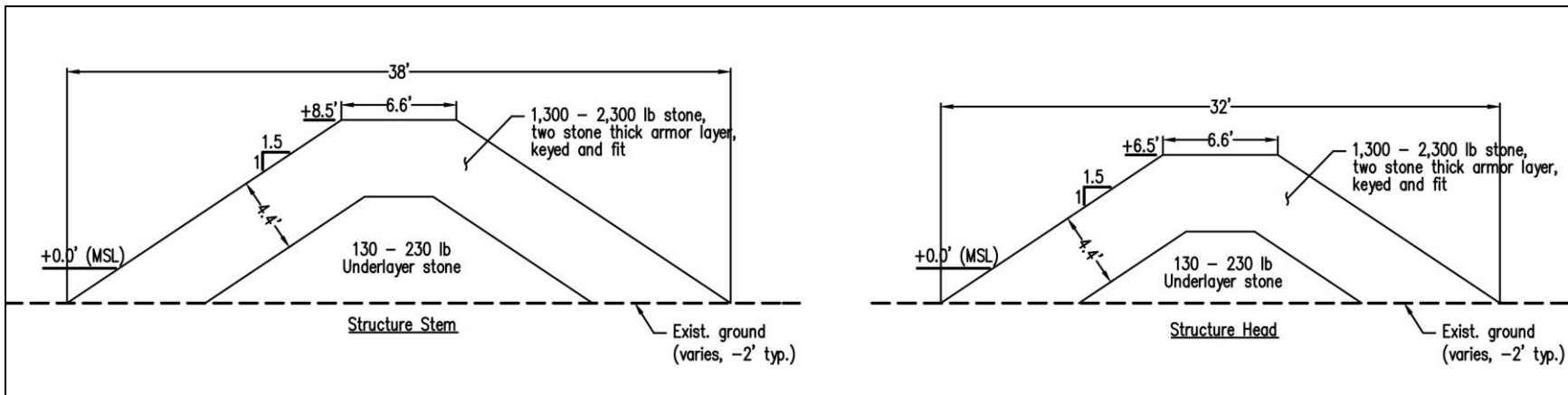


Figure 10-11. Hybrid stabilized pocket beaches - structure typical section views (stem and head sections)



10.6.1 *Alternative 5 – ROM Cost Estimate*

Table 10-10 below summarizes the ROM cost estimate breakdown for Alternative 5 – Hybrid Stabilized Pocket Beaches. The total ROM cost for this alternative is \$31,210,000.

Table 10-10. Alternative 5 ROM cost breakdown

Sand Recovery and Placement Task Descriptions:	ROM Cost Breakdown
Construction Mobilization and Demobilization	\$295,000
Environmental Controls and Safety Measures	\$450,000
Water Quality Monitoring and Surveying Services	\$180,000
Installation of HDPE Pipeline from Sand Recovery Area to the Shoreline	\$1,575,000
Dewatering Basin Construction	\$650,000
Hydraulic Suction Dredging of Offshore Sand and Transport to Dewatering Basin	\$8,740,000
Spread Dredged Sand Along Beach	\$920,000
Weather Contingency	\$75,000
Subtotal:	\$12,885,000
Stabilizing Structure Construction Task Descriptions:	
Construction Mobilization and Demobilization	\$250,000
Environmental Controls and Safety Measures	\$647,000
Water Quality Monitoring and Surveying Services	\$128,000
Furnish and Install Three (3) Headland Structures	\$8,850,000
Furnish and Install Downdrift Control Structure	\$6,300,000
Weather Contingency	\$200,000
Subtotal:	\$16,375,000
Backshore Dune Construction Task Descriptions:	
Construction Mobilization and Demobilization	\$50,000
Environmental Controls and Safety Measures	\$100,000
Backshore Dune Construction	\$1,800,000
Subtotal:	\$1,950,000
Total:	\$31,210,000

11. WAVE AND SEA LEVEL RISE INUNDATION MODELING

The concept beach restoration plans presented in Section 10 were assessed by incorporating them into the XBeach-NH numerical model. The model results for each alternative provide a comparison of modeled overland flooding for a combination of prevailing and annual wave conditions under existing sea level and with +1.6 and +3.2 ft of SLR. The timing for +1.6 ft is between 2051 and 2066 for the High to Intermediate SLR projections. For +3.2 ft, the timing is between 2067 and 2093 for the same projections (see Section 5.3). For each sea level case, the background water level is set as mean higher high water (MHHW) which is representative of mean high tide conditions. Alternative 1 – Beach Nourishment was only included in the existing sea level model simulations but not included in the modeling assessment for the +1.6 and +3.2 ft SLR cases with the assumption that the beach would have eroded by the time +1.6 and +3.2 ft of SLR occurs. This is a reasonable assumption assuming the shoreline migrates landward at least at the historical erosion rate. For Alternative 2 – Beach Nourishment with Buried Revetment, the beach fill is assumed to be eroded back to its pre-project position and only the exposed revetment structure and elevated backshore is included in the model domain. The elevation surface of Alternatives 2 through 5 were incorporated into the XBeach-NH model domain. Prevailing and annual waves associated with tradewind waves were chosen for the inundation modeling because they are the most common conditions and produce larger waves compared to north swell.

11.1 Prevailing Waves for Existing Sea Level

Modeled inundation for prevailing waves under current sea level for existing conditions and Alternatives 1/2 through 4 are shown in Figure 11-11 through Figure 11-15. Modeled flooding for the existing topography and all alternatives occurs primarily on the beach faces and structure slopes. It should be noted that the model results include passive (static) flooding in backshore areas where the topography is lower than the input water level. Table 11-1 summarizes the modeling results for each model setup.

Table 11-1. Summary of modeled flooding results for annual waves for existing sea level

Model Case	Flooding of Beach Park Area	Flooding of Highway
Existing Topography	None	None
Alt 1/2 – Beach Nourishment	None	None
Alt 3 – Stabilized Pocket Beaches	None	None
Alt 4 – Partially Stabilized Pocket Beaches	None	None
Alt 5 – Hybrid Stabilized Pocket Beaches	None	None

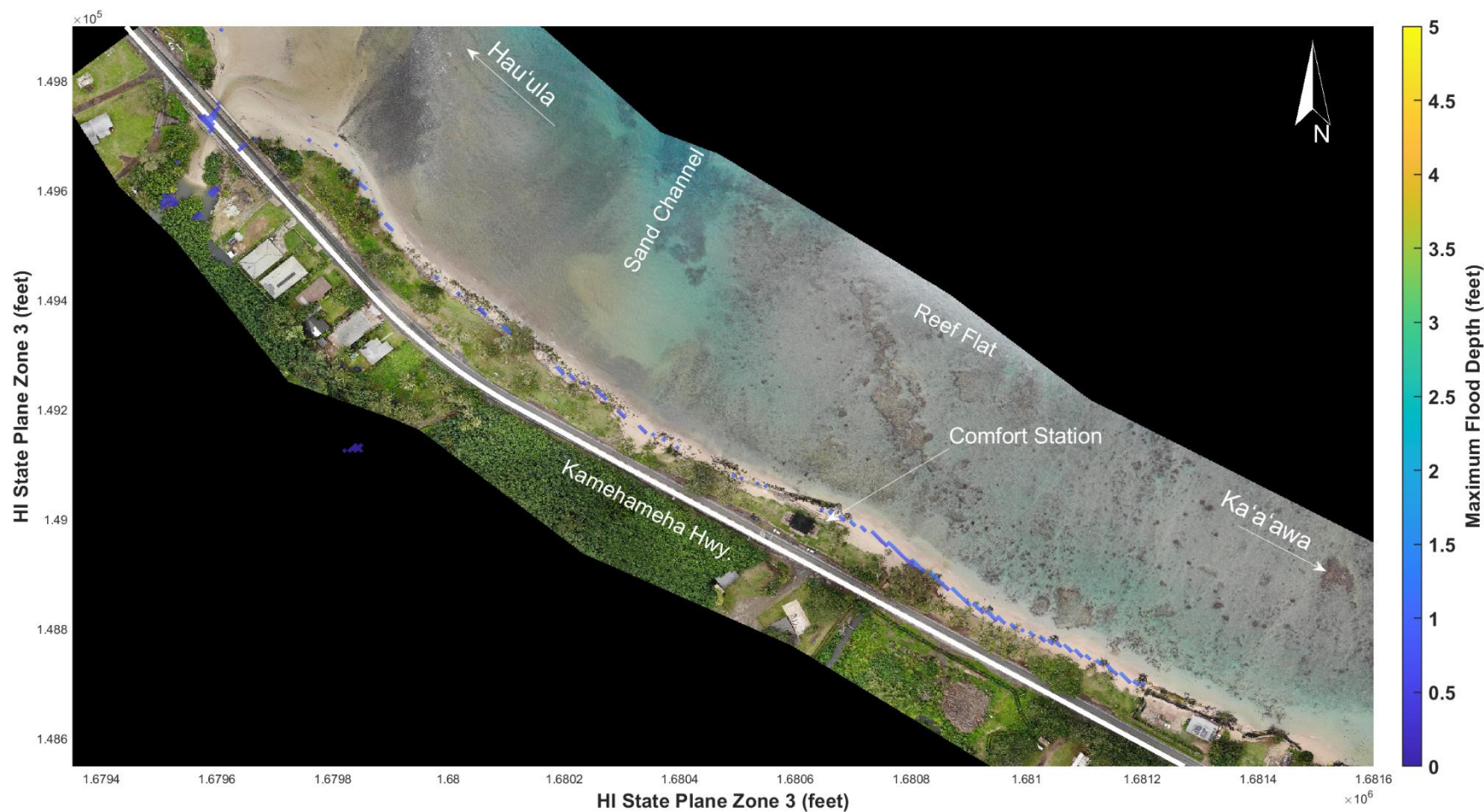


Figure 11-1. Maximum modeled flood depth for existing conditions for existing sea level during a prevailing wave event



Figure 11-2. Maximum modeled flood depth for the beach nourishment concept for existing sea level during a prevailing wave event

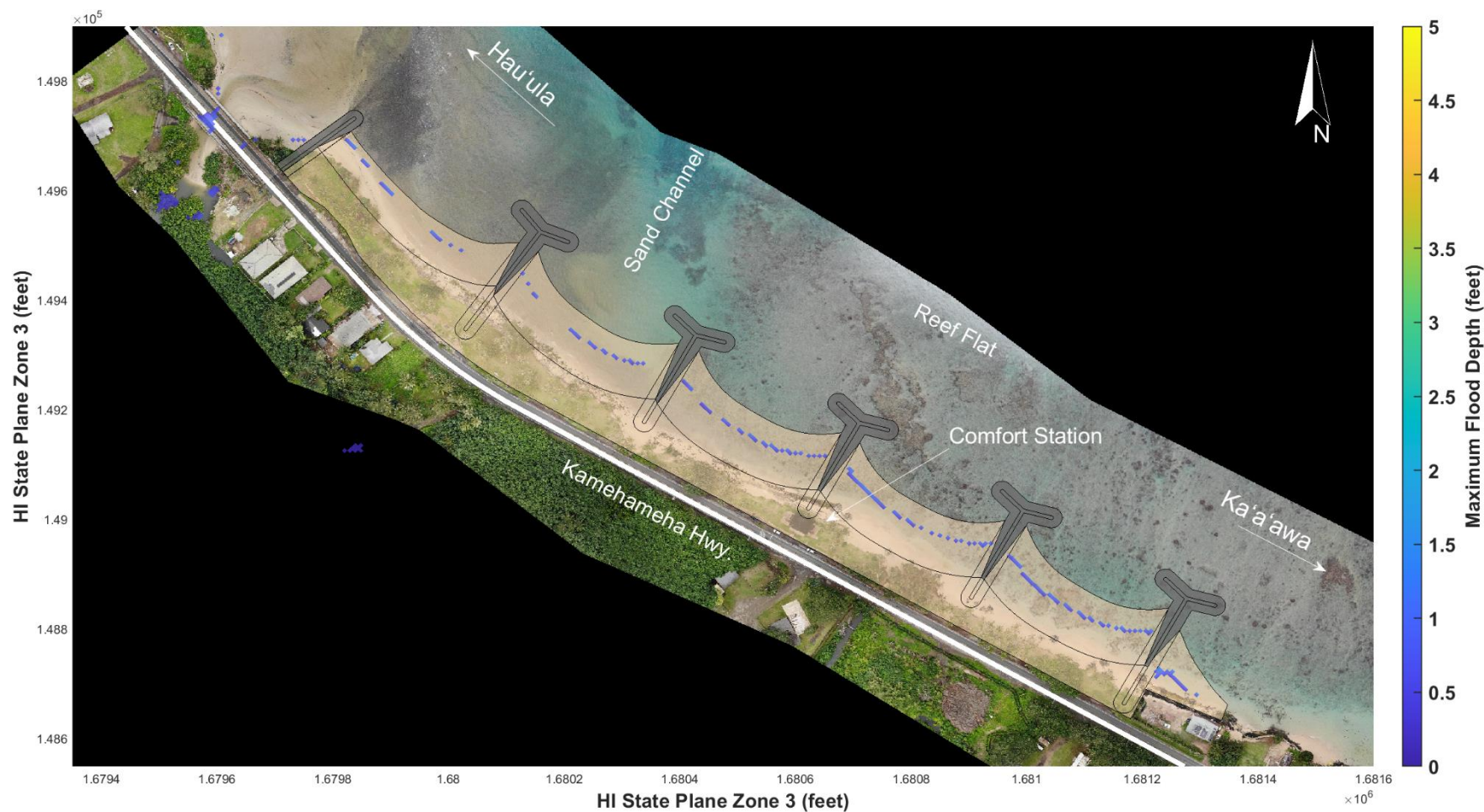


Figure 11-3. Maximum modeled flood depth for stabilized pocket beaches concept for existing sea level during a prevailing wave event

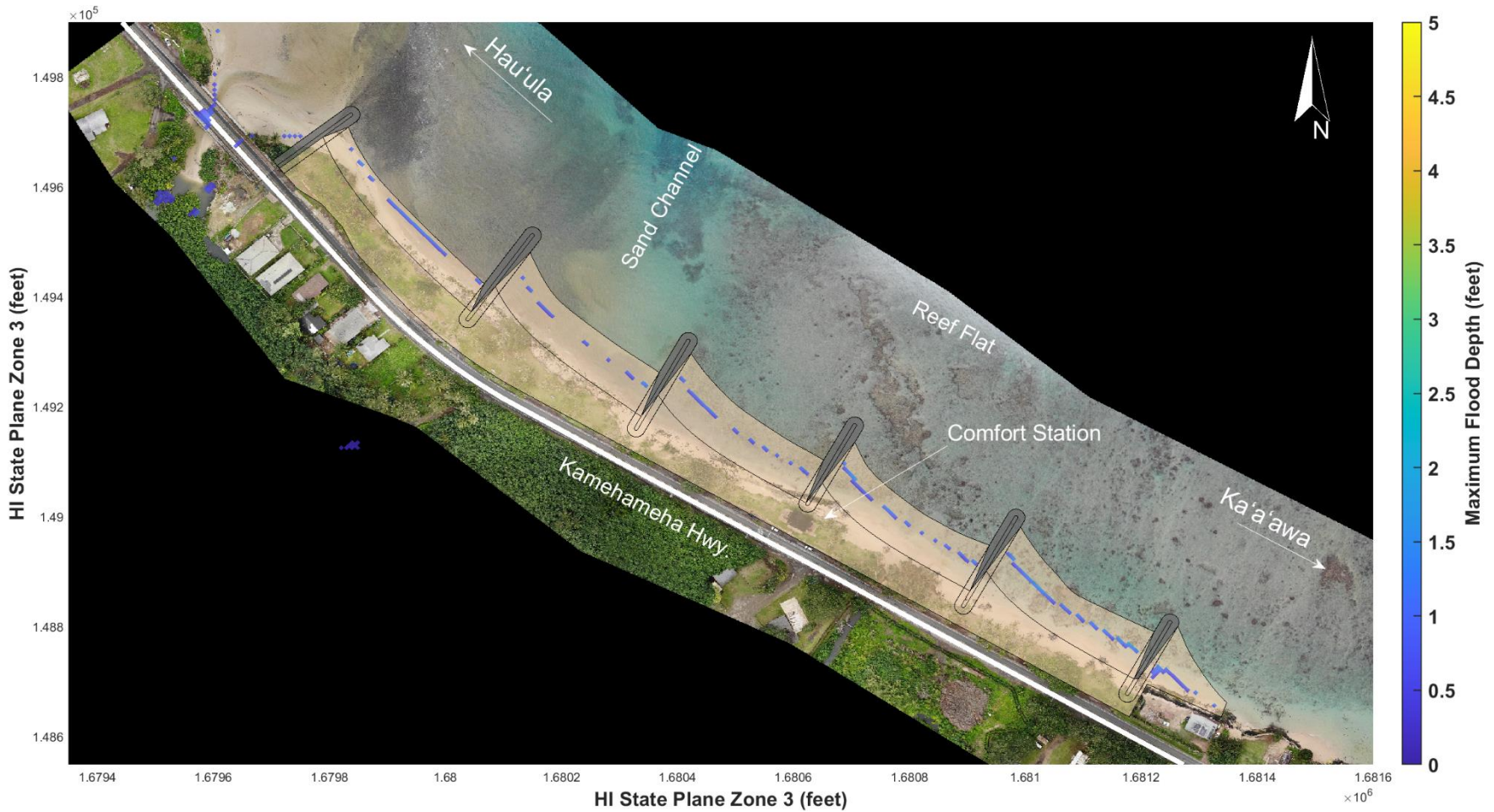


Figure 11-4. Maximum modeled flood depth for the partially stabilized pocket beaches concept for existing sea level during a prevailing wave event

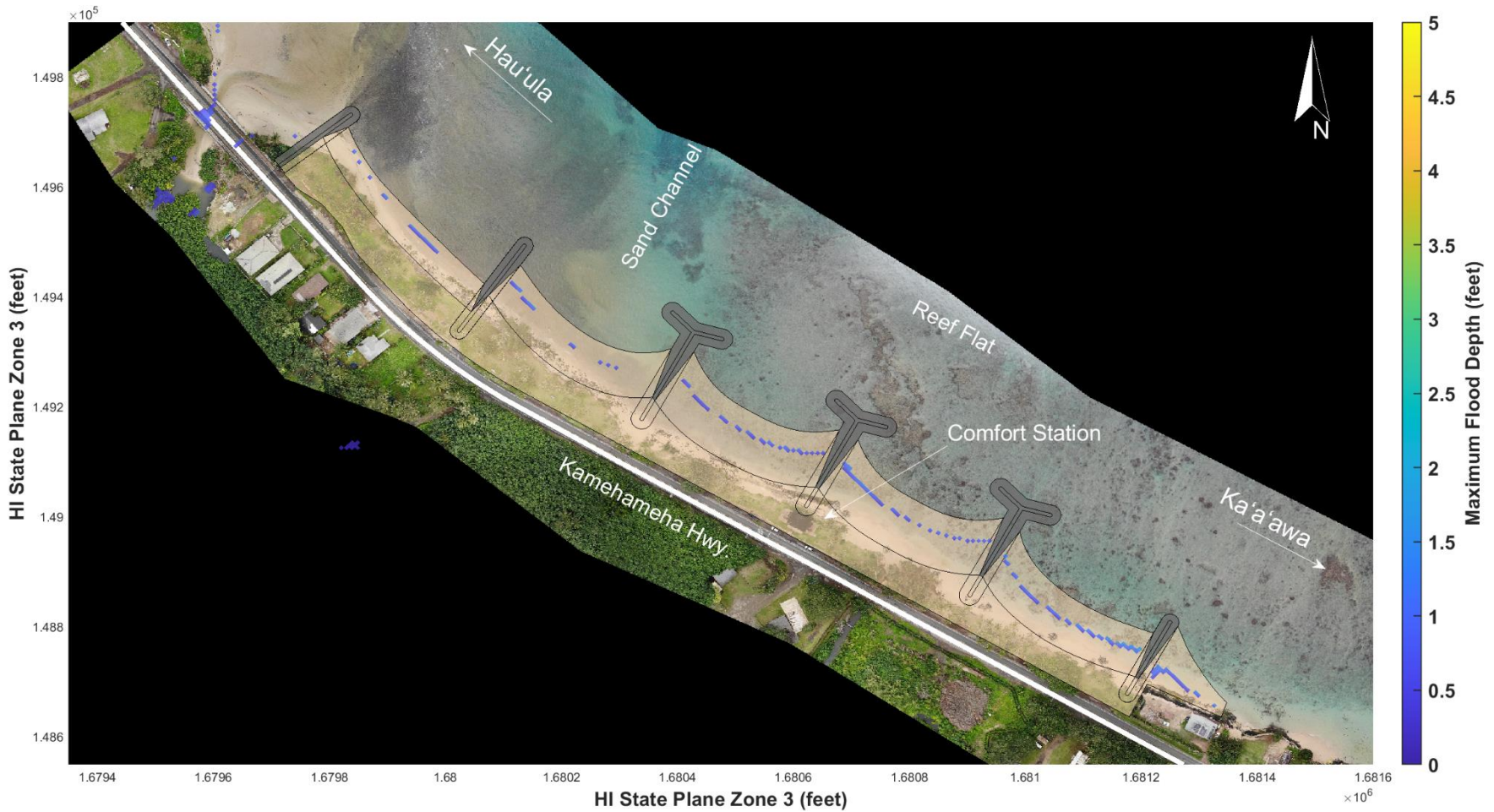


Figure 11-5. Maximum modeled flood depth for the hybrid stabilized pocket beaches concept for existing sea level during a prevailing wave event

11.2 Annual Waves Under Existing Sea Level

Modeled inundation for annual waves under current sea level for existing conditions and Alternatives 1/2 through 4 are shown in Figure 11-16 through Figure 11-20. Modeled flooding for the existing topography primarily occurs around the stream south of the comfort station and reaches near the edge of the highway in this area. It should be noted that the model results include passive (static) flooding in backshore areas where the topography is lower than the input water level. Alternatives 1/2 through 5 are projected to reduce inundation, restricting it to the nourished beach faces and structure slopes. Table 11-2 summarizes the modeling results for each model setup.

Table 11-2. Summary of modeled flooding results for annual waves for existing sea level

Model Case	Flooding of Beach Park Area	Flooding of Highway
Existing Topography	Low	None
Alt 1/2 – Beach Nourishment	None	None
Alt 3 – Stabilized Pocket Beaches	None	None
Alt 4 – Partially Stabilized Pocket Beaches	None	None
Alt 5 – Hybrid Stabilized Pocket Beaches	None	None

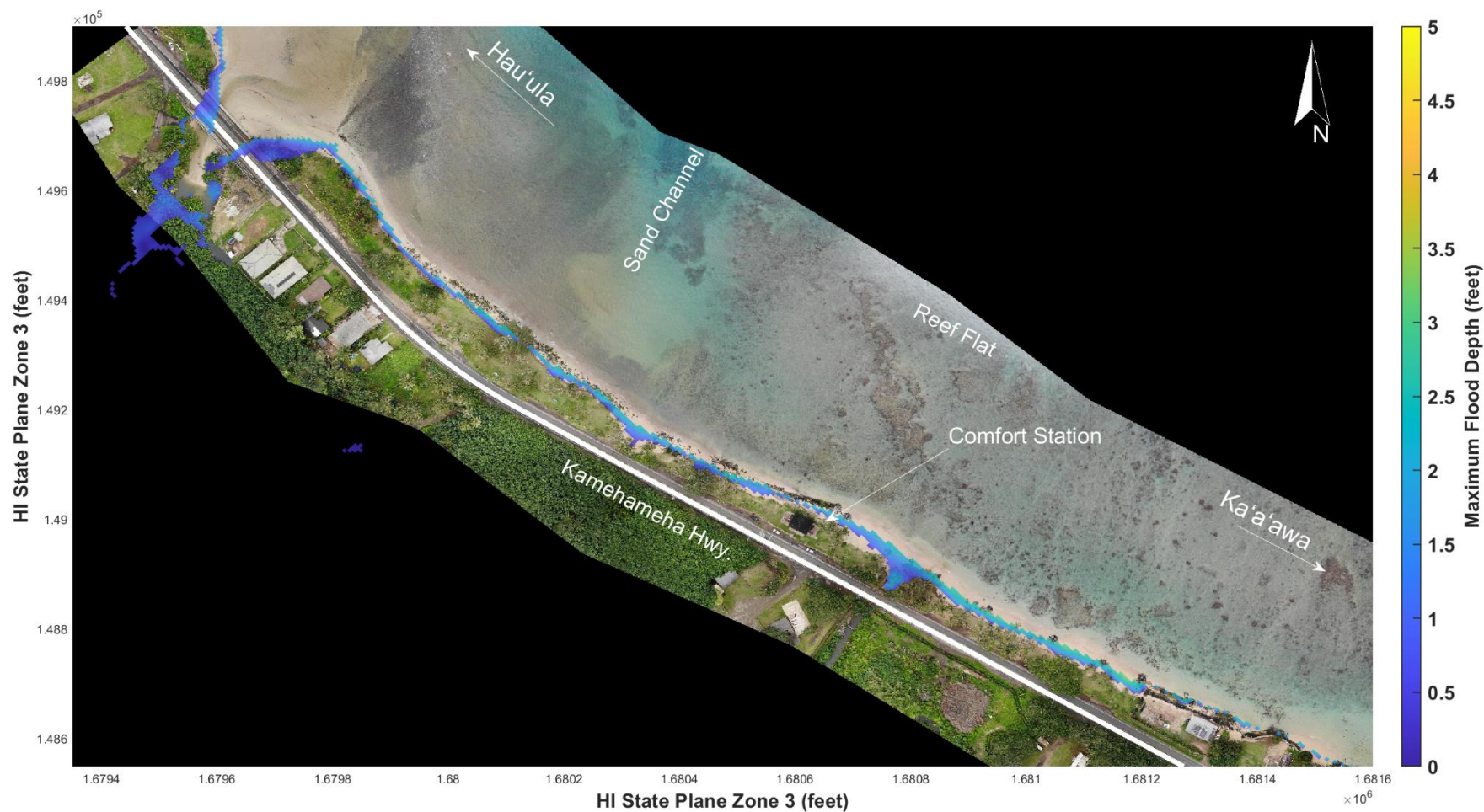


Figure 11-6. Maximum modeled flood depth for existing conditions for existing sea level during an annual wave event



Figure 11-7. Maximum modeled flood depth for the beach nourishment concept for existing sea level during an annual wave event



Figure 11-8. Maximum modeled flood depth for stabilized pocket beaches concept for existing sea level during an annual wave event



Figure 11-9. Maximum modeled flood depth for the partially stabilized pocket beaches concept for existing sea level during an annual wave event



Figure 11-10. Maximum modeled flood depth for the hybrid stabilized pocket beaches concept for existing sea level during an annual wave event

11.3 Prevailing Waves with 1.6 ft of SLR

Modeled inundation for prevailing waves with +1.6 ft of SLR for existing conditions and Alternatives 2 through 4 are shown in Figure 11-11 through Figure 11-15. Modeled flooding for the existing topography occurs primarily at the existing stream on either side of the comfort station. Modeled flooding also occurs at the bridge abutment at the north end of the shoreline. The model does not include the built environment which includes the elevated bridge so flooding shown on these figures would occur below the bridge structure for this case. It should be noted that the model results include passive (static) flooding in backshore areas where the topography is lower than the input water level. Alternatives 2 through 5 are projected to reduce inundation, restricting it to the nourished beach faces and structure slopes. Table 11-3 summarizes the modeling results for each model setup.

Table 11-3. Summary of modeled flooding results for prevailing waves with 1.6 ft of SLR

Model Case	Flooding of Beach Park Area	Flooding of Highway
Existing Topography	Minor	None
Alt 1/2 – Beach Nourishment	None	None
Alt 3 – Stabilized Pocket Beaches	None	None
Alt 4 – Partially Stabilized Pocket Beaches	None	None
Alt 5 – Hybrid Stabilized Pocket Beaches	None	None

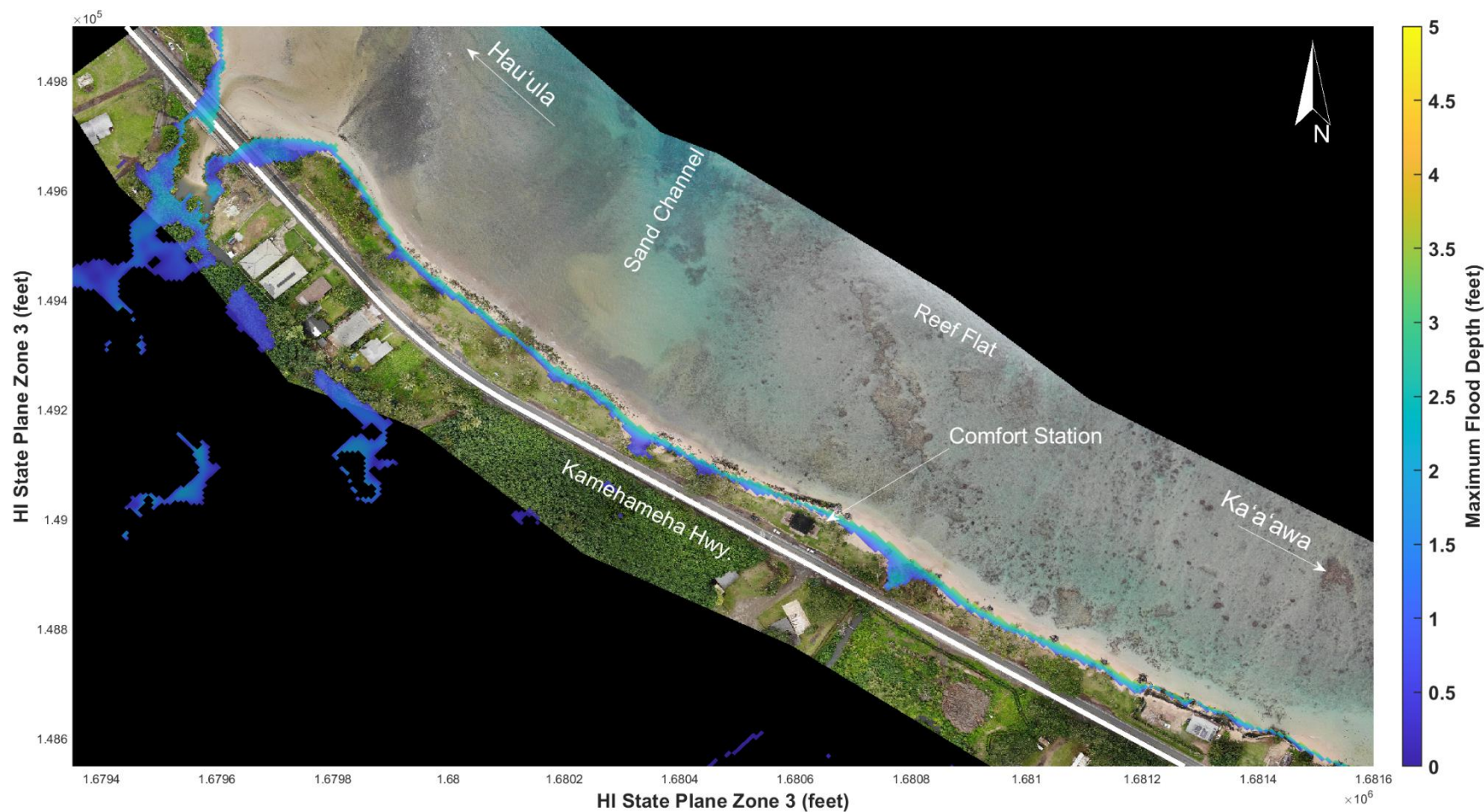


Figure 11-11. Maximum modeled flood depth for existing conditions with +1.6 ft of SLR during a prevailing wave event

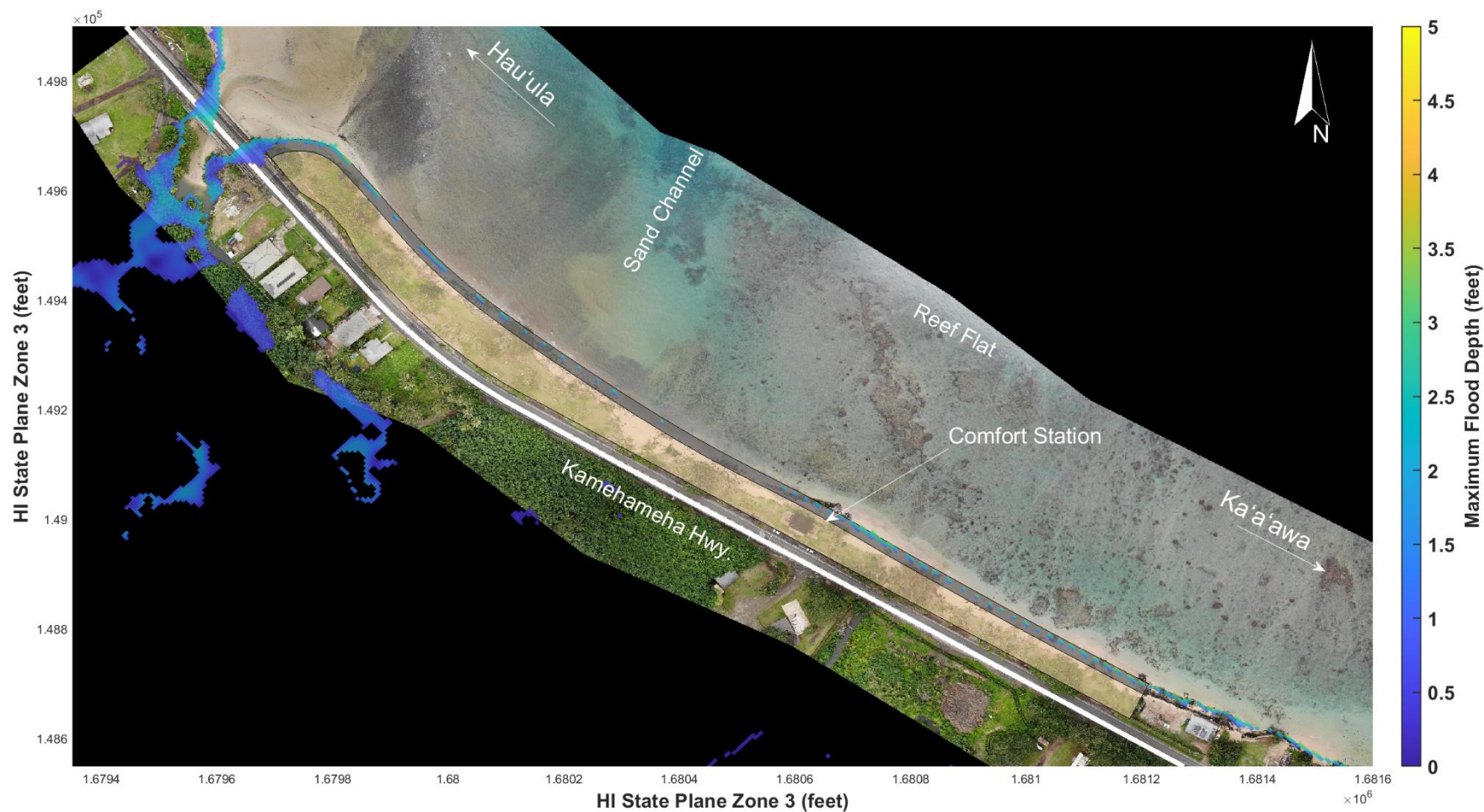


Figure 11-12. Maximum modeled flood depth for the revetement concept with +1.6 ft of SLR during a prevailing wave event



Figure 11-13. Maximum modeled flood depth for stabilized pocket beaches concept with +1.6 ft of SLR during a prevailing wave event

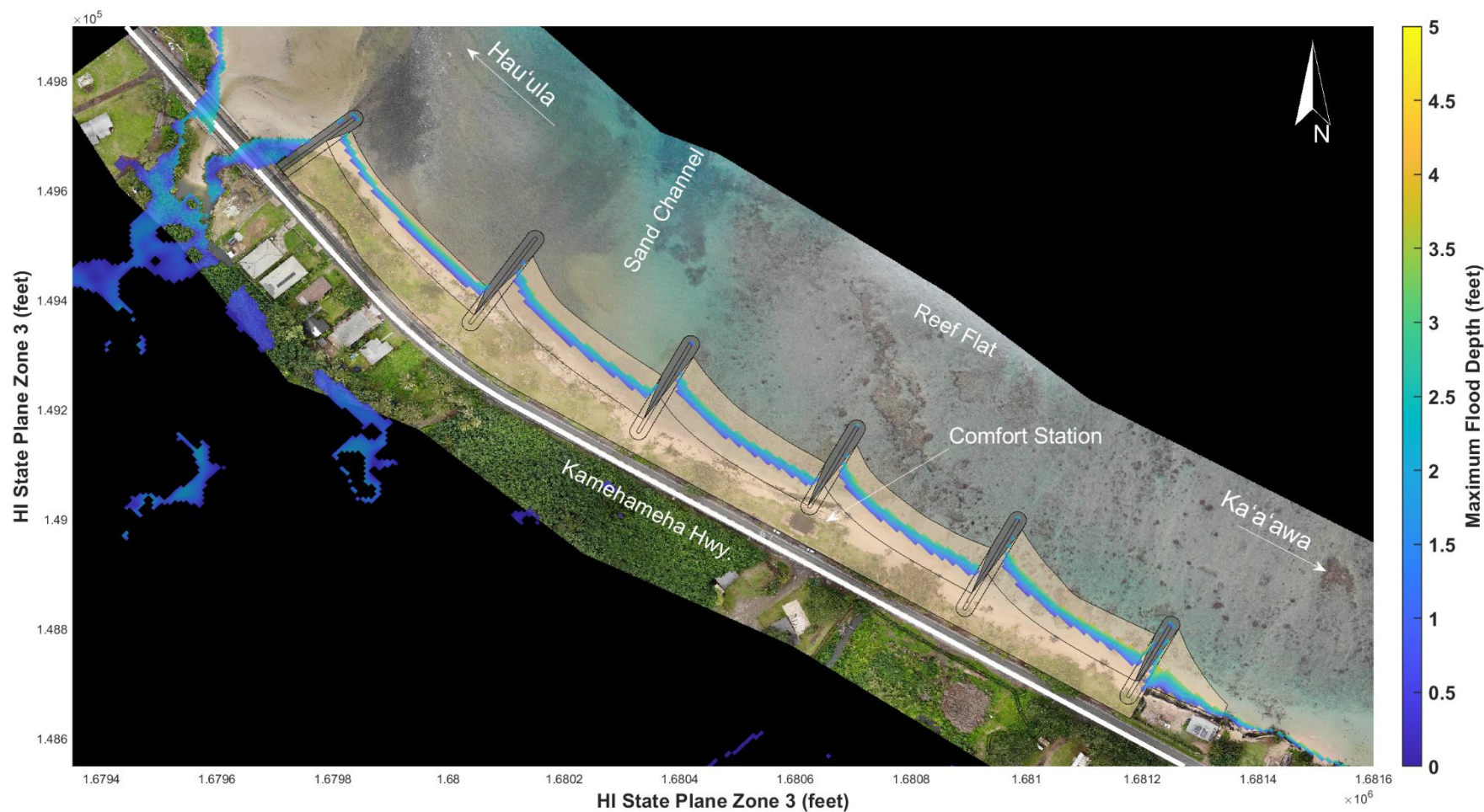


Figure 11-14. Maximum modeled flood depth for the partially stabilized pocket beaches concept with +1.6 ft of SLR during a prevailing wave event



Figure 11-15. Maximum modeled flood depth for the hybrid stabilized pocket beaches concept with +1.6 ft of SLR during a prevailing wave event

11.4 Annual Waves with 1.6 ft of SLR

Modeled inundation for annual tradewind waves with 1.6 ft of SLR for existing conditions and Alternatives 2 through 4 are shown in Figure 11-16 through Figure 11-20. Modeled flooding for the existing topography occurs throughout a majority of the backshore area and onto the highway in some areas. It should be noted that the model results include passive (static) flooding in backshore areas where the topography is lower than the input water level. Alternatives 2 through 5 are projected to prevent this inundation by restricting it to the nourished beach faces and structure slopes. Table 11-4 summarizes the modeling results for each model setup.

Table 11-4. Summary of modeled flooding results for annual waves with 1.6 ft of SLR

Model Case	Flooding of Beach Park Area	Flooding of Highway
Existing Topography	Extensive	Moderate
Alt 2 – Exposed Buried Revetment	None	None
Alt 3 – Stabilized Pocket Beaches	None	None
Alt 4 – Partially Stabilized Pocket Beaches	None	None
Alt 5 – Hybrid Stabilized Pocket Beaches	None	None

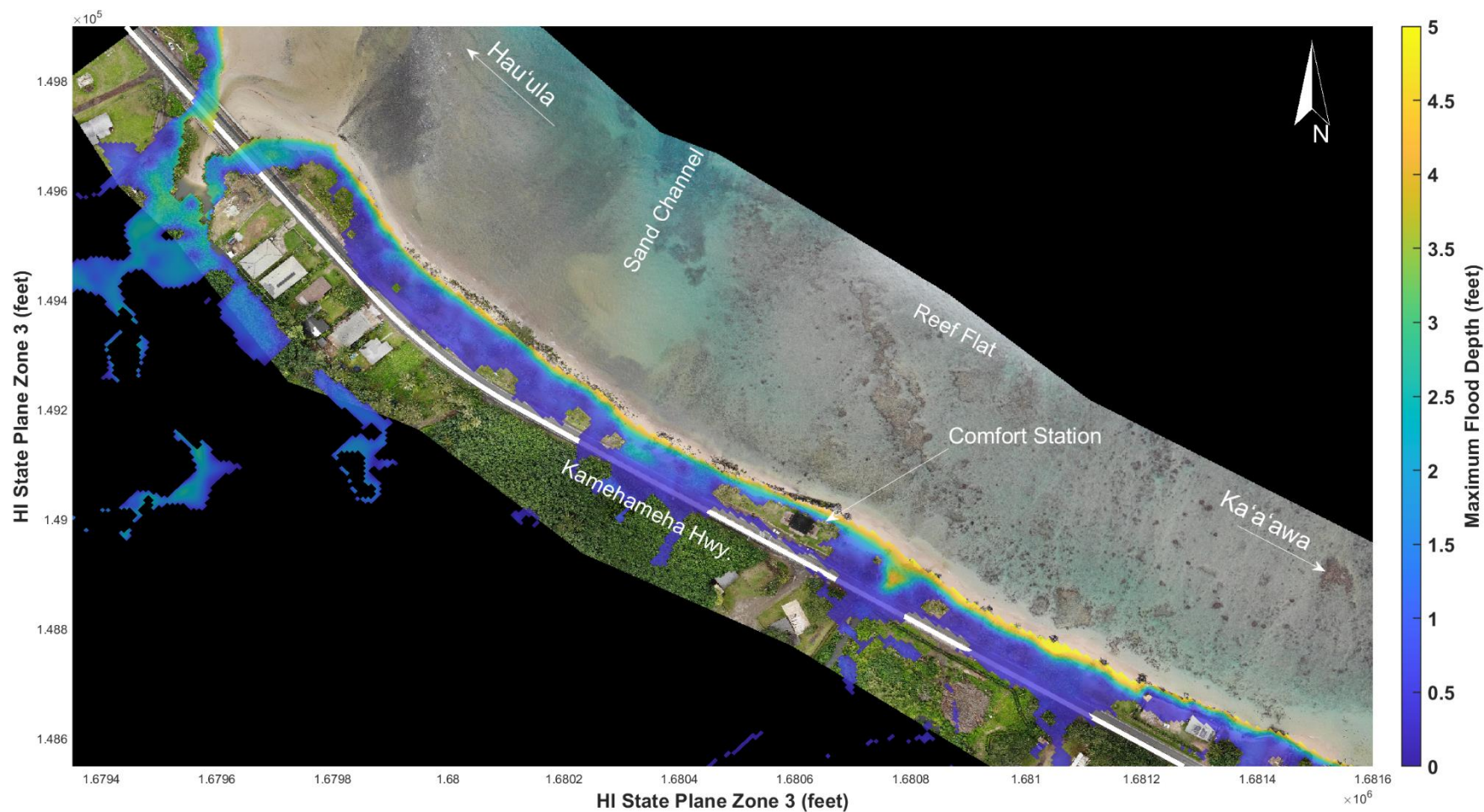


Figure 11-16. Maximum modeled flood depth for existing conditions with +1.6 ft of SLR during an annual wave event

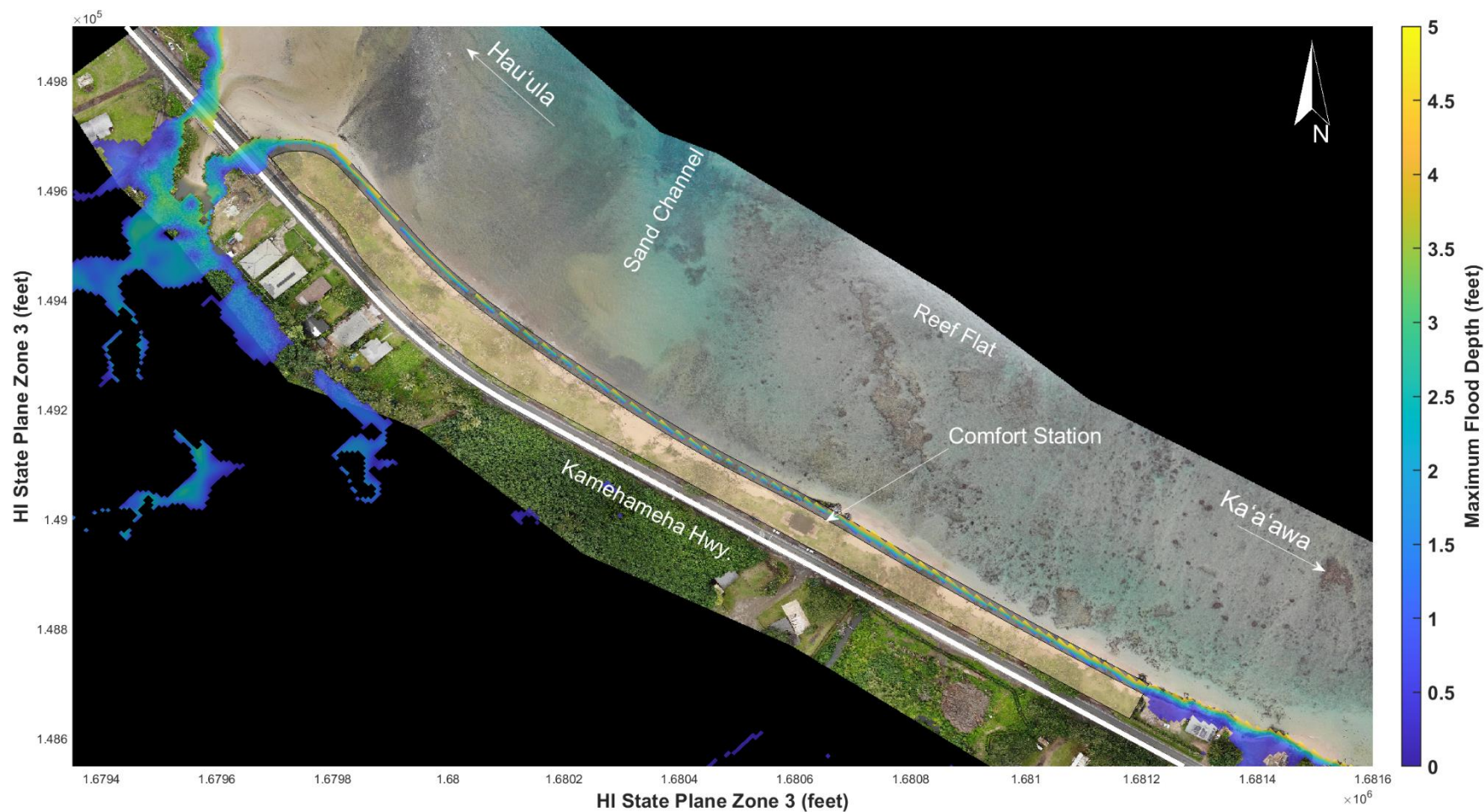


Figure 11-17. Maximum modeled flood depth for the revetment concept with +1.6 ft of SLR during an annual wave event

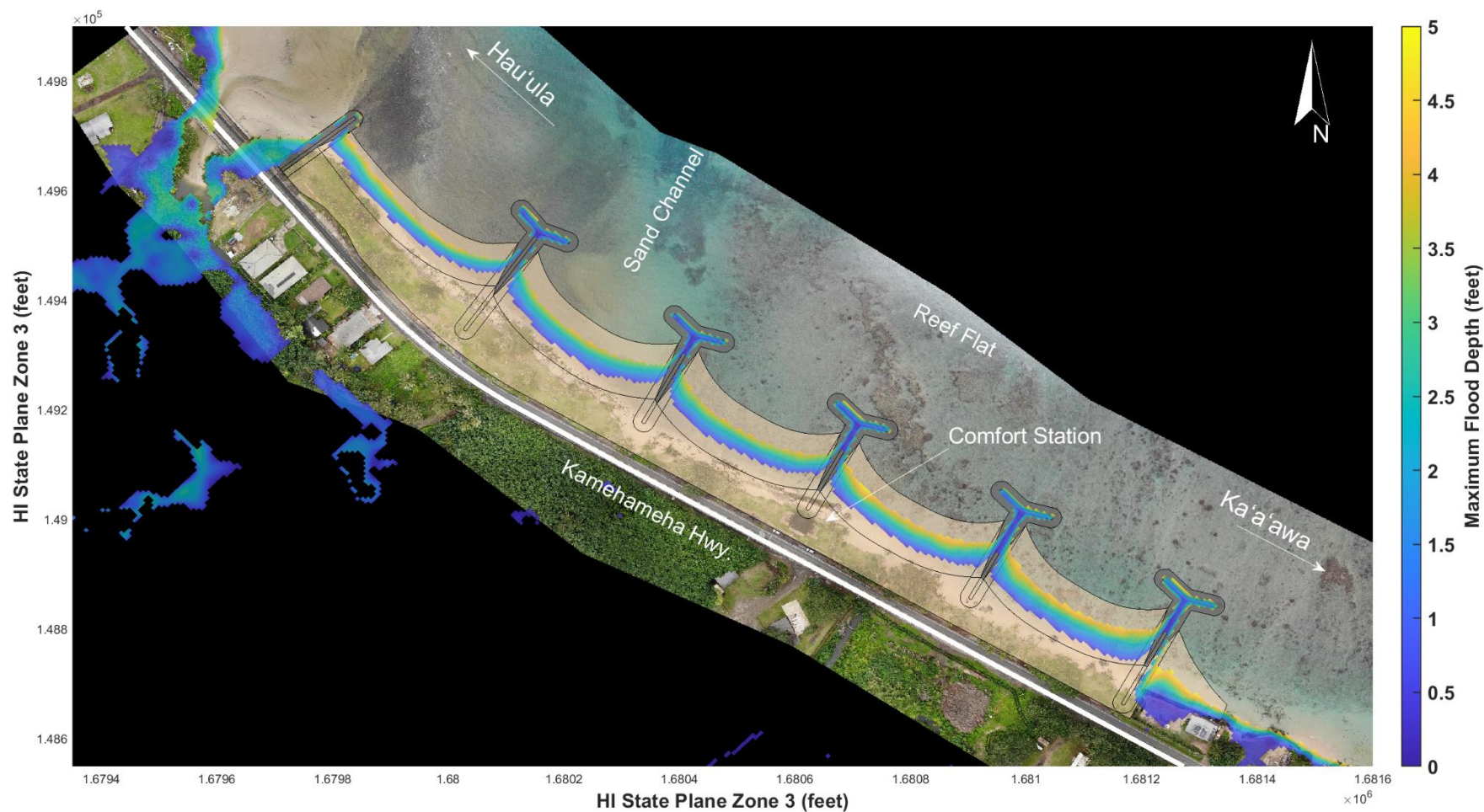


Figure 11-18. Maximum modeled flood depth for stabilized pocket beaches concept with +1.6 ft of SLR during an annual wave event

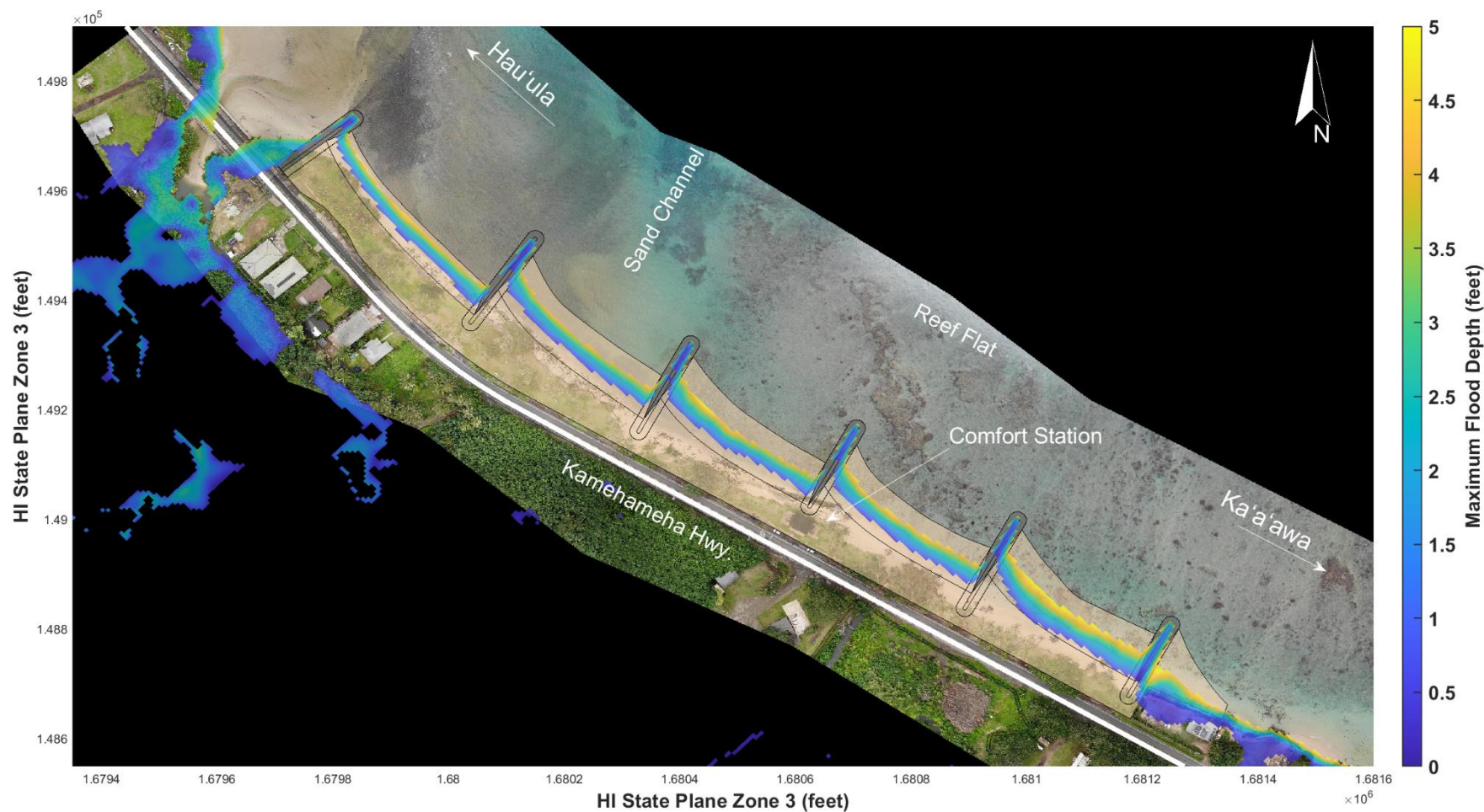


Figure 11-19. Maximum modeled flood depth for the partially stabilized pocket beaches concept with +1.6 ft of SLR during an annual wave event

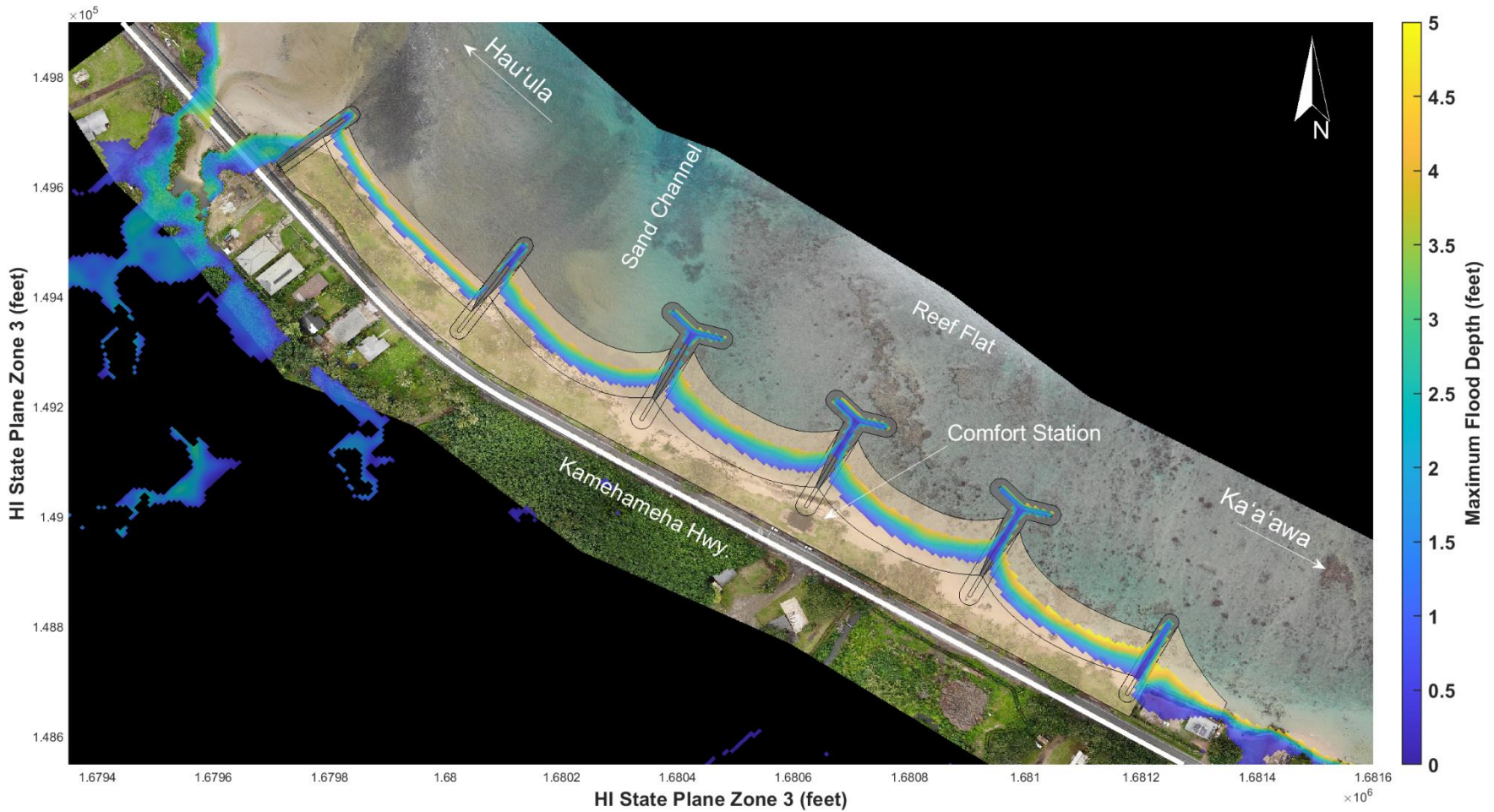


Figure 11-20. Maximum modeled flood depth for the hybrid stabilized pocket beaches concept with +1.6 ft of SLR during an annual wave event

11.5 Prevailing Waves with 3.2 ft of SLR

Modeled inundation for prevailing tradewind waves with 3.2 ft of SLR for existing conditions and Alternatives 2 through 4 are shown in Figure 11-21 through Figure 11-25. Modeled flooding for the existing topography occurs almost entirely throughout the backshore area and onto a majority of the highway landward of the beach park. Alternatives 2 through 5 are projected to prevent this inundation by restricting it to the nourished beach faces and structure slopes. The model results for each case show flooding landward of the highway which are low-lying areas that are statically flooded by the base water level. For all model simulations, the private properties to the south of the beach park are completely flooded during the simulation. These areas may become worse and more prone to flooding if they are left unprotected. Table 11-5 summarizes the modeling results for each model setup.

Table 11-5. Summary of modeled flooding results for prevailing waves with 3.2 ft of SLR

Model Case	Flooding of Beach Park Area	Flooding of Highway
Existing Topography	Extensive	Extensive
Alt 2 – Exposed Buried Revetment	None	None
Alt 3 – Stabilized Pocket Beaches	None	None
Alt 4 – Partially Stabilized Pocket Beaches	None	None
Alt 5 – Hybrid Stabilized Pocket Beaches	None	None

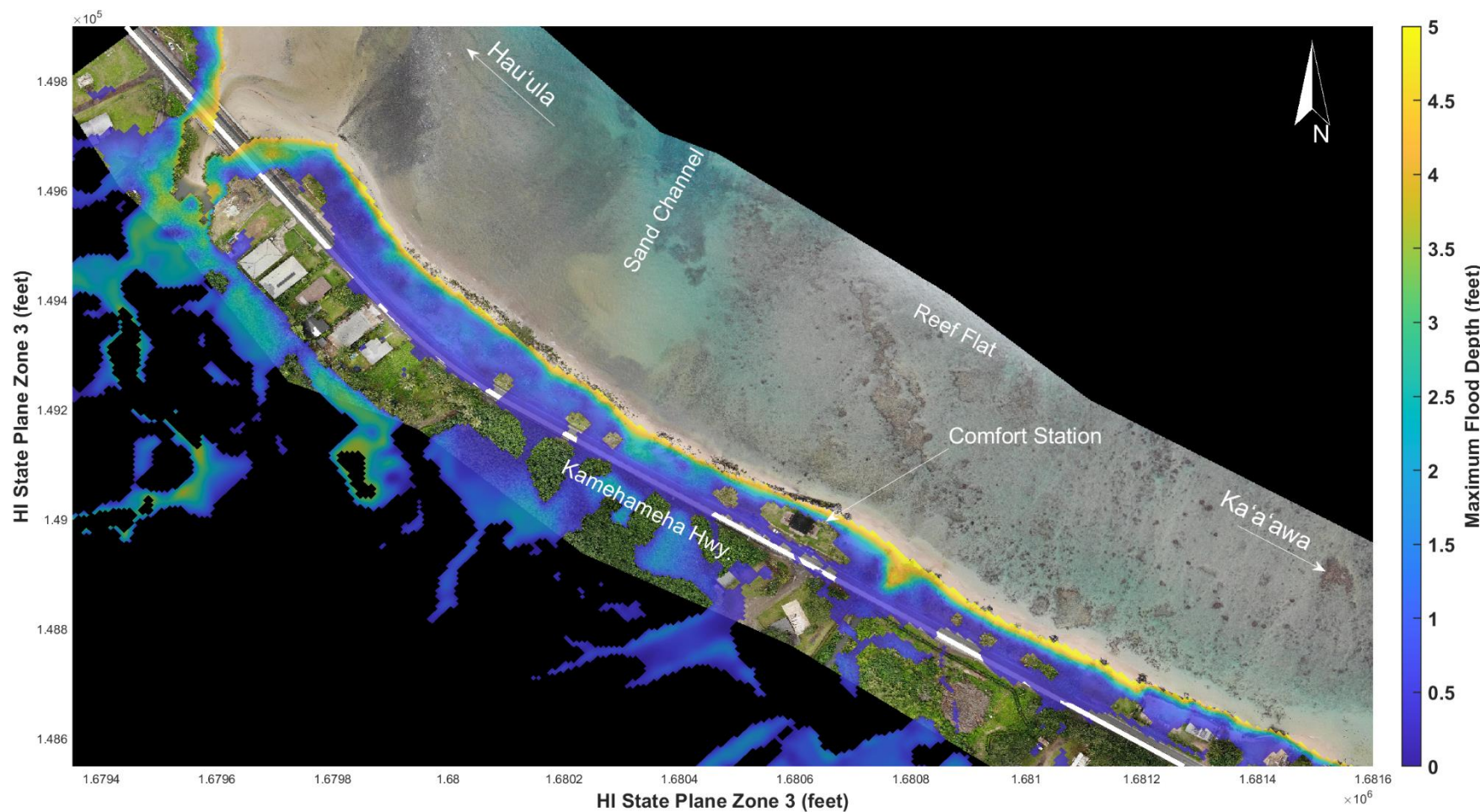


Figure 11-21. Maximum modeled flood depth for existing conditions with +3.2 ft of SLR during a prevailing wave event

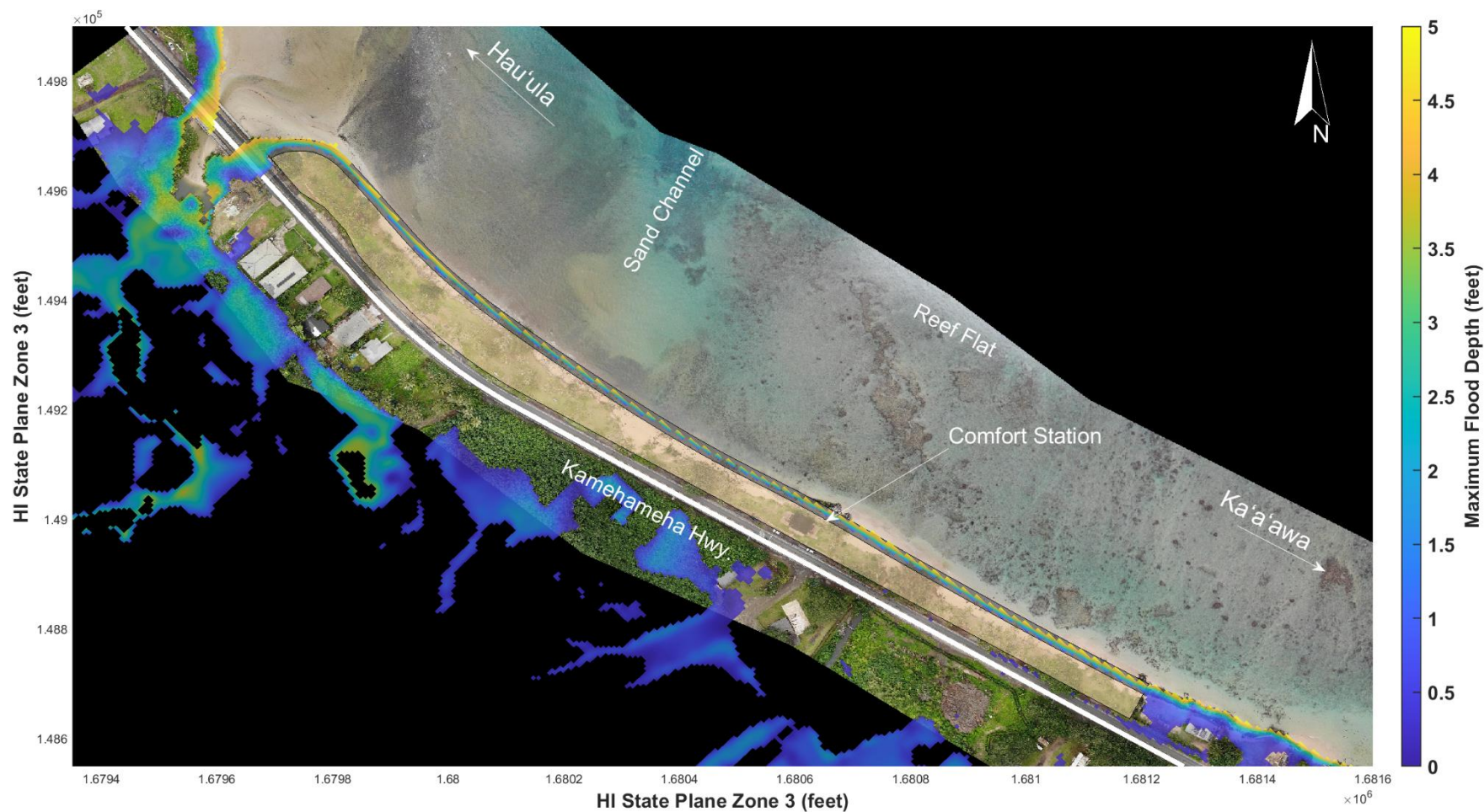


Figure 11-22. Maximum modeled flood depth for the revetment concept with +3.2 ft of SLR during a prevailing wave event

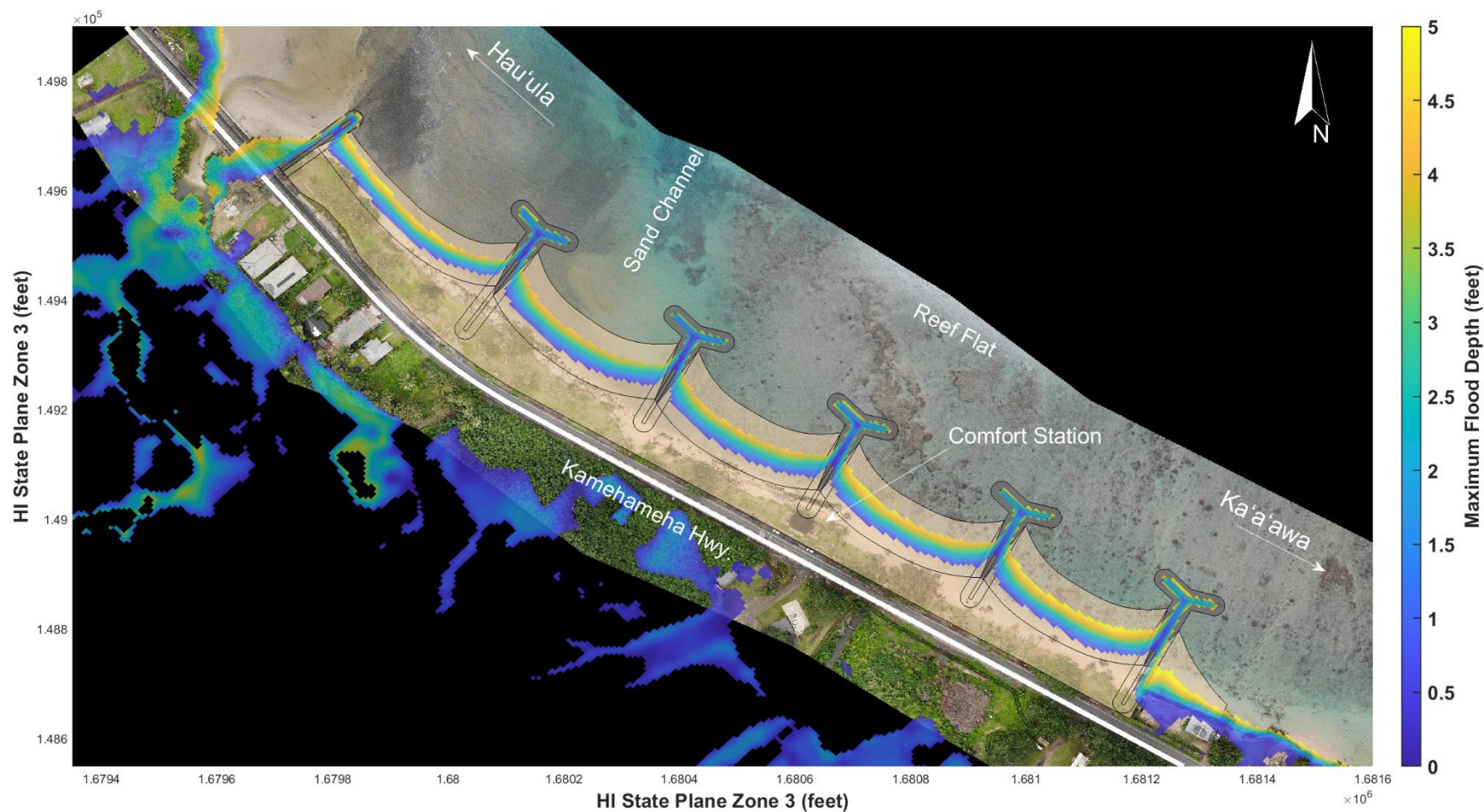


Figure 11-23. Maximum modeled flood depth for the stabilized pocket beaches concept with +3.2 ft of SLR during a prevailing wave event

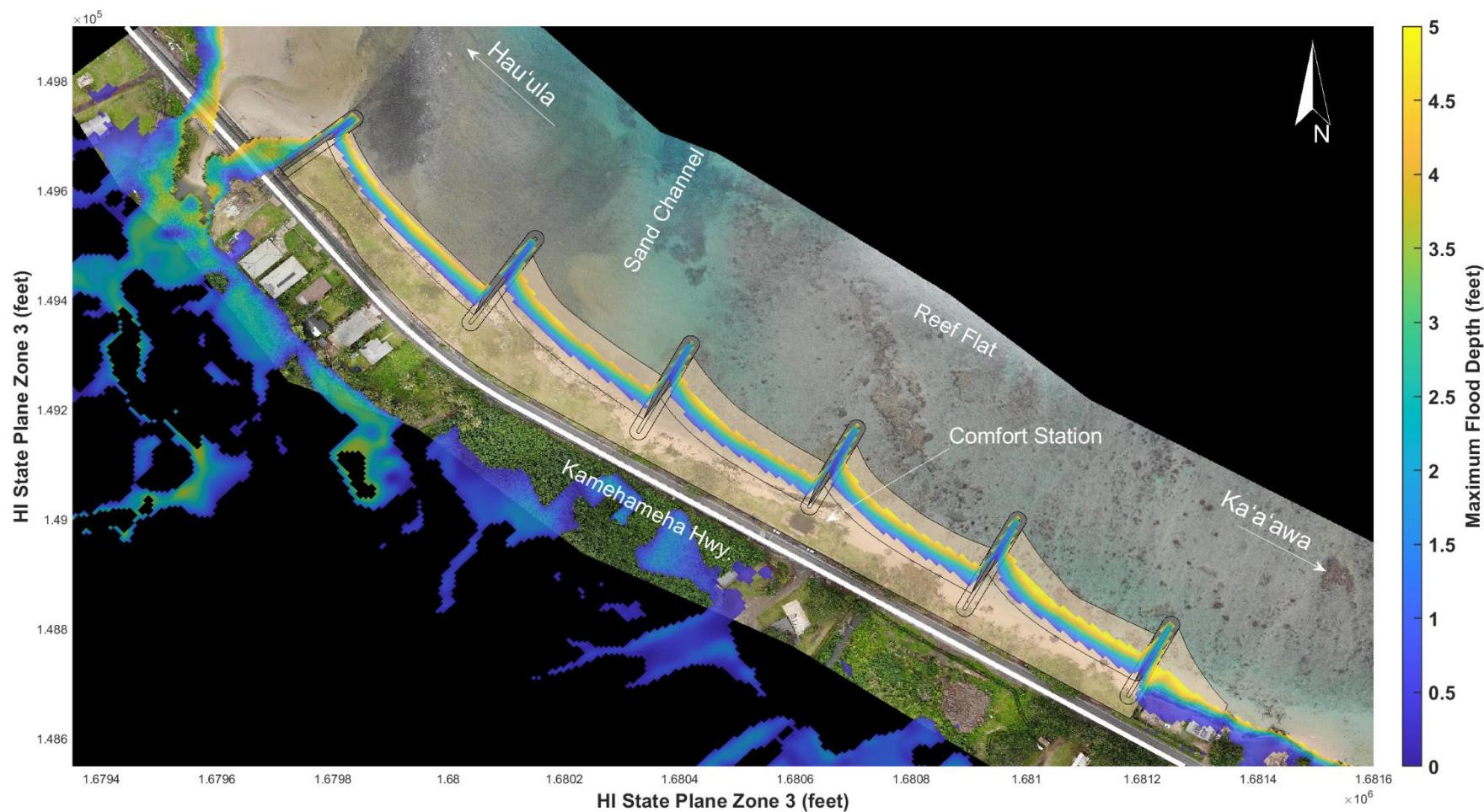


Figure 11-24. Maximum modeled flood depth for the partially stabilized pocket beaches concept with +3.2 ft of SLR during a prevailing wave event

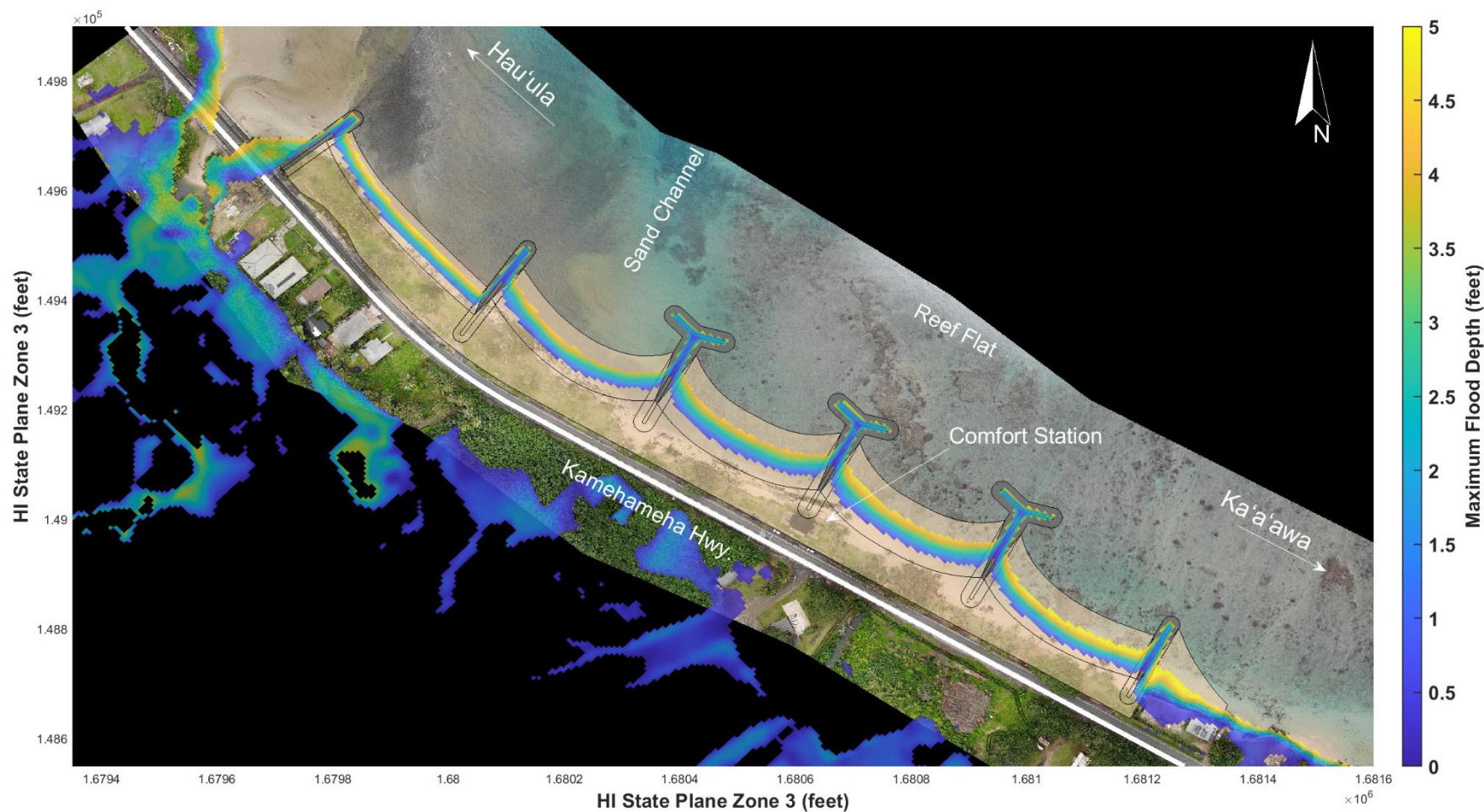


Figure 11-25. Maximum modeled flood depth for the hybrid stabilized pocket beaches concept with +3.2 ft of SLR during a prevailing wave event

11.6 Annual Waves with 3.2 ft of SLR

Modeled inundation for annual tradewind waves with +3.2 ft of SLR for existing conditions and alternatives 2 through 4 are shown in Figure 11-26 through Figure 11-30. Modeled flooding for the existing topography is total for the park and highway, and extensive inshore of the highway. The Alternative 2 revetment is projected to prevent inundation of the park and highway in the northern half of the park, but inundation is extensive in the southern half where waves are larger across the reef. The Alternative 3 pocket beach is most effective, preventing inundation of the park and highway in all but the southern pocket beach, where moderate inundation is projected. Alternatives 4 and 5 are projected to prevent most inundation in all but the southern two pocket beaches where moderate to extensive inundation is projected. This simulation case illustrates the challenges to design coastal infrastructure for +3.2 ft of SLR in the Punalu‘u region. As discussed previously in Section 6.4, the alternative concepts are only designed for +1.6 ft of SLR due to the low-lying elevation of the surrounding region. Even though these concepts can technically be designed to reduce flooding at the beach park and the highway, the surrounding region is vulnerable to extensive flooding and preservation of the beach park during these conditions may be impractical. Table 11-6 summarizes the modeling results for each model setup.

Table 11-6. Summary of modeled flooding results for prevailing waves with 3.2 ft of SLR

Model Case	Flooding of Beach Park Area	Flooding of Highway
Existing Topography	Total	Total
Alt 2 – Exposed Buried Revetment	Extensive south beach park, none elsewhere	Extensive south beach park, none elsewhere
Alt 3 – Stabilized Pocket Beaches	Moderate southern pocket beach, none elsewhere	Moderate southern pocket beach, none elsewhere
Alt 4 – Partially Stabilized Pocket Beaches	Moderate southern 2 pocket beaches, minor elsewhere	Moderate southern 2 pocket beaches, none elsewhere
Alt 5 – Hybrid Stabilized Pocket Beaches	Extensive southern pocket beach, minor elsewhere	Extensive southern pocket beach, none elsewhere

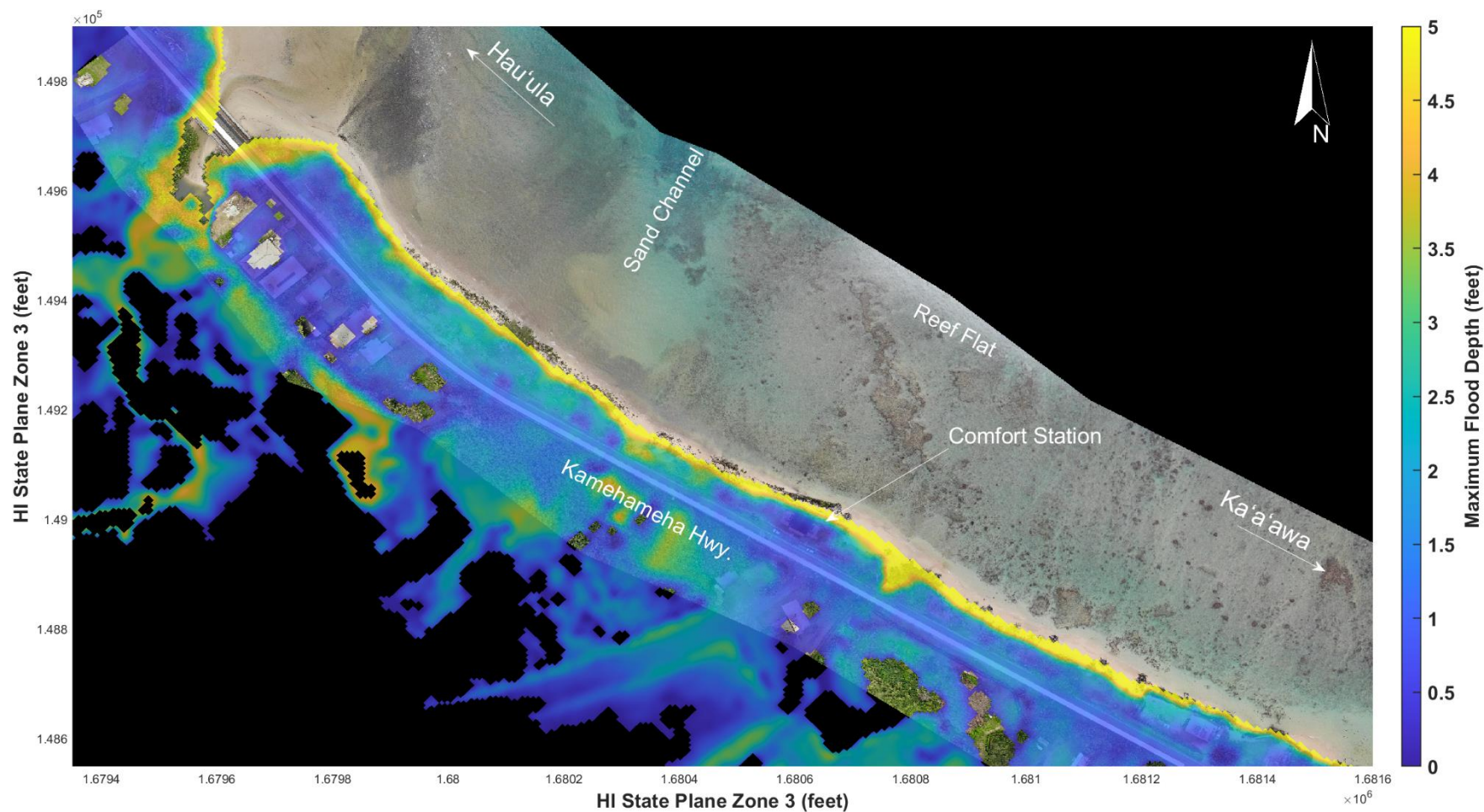


Figure 11-26. Maximum modeled flood depth for existing conditions with +3.2 ft of SLR during an annual wave event

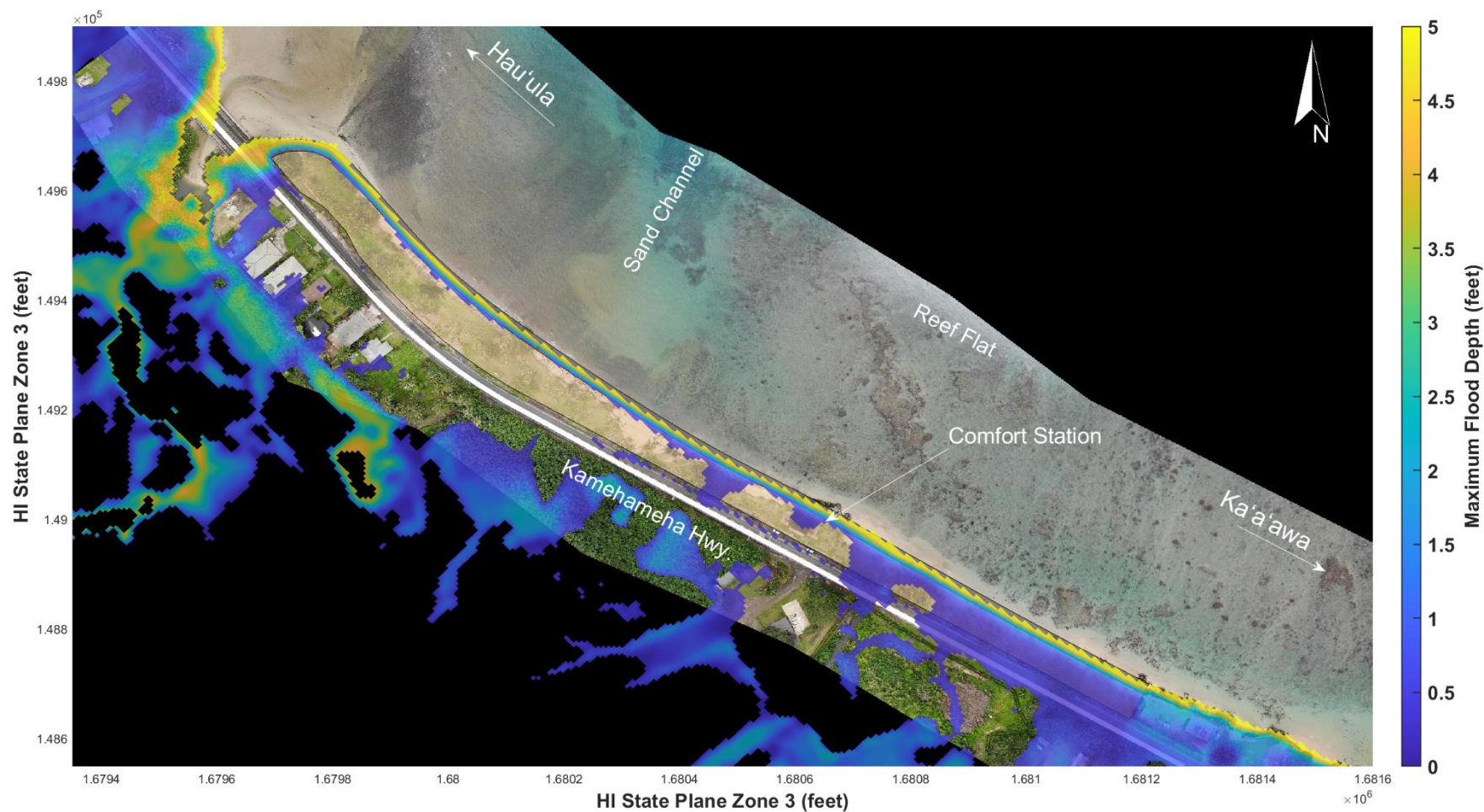


Figure 11-27. Maximum modeled flood depth for the revetment concept with +3.2 ft of SLR during an annual wave event

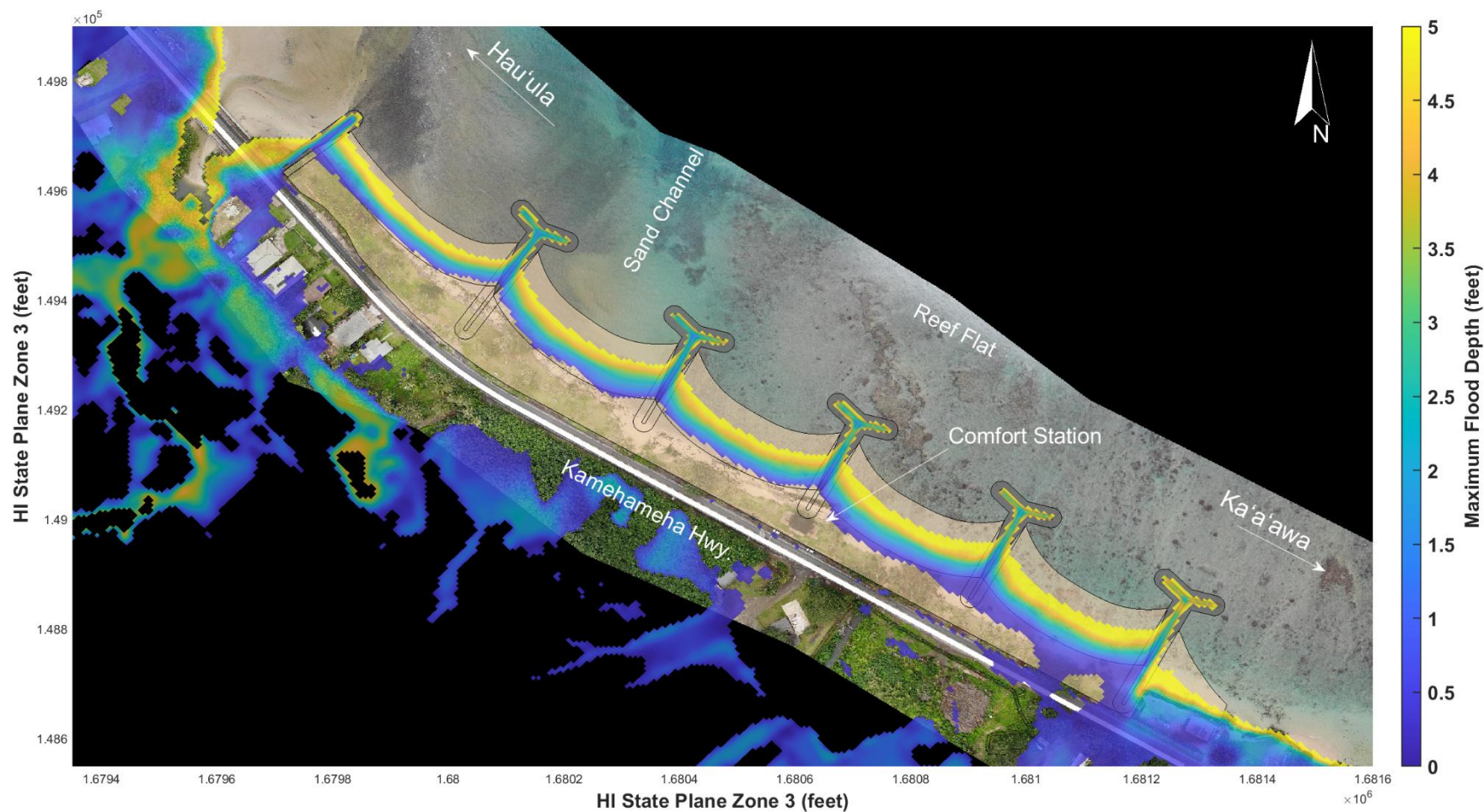


Figure 11-28. Maximum modeled flood depth for the stabilized pocket beaches concept with +3.2 ft of SLR during an annual wave event

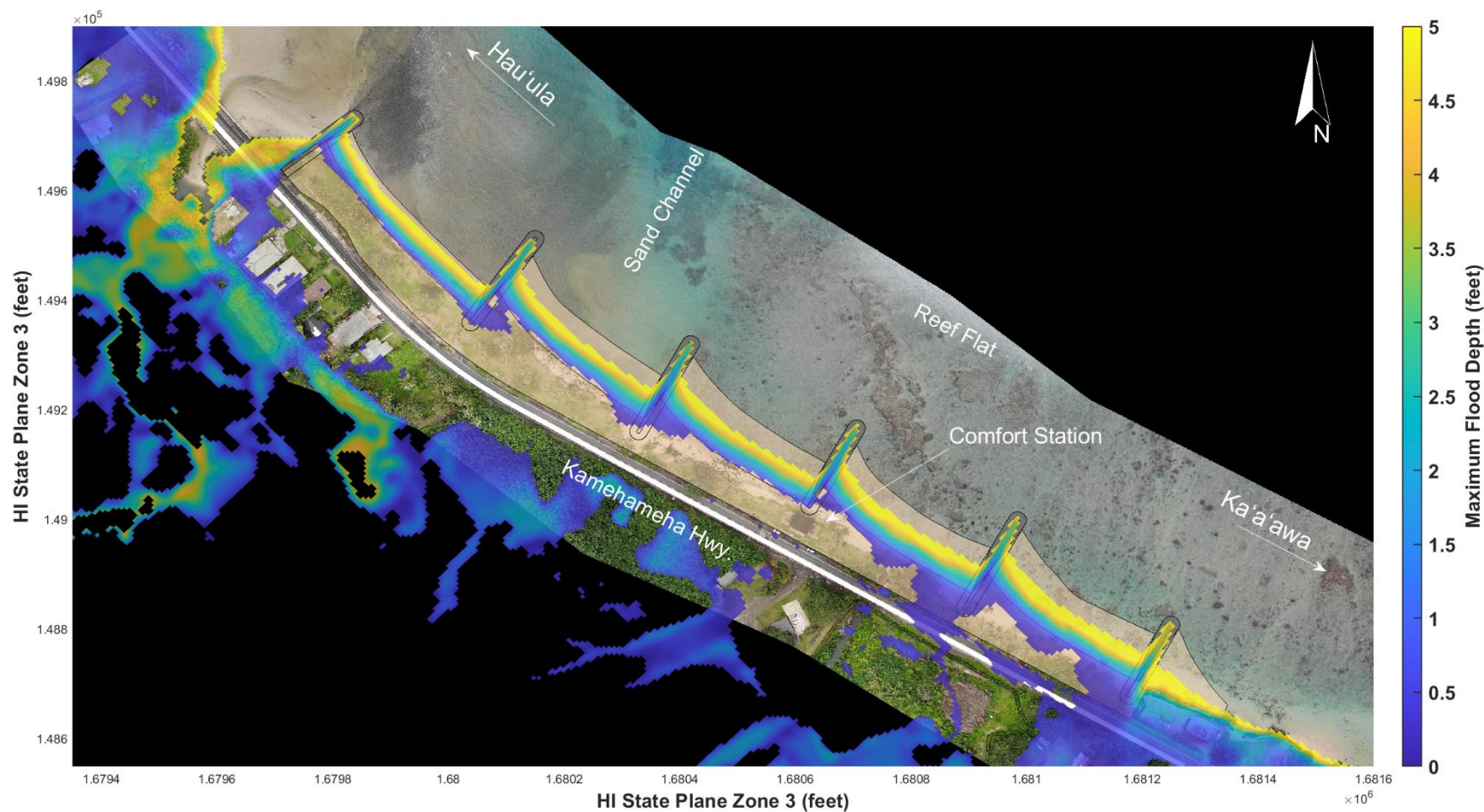


Figure 11-29. Maximum modeled flood depth for the partially stabilized pocket beaches concept with +3.2 ft of SLR during an annual wave event

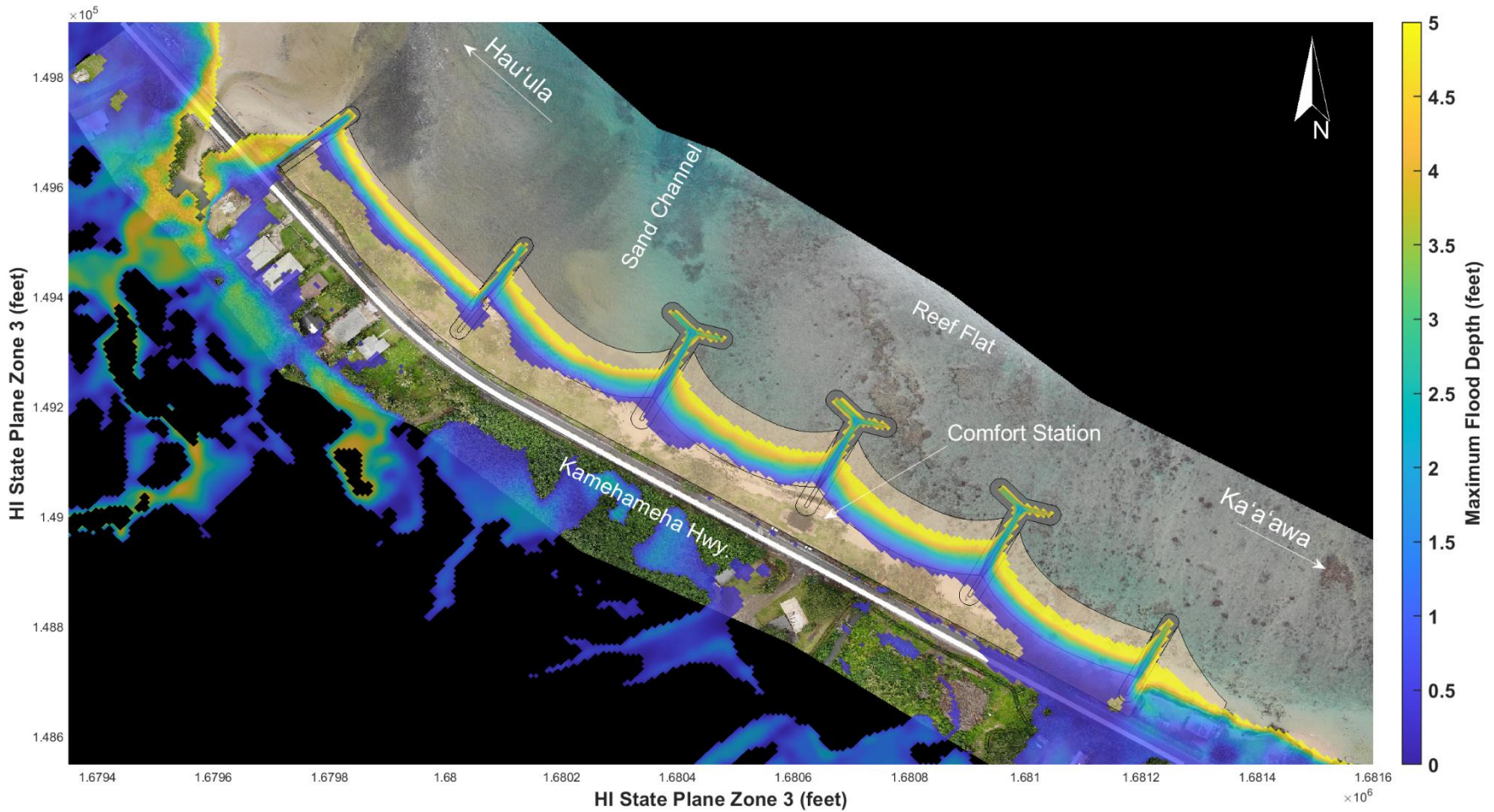


Figure 11-30. Maximum modeled flood depth for the hybrid stabilized pocket beaches concept with +3.2 ft of SLR during an annual wave event

12. SUMMARY, DISCUSSION, AND REGULATORY REQUIREMENTS

12.1 Summary

Development of beach restoration alternatives requires a site-specific analysis of the project site accounting for the oceanographic parameters, physical environment, and shoreline history specific to the site. The methodology utilized in this study to develop beach restoration alternatives provides an effective framework which can be applied to other locations in Hawai‘i. Key findings from this study include the following:

- The shoreline at Punalu‘u Beach Park is chronically eroding with historical erosion rates between -2.0 and -3.0 ft/yr (1988-2022). These erosion rates are expected to increase with rising sea levels as more wave energy reaches the shoreline.
- A broad shallow fringing reef protects the shoreline from the highly energetic offshore waves typical for this coastline. As sea level rises, the effectiveness of the reef at reducing waves decreases and backshore inundation increases drastically with both higher water levels and waves at the shoreline. This is shown through numerical modeling discussed in Section 11.
- A suitable offshore sand source exists about 2,000 ft offshore of Punalu‘u Beach Park with sand characteristics that match well with the existing beach sand.
- The most viable method to recover the sand and transport it to shore is to use a hydraulic suction pump deployed off a barge and pump the sand to shore through a temporary pipeline. Current regulation requires that the sand be dewatered prior to placement on the beach.
- While the source is reasonably close to shore, the windward coast of O‘ahu is one of the most energetic wave environments in Hawai‘i which makes the sand recovery challenging. Because of the challenges and high cost to recover sand it is recommended that stabilizing structures (particularly headland type structures) be used in conjunction with beach nourishment to prevent the need for re-nourishment to maintain the beach.
- Five (5) concept beach alternatives are proposed for Punalu‘u Beach Park along with ROM cost estimates. These concepts are considered nature-based or hybrid nature-based solution and include:
 - Alternative 1 – Beach Nourishment
 - **ROM Cost: \$14,835,000**
 - Alternative 2 – Beach Nourishment with Buried Revetment
 - **ROM Cost: \$22,396,00**
 - Alternative 3 – Stabilized Pocket Beaches
 - **ROM Cost: \$32,910,000**

- Alternative 4 – Partially Stabilized Pocket Beaches
 - **ROM Cost: \$28,539,000**
- Alternative 5 – Hybrid Stabilized Pocket Beaches
 - **ROM Cost: \$31,210,000**
- All concepts were modeled under a combination of existing/future sea level and wave conditions. The modeling results show that the alternatives reduce the expected wave inundation at the beach park compared to existing conditions. For the +3.2 ft SLR case, all alternative simulations show no inundation of the backshore park area and highway during prevailing waves compared to extensive inundation for existing topography. With annual waves under the same SLR case, flooding of the backshore and highway is reduced from total inundation for existing topography to moderate/extensive inundation of the southern portion of the park and highway for all alternatives.

12.2 Discussion

Primary project objectives of this study include the following:

- Restore the beach at Punalu‘u Beach Park
- Protect Kamehameha Highway from flooding and erosion
- Improve community resilience to sea level rise and coastal storms
- Provide recreational resources and native habitat

Alternatives 3 and 5 most effectively meet the project objectives and are projected to prevent inundation of the beach park and highway even up to +3.2 ft of SLR during an annual wave event.

Alternative 4 is similarly projected to prevent inundation of the beach park and highway, however, model results assume that the full beach within the cells remains in place. The longevity of beach fill with straight stabilization structures is uncertain. Sand loss through rip currents along the sides can occur. This could lead to loss of a recreational sand beach, and importantly, the inundation protection the sand beach provides. The use of straight stabilizing structures may not be effective in the long-term to stabilize the nourished beach. Further evaluation through physical model studies is recommended to assess effectiveness. However, a benefit of the straight stabilizing structures is that they can be expanded later to include headland features if they prove to not be effective at holding sand along the shoreline once installed.

Given rising sea levels, and the nearshore circulation dynamics that appear to transport sand into the deep sand channel, eventual loss of the protective sand beach fronting the beach park in Alternative 1 and fronting the buried revetment in Alternative 2 is expected. The rate of beach loss is not known but will likely be at a higher rate than the recent historical trend. Also, because there are no stabilizing structures, rapid, catastrophic sand loss is possible due to severe wave events. Alternatives 1 and 2 may therefore meet the primary project objective of restoring the beach for only a limited time into the future. Recurring and significant costs may then be required to periodically renourish the beach.

The current study includes a comprehensive analysis of the various aspects of beach restoration for Punalu‘u Beach Park. Additional studies for the subject property could include assessment of

the adjacent streams along the study area and how those may be impacted by the proposed beach restoration alternatives. Additional offshore sand source availability may also be conducted if beach re-nourishment (maintenance) is desired for the Alternatives 1 and 2.

12.3 Regulatory Requirements

The State's Conservation District extends 3 nautical miles offshore from the certified shoreline, which is defined by the highest wash of the waves during the season of high surf (not including hurricanes or tsunamis). SEI anticipates that the certified shoreline would be located along, or close to, the existing erosion scarp or near the road shoulder in some areas. This would put essentially all alternative options seaward of the shoreline in the Conservation District. It is likely that all alternative concepts would require Federal, State, and City approvals.

SEI anticipates that any of the proposed alternatives would require the following permits:

- Department of the Army (DA), Section 10 and Section 404 Individual Permit (IP).
- Hawai'i Department of Health (DOH), Standard Water Quality Certification (WQC).
- Hawai'i Department of Health (DOH), National Pollutant Discharge Elimination System (NPDES) Permit.
- Hawai'i Department of Health (DOH), Community Noise Permit.
- Hawai'i Department of Land and Natural Resources (DLNR), Shoreline Certification.
- Hawai'i Department of Land and Natural Resources (DLNR), Right of Entry Permit (ROE) or Revocable Permit (RP).
- Hawai'i Department of Land and Natural Resources (DLNR), Conservation District Use Permit (CDUP). Depending on the scope of the repairs and/or alterations, an Environment Assessment (EA) may be required. This determination will be made by DLNR during review of the CDUP application.
- Hawai'i Office of Planning (OP), Coastal Zone Management (CZM) Federal Consistency Review.
- Hawai'i State Historic Preservation Division, Chapter 6E-8 Historic Preservation Review.
- City and County of Honolulu, Special Management Area (SMA) Permit (SMA Minor if under \$500,000, SMA Major if over \$500,000). If an SMA Major is required, an Environmental Assessment (EA) will be required.
- City and County of Honolulu, Shoreline Setback Variance (SSV), if required.
- City and County of Honolulu, Building Permit, if required.
- City and County of Honolulu, Grading Permit, if required.

Final design, Environmental Impact Statement, permitting, and contract documents are estimated to cost an additional \$1M.

13. REFERENCES

Booij, N. R. R. C., Roeland C. Ris, and Leo H. Holthuijsen. 1999. "A third-generation wave model for coastal regions: 1. Model description and validation." *Journal of Geophysical Research: Oceans* 104, no. C4: 7649-7666., doi:10.1029/98JC02622.

Boudreau, R., Sloop, R., Holloway, A., and Rivera, J. (2018). "Maui's resilient living shoreline project provides adaptation strategy for critical infrastructure." *Shore & Beach*, 86(4), 26–35.

Bridges, T. S., J. K. King, J. D. Simm, M. W. Beck, G. Collins, Q. Lodder, and R. K. Mohan, eds. 2021. "International Guidelines on Natural and Nature-Based Features for Flood Risk Management." Vicksburg, MS: U.S. Army Engineer Research and Development Center.

Coastal Engineering Research Center (US). 2006. *Coastal Engineering Manual*. Department of the Army, Waterways Experiment Station, Corps of Engineers, Coastal Engineering Research Center.

Garza, J. A., P.-S. Chu, C. W. Norton, and T. A. Schroeder (2012), "Changes of the prevailing trade winds over the islands of Hawaii and the North Pacific", *J. Geophys. Res.*, 117, D11109, doi:10.1029/2011JD016888.

Hawai'i Dune Restoration Manual, 2022. University of Hawai'i Sea Grant College Program. National Sea Grant Office, Rapid Response Funds Funding opportunity NOAAOAR-SG-2019-2005864 (HH-21-01).

IPCC, 2021: *Climate Change 2021: The Physical Science Basis. Contribution of Working Group I to the Sixth Assessment Report of the Intergovernmental Panel on Climate Change*[Masson-Delmotte, V., P. Zhai, A. Pirani, S.L. Connors, C. Péan, S. Berger, N. Caud, Y. Chen, L. Goldfarb, M.I. Gomis, M. Huang, K. Leitzell, E. Lonnoy, J.B.R. Matthews, T.K. Maycock, T. Waterfield, O. Yelekçi, R. Yu, and B. Zhou (eds.)]. Cambridge University Press, Cambridge, United Kingdom and New York, NY, USA, In press, doi:[10.1017/9781009157896](https://doi.org/10.1017/9781009157896).

Knutson, T. R., Sirutis, J. J., Zhao, M., Tuleya, R. E., Bender, M., Vecchi, G. A., Chavas, D. (2015). "Global projections of intense tropical cyclone activity for the late twenty-first century from dynamical downscaling of CMIP5/RCP4.5 scenarios." *Journal of Climate*, 28(18), 7203-7224. doi:10.1175/jcli-d-15-0129.1

Stelling, G., and M. Zijlema. 2003. "An accurate and efficient finite-difference algorithm for non-hydrostatic free-surface flow with application to wave propagation." *International journal for numerical methods in fluids*, vol. 43, no. 1: 1-23.

Storlazzi, C.D., Shope, J.B., Erikson, L.H., Hegermiller, C.A., and Barnard, P.L., 2015, "Future wave and wind projections for United States and United States-affiliated Pacific Islands": U.S. Geological Survey Open-File Report 2015–1001, 426 p., <http://dx.doi.org/10.3133/ofr20151001>.

Sweet, W.V., R.E. Kopp, C.P. Weaver, J. Obeysekera, R.M. Horton, E.R. Thieler, and C. Zervas (2017). Global and Regional Sea Level Rise Scenarios for the United States. NOAA Technical

Report NOS CO-OPS 083. NOAA/NOS Center for Operational Oceanographic Products and Services.

Sweet, W.V., Mercy, D., Dusek, G., Marra, J.J., Pendleton, M. (2018). 2017 State of U.S. High Tide Flooding with a 2018 Outlook. National Oceanic and Atmospheric Administration (NOAA) Center for Operational Oceanographic Products and Services, NOAA Office of Coastal Management, NOAA National Centers for Environmental Information, The Baldwin Group, Inc.

Sweet, W.V., B.D. Hamlington, R.E. Kopp, C.P. Weaver, P.L. Barnard, D. Bekaert, W. Brooks, M. Craghan, G. Dusek, T. Frederikse, G. Garner, A.S. Genz, J.P. Krasting, E. Larour, D. Marcy, J.J. Marra, J. Obeysekera, M. Osler, M. Pendleton, D. Roman, L. Schmied, W. Veatch, K.D. White, and C. Zuzak (2022). *Global and Regional Sea Level Rise Scenarios for the United States: Updated Mean Projections and Extreme Water Level Probabilities Along U.S. Coastlines*. NOAA Technical Report NOS 01. National Oceanic and Atmospheric Administration, National Ocean Service, Silver Spring, MD, 111 pp. <https://oceanservice.noaa.gov/hazards/sealevelrise/noaa-nostechrpt01-global-regional-SLR-scenarios-US.pdf>

Van der Meer, J.W., Allsop, N.W.H., Bruce, T., De Rouck, J., Kortenhaus, A., Pullen, T., Schüttrumpf, H., Troch, P. and Zanuttigh, B., 2016. Eurotop-Manual on wave overtopping of sea defenses and related structures. An overtopping manual largely based on European research, but for worldwide application.

Webb, B., Dix, B. Douglass, S., Asam, S. Cherry, C., and Buhring, B. (2019) “*Nature-Based Solutions for Coastal Highway Resilience: An Implementation Guide*.” FHWA-HEP-19-042. Washington, D.C. Federal Highway Administration.

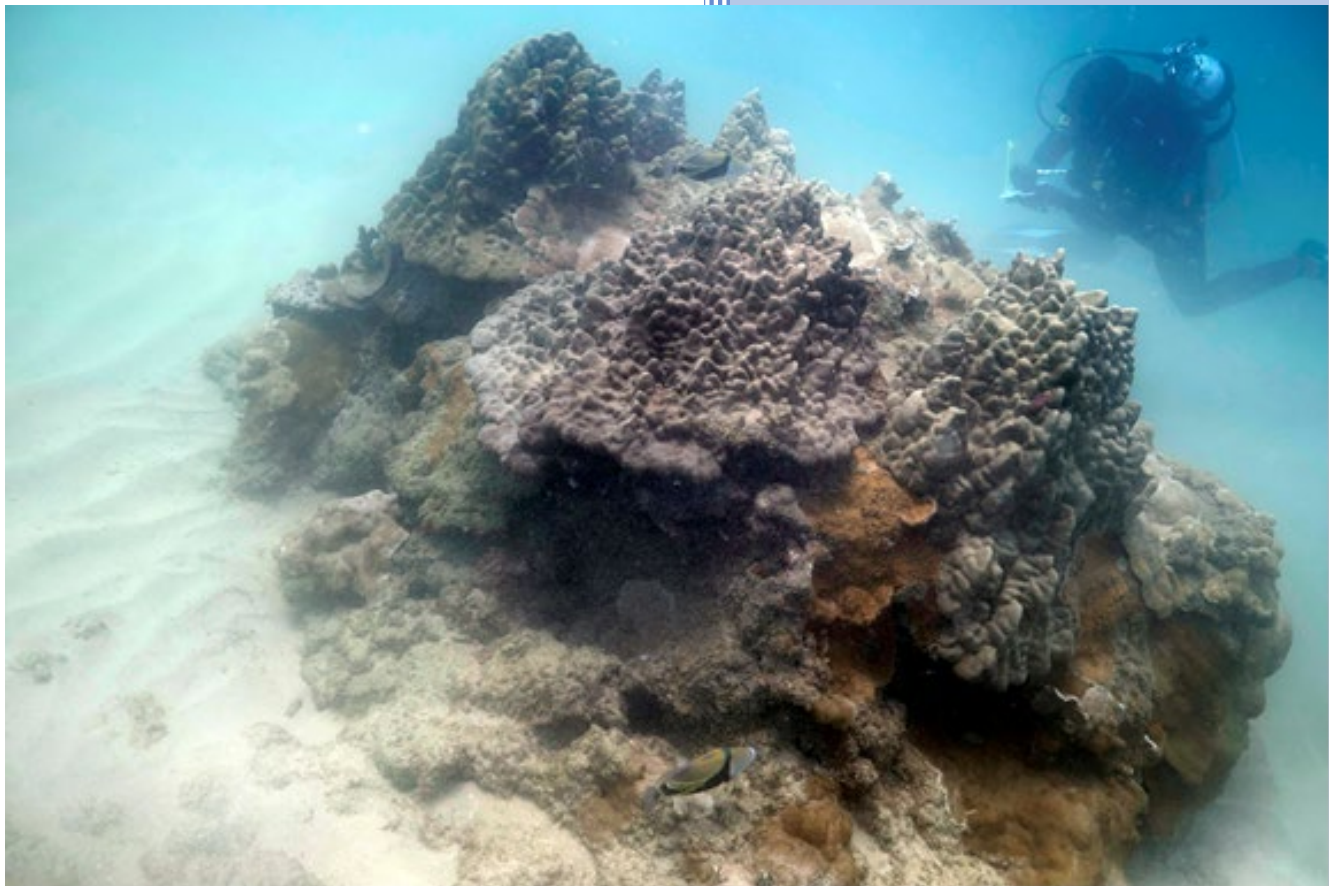


14. APPENDIX A: PUNALUU BEACH NOURISHMENT MARINE ASSESSMENTS



MARINE RESEARCH CONSULTANTS, INC.

PUNALUU BEACH NOURISHMENT MARINE ASSESSMENTS



SUBMITTED TO:

Sea Engineering, Inc.
41-305 Kalanianaʻole Hwy
Waimanalo, HI 96795

PREPARED BY:

Marine Research Consultants, Inc.
46-312C Haiku Rd
Kaneohe, HI 96744
808-779-4009

DATE: April 1, 2024

1 INTRODUCTION AND PURPOSE

In 2007, the City and County of Honolulu initiated a program to address erosion problems at City beach parks on Oahu. Haleiwa, Punaluu, and Hauula beach parks were identified as having the most severe erosion threats, and follow-up conceptual design studies were conducted at these beach parks in 2012 to develop shoreline improvement alternatives. Erosion has progressed since these studies were completed. At Punaluu the erosion has undermined the shoreline and is threatening to severely damage the park comfort station. Emergency shore protection was installed in 2016 and again in 2020 to prevent the collapse of the structure. The park grounds and Kamehameha Highway, which is as close as 25 to 50 feet from the shoreline in some locations, are at low elevation and occasionally inundated by large storm waves.

Kamehameha Highway is considered vital infrastructure as it is the only road to communities along northeast Oahu. Erosion and wave inundation of the highway and backshore are expected to increase in the future as sea level rises. To help protect Kamehameha Highway from flooding and erosion, improve community resiliency to sea level rise and coastal storms, and provide recreational resources and native habitat, the Hawaii Department of Natural Resources (DLNR) is conducting this green infrastructure project to restore the beach at Punaluu. The project is titled "Planning for Improved Resilience to Coastal Hazards through Green Infrastructure at Punaluu, Oahu." The 2012 conceptual design of shoreline improvements at the park, which included development of oceanographic design parameters, identification of a possible nearshore sand source, and development of alternative improvement concepts including groins and beach nourishment, provide a valuable basis and starting point for the present Green Infrastructure Project.

Multiple strategies are being investigated and analyzed as potential adaptation measures along the coastline. Benthic investigations were focused on options that include the recovery of sand from the nearshore paleo-channel, placement of sand along the shoreline as a beach restoration effort, and installation of stabilizing structures along the shoreline. The purpose of the present document is to provide an assessment of marine water chemistry, and results of a rapid ecological assessment (REA) to describe the marine biotic community structure at the Project sand donor and sand recipient areas.

Water chemistry was assessed by collecting a set of samples along two transects (T1 – T2) originating at the shoreline as well as from sites distributed across the donor site. The physical composition and biotic community structure of marine habitats were also documented within both the donor and the recipient areas. One primary focus of the assessment of the biotic community was to fully describe coral reef assemblages adjacent to the sand donor area and within the sand recipient area. As coral communities are both long-lived and attached to the bottom, they serve as the best indicators of the time-integrated forces that affect nearshore reef areas. Another focus of the biotic community assessment was to document the presence (if any) of seagrass (*Halophila* spp.) adjacent to the sand donor area or at Punaluu Beach Park in the sand

recipient area. Finally, long term monitoring sites were established offshore of the beach park to provide baseline data to evaluate changes in the biotic community over time.

Evaluation of the existing condition of water chemistry and marine communities provides an insight into the physical and chemical factors that influence the marine setting. Understanding the existing physical, chemical, and biological conditions of the marine environment provides a basis for predicting potential effects that might occur as a result of the proposed sand replenishment actions at Punaluu Beach Park.

2 METHODS

2.1 Water Chemistry

All water chemistry criteria specified for open coastal waters in Chapter 11 54, Section 06 (b) of the State of Hawaii Department of Health (DOH) were evaluated for the Punaluu Beach replenishment project. These criteria include total nitrogen (TN), nitrate + nitrite nitrogen ($\text{NO}_3^- + \text{NO}_2^-$, hereafter referred to as NO_3^-), ammonium nitrogen (NH_4^+), total phosphorus (TP), Chlorophyll a (Chl a), turbidity, temperature, pH, and salinity. In addition, dissolved silica (Si) and orthophosphate phosphorus (PO_4^{3-}) were reported as these constituents are sensitive indicators of biological activity and the degree of groundwater mixing.

The HDOH water quality standards (WQS) that apply to the areas offshore of Punaluu Beach Park are listed as “open coastal water” in HRS Chapter §11-54-6(b). Two sets of standards are listed depending on whether an area receives more than 3 million gallons per day (mgd) of freshwater input per shoreline mile (“wet standards”), or less than 3 mgd of freshwater input per shoreline mile (“dry”). As the Punaluu shoreline area receives substantial rainfall and input from Punaluu Stream, wet criteria were used for this evaluation.

The HDOH-WQS are also separated into three standards: geometric means, “not to exceed more than 10% of the time,” and “not to exceed more than 2% of the time.” As these classifications require multiple samplings, they cannot be used for a strict evaluation of whether waters at the sampling site were within compliance standards. However, these values provide a guideline to evaluate the overall status of sampled waters in terms of the relation with State standards.

EPA and Standard Methods (SM) methods that were employed for the Monitoring Program, as well as resolution / detection limits, are listed in the Code of Federal Regulations (CRF) Title 40, Chapter 1, Part 136, and are shown in Table 1. In situ field measurements included water temperature, dissolved oxygen, and salinity, which were acquired using an RBR Concerto data logger with sensors for pressure (depth), conductivity (salinity), temperature, and dissolved oxygen calibrated to factory specifications.

All sampling locations were recorded with a handheld global positioning system (Garmin GPS map 78sc). Samples were collected by filling 0.25-liter, triple-rinsed, polyethylene bottles at each depth at each collection station. Laboratory analyses

were conducted by Marine Consulting and Analytical Resources LLC (MCAR) (Lab number HI 00928). Analyses for Si, NH_4^+ , PO_4^{3-} , and NO_3^- were performed with a Seal Analytical AutoAnalyzer 3 HR (AA3HR) using standard methods for seawater analysis. TN and TP were analyzed in a similar fashion following digestion. Salinity was determined using a Mettler Toledo Seven Excellence Multi-parameter meter with an InLab 731-ISM conductivity probe.

Chl *a* was measured by filtering 150 ml through GFF/F glass-fiber filters; pigments on filters were extracted in 90% acetone in the dark at -20 °C for 24 hours. Fluorescence of the extract was measured with a Turner Designs Trilogy Fluorometer model 7200-000 equipped with an extracted chlorophyll non-acidification module. Salinity was determined using a Mettler Toledo Seven Excellence Multi-parameter meter with an InLab 731-ISM conductivity probe, calibrated to a Hach Instruments traceable salinity standard of 35.00 parts per thousand (‰ or ppt), 53.0 mS/cm, with a readability of 0.01 ppt. Turbidity was determined using a Hanna Instruments Model #HI88703 Turbidimeter and reported in nephelometric turbidity units (NTU) (precision of 0.01 NTU). Measurements of pH were acquired with a Thermo Scientific Orion Star meter with a Thermo Scientific 8107UWMMD electrode.

2.1.1 Sand Donor Area

Fieldwork for the water chemistry assessment at the sand donor area was conducted on September 6, 2023. Water chemistry samples were collected at six stations over the sand bed and two stations in the channel leading to Punaluu Beach Park. At each station two samples were collected; one sample was collected within 20 cm of the ocean surface and one sample collected approximately 1 m above the ocean floor. In addition, samples were collected at two sites within the channel originating at the stream mouth adjacent to Punaluu Beach Park, and extending to the open ocean.

Samples were collected from a small boat using a 1.8-liter Niskin bottle. The bottle was lowered through the water column with spring loaded endcaps cocked in an open position allowing free flow of water through the bottle. At the desired sampling depth, endcaps were triggered to close by a messenger weight released from the surface. Upon retrieval, samples was transferred to a triple-rinsed polyethylene bottle until further processing.

2.1.2 Punaluu Beach Park

Fieldwork for the water chemistry assessment at Punaluu Beach Park was conducted on January 4, 2024. Water chemistry samples were collected along two transects extending from the shoreline to a distance of approximately 150 m offshore (Figure 1). Water samples were collected by wading or swimming at 7 locations along each transect. Transect 1 originated at the mouth of the Punaluu Stream and extended through the channel leading to the sand donor area. Samples were collected at distances of approximately 0.1, 10, 20, 30, 50, 100, and 150 m from the mouth of the stream. Transect 2 originated at the approximate center of the project area and extended directly offshore. Samples were collected at 0.1, 2, 5, 10, 30, 80, and 150 m from the shoreline (Figure 1). At sites where water depth was less than 2 m, only surface

samples (within 20 centimeters [cm] of the surface) were collected. At sites where water depth was greater than 2 m, surface and near bottom samples were collected.

Sampling was concentrated close to the shoreline as this area receives the most terrestrial input, and hence is most important with respect to identifying the effects of shoreline modification.

2.2 Marine Biotic Community Structure

2.2.1 Sand Donor Area

A rapid ecological assessment (REA) survey was conducted on September 6, 2023, at the sand donor site. The physical and biotic composition was assessed by biologists on SCUBA working from a small boat. Biologists conducted two dives within and around the boundaries of the donor site and one dive in the channel (Figure 1). The first dive originated at the west side and progressed in a clockwise direction; the second dive originated at the west side and progressed in a counterclockwise direction. The channel dive originated at the southwest edge of the sand bed and progressed shoreward through the channel towards the beach. During all dives on the sand bed and in the channel, underwater visibility ranged from 3 m to 5 m.

During underwater investigations at the sand donor area, notes on species composition were recorded and numerous digital photographs were collected to document the existing conditions of the area. Species lists were compiled of all fish, corals, non-coral invertebrates, and macroalgae. During all dives investigators noted the presence or absence of seagrass (*Halophila* spp.).

2.2.2 Punaluu Beach Park

A REA survey was conducted on January 4, 2024, at the sand recipient site by biologists snorkeling and working from the shore. Snorkel surveys were conducted by swimming in a zigzag pattern from the shoreline to approximately 75 m offshore throughout the area that fronted Punaluu Beach Park (Figure 1). Underwater visibility during the shoreline snorkel ranged from 2.5 m at the southeast end to 1.0 m near the stream mouth at the northwest end.

During underwater investigations offshore of the beach park, notes on species composition were recorded and numerous digital photographs were collected to document the existing conditions of the area. Species lists were compiled of all fish, corals, non-coral invertebrates, and macroalgae. During all dives investigators noted the presence or absence of seagrass (*Halophila* spp.).

In addition to the REA, four sites that provide a valid representation of the offshore marine environment near the beach park were selected for establishment of long-term quantitative survey locations. Each of these sites was georeferenced for future relocation using high-resolution GPS devices provided by Sea Engineering, Inc. Each site consisted of an area of approximately 5 m x 5 m (16.4 ft x 16.4 ft). Pastic tie-wraps were fixed to non-living surfaces to mark the corners of the sites for relocation in future surveys. Thus, all subsequent surveys will evaluate the same 5 m x 5 m area of reef, providing a time-course analysis of change related to sand nourishment activities.

Where conditions allowed (primarily adequate water depth) each survey site was photographically documented using orthomosaic techniques. To carry out orthomosaic acquisition, scale bars marked with colored tape at 10-cm intervals were placed on the corners of each site. Using digital mirrorless cameras fitted with 24-mm lenses in underwater housings, each 5 m x 5 m survey site was photographed by a diver in an overlapping boustrophedonic (“lawnmower”) pattern. This method of photo acquisition resulted in several hundred digital photographs that completely record the bottom composition of each survey area. Following fieldwork, all photographs for each area were processed using Agisoft Metashape software to produce a seamless orthomosaic image that shows the entire area as a single high-resolution image. In addition to the diver acquiring the photographic images, a second diver examined the survey site to compile a species list to ensure that any rare, small, or cryptic organisms that are not visible in the orthomosaic image are included in the survey results.

Following processing of photographs each orthomosaic was analyzed by trained personnel using the commercially available software Coral Point Count for Excel (CPCe). This software places 200 random points on each orthomosaic that are then systematically categorized in an Excel worksheet as living coral species, algae, and non-living bottom types (sand, rubble, mud, limestone fossil reef, dead coral, etc). The resulting data set provides percent cover of all bottom types and can be used to determine size-frequency distribution of corals, as well as rugosity of substratum. Replication of these methods as time-course surveys will provide an accurate representation of changes to the marine biotic communities and physical structure of the bottom with respect to activities related to shoreline modification.

3 RESULTS

3.1 Water Chemistry

3.1.1 Sand Donor Area

Results of water chemistry analyses for samples collected above the sand donor area are shown in Table 2 and Table 3. Dissolved nutrient concentration in Table 1 are shown as micromoles (μM); dissolved nutrient concentrations in Table 2 are shown as micrograms per liter ($\mu\text{g/L}$).

3.1.1.1 Distribution of Chemical Constituents

Examination of the data reveals that water chemistry over the sand donor area was fairly consistent for Stations 2 – 8 (Table 2 and Table 3). At all sampling stations concentrations of Si and NO_3^- were higher in surface samples relative to near-bottom samples. Salinity showed a mirror-image pattern, with all surface samples lower than respective bottom samples. As Si and NO_3^- are typically found in substantially higher concentrations in groundwater and surface water discharge compared to ocean water, the consistent profile at all sample sites indicates that the entire source area

contains a surface layer that contains input from land. Sample station 1, located closed to the shoreline and the mouth of Punaluu Stream showed the highest values of Si and NO_3^- , and the lowest values of salinity, as well as the greatest differences between surface and bottom samples. These elevated values indicate that flow of stream water and/or concentrated groundwater are resulting in the stratified water column over the sand donor site.

Other dissolved inorganic nutrients (PO_4^{3-} , NH_4^+) that are not normally found in elevated concentrations in groundwater do not show the same consistent pattern of elevated values in surface samples as was evident for Si and NO_3^- .

Values of turbidity also showed a peak value at the surface at station 1, with relatively consistent values at all of the offshore stations between 0.33 and 0.96 nephelometric turbidity units (NTUs). There was not a consistent vertical pattern of elevated values in surface samples. Conversely, measurements of Chl *a* did reveal a pattern of lower values at the surface relative to the bottom at all survey sites. Such a pattern may indicate that freshwater input from streams and groundwater contain lower values of Chl *a* than background ocean waters. Elevated temperature at the surface in all sample pairs again indicates the effect of stream water and groundwater on the water chemistry in the vicinity of the proposed sand donor area.

3.1.1.2 Compliance with DOH Criteria

All but one sample was in compliance with the DOH-WQS for all measured constituents. The single exception was for NH_4^+ and turbidity in the surface sample at Station 1, which exceeded the NTE more than 10% of the time criteria for wet conditions (Table 2 and Table 3). These elevated values are an indicator of the input of terrigenous materials to the ocean from Punaluu Stream. All values of PO_4^{3-} , nitrate, total phosphorous, total nitrogen, and chlorophyll *a* were within the DOH-WQS criteria for wet conditions.

3.1.2 Punaluu Beach Park

Water chemistry samples were collected along two transects originating at and perpendicular to the shoreline at Punaluu Beach Park (Figure 1). The western transect originated at the mouth of Punaluu Stream and extended through the channel towards Station 1, which was the most shoreward water sampling site at the sand donor area. Dissolved nutrient concentration along transects offshore of Punaluu Beach Park are shown in Table 4 as μM and in Table 5 as $\mu\text{g/L}$.

3.1.2.1 Distribution of Chemical Constituents

Examination of the water chemistry data on the transects originating at the shoreline of Punaluu Beach Park reveal a distinct influence of stream input to the nearshore ocean. All nutrients show distinct patterns of horizontal gradation with highest values at the shoreline and progressively decreasing concentrations with distance from shore. Salinity displays the opposite trend, with lowest concentrations in the nearshore samples and progressive increases with distance from shore. Over the West sampling transect, the range in NO_3^- is approximately 12.6 $\mu\text{g/L}$, while the range of salinity is approximately 30 ppt. On

the East sampling transect, which originates approximately 400 m from the stream mouth, the range in NO_3^- is approximately 7 $\mu\text{g/L}$, while the range of salinity is approximately 1.5 ppt. Hence, it is apparent that input from stream discharge has a substantial effect on nutrient concentrations in the nearshore ocean. Temperature also displays a distinct gradient off the stream mouth with lowest values near the point of discharge, and progressive increases with distance from shore.

Unlike the patterns of dissolved inorganic nutrients (particularly Si and NO_3^-), the distributions of turbidity and Chl *a* on the West Beach Park transect do not display highest values near the shoreline, with diminishing values moving seaward (Table 4 and Table 5). Overall, values of Chl *a* are considered low with all values below 0.75 $\mu\text{g/L}$. On the East transect, however, there are peak values at the shoreline for turbidity and Chl *a*, with progressive decreases with distance from shore. Such a pattern is likely a response to resuspension of fine-grained particulate material, including plant fragments, stirred by breaking waves in the shallow nearshore zone. With decreasing wave energy and increasing water depth, turbidity in the water column decreases. Temperature displays no gradient of consistent change across the East transect.

3.1.3 Compliance with DOH Criteria

Of the samples collected along the two transects off of Punaluu Beach Park the only constituents to exceed State of Hawaii water quality standards criteria under wet conditions were turbidity and Chl *a*. The highest values above the standards were turbidity in the nearshore stations on the East transect. As discussed above the elevated levels of turbidity off the beach are a function of wave stirring in the shallow nearshore zone. Of note is that the elevated levels of inorganic nutrients originating from stream input do not raise the concentrations above the DOH Open Coastal Ocean wet limits.

3.2 Marine Biotic Community Structure

3.2.1 Sand Donor Area

3.2.1.1 Physical Structure

The donor area consists of a bed of uniform sand with no macrobiotic components. The sand surface is structured into waves that cover the entirety of the donor area (Figure 2 A). The seafloor outside of the perimeter of the bed of sand transitions to hard substrate consisting of coral rock rubble and limestone fossil reef (Figure 2 B). The presence of living coral tissue buried in sand waves indicates that the sand likely moves into, out of, and around the sand bed (Figure 2 C). The south edge of the patch is adjacent to a vertical wall that reaches to within several feet of the surface of the water. The wall provides a solid surface for the attachment of stony corals (Figure 2 D).

3.2.1.2 Biotic Community Structure

As macrobiota were not present within the sand bed, biotic community structure analysis will focus on the community immediately surrounding the sand bed. Best management practices should be mandated to protect these nearby resources during all in-water operations.

3.2.1.2.1 Seagrass

One primary resource in the vicinity of the sand donor bed is seagrass. Dense meadows of seagrass rim the perimeter of the west edge of the donor patch as well as throughout the channel between the donor area and the shore (Figure 3). Note, seagrass was not observed within the bounds of the sand donor bed. It is likely that the shifting nature of the sand bed prevents colonization by seagrass as this species requires substrate with some stability. Seagrass is present in areas of hard substrate covered with sand and sand pockets between areas of hard substrate.

3.2.1.2.2 Coral

Corals were common on the hard substrate outside the perimeter of the sand donor bed. When considering the entire survey area around the outside of the sand donor site, eight species of stony corals were documented (Table 6). *Montipora capitata*, *M. patula*, *Pocillopora meandrina*, and *Porites evermanni* can be considered common; while *Montipora flabellata*, *Pavona varians*, *Pocillopora damicornis*, and *Porites lobata* can be considered rare within the survey area (Figure 4 and Figure 5). At the time of the survey, the water column above the sand donor area was highly turbid owing to resuspended fine-grained sediment and sand. As a result of persistent wave energy, it is likely that these conditions are common and corals in this zone have adapted to the high turbidity and low light conditions present in the coastal area of the northwest shore of Oahu.

Montipora capitata and *M. patula* were present as encrusting colonies often found competing for available hard substrate with mounding colonies of *Porites evermanni* and, to a lesser extent, *P. lobata* (Figure 4 B and C, and Figure 5 A). Colonies of *M. capitata* were also found with a branching morphology. These corals heads of mixed *Montipora* and *Porites* species were often large with longest diameters of 2 meters (Figure 4 C). Several branching colonies of *P. meandrina* were observed with deeply pigmented tissue and longest diameters of approximately 40 cm on the hard substrate around the sand bed (Figure 4 D). Several colonies of encrusting *Montipora flabellata* with longest diameters of approximately 30 cm were also observed on the west side of the survey area (Figure 5 C). Several colonies of *Pocillopora damicornis* were observed, all less than 20 cm in diameter and with bleached tissue (Figure 5 D). A single colony of *Pavona varians* was found with a typical encrusting growth form on the vertical side of a boulder off the west side of the sand donor bed.

The nearly vertical wall on the south side of the sand donor bed provided adequate hard substrate above the scour of sand for coral colonization (Figure 2 D). This wall was estimated to have coral cover of approximately 40%. The most common species of coral on the wall were encrusting and plating colonies of *Montipora capitata* and *M. patula* followed by mounding and encrusting colonies of *P. lobata* and branching

colonies of *Pocillopora meandrina*. Crustose coralline algae and turf algae were also common on the vertical wall.

3.2.1.2.3 Algae

The most common algal group at the sand donor area was turf algae, which colonized nearly all available abiotic hard substrate. The turf algae collected sand and fine-grained sediment and often created a carpet of sediment-bound turf (Figure 2 B, and Figure 6 A and B). None of the observed macroalgal species groups were classified as abundant (Figure 6). Species/species groups classified as common were cyanobacteria, *Acanthophora spicifera*, and crustose coralline algae (Table 7). Tufts of cyanobacteria were found on the seafloor attached to small stones in the sand as well as to larger expanses of hard substrate (Figure 6 C). *Acanthophora spicifera* was common on the west side of the sand bed and was often found growing in conjunction with other macroalgae (Figure 6 B). *Acanthophora spicifera* is a red alga that is classified as invasive alien by the Hawaii Department of Land and Natural Resources, Division of Aquatic Resources (DAR). In the 50 years since its unintended introduction from Guam, *A. spicifera* has become one of the most successful and abundant algae on Hawaiian reef flats. Crustose coralline algae was ubiquitous throughout the survey area and was commonly found on the wall off the south end of the donor bed as well as on rubble and boulders.

3.2.1.2.4 Fish

Fish were relatively uncommon within the sand donor survey area. Fish paucity is likely partially a result of low detectability owing to poor visibility at the time of the survey. In total, 26 species of fish were detected (Table 8, Figure 7). The most common and conspicuous groups were the surgeonfish and damselfish, which were comprised of 3 species and 5 species, respectively. The wrasses were also well-represented with 4 species, however, 3 of these 4 species were considered rare within the survey area.

The saddle wrasse (*Thalassoma duperrey*) and the blackfin chromis (*Chromis vanderbilti*) were the only species classified as abundant around the perimeter of the sand donor bed. The saddle wrasse was ubiquitous throughout the survey area as both juveniles and adults. The blackfin chromis was commonly observed schooling over large coral heads in groups of up to 50 individuals (Figure 4 C). Groups of Hawaiian Dascyllus (*Dascyllus albisella*) were schooling over rocks with mixed encrusting corals (Figure 7 A).

3.2.1.2.5 Non-Coral Invertebrates

In general, non-coral macro-invertebrates were conspicuously sparse around the perimeter of the sand bed with only five species/species groups detected (Table 9, Figure 8 A and B). All of the species observed around the perimeter of the sand donor bed were classified as rare (low abundance at the site) except for the collector urchin (*Tripneustes gratilla*), which can be considered common within the survey area (Figure 8 A). One species of lobster (*Parribacus antarcticus*, Figure 4 B), one sea cucumber (*Actinopyga varians*, Figure 8 B), one additional species of sea urchin (*Echinothrix calamaris*, Figure 8 A), and several sponges were observed and classified as rare. Note that all five of these species/groups are common nearshore Hawaii invertebrates.

3.2.1.2.5.1 Debris

Large anthropogenic debris was found around the perimeter of the sand donor area (Figure 8 C and D). A large chain and an unidentifiable metal structure were located east of the donor area. These objects provided hard substrate for colonization by macroalgae and coral.

3.2.2 Punaluu Beach Park

3.2.2.1 Physical Structure

The composition of the shoreline varies along the length of Punaluu Beach Park where mitigation procedures are being planned (Figure 9 A). Some portions of the shoreline along the highway are comprised of eroded grass lawns where the high wash of waves reaches to the edge of the lawn (Figure 9 B). Other sections adjacent to the highway consist of sandy beaches up to 10 m in width (Figure 9 C). Some of these sandy stretches include rocks and boulders up to 1 m in diameter distributed on the surface of the sand (Figure 9 D). Apparent mitigation measures have been installed makai of the bathhouse in what appears to be an attempt to stabilize and preserve the structure.

In areas where the shoreline consists of sandy beaches, the sand extends through the intertidal zone and transitions into a mixed sand and rubble zone (Figure 10). The sand and rubble zone extends seaward for the entire offshore range of the study area and beyond. In general, the amount of sand decreases while the amount of solid rock bottom increases with distance from shore. Sand beds are also more common and persist further from shore at the northwest end of the survey area near the mouth of the Punaluu Stream. Occasional boulders and cracks forming small ledges add some rugosity to an otherwise flat, sloping seafloor in the nearshore zone.

The entire sand/rubble/rock zone within the study area is shallow in depth, never deeper than approximately 2 m. The offshore area beyond the sandy intertidal zone consists of a relatively homogeneous environment with little distinct zonation in physical structure.

3.2.2.2 Biotic Community Structure

3.2.2.2.1 Algae

The biotic composition of the reef community fronting Punaluu Beach Park can generally be considered an algal dominated system. Most of the sand and rubble/rock surfaces were covered with a variety of turf and macroalgae (Figure 11 and Figure 12). In total, 30 macroalgae species/species groups were identified in the Punaluu Beach Park survey area (Table 7). The most common species/species groups were *Acanthophora spicifera*, crustose coralline algae, and cyanobacteria (Figure 11 A, B, and C). These three macroalgae were categorized as abundant in the sand recipient area at Punaluu Beach Park. *Acanthophora spicifera* is a red alga that is classified as invasive alien by the Hawaii Department of Land and Natural Resources, Division of Aquatic Resources (DAR). In the 50 years since its unintended introduction from Guam, *A. spicifera* has become one of the most successful and abundant algae on Hawaiian reef flats. Other common species were *Boodleia composita* (Figure 11 D), *Cladophora* sp., *Codium edule* (Figure 12 A), *Dictyosphaeria cavernosa* (Figure 12 A), *D. versluysii*,

Galaxaura rugosa, *Halimeda discoidea* (Figure 12 B), *Hormothamnion enteromorphioides*, *Hypnea* spp., *Laurencia* spp., *Liagora ceranoides*, *Ulva fasciata*, and *Ulva* spp.

Halophila spp. was not observed within the Punaluu beach Park survey area.

3.2.2.2 Coral

Reef building corals were present throughout the rubble and rock zones. However, colonies were generally isolated with no true accreting reef structure. Over the entire survey area along Punaluu Beach Park, eight species of stony corals were documented (Table 6). *Porites lobata* can be considered common, while all seven of the other species can be considered rare within the survey area.

Porites lobata was present as mounding colonies all less than 40 cm in diameter (Figure 13 A). *Cyphastrea ocellina* (Figure 13 B), *Montipora capitata* (Figure 13 C), *M. patula*, and *Leptastrea purpurea* were observed as encrusting colonies growing on pieces of dead coral rubble. Unlike *M. patula*, *M. capitata* and *C. ocellina* were observed with small lumps that protruded from the otherwise encrusting colonies. *Pocillopora damicornis* (Figure 13 D), *P. meandrina* (Figure 13 E), and *Porites compressa* were observed as small branching colonies not exceeding 20 cm, 40 cm, and 20 cm, respectively.

Four permanent survey sites were established along the length of the surveyed shoreline approximately 200 m offshore. GPS coordinates for the sites are shown in Table 10. To assist in relocation of sites plastic tie-wraps were attached to non-coral structures at sites 2, 3 and 4. At sites 2, 3 and 4 orthomosaic images were acquired of the bottom to determine baseline conditions prior to any sand relocation activities (Figure 14 and Figure 15). Site 1 consisted entirely of weathered rocks <10 cm in diameter and covered in turf algae and crustose coralline algae. This site was documented with representative photographs (Figure 16).

Bottom composition of sites 2, 3 and 4 consisted entirely of sand, coral rubble, and rocks with scattered small coral colonies and algae. Table 11 shows results of size frequency analysis of corals within the orthomosaics at permanent survey sites 2, 3, and 4. In total, 24 corals were counted; one each at sites 2 and 3 and the remaining 22 colonies at site 4. Seven species of coral were present with *Montipora capitata* as the most abundant (7 colonies). The most abundant size class was >10 - 20 cm (8 colonies) with 20 colonies less than 20 cm. Only a single coral was greater than 40 cm in long diameter (*Montipora capitata* at site 4).

3.2.2.3 Non-Coral Macroinvertebrates

In general, non-coral macro-invertebrates were conspicuously sparse on the reef flat with only five species/species groups detected (Table 9). All of the species observed at Punaluu Beach Park were classified as rare (low abundance at the site) with three sightings or fewer. Two species of sea cucumbers were detected (*Actinopyga varians* [Figure 17 A] and *Holothuria atra*), one sea star (*Ophiocoma erinaceus*), one sea urchin (*Echinometra mathaei*), and several sponges. All five of these species/groups are common nearshore Hawaii organisms.

3.2.2.2.4 Fish

Fish were relatively uncommon on the reef flat, and the fish that were observed were generally small (less than 20 cm). In total, 11 species of fish were detected (Table 8). The most common and conspicuous groups were the surgeonfish and wrasses, which were each comprised of 3 species (Figure 17 B, C, and D). The ringtail surgeonfish (*Acanthurus blochii*, Figure 17 B), the Hawaiian whitespotted pufferfish (*Canthigaster jactator*, Figure 17 B and E), and the saddle wrasse (*Thalassoma duperrey*, Figure 17 B) were the only fish observed to be common within the survey area. No species of fish were observed to be abundant. The majority of fish were observed under small ledges and sheltering in boulders. The relative paucity of fish is likely a result of the lack of shelter for fish on the flat bottom structure of the nearshore area at Punaluu Beach Park.

4 DISCUSSION AND CONCLUSIONS

The purpose of this assessment is to assemble information to make valid evaluations of the potential for impact to the marine environment from the proposed Punaluu Beach Replenishment project in Punaluu on the northeast shoreline of Oahu, Hawaii. Shoreline mitigation protection is intended to prevent future erosion damage and avoid recurring efforts at temporary emergency protection measures. Specifically, protective measures will help defend Kamehameha Highway from flooding and erosion, improve community resiliency to sea level rise and coastal storms, and provide recreational resources and native habitat.

Evaluation of water chemistry along two transects originating at the shoreline at Punaluu Beach Park and extending seaward reflect input of groundwater and stream water. Concentrations of dissolved nutrients were highest at the shoreline and decreased with distance from shore. On the transect located off the center of the beach park Chl *a* and turbidity displayed horizontal gradients with highest values nearest the shoreline. This pattern is likely a result of resuspension of sediment and algal fragments by wave action in the nearshore zone. On the transect originating in Punaluu Stream, there was not a similar gradient for Chl *a* and turbidity as the stream water did not contain substantial sediment loads.

Evaluation of water chemistry at the sand donor site revealed a vertically stratified water column with a surface layer consisting of lower salinity and higher nutrients than the underlying water column. With a single exception (NH_4^+ at Station 1 in the channel), the only constituents that exceed the DOH-WQS were Chl *a* and turbidity.

Results of the biological assessment reveal that the composition of the sand donor survey area consists of a uniform bed of sand. No macrobiota were observed within the bounds of sand donor bed. Outside the perimeter of the sand bed, bottom composition consists of a mix of hard substrate that is primarily covered with turf algae and macroalgae. Stony corals are common on the hard substrate while seagrass is common on regions of sand-covered hard bottom. In total, eight species of coral were documented with *Montipora capitata*, *M. patula*, *Pocillopora meandrina*, and *Porites evermanni* classified as common. With respect to macroalgae, 18 species/species

groups were identified in the vicinity of the sand donor survey area. Species/species groups classified as common were cyanobacteria, *Acanthophora spicifera* (an invasive red algae), and crustose coralline algae.

The nearshore area at Punaluu Beach Park where beach nourishment is planned consists of a homogeneous shallow sand and rubble/rock reef flat. The biotic composition of the area is comprised primarily of a varied assemblage of macroalgae and turf algae. In total, 30 macroalgae species/species groups were identified. The most common species/species groups were *Acanthophora spicifera* (an invasive red algae), crustose coralline algae, and cyanobacteria. Seagrass was not observed within the Punaluu Beach Park survey area. Reef building corals were present throughout the rubble and rock zones. However, colonies were typically small, rare, and generally isolated with no true accreting reef structure. Over the entire survey area along Punaluu Beach Park, eight species of stony corals were documented. *Porites lobata* can be considered common, while all seven of the other species can be considered rare within the survey area.

Four permanent biological monitoring sites were established offshore of Punaluu Beach Park at a distance of approximately 200 m from the shoreline. These four sites were surveyed to establish a baseline of the physical structure and marine biotic community structure prior to any sand relocation activities. Site 1, which was documented with representative photographs, consisted entirely of small, weathered rocks covered in algae and crustose coralline algae. Sites 2, 3 and 4, which were documented with orthomosaics, consisted of sand, coral rubble, and rocks with scattered small coral colonies and algae. In total, 24 corals within seven species were enumerated within the three orthomosaic monitoring sites. The majority of the colonies were less than 20 cm in longest diameter, and all colonies were less than 80 cm in longest diameter.

The paucity of corals in the nearshore area at Punaluu Beach Park is likely a result of high wave energy and limited availability of hard bottom substratum on the reef flat. High sedimentation and competition with algae and encrusting invertebrates are contributing negative factors to coral settlement and growth. The installation of stabilizing structures may provide solid surfaces for colonization by corals and other encrusting organisms. Such structures in other nearshore areas on Oahu have shown colonization by corals that occur commonly in shallow, turbid environments (e.g. *Leptastrea purpurea*, *Pocillopora damicornis*, *Pocillopora ligulata*, and *Porites lobata*; AECOS, 2020). The stabilizing structures may also provide shelter for juvenile reef fishes, and the interstitial spaces may provide shelter for reclusive fishes. Such results were observed by AECOS (2020) at Iroquois Point, Oahu, where fish abundance and fish species density increased after the installation of similar type structures.

The information collected in this study provides a baseline data set that describes the physical, chemical, and biotic structure of the area. This information can be used to address any concerns that might arise regarding effects to the marine environment during the planning process for the shoreline mitigation.

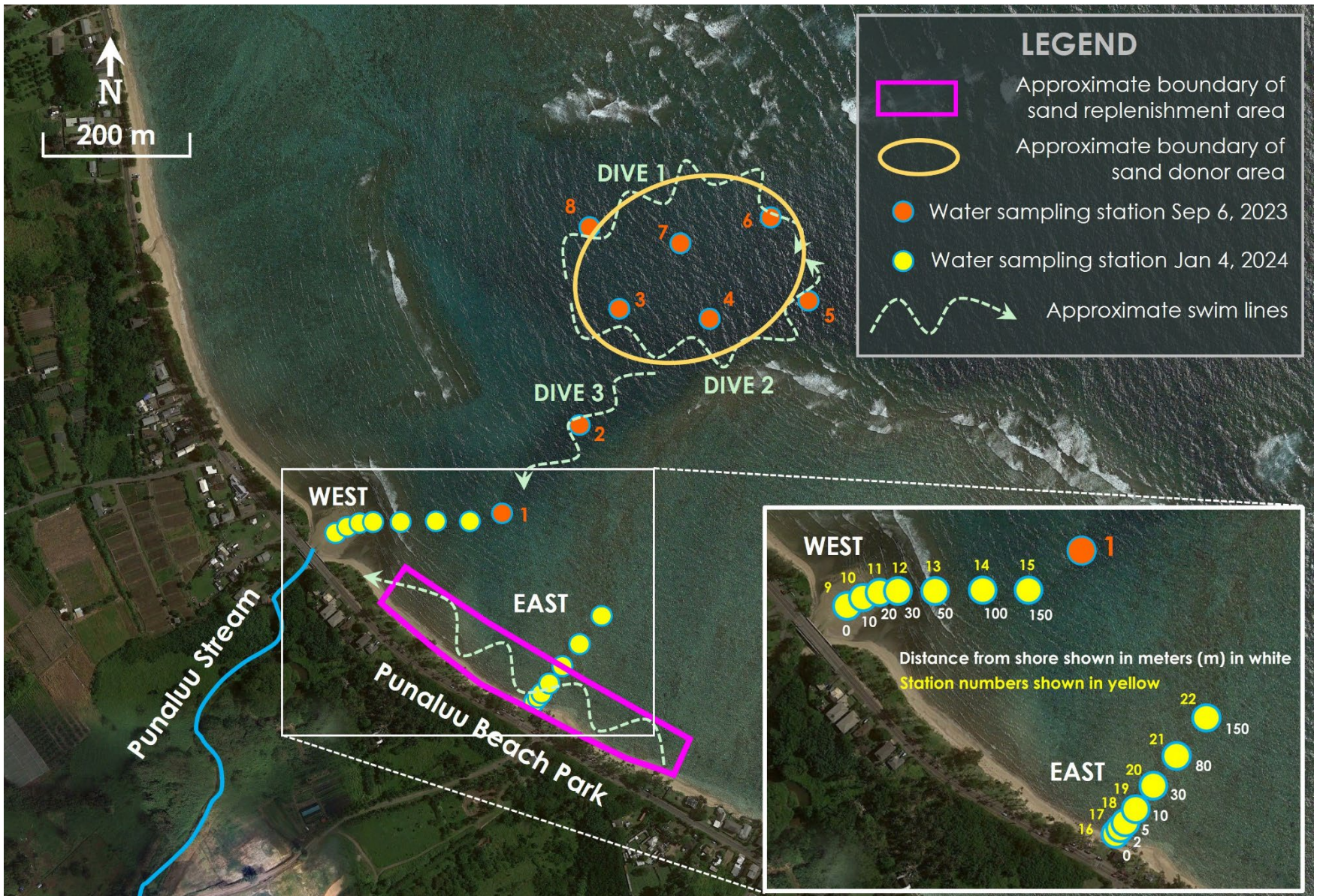


Figure 1 Vicinity Map Showing Locations of Water Sampling Stations, Sand Donor Area, Sand Replenishment Area, and Diver Swim Tracks

Table 1 Water quality constituents, Methods, and Detection Limits/Readability for Samples Collected along Two Transects

Constituent	Method	Detection Limit/Readability
NH ₄ ⁺	EPA 350.1, Rev. 2.0 or SM4500-NH3 G	0.042 micrograms/liter (µg/L)
NO ₃ ⁻ + NO ₂ ⁻	EPA 353.2, Rev. 2.0 or SM4500-NO3F	0.084 µg/L
PO ₄ ³⁻	EPA 365.5 or SM4500-P F	0.28 µg/L
Total P	EPA 365.1, Rev. 2.0 or SM4500-P E J	0.93 µg/L
Total N	SM 4500-N C	1.96 µg/L
Si	EPA 370.1 or SM 4500 SiO ₂ E	0.45 µg/L
Chlorophyll <i>a</i>	SM 10200	0.006 µg/L
pH	EPA 150.1 or SM4500H+B	0.002 pH units
Turbidity	EPA 180.1, Rev. 2.0 or SM2130 B	0.008 nephelometric turbidity units (NTU)
Temperature	SM 2550 B	0.001 degrees Celsius (°C)
Salinity	SM 2520	0.001 parts per thousand (‰)
Dissolved Oxygen	SM4500 O G	0.001% saturation (% sat)

Table 2 Water chemistry measurements from samples collected above the sand donor patch. Nutrient concentrations are shown in micromoles ($\mu\text{M}/\text{L}$). Also shown are the State of Hawaii, Department of Health (DOH) “not to exceed more than 10% of the time” and “not to exceed more than 2% of the time” water quality standards (WQS) for open coastal waters under “wet” conditions. For sampling locations, see Figure 1.

SURVEY AREA	STATION	S or B	PO_4^{3-}	$\text{NO}_3^- + \text{NO}_2^-$	NH_4^+	Si	TP	TOP	TN	TON	TURB	Salt	pH	Chl-a	TEMP	Diss. O_2
			μM	μM	μM	μM	μM	μM	μM	μM	μM	(NTU)	(ppt)	(rel)	($\mu\text{g}/\text{l}$)	deg. C
DONOR AREA	1	S	0.21	0.25	0.94	45.92	0.39	0.18	8.67	7.49	1.31	31.65	8.07	0.41	28.00	97.49
		B	0.09	0.10	0.06	4.51	0.29	0.20	6.89	6.73	0.96	34.68	8.04	0.44	26.80	91.76
	2	S	0.06	0.14	0.07	4.99	0.30	0.25	7.50	7.29	0.69	34.61	8.13	0.34	27.34	103.97
		B	0.07	0.10	0.07	3.81	0.32	0.25	7.45	7.29	0.60	34.72	8.01	0.47	26.57	86.09
	3	S	0.07	0.11	0.07	3.57	0.31	0.24	7.83	7.65	0.52	34.68	8.10	0.38	27.15	100.14
		B	0.08	0.02	0.06	2.01	0.30	0.21	7.01	6.94	0.35	34.83	8.11	0.50	26.67	111.25
	4	S	0.07	0.07	0.09	3.05	0.29	0.22	7.50	7.35	0.54	34.76	8.13	0.36	27.20	107.58
		B	0.08	0.07	0.10	1.89	0.34	0.26	7.88	7.72	0.79	34.80	8.07	0.79	26.61	103.31
	5	S	0.06	0.10	0.00	5.50	0.30	0.24	8.91	8.81	0.51	34.55	8.13	0.37	27.37	105.55
		B	0.10	0.02	0.11	1.80	0.38	0.29	8.25	8.12	0.33	34.80	8.13	0.69	26.47	103.98
	6	S	0.06	0.12	0.11	4.40	0.28	0.22	8.33	8.11	0.43	34.58	8.12	0.36	27.27	104.56
		B	0.08	0.03	0.11	1.89	0.31	0.23	7.65	7.51	0.48	34.80	8.11	0.57	26.58	98.95
	7	S	0.07	0.12	0.12	3.09	0.30	0.24	7.31	7.07	0.40	34.72	8.12	0.35	27.18	102.44
		B	0.10	0.03	0.12	1.99	0.37	0.27	7.32	7.17	0.38	34.79	8.11	0.48	26.66	99.32
	8	S	0.07	0.13	0.11	3.76	0.31	0.24	7.51	7.27	0.58	34.65	8.10	0.36	27.16	97.90
		B	0.07	0.03	0.13	2.28	0.30	0.23	6.81	6.65	0.67	34.80	8.12	0.73	26.73	101.87
DOH OCW WET limits:			NTE 10%	1.00	0.61	-	1.29	-	17.85	-	1.25	*	**	0.90	***	-
			NTE 2%	1.78	1.07	-	1.93	-	25.00	-	2.00	*	**	1.75	***	-

* Salinity shall not vary more than 10% from natural or seasonal changes considering hydrologic input and oceanographic conditions.

** Temperature shall not vary by more than one C from ambient conditions.

*** pH shall not deviate more than 0.5 units from 8.1.

Green shaded values exceed the NTE more than 10% of the time DOH WQS for “wet” conditions; yellow shaded values exceed the NTE more than 2% of the time WQS.

Table 3 Water chemistry measurements from samples collected above the sand donor patch. Nutrient concentrations are shown in micromoles (µg/L). Also shown are the State of Hawaii, Department of Health (DOH) “not to exceed more than 10% of the time” and “not to exceed more than 2% of the time” water quality standards (WQS) for open coastal waters under “wet” conditions. For sampling locations, see Figure 1.

SURVEY AREA	STATION	S or B	PO ₄ ³⁻	NO ₃ ⁻ +NO ₂ ⁻	NH ₄ ⁺	Si	TP	TOP	TN	TON	TURB	Salt	pH	Chl-a	TEMP	Diss. O ₂
			(µg/L)	(µg/L)	(µg/L)	(µg/L)	(µg/L)	(µg/L)	(µg/L)	(µg/L)	(µg/L)	(µg/L)	(NTU)	(ppt)	(rel)	(µg/l)
DONOR AREA	1	S	6.51	3.46	13.16	1,290.26	12.20	5.69	121.44	104.81	1.31	31.65	8.07	0.41	28.00	97.49
		B	2.67	1.39	0.84	126.83	9.01	6.35	96.45	94.22	0.96	34.68	8.04	0.44	26.80	91.76
	2	S	1.71	2.00	1.02	140.24	9.36	7.65	105.01	101.99	0.69	34.61	8.13	0.34	27.34	103.97
		B	2.08	1.37	0.99	107.20	9.93	7.85	104.36	101.99	0.60	34.72	8.01	0.47	26.57	86.09
	3	S	2.05	1.51	1.04	100.43	9.60	7.56	109.62	107.07	0.52	34.68	8.10	0.38	27.15	100.14
		B	2.60	0.27	0.77	56.59	9.19	6.59	98.18	97.14	0.35	34.83	8.11	0.50	26.67	111.25
	4	S	2.17	1.00	1.22	85.66	8.99	6.82	105.06	102.84	0.54	34.76	8.13	0.36	27.20	107.58
		B	2.39	0.97	1.33	52.97	10.60	8.21	110.38	108.08	0.79	34.80	8.07	0.79	26.61	103.31
	5	S	1.71	1.37	0.01	154.42	9.29	7.58	124.74	123.36	0.51	34.55	8.13	0.37	27.37	105.55
		B	2.98	0.26	1.47	50.48	11.85	8.87	115.43	113.70	0.33	34.80	8.13	0.69	26.47	103.98
	6	S	1.83	1.63	1.47	123.69	8.58	6.75	116.62	113.52	0.43	34.58	8.12	0.36	27.27	104.56
		B	2.57	0.38	1.58	53.03	9.65	7.08	107.13	105.16	0.48	34.80	8.11	0.57	26.58	98.95
	7	S	2.14	1.64	1.62	86.79	9.43	7.29	102.27	99.01	0.40	34.72	8.12	0.35	27.18	102.44
		B	3.07	0.41	1.65	55.94	11.32	8.26	102.45	100.39	0.38	34.79	8.11	0.48	26.66	99.32
	8	S	2.11	1.77	1.57	105.77	9.51	7.40	105.11	101.77	0.58	34.65	8.10	0.36	27.16	97.90
		B	2.05	0.38	1.85	64.01	9.19	7.14	95.27	93.05	0.67	34.80	8.12	0.73	26.73	101.87
DOH OCW WET limits:			NTE 10%	14.00	8.50	-	40.00	-	250.00	-	1.25	*	**	0.90	***	-
			NTE 2%	25.00	15.00	-	60.00	-	350.00	-	2.00	*	**	1.75	***	-

* Salinity shall not vary more than 10% from natural or seasonal changes considering hydrologic input and oceanographic conditions.

** Temperature shall not vary by more than one C from ambient conditions.

*** pH shall not deviate more than 0.5 units from 8.1.

Green shaded values exceed the NTE more than 10% of the time DOH WQS for “wet” conditions; yellow shaded values exceed the NTE more than 2% of the time WQS.

Table 4 Water chemistry measurements from samples collected along two transects offshore of Punaluu Beach Park. Nutrient concentrations are shown in micromoles (µM). Also shown are the State of Hawaii, Department of Health (DOH) “not to exceed more than 10% of the time” and “not to exceed more than 2% of the time” water quality standards (WQS) for open coastal waters under “wet” conditions. For sampling locations, see Figure 1.

SURVEY AREA	STATION	DFS (m)	PO ₄ ³⁻	NO ₃ ⁻ +NO ₂ ⁻	NH ₄ ⁺	Si	TP	TOP	TN	TON	TURB	Salt	pH	Chl-a	TEMP	Diss. O ₂
		S or B	µM	µM	µM	µM	µM	µM	µM	µM	µM	(NTU)	(ppt)	(rel)	(µg/l)	deg. C
PUNALUU BEACH PARK WEST	9	0	0.45	0.90	0.36	397.52	0.50	0.05	7.76	6.50	1.04	4.18	7.78	0.61	22.16	99.88
	10	10	0.47	0.88	0.53	390.34	0.54	0.07	7.65	6.24	1.00	4.81	7.74	0.74	22.32	99.84
	11	20	0.44	0.88	0.42	377.60	0.50	0.06	7.47	6.17	1.44	5.56	7.82	0.67	22.27	98.32
	12	30	0.34	0.31	0.23	136.46	0.56	0.22	6.63	6.09	1.30	24.55	8.08	0.55	23.32	100.04
	13	50S	0.51	0.74	0.30	329.51	0.53	0.02	6.86	5.82	0.78	9.41	7.94	0.56	23.11	99.95
		50B	0.30	0.16	0.17	78.52	0.43	0.13	6.64	6.31	1.04	29.14	8.09	0.44	23.98	101.43
	14	100S	0.14	0.01	0.10	16.28	0.40	0.26	6.86	6.75	1.23	33.78	8.07	0.35	24.08	102.44
		100B	0.15	0.01	0.12	16.09	0.36	0.21	6.69	6.56	1.57	33.81	8.08	0.42	24.08	103.05
15	150S	0.19	0.10	0.07	22.74	0.35	0.16	6.95	6.78	1.15	33.27	8.09	0.36	24.06	101.73	
	150B	0.08	-	0.05	12.60	0.30	0.23	6.94	6.88	2.42	34.03	8.09	0.54	24.12	103.25	
PUNALUU BEACH PARK EAST	16	0	0.38	0.51	0.29	30.33	0.55	0.18	7.83	7.03	16.10	33.32	8.13	1.98	24.25	99.75
	17	2	0.29	0.48	0.26	20.66	0.43	0.14	7.55	6.81	10.60	33.80	8.11	1.25	24.26	99.86
	18	5	0.20	0.39	0.20	12.91	0.35	0.15	7.40	6.82	5.22	34.25	8.12	0.93	24.26	102.44
	19	10	0.20	0.36	0.21	12.33	0.40	0.21	7.91	7.33	4.23	34.25	8.13	0.64	24.27	103.84
	20	30S	0.17	0.33	0.16	12.41	0.43	0.26	7.94	7.45	1.75	34.25	8.11	0.51	24.29	102.84
		30B	0.13	0.10	0.16	5.49	0.38	0.25	8.02	7.76	2.75	34.61	8.14	1.13	24.28	103.55
	21	80S	0.11	0.05	0.21	2.26	0.35	0.24	7.74	7.47	0.85	34.75	8.15	0.42	24.29	103.02
		80B	0.09	0.04	0.14	2.19	0.34	0.24	7.33	7.15	0.88	34.75	8.14	0.48	24.30	103.74
22	150S	0.08	0.03	0.14	2.30	0.32	0.24	7.29	7.12	1.02	34.76	8.14	0.40	24.25	102.90	
	150B	0.06	0.04	0.12	2.26	0.32	0.25	6.89	6.74	0.67	34.72	8.15	0.42	24.25	103.41	
DOH OCW WET limits:			NTE 10%	1.00	0.61	-	1.29	-	17.85	-	1.25	*	**	0.90	***	-
			NTE 2%	1.78	1.07	-	1.93	-	25.00	-	2.00	*	**	1.75	***	-

* Salinity shall not vary more than 10% from natural or seasonal changes considering hydrologic input and oceanographic conditions.

** Temperature shall not vary by more than one C from ambient conditions.

*** pH shall not deviate more than 0.5 units from 8.1.

Green shaded values exceed the NTE more than 10% of the time DOH WQS for “wet” conditions; yellow shaded values exceed the NTE more than 2% of the time WQS.

Table 5 Water chemistry measurements from samples collected along two transects offshore of Punaluu Beach Park. Nutrient concentrations are shown in micromoles (µg/L). Also shown are the State of Hawaii, Department of Health (DOH) “not to exceed more than 10% of the time” and “not to exceed more than 2% of the time” water quality standards (WQS) for open coastal waters under “wet” conditions. For sampling locations, see Figure 1.

SURVEY AREA	STATION	DFS (m)	PO ₄ ³⁻	NO ₃ ⁻ +NO ₂ ⁻	NH ₄ ⁺	Si	TP	TOP	TN	TON	TURB	Salt	pH	Chl-a	TEMP	Diss. O ₂
		S or B	(µg/L)	(µg/L)	(µg/L)	(µg/L)	(µg/L)	(µg/L)	(µg/L)	(µg/L)	(µg/L)	(NTU)	(ppt)	(rel)	(µg/l)	deg. C
PUNALUU BEACH PARK WEST	9	0	0.45	0.90	0.36	397.52	0.50	0.05	7.76	6.50	1.04	4.18	7.78	0.61	22.16	99.88
	10	10	0.47	0.88	0.53	390.34	0.54	0.07	7.65	6.24	1.00	4.81	7.74	0.74	22.32	99.84
	11	20	0.44	0.88	0.42	377.60	0.50	0.06	7.47	6.17	1.44	5.56	7.82	0.67	22.27	98.32
	12	30	0.34	0.31	0.23	136.46	0.56	0.22	6.63	6.09	1.30	24.55	8.08	0.55	23.32	100.04
	13	50S	0.51	0.74	0.30	329.51	0.53	0.02	6.86	5.82	0.78	9.41	7.94	0.56	23.11	99.95
		50B	0.30	0.16	0.17	78.52	0.43	0.13	6.64	6.31	1.04	29.14	8.09	0.44	23.98	101.43
	14	100S	0.14	0.01	0.10	16.28	0.40	0.26	6.86	6.75	1.23	33.78	8.07	0.35	24.08	102.44
		100B	0.15	0.01	0.12	16.09	0.36	0.21	6.69	6.56	1.57	33.81	8.08	0.42	24.08	103.05
15	150S	0.19	0.10	0.07	22.74	0.35	0.16	6.95	6.78	1.15	33.27	8.09	0.36	24.06	101.73	
	150B	0.08	-	0.05	12.60	0.30	0.23	6.94	6.88	2.42	34.03	8.09	0.54	24.12	103.25	
PUNALUU BEACH PARK EAST	16	0	0.38	0.51	0.29	30.33	0.55	0.18	7.83	7.03	16.10	33.32	8.13	1.98	24.25	99.75
	17	2	0.29	0.48	0.26	20.66	0.43	0.14	7.55	6.81	10.60	33.80	8.11	1.25	24.26	99.86
	18	5	0.20	0.39	0.20	12.91	0.35	0.15	7.40	6.82	5.22	34.25	8.12	0.93	24.26	102.44
	19	10	0.20	0.36	0.21	12.33	0.40	0.21	7.91	7.33	4.23	34.25	8.13	0.64	24.27	103.84
	20	30S	0.17	0.33	0.16	12.41	0.43	0.26	7.94	7.45	1.75	34.25	8.11	0.51	24.29	102.84
		30B	0.13	0.10	0.16	5.49	0.38	0.25	8.02	7.76	2.75	34.61	8.14	1.13	24.28	103.55
	21	80S	0.11	0.05	0.21	2.26	0.35	0.24	7.74	7.47	0.85	34.75	8.15	0.42	24.29	103.02
		80B	0.09	0.04	0.14	2.19	0.34	0.24	7.33	7.15	0.88	34.75	8.14	0.48	24.30	103.74
22	150S	0.08	0.03	0.14	2.30	0.32	0.24	7.29	7.12	1.02	34.76	8.14	0.40	24.25	102.90	
	150B	0.06	0.04	0.12	2.26	0.32	0.25	6.89	6.74	0.67	34.72	8.15	0.42	24.25	103.41	
DOH OCW WET limits:			NTE 10%	1.00	0.61	-	1.29	-	17.85	-	1.25	*	**	0.90	***	-
			NTE 2%	1.78	1.07	-	1.93	-	25.00	-	2.00	*	**	1.75	***	-

* Salinity shall not vary more than 10% from natural or seasonal changes considering hydrologic input and oceanographic conditions.

** Temperature shall not vary by more than one C from ambient conditions.

*** pH shall not deviate more than 0.5 units from 8.1.

Green shaded values exceed the NTE more than 10% of the time DOH WQS for “wet” conditions; yellow shaded values exceed the NTE more than 2% of the time WQS.

Table 6 Species of Coral Detected within the Donor Area and at Punaluu Beach Park

SPECIES	DONOR AREA	PUNALUU BEACH PARK
<i>Cyphastrea ocellina</i>	-	R
<i>Leptastrea purpurea</i>	-	R
<i>Montipora capitata</i>	C	R
<i>Montipora flabellata</i>	R	-
<i>Montipora patula</i>	C	R
<i>Pavona varians</i>	R	-
<i>Pocillopora damicornis</i>	R	R
<i>Pocillopora meandrina</i>	C	R
<i>Porites compressa</i>	-	R
<i>Porites evermanni</i>	C	-
<i>Porites lobata</i>	C	C
TOTAL NUMBER OF SPECIES OBSERVED	8	8

Notes: R = Rare, C = Common

Table 7 Species of Macroalgae Detected within the Donor Area and at Punaluu Beach Park

DIVISION	SPECIES	DONOR AREA	PUNALUU BEACH PARK
CHLOROPHYTA	<i>Avrainvillea amadelpha</i>	R	-
	<i>Boodlea composita</i>	R	C
	<i>Cladophora</i> sp.	-	C
	<i>Codium arabicum</i>	-	R
	<i>Codium edule</i>	-	C
	<i>Derbesia fastigiata</i>	R	-
	<i>Dictyosphaeria cavernosa</i>	-	C
	<i>Dictyosphaeria versluysii</i>	R	C
	<i>Halimeda discoidea</i>	R	C
	<i>Microdictyon setchellianum</i>	R	R
	<i>Neomeris</i> spp.	-	R
	<i>Pseudobryopsis oahuensis</i>	-	R
	<i>Ulva fasciata</i>	-	C
	<i>Ulva</i> spp.	-	C
	<i>Ventricaria ventricosa</i>	-	R
CYANO-BACTERIA	General	C	A
	<i>Hormothamnion enteromorphioides</i>	-	C
	<i>Leptolyngbia cosbyana</i>	R	-
	<i>Lyngbya majuscula</i>	R	-
OCHRO-PHYTA	<i>Dictyota acutiloba</i>	-	R
	<i>Dictyota sandvicensis</i>	R	R
	<i>Padina australis</i>	-	R
	<i>Turbinaria ornata</i>	-	R
RHODOPHYTA	<i>Acanthophora spicifera</i>	C	A
	<i>Amansia glomerata</i>	-	R
	<i>Amphiroa beauvoisii</i>	R	R
	<i>Asparagopsis taxiformis</i>	R	R
	<i>Coelothrix irregularis</i>	-	R
	Crustose Coralline Algae	C	A
	<i>Galaxaura rugosa</i>	R	C
	<i>Gracilaria coronopifolia</i>	R	-
	<i>Hypnea</i> spp.	R	C
	<i>Laurencia</i> spp.	-	C
	<i>Liagora ceranoides</i>	-	C
	<i>Portieria hornemannii</i>	-	R
<i>Treicleocarpa cylindrica</i>	R	-	
TOTAL NUMBER OF SPECIES OBSERVED		18	30

Notes: R = Rare, C = Common

Table 8 Species of Fish Detected within the Donor Area and at Punaluu Beach Park

FAMILY and SPECIES	DONOR AREA	PUNALUU BEACH PARK
Acanthuridae (Surgeonfishes)		
<i>Acanthurus blochii</i>	C	C
<i>A. nigrofuscus</i>	C	R
<i>Ctenochaetus strigosus</i>	C	R
Antennariidae (Frogfishes)		
<i>Antennarius sp.</i>	R	-
Apogonidae (Cardinalfishes)		
<i>Pristiapogon kallopterus</i>	C	R
Balistidae (Triggerfishes)		
<i>Rhinecanthus rectangulus</i>	R	-
<i>Sufflamen bursa</i>	R	-
Chaetodontidea (Butterflyfishes)		
<i>Heniochus diphreutes</i>	C	-
Cirrhitidae (Hawkfishes)		
<i>Paracirrhites pinnulatus</i>	R	-
Holocentridae (Squirrelfishes and Soldierfishes)		
<i>Myripristis berndti</i>	R	-
Labridae (Wrasses)		
<i>Bodianus albotaeeniatus</i>	R	-
<i>Cheilio inermis</i>	-	R
<i>Gomphosus varius</i>	R	-
<i>Novaculichthys taeniourus</i>	R	R
<i>Thalassoma duperrey</i>	A	C
Lutjanidae (Snapper)		
<i>Lutjanus kasmira</i>	R	-
Mullidae (Goatfishes)		
<i>Parupeneus multifasciatus</i>	R	-
<i>Parupeneus porphyreus</i>	-	R
Muraenidae (Eels)		
<i>Gymnothorax eurostus</i>	R	R
Ostraciidae (Boxfishes)		
<i>Ostracion meleagris</i>	R	R
Pomocentridae (Damselﬁshes)		
<i>Chromis hanui</i>	R	-
<i>C. vanderbilti</i>	A	-
<i>Dascyllus albisella</i>	C	-
<i>Plectroglyphidodon johnstonianus</i>	R	-
<i>P. marginatus</i>	R	-
Serranidae (Groupers)		
<i>Cephalopholis argus</i>	R	-
Tetraodontidae (Pufferfishes)		
<i>Canthigaster jactator</i>	C	C
Zanclidae (Moorish Idol)		
<i>Zanclus cornutus</i>	R	-
TOTAL SPECIES	26	11

Notes: R = Rare, C = Common

Table 9 Species of Non-Coral Invertebrates Detected within the Donor Area and at Punaluu Beach Park

GROUP AND SPECIES NAMES	DONOR AREA	PUNALUU BEACH PARK
LOBSTERS		
<i>Parribacus antarcticus</i>	R	-
SEA CUCUMBERS		
<i>Actinopyga varians</i>	R	R
<i>Holothuria atra</i>	-	R
SEA STARS		
<i>Ophiocoma erinaceus</i>	-	R
SEA URCHINS		
<i>Echinometra mathaei</i>	-	R
<i>Echinothrix calamaris</i>	R	-
<i>Tripneustes gratilla</i>	C	-
SPONGES		
Porifera (phylum)	R	R
TOTAL NUMBER OF SPECIES OBSERVED	5	5

Notes: R = Rare, C = Common

Table 10 GPS coordinates for four permanent orthomosaic monitoring sites

ORTHOMOSAIC SITE	LATITUDE	LONGITUDE
1	21° 34.718'	-157° 53.002'
2	21° 34.659'	-157° 52.905'
3	21° 34.638'	-157° 52.846'
4	21° 34.609'	-157° 52.810'

Table 11 Size class frequency of corals at four permanent orthomosaic monitoring sites

ORTHOMOSAIC SITE	SPECIES	SIZE CLASS (cm)					TOTAL
		0 - 5	>5 - 10	>10 - 20	>20 - 40	>40 - 80	
2	<i>Pocillopora damicornis</i>	1	-	-	-	-	1
3	<i>Porites compressa</i>	-	-	-	1	-	1
4	<i>Cyphastrea ocellina</i>	1	1	-	-	-	2
	<i>Leptastrea purpurea</i>	3	-	-	-	-	3
	<i>Montipora capitata</i>	-	1	5	-	1	7
	<i>Montipora patula</i>	1	2	1	1	-	5
	<i>Pocillopora damicornis</i>	-	2	2	-	-	4
	<i>Porites lobata</i>	-	-	-	1	-	1
TOTAL CORALS		6	6	8	3	1	24

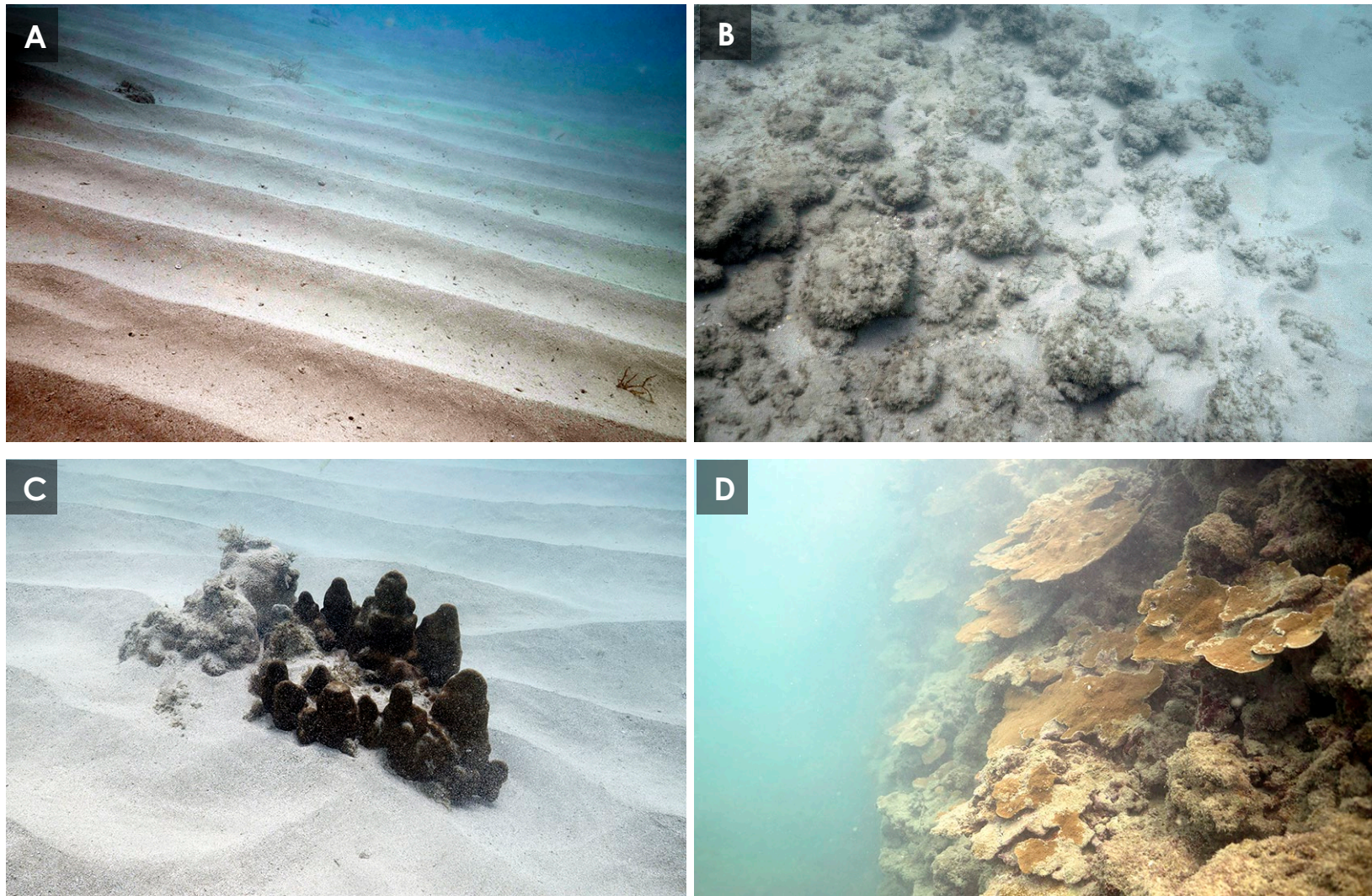


Figure 2 Representative Images of the Center and Perimeter of the Sand Donor Area.

Notes: A – Uniform bed of sand with sand waves in center of donor area; B – Rubble at edge of sand bed; C – Vertical wall at south side of sand bed; and D – partially buried coral at edge of sand bed



Figure 3 Representative Images of Seagrass at the Perimeter of the Sand Donor Area.

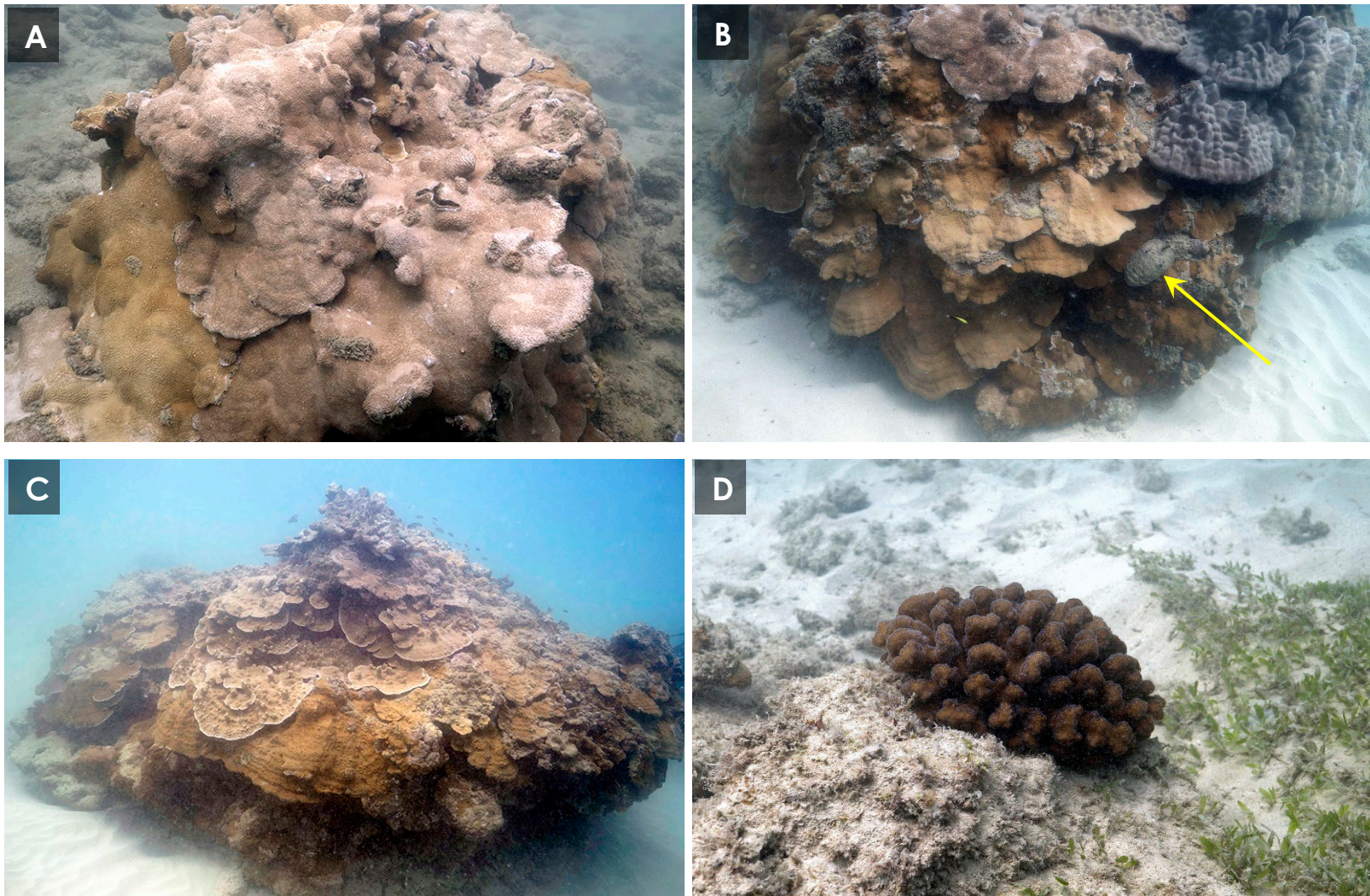


Figure 4 Representative Images of Coral Outside the Perimeter of the Sand Donor Area.

Notes: A – *Montipora capitata*; B – *Montipora patula*, *M. capitata*, and *Porites evermanni* with *Parribacus antarcticus* (yellow arrow); C – *M. capitata* and *M. patula*; and D – *Pocillopora meandrina*.

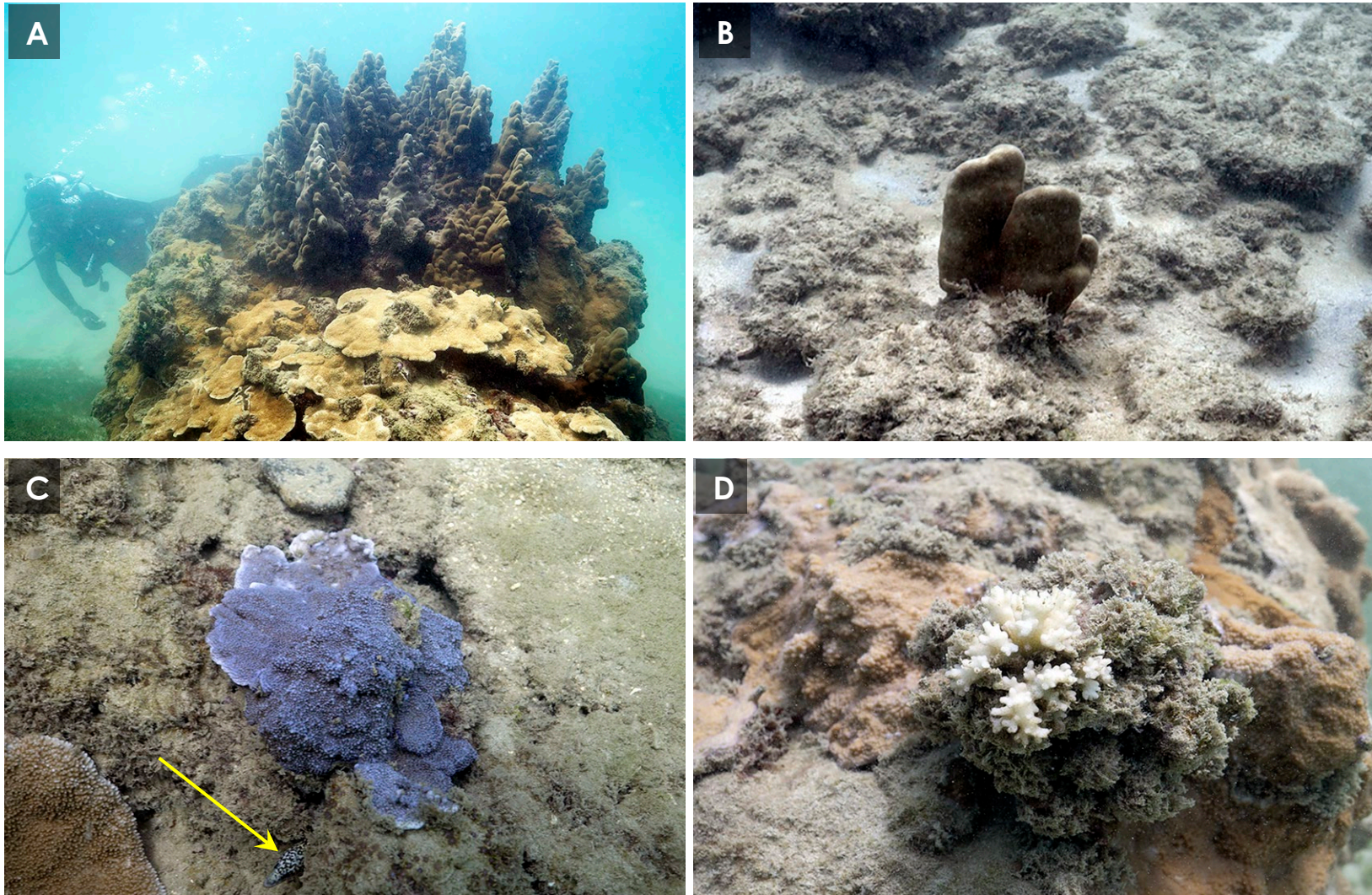


Figure 5 Representative Images of Coral Outside the Perimeter of the Sand Donor Area.

Notes: A – *Porites evermanni* (center) and *Montipora capitata* (foreground); B – *Porites lobata*; C – *Montipora flabellata* with *Gymnothorax eurostus* (yellow arrow); and D – *Pocillopora damicornis* (center) and *M. patula* (background)

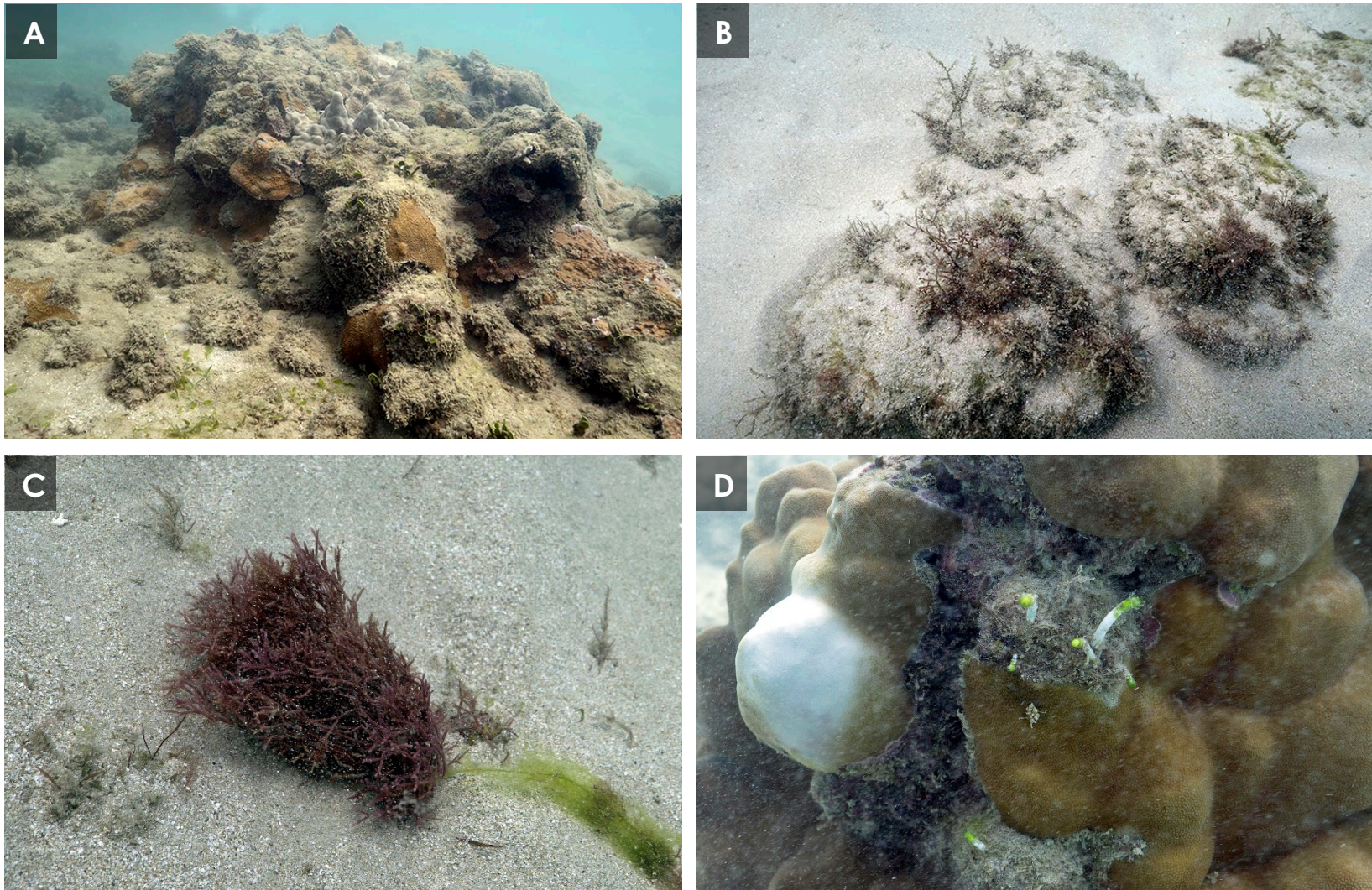


Figure 6 Representative Images of the Center and Perimeter of the Sand Donor Area.

Notes: A – Turf algae trapping sediment, some macroalgae, and seagrass (foreground) on hard substrate and coral; B – Turf algae, *Acanthophora spicifera*, *Gracilaria coronopifolia*, and *Hypnea* sp.; C – *Galaxaura rugosa* (red) and cyanobacteria (green, lower right); and D – *Neomeris* sp. on dead portion of colony of *Porites lobata*.

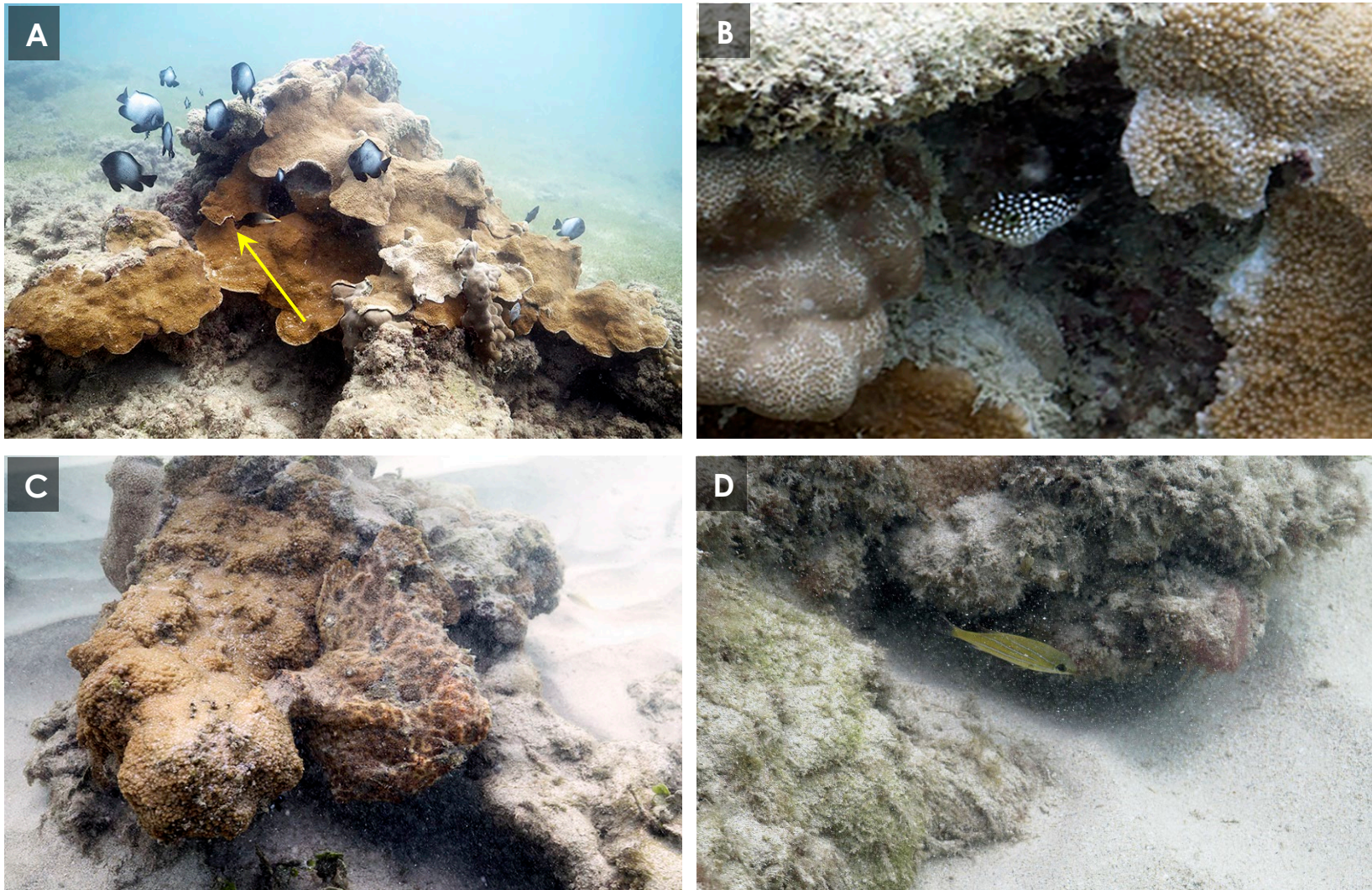


Figure 7 Representative Images of Fish Outside the Perimeter of the Sand Donor Area.

Notes: A – *Dascyllus albisella* (black and white) and *Gomphosus varius* (yellow arrow); B – *Canthigaster jactator*; C – *Antennarius* sp.; and D – *Lutjanus kasmira*

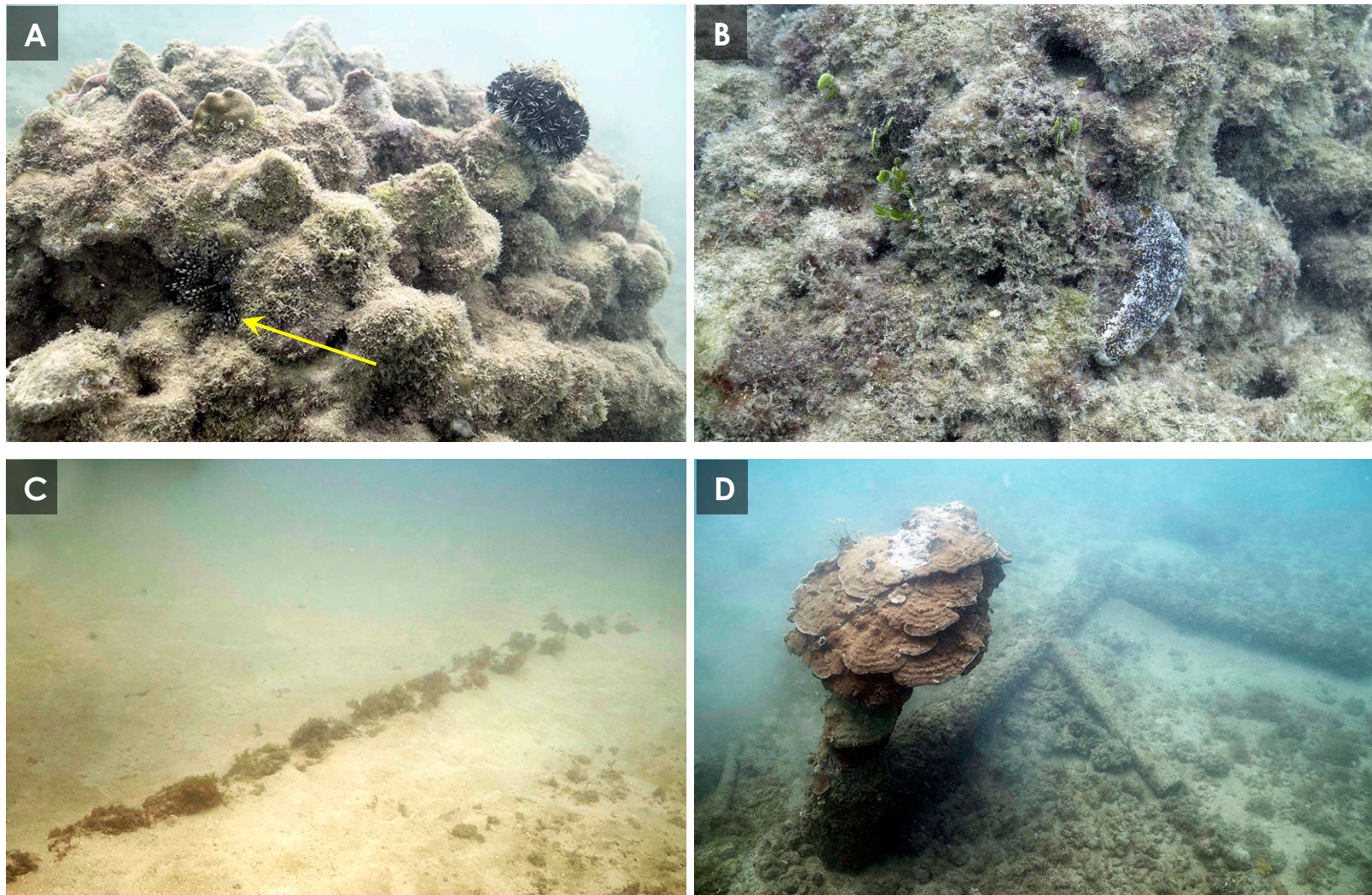


Figure 8 Representative Images of Invertebrates and Debris Outside the Perimeter of the Sand Donor Area.

Notes: A – *Echinothrix calamaris* (yellow arrow) and *Tripneustes gratilla* (top right); B – *Actinopyga varians*; C – Chain mostly buried in sand with macroalgal cover; and D – Unknown debris with *Montipora patula*



Figure 9 Representative Images of the Shoreline at Punaluu Beach Park.

Notes: A – Looking onshore near the south end of the survey area; B – Interface between grassy lawn and sandy beach where the high wash of waves creates erosion at the shoreline; C – Section of shoreline with a relatively wide sandy beach; and D – Sandy beach with rocks and boulders.

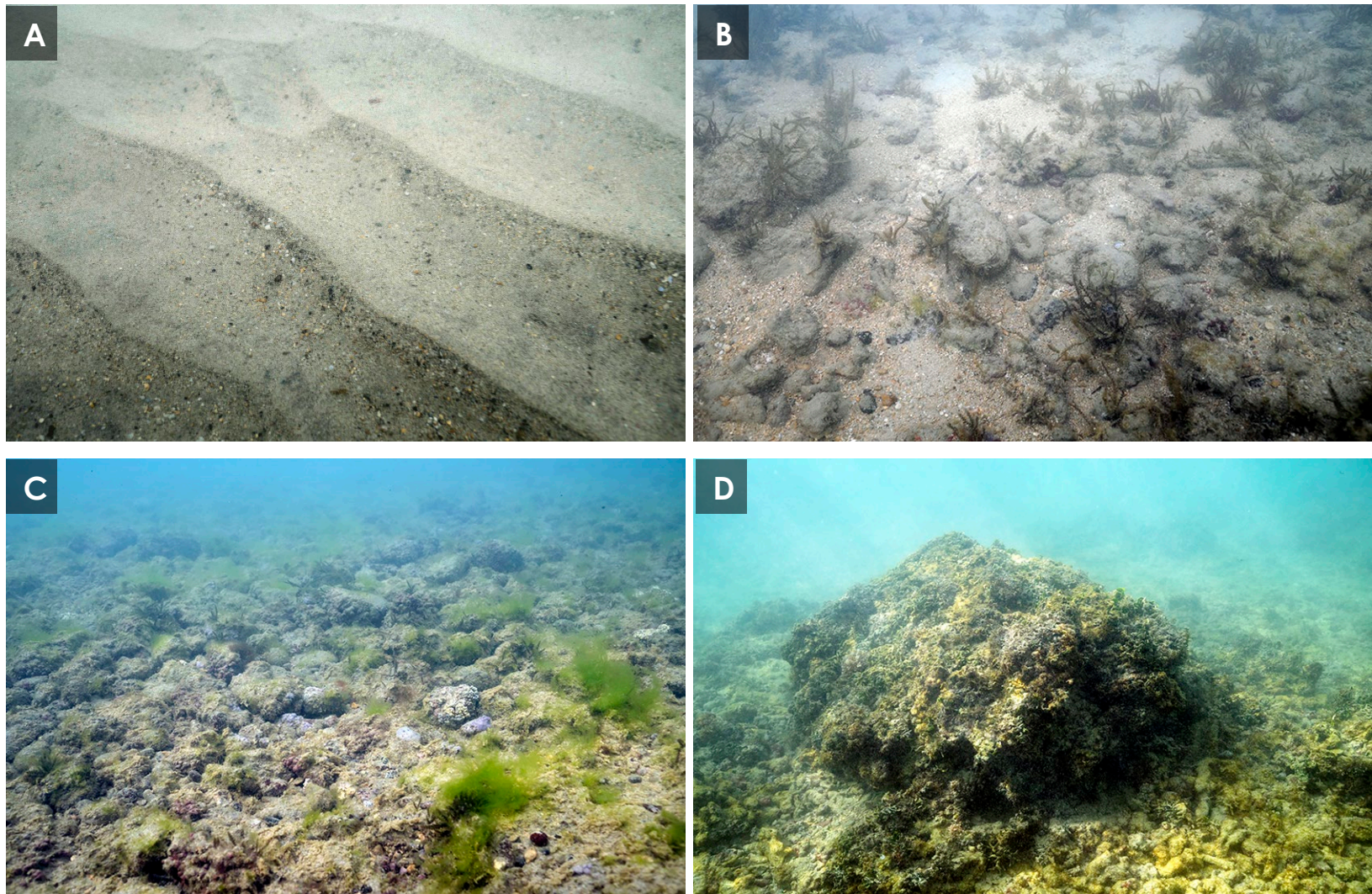


Figure 10 Representative Images of the Seafloor at Punaluu Beach Park.

Notes: A – Sand waves; B and C – Mix of sand and rock rubble with turf and macroalgae; and D – Boulder covered with turf and macroalgae

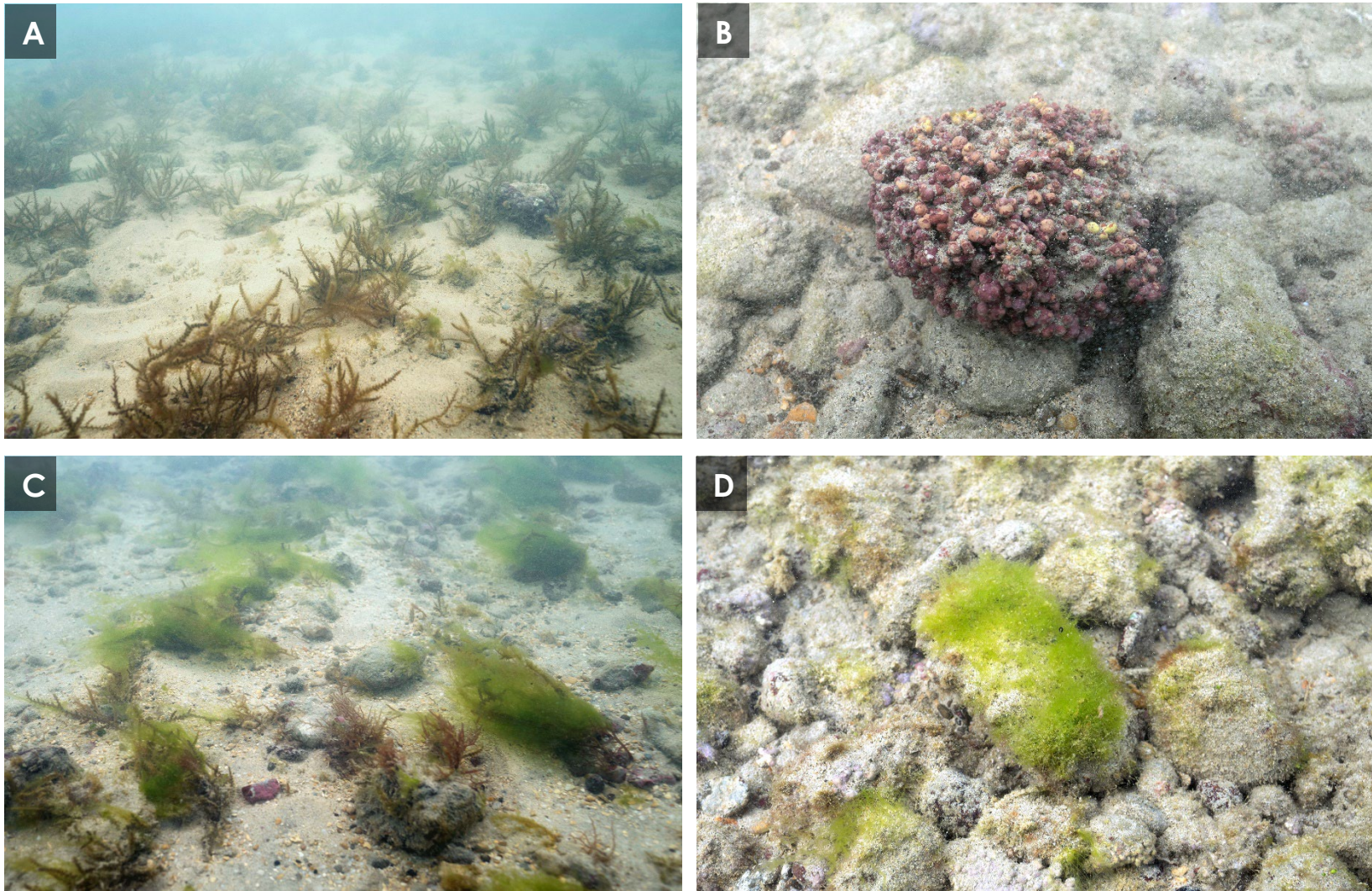


Figure 11 Representative Images of Macroalgae at Punaluu Beach Park.

Notes: A – *Acanthophora spicifera*; B – Crustose Coralline Algae; C – Cyanobacteria (green); and D – *Boodlea composita*.

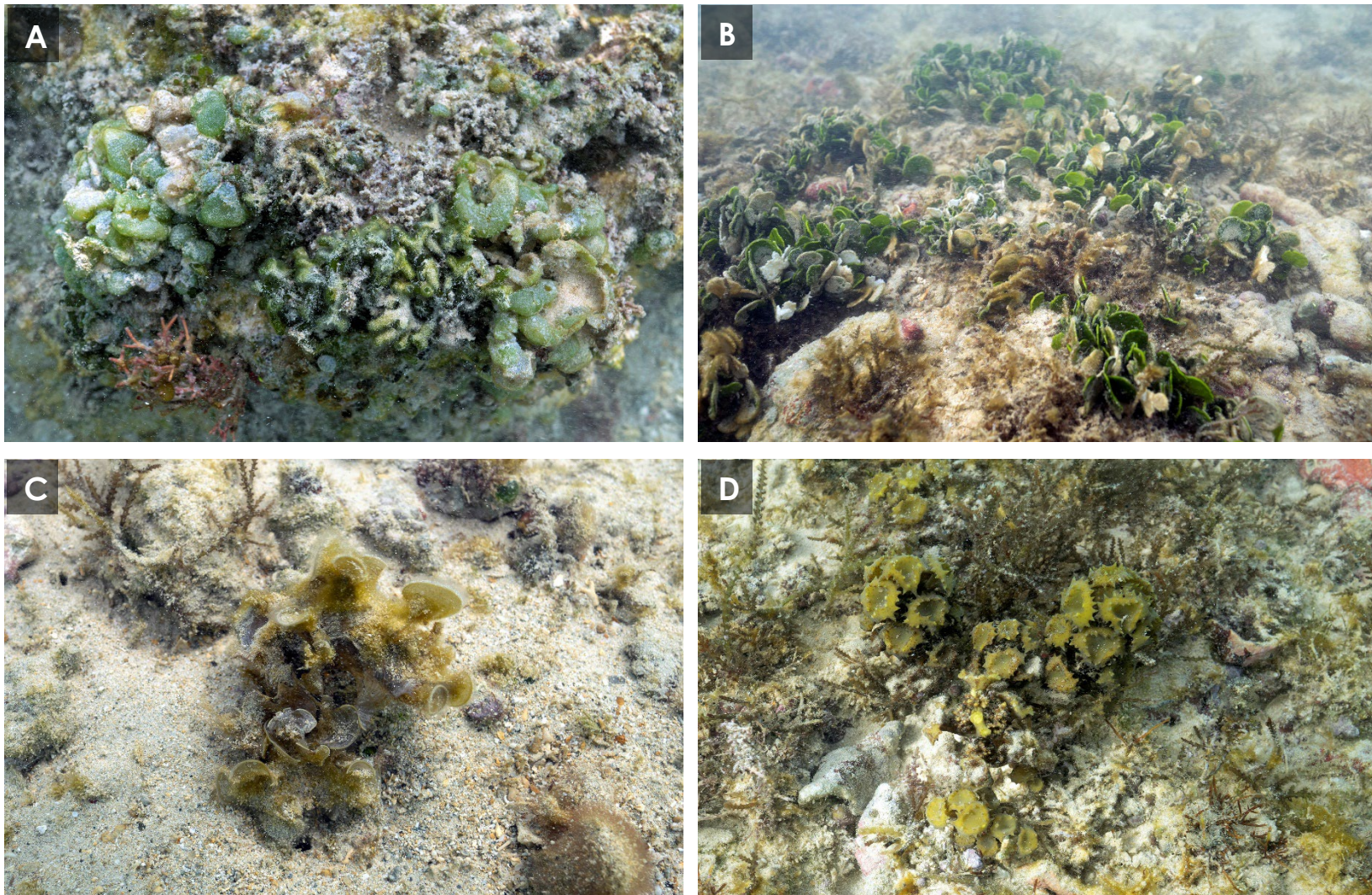


Figure 12 Representative Images of Macroalgae at Punaluu Beach Park.

Notes: A – *Codium edule* and *Dictyosphaeria* sp.; B – *Halimeda discoidea*; C – *Padina australis*; and D – *Turbinaria ornata*.

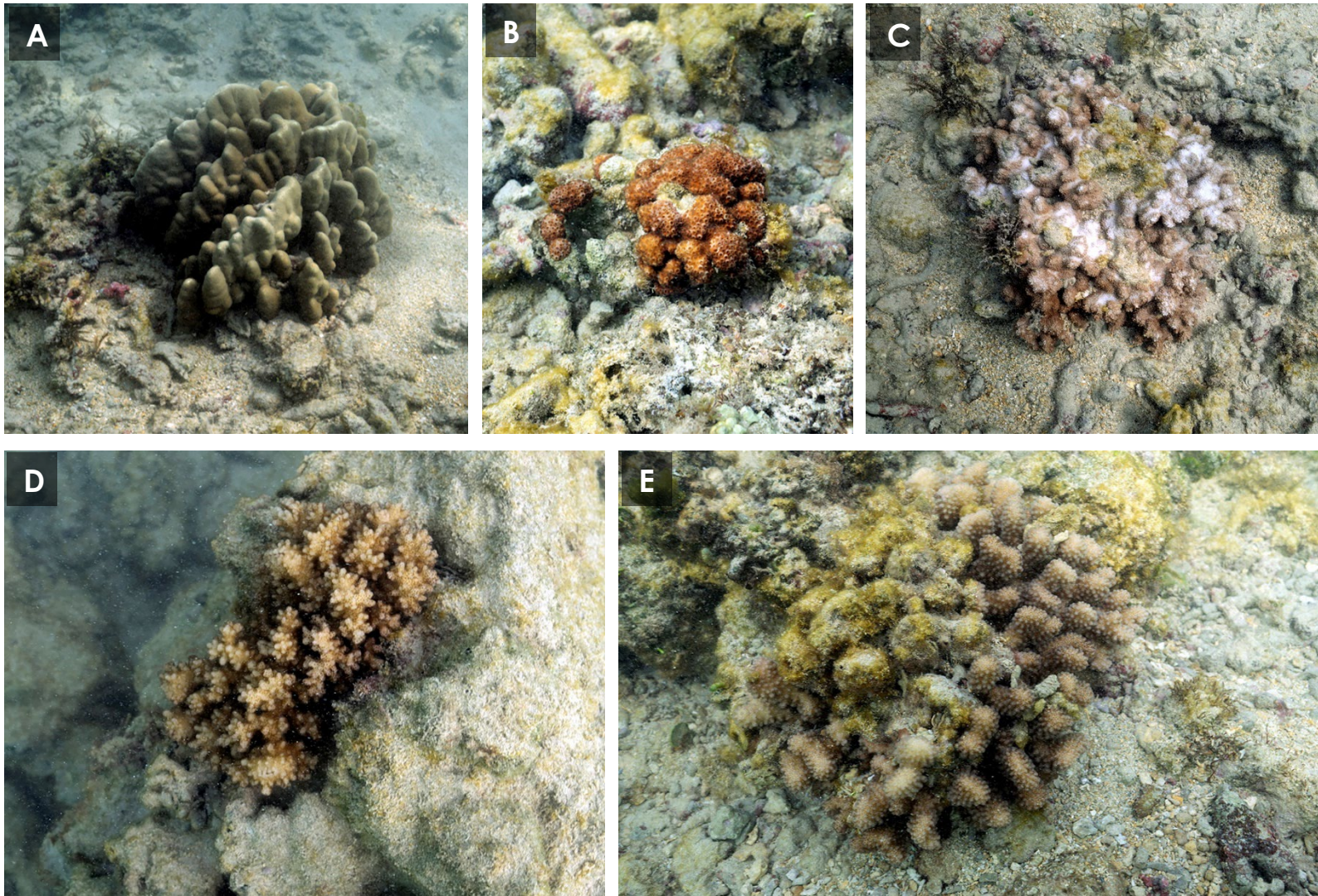


Figure 13 Representative Images of Corals at Punaluu Beach Park.

Notes: A – *Porites lobata*; B – *Cyphastrea ocellina*; C – *Montipora capitata*; D – *Pocillopora damicornis*; and *Pocillopora meandrina*.

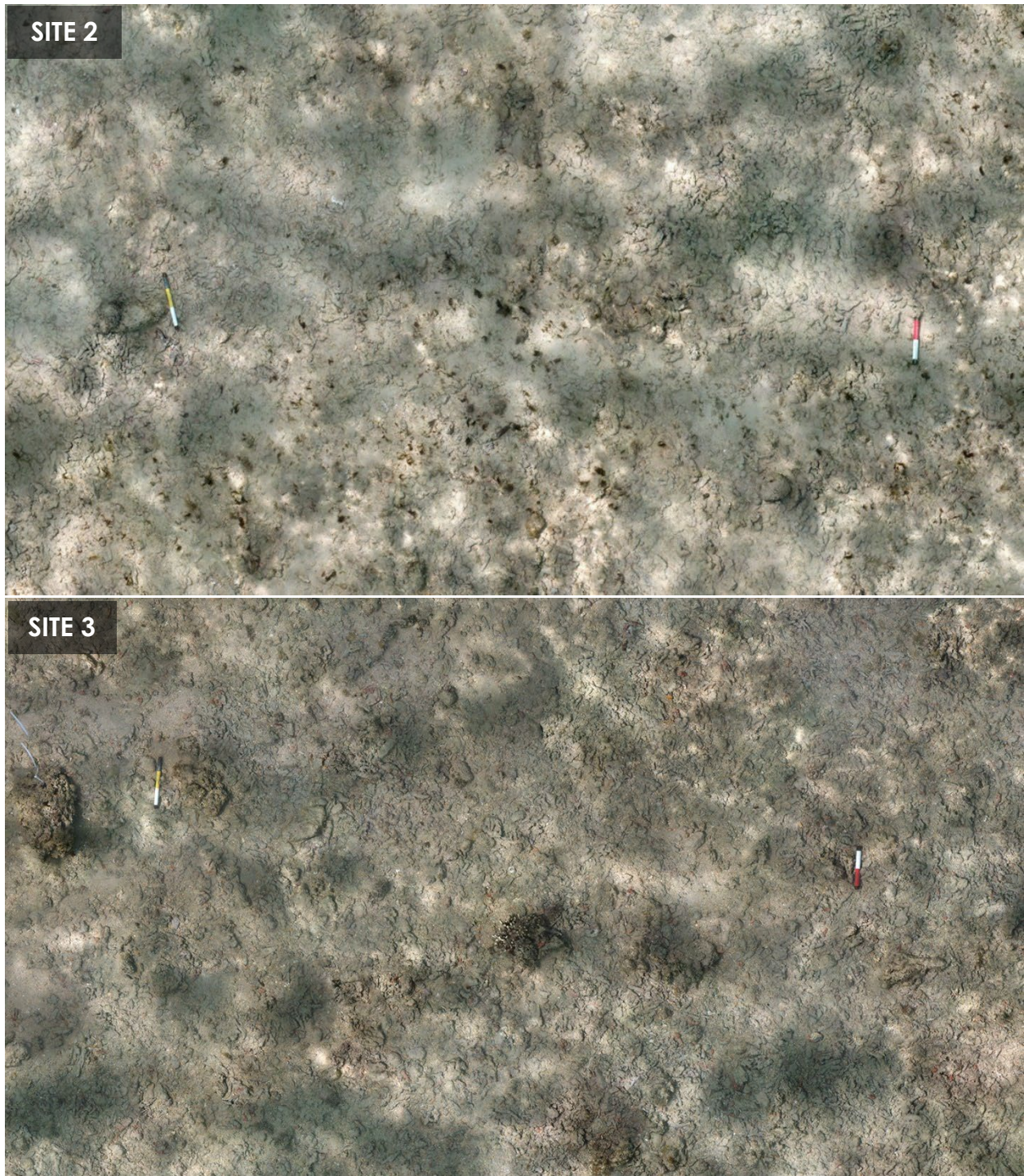


Figure 14 Orthomosaics at Permanent Monitoring Sites 2 and 3.

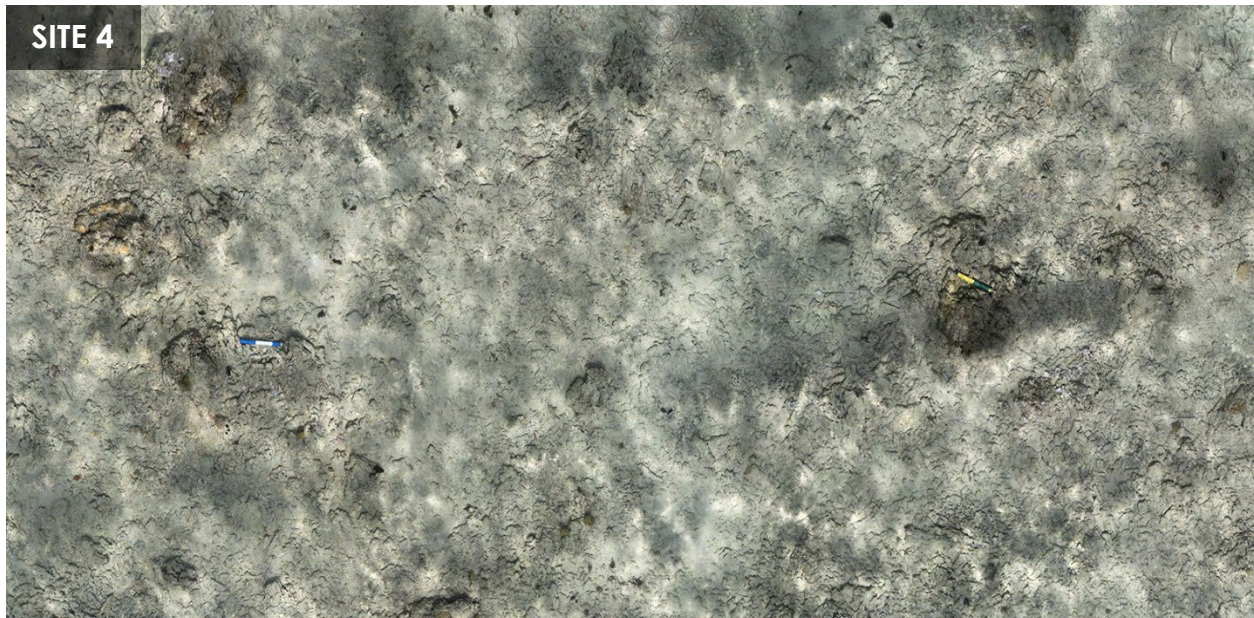


Figure 15 Orthomosaics at Permanent Monitoring Site 4.

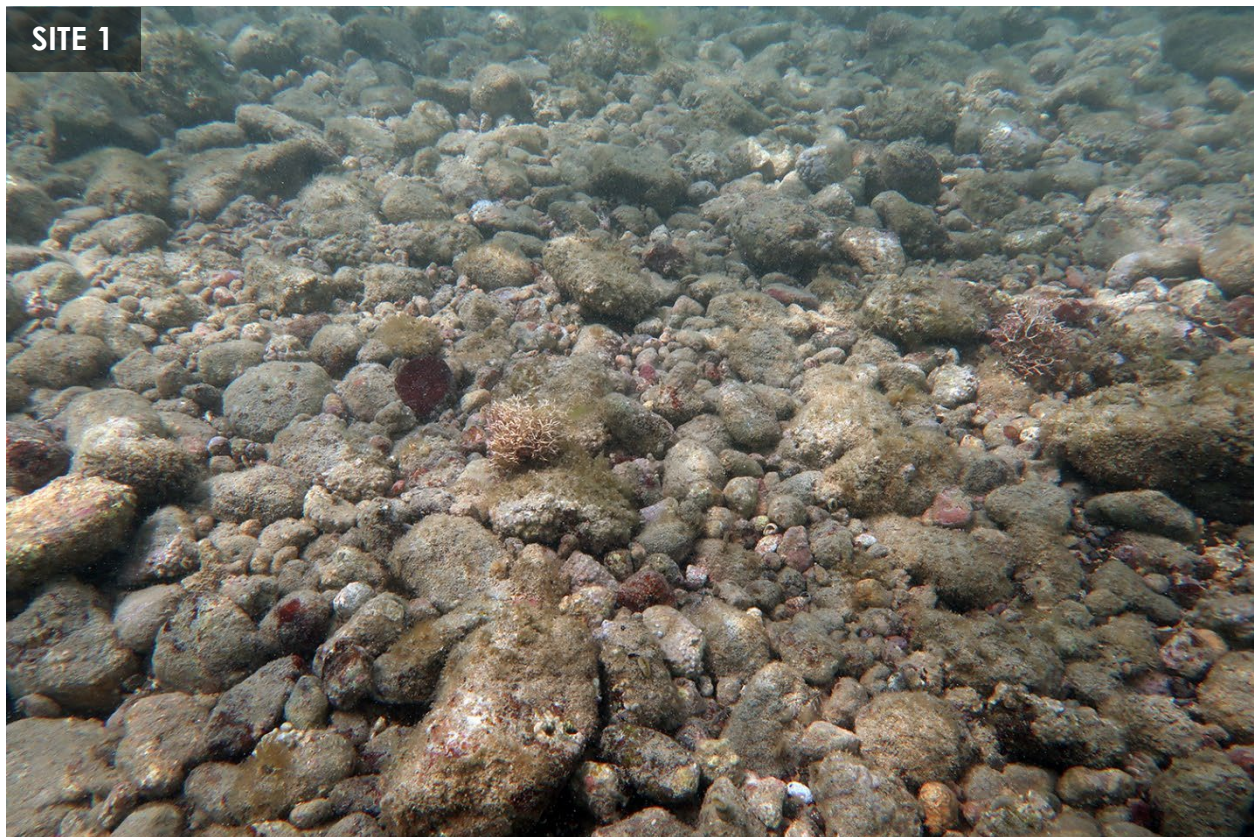


Figure 16 Representative Photograph of Rocks Covered in Crustose Coralline Algae, Turf Algae, and Macroalgae on the Seafloor at Site 1

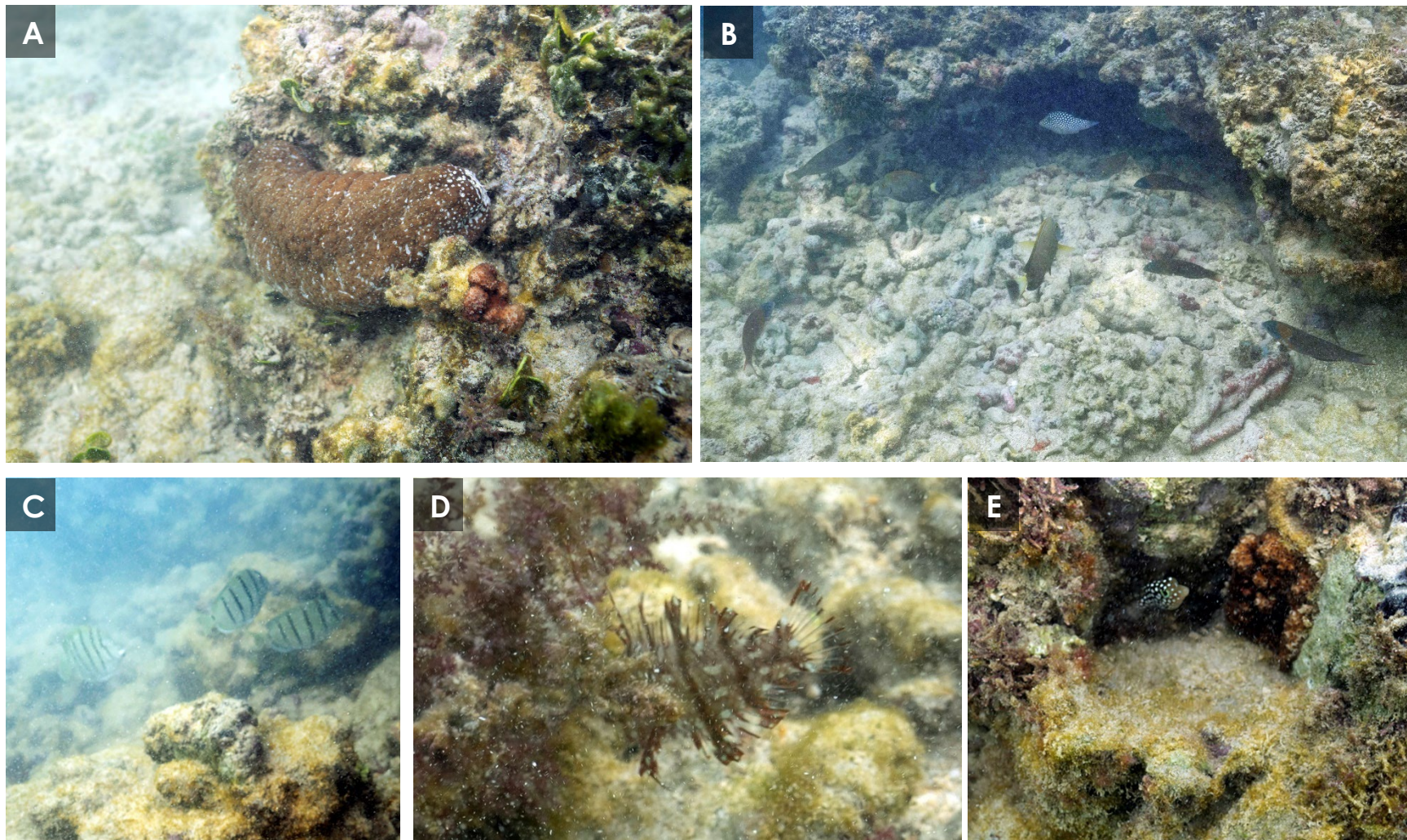


Figure 17 Representative Images of a Sea Cucumber and Fish at Punaluu Beach Park

Notes: A – *Actinopyga varians*; B – Mixed school of fish including *Acanthurus blochii*, *Canthigaster jactator*, and *Thalassoma duperrey*; C – *Acanthurus triostegus*; D – *Novaculichthys taeniourus*; and E – *Canthigaster jactator*